TU Delft

Delft University of Technology

Phosphate recovery from wastewater via reversible adsorption

Suresh Kumar, Prashanth

DOI
10.4233/uuid:f75d3713-8ef2-4f92-884f-06664b040f47

Publication date
2018

Document Version
Final published version

Citation (APA)
Suresh Kumar, P. (2018). *Phosphate recovery from wastewater via reversible adsorption*. [Dissertation (TU Delft), Delft University of Technology]. https://doi.org/10.4233/uuid:f75d3713-8ef2-4f92-884f-06664b040f47

Important note
To cite this publication, please use the final published version (if applicable).
Please check the document version above.

Copyright
Other than for strictly personal use, it is not permitted to download, forward or distribute the text or part of it, without the consent of the author(s) and/or copyright holder(s), unless the work is under an open content license such as Creative Commons.

Takedown policy
Please contact us and provide details if you believe this document breaches copyrights.
We will remove access to the work immediately and investigate your claim.

This work is downloaded from Delft University of Technology.
For technical reasons the number of authors shown on this cover page is limited to a maximum of 10.

Phosphate recovery from wastewater via reversible adsorption

Dissertation

For the purpose of obtaining the degree of doctor
at Delft University of Technology
by the authority of the Rector Magnificus Prof. dr. ir. T.H.J.J. van der Hagen
Chair of the Board for doctorates,
to be defended publicly on
16 November 2018 at 15:00
by

Prashanth Suresh Kumar,
Master of Science in Applied Biotechnology,
Uppsala University, Sweden,
born in Jamshedpur, India

This dissertation has been approved by the promotors:

Prof. dr. G.J. Witkamp and prof. dr.ir. M.C.M. van Loosdrecht.

Composition of the doctoral committee:

Rector Magnificus	Chairman
Prof. dr. G.J. Witkamp	Delft University of Technology, promotor
Prof. dr.ir. M.C.M. van Loosdrecht	Delft University of Technology, promotor

Independent members:

Prof. dr. R.N.J. Comans	Wageningen University and Research,
Prof. dr.ir. J.A.M.Hofman	University of Bath,
Prof.dr. E.H.Brück	Delft University of Technology,
Prof.dr. S.J. Picken	Delft University of Technology

Other members:

Ir. Leon Korving	Wetsus, European centre of excellence for sustainable water technology

Phosphate recovery

from wastewater

via reversible adsorption

M.Sc. Prashanth Suresh Kumar,

Phosphate recovery from wastewater via reversible adsorption,

250 pages,

PhD thesis, TU Delft, Delft, The Netherlands (2018)

This work was financially supported by Wetsus – European Centre of Excellence for sustainable Water technology, Oostergoweg 9, 8911 MA Leeuwarden, The Netherlands.

Cover design by Vriksha – a presentation port (www.vriksha.co.in)

ISBN: 978-94-6332-429-8

Popular Science Summary

A schoolboy once came to me with a bag of potato chips and asked: “Do these also have phosphate in them?”

Whenever we buy food, we can see that on the backside of the package, the amount of carbohydrates, proteins, and fats are mentioned. While it is true that these macronutrients are very essential for us, there are also micronutrients that are equally essential. Phosphate, a molecule containing phosphorus (P), is one such vital nutrient. It is required by all life and is present in our DNA. It is used as fertilizer for growing plants. We consume it in our food and our excrete containing phosphate ends up in the municipal wastewater plant. Whatever phosphate is left behind after the treatment passes on to surface waters like lakes and rivers.

It is said that one person’s waste is another one’s resource. It is so true in this case because the human waste ends up being used as a resource in water bodies by organisms called algae. This results in algal bloom, the green coloring seen in water bodies. This is often associated with dirty or polluted water. An algal bloom has serious implications and causes economic as well as environmental damages. It poses health risks for humans as well other organisms in the ecosystem. It affects industries like fishing, tourism, housing, and water treatment.

Cleaning the water from phosphate can prevent the algal bloom. But phosphate is such a vital nutrient that it is also desirable to recover whatever phosphate is removed from the water. Thus a more appropriate approach than cleaning would be transporting. A waste is something that is in the wrong amount in the wrong place. Transporting this something to a place where it is needed will make it into a valuable product.

In this research, the idea is to design an optimum phosphate transport vehicle called the adsorbent. This can be any solid material that can remove phosphate, for e.g. iron oxide (also known as rust). This adsorbent can remove the phosphate from the wastewater and recover it to a form which can be used as a raw material for fertilizer. It can be thought similar to a bus which transports people from one place to another. The bus needs to be able to transport as many people as possible, as fast as possible. The adsorbent needs to transport phosphate instead of people.



A big aspect of making any technology translate into application is the economic feasibility, i.e. how low can the costs of treatment be. In terms of phosphate removal, this can be measured as $/Kg P removed. This is similar to the cost of a bus ticket in our analogy, $/Ticket. If a bus is bought for just a one-time use, it will be an extremely expensive investment. But reusing the

bus several times allows the passengers to travel for a cheaper price. Similarly, the adsorbent needs to be reused several times to make the whole process economically viable.

The different aspects that characterize a good phosphate adsorbent, including the amount of phosphate transported, speed of transport and reusability of the material are studied in this thesis. Based on the observations the economics of the process are also discussed along with research gaps and suggestions.

Populaire Wetenschappelijke Samenvatting

Een schooljongen kwam ooit met een zak chips naar me toe en vroeg: "Zit hier ook fosfaat in?"

Wanneer we eten kopen, kunnen we zien dat er een etiket op het product zit waarop de hoeveelheden koolhydraten, eiwitten en vetten worden vermeld. Hoewel deze macronutriënten erg belangrijk voor ons zijn, zijn er ook micronutriënten die eveneens zeer belangrijk zijn. Fosfaat, een afgeleide vorm van fosfor (P), is zo'n belangrijke voedingsstof. Het is door al het leven vereist en is aanwezig in ons DNA. We gebruiken het als meststof om planten te laten groeien, we consumeren het in ons voedsel en onze uitscheiding met fosfaat komt terecht in het rioolwater. Het fosfaat dat na behandeling van het rioolwater achterblijft, stroomt naar oppervlaktewateren zoals meren en rivieren.

Er wordt wel eens gezegd dat het afval van een persoon voor een ander een grondstof is. Dat gaat helemaal ook op in dit geval, omdat het menselijke afval uiteindelijk wordt gebruikt als een grondstof in oppervlaktewater door organismen die algen worden genoemd. Dit resulteert in algenbloei, de groene verkleuring die te zien is in oppervlaktewater. Dit wordt vaak geassocieerd met vies of vervuild water. Algenbloei heeft ernstige gevolgen voor andere organismen in het water, zoals vissen, en kan ook leiden tot voedselvergiftiging. Het beïnvloedt industrieën zoals visserij, toerisme, huisvesting en waterzuivering.

Het verwijderen van fosfaat uit het water kan algenbloei voorkomen. Maar fosfaat is zo'n essentiële voedingsstof dat het wenselijker is om het fosfaat uit het water terug te winnen. Dus een meer geschikt woord dan reinigen zou transporteren zijn. Een verspilling is iets dat in de verkeerde hoeveelheid op de verkeerde plaats staat. Door dit naar een plaats te transporteren waar het nodig is, wordt het weer waardevol.

De kern van dit onderzoek is het idee om een optimaal fosfaattransportvoertuig te ontwerpen. Dit voertuig wordt een adsorptiemiddel genoemd. Het adsorptiemiddel kan het fosfaat uit het afvalwater onttrekken en terugwinnen tot een vorm die kan worden gebruikt als grondstof voor kunstmest. Het kan als een bus worden beschouwd die mensen van de ene plaats naar de andere vervoert. De bus moet zo veel mogelijk passagiers zo snel mogelijk kunnen vervoeren. Het adsorptiemiddel moet fosfaat vervoeren in plaats van mensen.



Bij het vertalen van een technologie naar toepassing is de economische haalbaarheid een belangrijk aandachtspunt, met andere woorden hoe laag kunnen de kosten van de behandeling

zijn. In termen van fosfaatverwijdering kan dit worden gemeten als € / kg P verwijderd. Dit is vergelijkbaar met de kosten van een bus ticket waarbij de prijs wordt uitgedrukt in € / ticket. Als een bus voor eenmalig gebruik wordt gekocht, is het een extreem dure investering. Maar als de bus meerdere keren wordt hergebruikt nemen de kosten per rit af en kunnen passagiers reizen tegen een lagere prijs. Het adsorptiemiddel moet eveneens verschillende keren worden hergebruikt om het gehele proces economisch levensvatbaar te maken.

De verschillende aspecten die kenmerkend zijn voor een goed fosfaat adsorptiemiddel, de hoeveelheid getransporteerd fosfaat, transportsnelheid en herbruikbaarheid van het materiaal, worden in dit proefschrift bestudeerd. Op basis van de waarnemingen worden de economische aspecten van het proces besproken en suggesties gedaan voor onderwerpen die nader onderzoek behoeven.

Table of contents

POPULAR SCIENCE SUMMARY 5

POPULAIRE WETENSCHAPPELIJKE SAMENVATTING 7

CHAPTER - 1

INTRODUCTION **13**

1.1. INTRODUCTION AND OUTLINE 14

CHAPTER -2

THE RELEVANCE OF PHOSPHORUS AND IRON CHEMISTRY TO THE RECOVERY OF PHOSPHORUS FROM WASTEWATER: A REVIEW **17**

2.1. PROLOGUE 18
2.2. ABSTRACT 19
2.3. INTRODUCTION 19
2.4. IRON AS A KEY ELEMENT IN WASTEWATER TREATMENT PLANTS OF THE FUTURE 21
2.5. IRON AND PHOSPHORUS INTERACTIONS 24
2.6. TRANSFORMING IRON–PHOSPHORUS COMPOUNDS 30
2.7. APPROACHES TO RECOVER PHOSPHORUS FROM IRON 36
2.8. SUPPLEMENTARY INFORMATION 39

CHAPTER - 3

EFFECT OF PORE SIZE DISTRIBUTION ON IRON OXIDE COATED GRANULAR ACTIVATED CARBONS FOR PHOSPHATE ADSORPTION – IMPORTANCE OF MESOPORES **45**

3.1. PROLOGUE 46
3.2. ABSTRACT 48
3.3. INTRODUCTION 48
3.4. EXPERIMENTAL 49
3.5. RESULTS AND DISCUSSION 52
3.6. CONCLUSION 64
3.7. SUPPORTING INFORMATION 65

CHAPTER - 4

EFFECT OF PORE SIZE DISTRIBUTION AND PARTICLE SIZE OF POROUS METAL OXIDES ON PHOSPHATE ADSORPTION CAPACITY AND KINETICS **73**

4.1. PROLOGUE 74
4.2. ABSTRACT 76
4.3. INTRODUCTION 76
4.4. MATERIALS AND METHODS 77
4.5. RESULTS AND DISCUSSION 79
4.6. CONCLUSION 92
4.7. SUPPORTING INFORMATION 93

CHAPTER - 5

BIOGENIC IRON OXIDES FOR PHOSPHATE REMOVAL **97**

5.1. PROLOGUE 98
5.2. ABSTRACT 98
5.3. INTRODUCTION 99
5.4. MATERIAL AND METHODS 100
5.5. RESULTS AND DISCUSSION 101
5.6. SUPPLEMENTARY INFORMATION 105

CHAPTER – 6

UNDERSTANDING AND IMPROVING THE REUSABILITY OF PHOSPHATE ADSORBENTS FOR WASTEWATER EFFLUENT POLISHING **111**

6.1. PROLOGUE 112
6.2. ABSTRACT 114
6.3. INTRODUCTION 114
6.4. MATERIALS AND METHODS 115
6.5. RESULTS AND DISCUSSION 120
6.6. CONCLUSION 135
6.7. SUPPORTING INFORMATION 136

CHAPTER - 7

ADSORPTION AS A TECHNOLOGY FOR ACHIEVING ULTRA-LOW CONCENTRATIONS OF PHOSPHATE: RESEARCH GAPS AND ECONOMIC ANALYSIS **147**

7.1. PROLOGUE 148
7.2. ABSTRACT 150
7.3. INTRODUCTION 150
7.4. FACTORS GOVERNING THE CHEMICAL COSTS OF PHOSPHATE ADSORPTION 154
7.5. ECONOMIC ANALYSIS FOR PHOSPHATE ADSORPTION 163
7.6. CONCLUSION 176
7.7. SUPPORTING INFORMATION 177

CHAPTER - 8

VALORIZATION OF PHOSPHATE ADSORPTION **193**

8.1. PROBLEM STATEMENT AND THE CAPABILITY OF ADSORPTION 194
8.2. EXISTING MARKET(S) AND POTENTIAL CUSTOMERS 194
8.3. COST ANALYSIS 194
8.4. VALUE TO CUSTOMERS 195
8.5. EXAMPLE OF APPLICATION 196
8.6. POTENTIAL BUSINESS MODEL 197

CHAPTER - 9

CONCLUSION AND OUTLOOK **199**

REFERENCES **203**

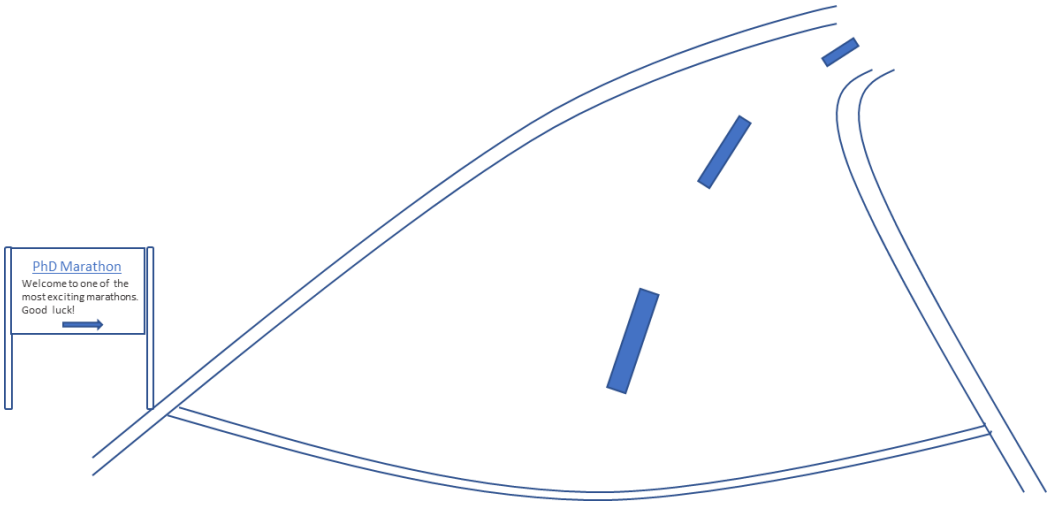
ACKNOWLEDGMENTS **241**

CURRICULUM VITAE **249**

LIST OF PUBLICATIONS **250**

Chapter - 1

Introduction



1.1. Introduction and outline

What is a waste? We talk about it in our day to day lives. Do not waste food, do not waste electricity, do not waste paper and so on. While these phrases imply the action of wasting, Oxford dictionary defines waste the noun as unwanted or unusable materials, substances or byproducts. However, in the world of chemistry that is not true. Our planet is composed of more than 100 elements and the world around us is made up of a huge permutation and combination of extremely small building blocks of these elements called atoms. An element is in fact defined by its atomic number, which implies the number of protons it has per atom. A proton has a predicted lifetime of more than 10^{30} years (Walker J. 2014). To put it in perspective, the universe has an estimated age of about 10^{10} years so far. The point is, from a chemical perspective, there is nothing that cannot be reused again. Atoms can react to form molecules, which can react to form living or non-living compounds. It is true that the compounds themselves can naturally break down, as can molecules and after a very long time atoms too can disintegrate. However, these atoms can interact with other atoms again, form molecules and form complex compounds once more.

In fact, what we refer to as waste is basically something that is at the wrong place, in the wrong amount or wrong time. We waste food if we have an excess of food. If the food is distributed somewhere else in the world where it was needed, it is actually a resource. Along similar lines, nothing is actually a waste if it can be reused. This applies to many things in our day to day life, even the food we already ate. The food has nutrients and once we eat and excrete it, these nutrients go to the municipal wastewater/sewage treatment plant. If these nutrients are just let go, they are indeed a waste. But if they can be recovered they become valuable.

One such nutrient is phosphate, a molecule consisting of the elements phosphorus (P) and oxygen. Phosphate is an essential nutrient for all life. It is present in the DNA, the hereditary material of humans and nearly all other organisms. Phosphate is present in ATP, also called the currency for molecules, which is the carrier of energy for our cells. Phosphate is present in our teeth and bones. We need phosphate in our food, as do plants and animals. In fact, phosphate is an essential component of fertilizers. Simply put, there is no substitute for phosphate, and lack of phosphate is equivalent to being without food. However, as implied earlier, any resource can become a waste and phosphate is no exception. Phosphate can enter surface waters through agricultural run-off or through the municipal wastewater. Once it reaches surface water, it can threaten the ecosystem even at concentrations as low as 0.01 mg P/L. This concentration is so low, that it is analogous to the concentration of sugar obtained by adding one tablespoon of sugar in a 1000 m^3 swimming pool. Just like it would be impossible to taste the sugar from the swimming pool, it is very hard to grasp such low levels of phosphate. However, this concentration is enough for certain microorganisms to grow. The presence of phosphate even in such low concentrations leads to a condition called eutrophication which causes the formation of harmful algal bloom.

Algal blooms are a disaster both from an environmental as well as economic point of view. Decomposition of algae after their death leads to oxygen depletion which leads to the death of many aquatic organisms like fishes. The toxins produced by these algae can reach other

organisms through the food chain including birds and humans and can cause fatalities. Moreover, they also cause economic losses by affecting various industries like fishing, housing, water treatment, recreation, and tourism. The annual damage costs due to freshwater eutrophication were estimated to be between $ 105 to 160 million in England and Wales (Pretty et al. 2003). The overall annual costs incurred as a result of eutrophication in US freshwaters was rounded to $ 2.2 billion (Dodds et al. 2009). As such, there is an urgent need to combat eutrophication by controlling the phosphate or bioavailable P in water bodies. Management of P from diffuse sources like agricultural run-off is vital and includes practices that monitor fertilizer usage, livestock numbers and P input from manure (Knowlton et al. 2004, Sharpley 2016). Regulation of non-point/diffuse sources can nonetheless be difficult since they arise due to activities distributed over wide areas and are more variable over time due to changes in weather (Carpenter et al. 1998).

Unlike diffuse sources, point sources of P like sewage effluent are easier to monitor and regulate (Dodds and Whiles 2010). Moreover, P loads from sewage effluent have been shown to have a higher fraction of bioavailable P compared to nonpoint sources (Gerdes and Kunst 1998, Maccoux et al. 2016). Conventional treatments to remove P in wastewater plants include chemical precipitation with metal salts and can generally reduce the levels between 0.5 to 1 mg P/L in the effluent depending on the salt dosage (Clark et al. 1997, Sedlak 1991). However, using chemical precipitation at concentrations below 0.1 mg P/L requires a significant increase in metal salt dosing due to the limitation related to solubility product, which in turn leads to high sludge production (Neethling 2013, Sedlak 1991). Technologies that can reduce phosphate concentrations to less than 0.15 mg P/L (referred to as ultra-low phosphate concentration) include wetlands, microalgal biofilms, precipitation combined with sand filtration (reactive filtration), precipitation or coagulation combined with ultrafiltration (Boelee et al. 2011, Dierberg et al. 2002, Mitchell and Ullman 2016b, Newcombe et al. 2008). However, each technique has its own demerits such as the need for large areas, optimal nutrient loading and illumination, fouling, or high sludge production by addition of metal salts. Hence there is a need for technology that can reduce P consistently to ultra-low levels, with less reliance on ideal conditions, a high throughput without fouling issues, with a low footprint, minimum waste generation and where the P is recoverable.

Adsorption is a technology that can achieve ultra-low concentrations of phosphate (Awual et al. 2014, Genz et al. 2004, Luo et al. 2016, Midorikawa et al. 2008, Sengupta and Pandit 2011). It involves the use of a solid material called adsorbent to remove the substance of interest called adsorbate, which is phosphate in this case. Apart from removing phosphate to very low concentrations, adsorption also offers the possibility to recover phosphate by regeneration of the adsorbent. This contributes to a circular economy. Extensive literature showcases the potential of adsorption to reach low P concentrations. But surprisingly, there is little information regarding their implementation at larger scales. This is likely due to insufficient information regarding the parameters essential for an economic assessment of phosphate adsorption, which is vital for scaling it up.

The goal of this thesis was thus based on two important questions:

i) What are the parameters that can be optimized for making adsorption an economically viable technology?
ii) How can these essential parameters be optimized using scientific research?

The following chapters highlight the studies undertaken to understand these aspects.

In the 2nd chapter, the role of iron is seen in its interaction with phosphorus in sewage treatment plants. It is discussed that the presence of iron in wastewater plants is common and this leads to a wide variety of possible interactions with phosphorus. Iron oxide based phosphate adsorbents are seen as interesting candidates for effluent polishing. The differences in binding properties of different iron oxides to phosphate are seen as offering interesting possibilities to design phosphate adsorbents.

In the 3rd chapter, describes the development of high surface area adsorbent composite by coating iron oxides on granular activated carbon (Fe-GAC). The effect of pore size distribution of granular activated carbons is seen as key moderator in making the maximum use of the available surface area and improving phosphate adsorption.

In the 4th chapter, the use of granular porous metal oxide adsorbents for phosphate removal is discussed. The role of the pore size distribution is discussed in the context of adsorption kinetics. The information from this chapter gives an idea in designing the adsorbents with ideal porosity.

In the 5th chapter, biogenic iron oxides are tested as a possible alternative to high affinity chemical phosphate adsorbents. The mechanism of adsorption involved with the biogenic iron oxides and their potential for use as an adsorbent is discussed.

In the 6th chapter, the reusability of iron oxide based adsorbents which were tested in real municipal wastewater effluent is described. The effect of adsorbent regeneration on adsorbent properties as well release of competing ions is discussed. Attention is given to the dual role of calcium.

In the 7th chapter, the potential of adsorption as effluent polishing technology is reviewed with a focus on the economic aspect. Research gaps regarding essential cost factors are indicated and a scenario analysis is done to predict the chemical cost for different types of adsorbents.

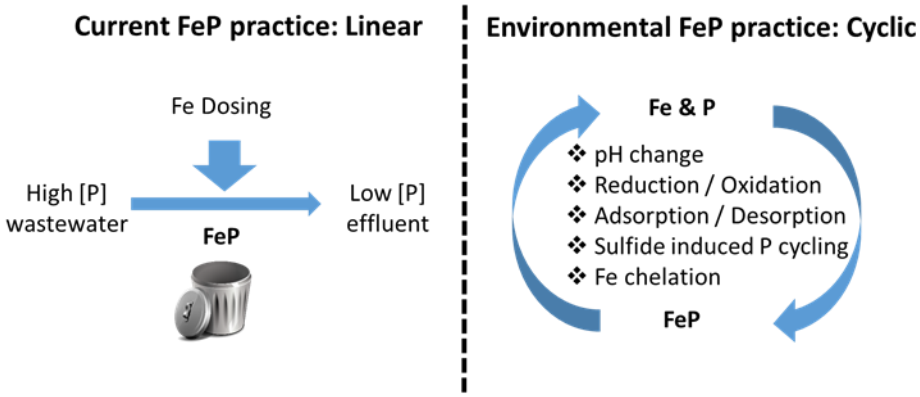
In the 8th chapter, the valorization of adsorption as a technology to reach ultra-low phosphate concentrations is discussed. This includes assessing the market potential for phosphate adsorption as well as generating a business canvas model that maps the possible activities to make a business out of this.

The final chapter gives a summary of the main discussions/findings from this thesis and future perspectives. There are recommendations and new possible routes suggested for exploration in the field of phosphate removal and recovery using adsorption.

Chapter -2

The relevance of phosphorus and iron chemistry to the recovery of phosphorus from wastewater: a review

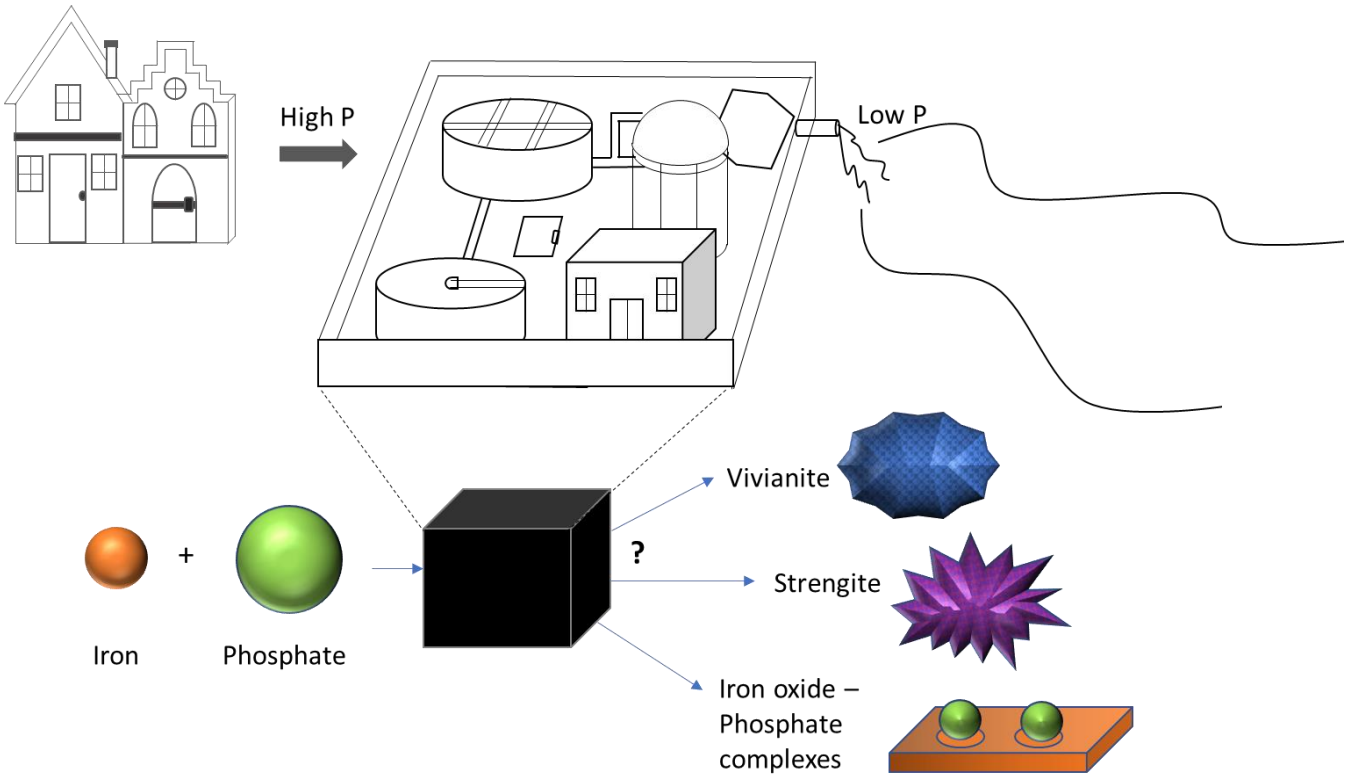
Wilfert, P.; Kumar, P. S.; Korving, L.; Witkamp, G.-J.; van Loosdrecht, M. C. M., The Relevance of Phosphorus and Iron Chemistry to the Recovery of Phosphorus from Wastewater: A Review. Environmental Science & Technology 2015, 49 (16), 9400-9414.



2.1. Prologue

2.1.1. Backdrop

- Although iron (Fe) is often employed in municipal wastewater treatment plants (WWTP) to remove Phosphorus (P), the involved chemistry is complex.
- This results in diverse chemical reactions between Fe and P (including phosphate) in the WWTP which often, like a black box, are not well understood.
- Understanding these interactions will help in designing optimal methods for phosphate recovery.



2.1.2. Research questions

i) What are the products formed between iron and phosphate, is it strengite (ferric phosphate), vivianite (ferrous phosphate) or iron (hydr)oxide phosphate complexes?

ii) How does phosphate adsorption vary with the different types of iron oxides?

iii) What type of phosphate recovery process can be envisioned with this knowledge of iron and phosphorus chemistry?

2.2. Abstract

The addition of iron is a convenient way for removing phosphorus from wastewater, but this is often considered to limit phosphorus recovery. Struvite precipitation is currently used to recover phosphorus, and this approach has attracted much interest. However, it requires the use of enhanced biological phosphorus removal (EBPR). EBPR is not yet widely applied and the recovery potential is low. Other phosphorus recovery methods, including sludge application to agricultural land or recovering phosphorus from sludge ash, also have limitations. Energy-producing wastewater treatment plants increasingly rely on phosphorus removal using iron, but the problem (as in current processes) is the subsequent recovery of phosphorus from the iron. In contrast, phosphorus is efficiently mobilized from iron by natural processes in sediments and soils. Iron–phosphorus chemistry is diverse, and many parameters influence the binding and release of phosphorus, including redox conditions, pH, the presence of organic substances, and particle morphology. We suggest that the current poor understanding of iron and phosphorus chemistry in wastewater systems is preventing processes being developed to recover phosphorus from iron–phosphorus rich wastes like municipal wastewater sludge. Parameters that affect phosphorus recovery are reviewed here, and methods are suggested for manipulating iron–phosphorus chemistry in wastewater treatment processes to allow phosphorus to be recovered.

2.3. Introduction

2.3.1. Background

Phosphorus is an essential nutrient and is very important for global food production. In 2000, 19.7 Mt of phosphorus was mined as phosphate rock. The major part, 15.3 Mt phosphorus, was used to produce fertilizers (van Vuuren et al., 2010). The demand for phosphorus will further increase in the future due to a growing global population, dietary changes and a rising share of biofuels (Cordell et al., 2009). Apart from the partial recycling of phosphorus by applying manure to agricultural land, the usage of phosphorus around the world is linear, with very few recycling routes and huge inefficiencies in its production and use (Cordell et al., 2009; Reijnders, 2014; van Vuuren et al., 2010). Ecological, geopolitical and economic concerns demand phosphorus recovery (Cooper et al., 2011; Cordell et al., 2009; De Ridder et al., 2012; Reijnders, 2014; van Vuuren et al., 2010). Hence, a cyclic use of phosphorus and thus the development of technologies that allow the recovery of phosphorus from secondary sources is required. Globally, about 1.3 Mt phosphorus/year is treated in municipal wastewater treatment plants (WWTPs) (van Vuuren et al., 2010). We focus in this review on municipal wastewater as a major secondary source of phosphorus. The implications of the interactions described for phosphorus and iron are also relevant to other wastewaters and even surface water.

Phosphorus is removed from wastewater to prevent eutrophication in effluent receiving surface waters (Conley et al., 2009; Jarvie et al., 2006). The most popular phosphorus removal techniques are enhanced biological phosphorus removal (EBPR) and the more widely used chemical phosphorus removal (CPR) using Iron or aluminium salts (Table S2-1

in supporting information) (Carliell-Marquet and Cooper, 2014; De-Bashan and Bashan, 2004; DWA, 2005; Korving, 2012; Morse et al., 1998; Paul et al., 2001). Iron salts are usually preferred. They are cheaper than aluminium salts (Geraarts et al., 2007; Paul et al., 2001). Also in EBPR plants, Iron is often dosed to support phosphorus removal (Table S2-1 in supporting information). Apart from phosphorus removal, iron plays an important role in modern wastewater treatment in general. It is used to prevent hydrogen sulphide emissions during anaerobic digestion and acts as a coagulant to improve sludge dewatering (Charles et al., 2006; Ge et al., 2013; Higgins and Murthy, 2006). Wastewater pumping stations dose iron to control odours and corrosion (Nielsen et al., 2005) and this practice may even aid the removal of phosphorus in WWTPs (Gutierrez et al., 2010). Furthermore, significant amounts of iron (typically: 0.5–1.5 mg Fe/L, Hvitved-Jacobsen et al., 2013) can already be present in the influent of WWTPs. For instance, data from 19 WWTPs in the Waterschap Vechtstromen in The Netherlands showed influent iron concentrations between 1 and 10 mg/L resulting in an average Fe/P molar ratio of about 0.26 (unpublished data). These examples illustrate that iron is omnipresent in modern WWTPs (Table S2-2 in supporting information) and thus, that significant amounts of phosphorus can be iron bound, also in WWTPs that do not rely on iron based CPR.

The presence of iron is often perceived as negative when evaluating phosphorus recovery options (ACHS, 2009; Egle et al., 2014; Morse et al., 1998; Römer, 2006; Samie and Römer, 2001; Schipper et al., 2001; Schipper and Korving, 2009). However, we will show that phosphorus is efficiently mobilized from various iron–phosphorus compounds (FePs) in environmental systems. This apparent mismatch can be explained by the current lack of understanding of the iron and phosphorus chemistry. We will evaluate the literature that we believe is important to help understanding iron and phosphorus interactions in WWTPs. We will also present possible directions that research and technology related to phosphorus recycling from wastewater could take, as inspired by the science of environmental mobilization mechanisms.

2.3.2. Critical evaluation of current phosphorus recovery options

Currently, phosphorus recovery methods from wastewater, applied on practical scales, include the agricultural use of sludge, production of struvite in EBPR plants and recovery of phosphorus from sludge ash. After hygienisation, sludge (often termed biosolids) can be applied to agricultural land. This practice is a widespread, low-cost option for phosphorus recycling. About 50% of all sludge in the USA(Moss et al., 2013) and about 40% of all sludge in the 27 EU countries (Kelessidis and Stasinakis, 2012) was applied in agriculture in 2004 and 2005 respectively. (Kelessidis and Stasinakis 2012) Public concerns about pathogens, heavy metals, and organic micropollutants in biosolids are widespread (Aubain et al., 2002; Beecher and Harrison, 2005; Langenkamp et al., 2001; Robinson et al., 2012). But several studies showed that associated risks are low (Lu et al., 2012; Smith, 2009). Increasing regulations may further reduce concentrations of certain compounds (Oliver et al., 2005; Olofsson et al., 2012) but at the same time emerging contaminants create new concerns (Clarke and Smith, 2011). The presence of iron in biosolids lowers the water-soluble phosphorus fraction (Brandt et al., 2004; Krogstad et al., 2005; Miller and O'Connor, 2009; O'Connor et al., 2004). This can be considered positive, because it may prevent phosphorus loss by surface runoff (Elliott and

O'Connor, 2007; Lu et al., 2012). Some authors perceive the presence of iron in biosolids as negative as it resulted in a reduced plant availability of phosphorus (Kidd et al., 2007; Krogstad et al., 2005; Römer, 2006; Samie and Römer, 2001). However, other studies show iron bound phosphorus can still be plant available (Kahiluoto et al., 2015; Nanzer et al., 2014; Prochnow et al., 2008). The biggest problem of biosolid application is perhaps the fact that there are areas with surpluses of phosphorus on agricultural land due to manure surpluses (Macdonald et al., 2011; Schröder et al., 2011). Transporting sludge from such areas to areas with phosphorus deficits is problematic because of the transport costs and logistics involved. Thus, a pure and high-value phosphorus recovery product is preferred over a complex product like sludge.

Several options exist for phosphorus recovery to produce high-value products (Cornel and Schaum, 2009; Desmidt et al., 2015; Hermann, 2009; Morse et al., 1998; Petzet and Cornel, 2011). Currently, struvite precipitation is attracting the most interest despite limited phosphorus recovery potential. This technique requires a combination of EBPR and sludge digestion, ideally in combination with a phosphorus stripping process (Cullen et al., 2013). But in many countries iron based CPR plants dominate (Table S2-1 in supporting information). Furthermore, the efficiency to recover phosphorus as struvite is typically only 10–50 % of the total influent phosphorus load (Cornel and Schaum, 2009; Hermann, 2009; Lodder et al., 2011). This is due to the presence of phosphorus fractions that are not extracted during anaerobic digestion (phosphorus fixed in biomass or bound to metals like iron).

In a few countries, a significant proportion of the sludge is incinerated in mono-incinerators (Kelessidis and Stasinakis, 2012). Recovery of phosphorus from sludge ash has advantages: (1) economies of scale due to centralized incinerators, (2) nearly all phosphorus removed can be recovered, (3) destruction of unwanted compounds and (4) phosphorus is present in a concentrated form. Various promising thermo- and wet-chemical technologies have been developed to recover phosphorus from sludge ash (Adam et al., 2009; Cornel and Schaum, 2009; Desmidt et al., 2015; Donatello and Cheeseman, 2013; Hermann, 2009, 2014; Langeveld and Wolde, 2013a; Schipper et al., 2001). Iron plays a role in these technologies as well. It is influencing the extractability of phosphorus (Langeveld and Wolde, 2013a) or the water solubility of phosphorus in the final product (Adam et al., 2009). These techniques depend on expensive infrastructure for incineration. Phosphorus recovery alone will not be a sufficient reason to build sludge incinerators.

2.4. Iron as a key element in wastewater treatment plants of the future

2.4.1. A future treatment plant

The presence of iron is important in wastewater treatment already today. In the future, iron could play an even more important role in WWTPs (Figure 2-1). Adding iron is a key step in upcoming WWTPs as energy and phosphorus factories. Energy-producing WWTPs already exist (Nowak et al., 2011). Such plants often apply the A-B process, using a very high loaded biological treatment (adsorption or A-stage) followed by a bio-oxidation process or B-stage to remove nitrogen (Böhnke et al., 1997). During the A-stage, soluble chemical oxygen demand (COD) in the wastewater is used for microbial growth and (bio)flocculation removes the biomass and colloidal and particulate COD from the wastewater. Iron addition is the cheapest option for the required coagulation and flocculation of the COD and for phosphorus elimination

in the A-stage (Böhnke et al., 1997, 1997; Li, 2005). Anaerobic digestion of A-stage sludge produces a large amount of biogas (Böhnke et al., 1997). Meanwhile, the A-B process has been further improved by using anaerobic ammonium oxidation (anammox) to remove nitrogen in the side streams of several WWTPs at elevated temperatures (25–40 °C) (Abma et al., 2007; Jetten et al., 1997; Lackner et al., 2014; Nowak et al., 2015). The anammox process does not need COD for nitrogen removal while reducing the energy demand simultaneously. The use of anammox at lower temperatures of 10-20 °C (cold anammox) in the main treatment lines of WWTPs is being researched (Lotti et al., 2014). Using anammox in the main line could potentially allow a WWTP to produce energy at a net rate of 86 J/(person d). A typical WWTP, using a classical activated sludge process, consumes 158 J/(person d) (Kartal et al., 2010).

In the future WWTP (Figure 2-1), phosphorus and COD removal can be achieved by adding iron in the A-stage. Nitrogen is removed using cold anammox. The settled sludge would be digested to produce biogas and subsequently, phosphorus could be recovered from the digested sludge. Phosphorus recovery could be done by selectively bringing iron-bound phosphorus into solution using a chemical or biotechnological phosphorus recovery process that is yet to be developed. The sludge would then be dewatered and the phosphorus precipitated and recovered as struvite or apatite.

Alternatively, phosphorus could be removed using an adsorption stage after the cold anammox. Owing to environmental concerns like eutrophication, more stringent regulations on phosphorus discharge limits (Oleszkiewicz and James L. B., 2006; UK technical advisory group, 2008) may anyway require phosphorus polishing of the effluent. To achieve low phosphorus concentrations in the effluent, iron based adsorbents have already been used (Pratt et al., 2012; Ragsdale, 2007) due to the high affinity of iron oxides for ortho-phosphate (o-P) (Blaney et al., 2007; Genz et al., 2004; Martin et al., 2009). Adsorption also offers the possibility of phosphorus recovery and the re-use of the adsorbents (Loganathan et al., 2014).

Most of the wastewater treatment techniques described above are already being used or tested at the pilot scale. Currently, the only missing process (as in current treatment processes) is economically feasible phosphorus recovery from FePs-containing sludge. We envisage developing a phosphorus recovery process which is inspired by environmental mechanisms.

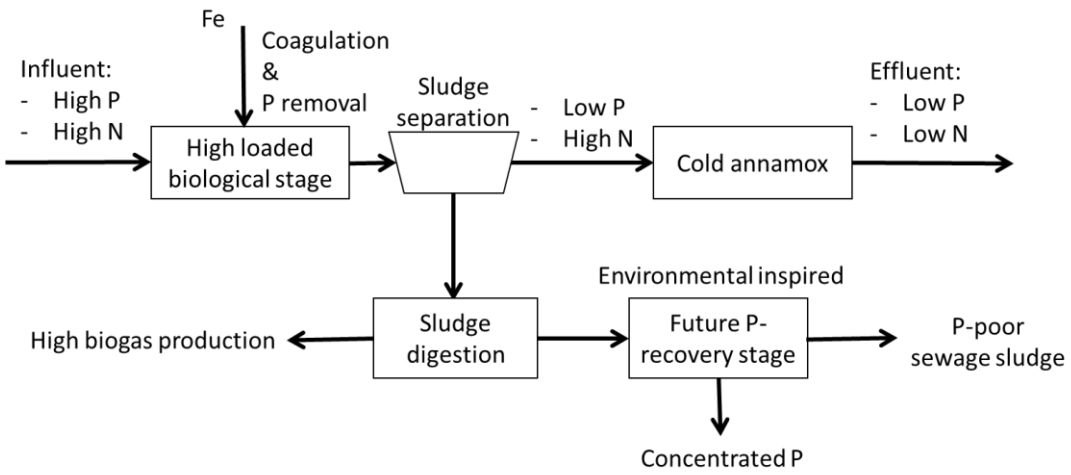


Figure 2-1: Proposed processes for an energy-producing wastewater treatment plant in which P is recovered.

2.4.2. Environmental cycling: inspiration for recovering phosphorus?

A combination of iron and phosphorus is often considered to have a negative impact when evaluating the potential for using sludge in agriculture (Römer, 2006; Samie and Römer, 2001) or phosphorus recovery (ACHS, 2009; Egle et al., 2014; Morse et al., 1998; Schipper et al., 2001; Schröder et al., 2010). Current processes for recovering phosphorus from FePs-containing sludge and ash require large changes in pH, pressure, or temperature, e.g., the Krepro, Seaborne, Mephrec, Ashdec, and Ecophos processes (Adam et al., 2009; Hermann, 2009, 2014; Langeveld and Wolde, 2013a; Levlin et al., 2002; Schipper and Korving, 2009). Usually, it is not economically feasible to use these processes. In contrast, phosphorus is mobilized very efficiently from FePs in aquatic and terrestrial ecosystems (Bolan et al., 1987; Chacon et al., 2006; Hinsinger, 2001; Roden and Edmonds, 1997). A biomimetic process could therefore be a more attractive alternative.

Fungi, bacteria, and plants are able to mobilize iron bound phosphorus and allow phosphorus cycling. The mobilization of phosphorus can be so efficient that it results in environmental damage by causing eutrophication in freshwater systems (Smolders et al., 2006). Phosphorus can be released from FePs by iron-reducing (Chacon et al., 2006; Roden and Edmonds, 1997) or sulphate reducing bacteria (Chacon et al., 2006; Roden and Edmonds, 1997; Smolders et al., 2006). Plants and fungi have developed a wide variety of strategies to access iron and phosphorus in FePs (Cardoso and Kuyper, 2006; Hinsinger, 2001). For example, excretion of carboxylate anions (such as oxalate or citrate) that chelate iron and release phosphorus (Geelhoed et al., 1999; Gerke et al., 2000), exudations of anions (e.g., bicarbonate or hydroxide) to desorb phosphorus from iron oxides (Dakora and Phillips, 2002; Gahoonia et al., 1992) or reduction of FePs (Gardner et al., 1983) and inducing pH changes to release phosphorus from FePs (Hinsinger, 2001). Mechanisms presumed to be predominantly related to the mobilization of iron, e.g., excretion of siderophores or iron reduction (Altomare et al., 1999) may also play a role in mobilizing phosphorus (Gardner et al., 1983; Reid et al., 1985). Dissolved organic matter can assist in the mobilization of phosphorus from FePs by chelating iron (Lobartini et al., 1998) or by facilitating the microbial reduction of iron (Lovley et al., 1996; Lovley et al., 1998; Peretyazhko and Sposito, 2005).

Iron plays an important role in controlling the mobilization of phosphorus in soil and sediment systems. Therefore, a great deal of research has been performed on the role of iron in the phosphorus cycle. The results show that iron and phosphorus cycling is possible, and this implies that recovering phosphorus from FePs is achievable as well. Insufficient understanding of the iron and phosphorus chemistry in WWTPs has prevented the environmental mechanisms responsible for mobilizing phosphorus from being transferred to industrial processes.

In section 2.5, we highlight the need for distinguishing between the different kinds of FePs to better understand the binding and release of phosphorus. In section 2.6, we will show that various FePs are formed and transformed during wastewater treatment processes but that little information is available on the occurrence and behaviour of these FePs. In section 2.7, we will describe the findings on the mobilization of phosphorus from FePs that could offer inspiration for the development of new phosphorus recovery technologies.

2.5. Iron and phosphorus interactions

2.5.1. Diversity of iron–phosphorus compounds

2.5.1.1. Introduction to iron–phosphorus compounds

Iron is a transition metal and its chemistry is very diverse (Cornell and Schwertmann, 2003b). It can exist in several oxidation states varying between -2 to +6 although +2 (ferrous) and +3 (ferric) are the most common oxidation states encountered. The solubility of ferrous and ferric ions vary with pH and oxidation-reduction potential (ORP) (Figure 2-2). Depending on the pH, the ferrous and ferric ions can form various insoluble oxides, oxyhydroxides and hydroxides, collectively termed iron oxides (Cornell and Schwertmann, 2003b).

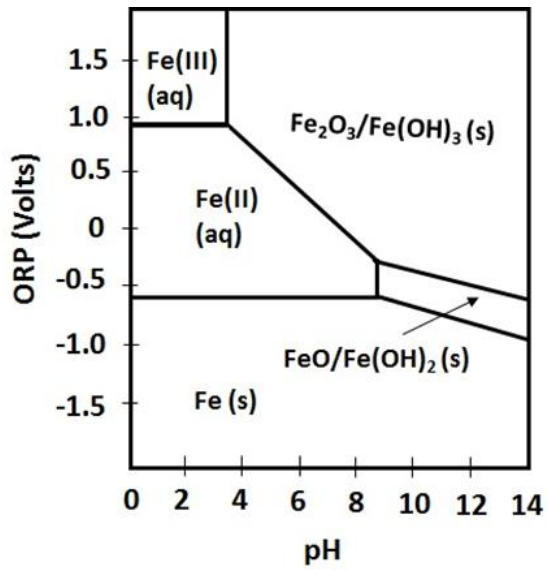


Figure 2-2: Simplified Pourbaix diagram showing the stable iron species under different conditions (modified from Tilley, 2005).

The FePs found in WWTPs can be either iron phosphate minerals or adsorption complexes which involve adsorption of o-P to iron oxides (Frossard et al., 1997; Huang and Shenker, 2004; Luedecke et al., 1989; Smith et al., 2008). Different methods to characterize FeP

interactions are listed in Table S2-3). These FePs have often not been well described. This has led to publications on the removal of phosphorus using iron or on the recovery of phosphorus from FePs often containing unspecific expressions such as “insoluble iron phosphates”, “metal phosphates”, and “iron (III) phosphates”. We will give examples which illustrate that phosphorus can be bound to iron in various ways and that the amount and strength of phosphorus bound to iron differ. This suggests that there is a range of mechanisms through which FePs can be altered resulting in phosphorus release, underlining the importance to differentiate between various FeP.

2.5.1.2. Iron oxides and their interaction with o-P

At least 16 iron oxides exist (Cornell and Schwertmann, 2003b). Prominent examples of ferric iron oxides are goethite, ferrihydrite, lepidocrocite, akaganeite, and hematite. Green rust iron oxides and magnetite are examples of iron oxides that contain both ferrous and ferric iron. The different iron oxides have different crystalline structures or are amorphous, and these structures largely determine properties such as porosity, specific surface area, the number of exposed surface sites, solubility, and reducibility. These properties, in turn, affect the o-P binding properties of the iron oxides and the bioavailability of adsorbed o-P (Barron et al., 1988; Guzman et al., 1994; McLaughlin et al., 1981; Parfitt et al., 1975; Wang et al., 2013). The surface area of the iron oxide usually correlates with its capacity to adsorb o-P (Figure S2-8 in supporting information). Amorphous or less crystalline iron oxides have higher o-P adsorption capacities than more crystalline iron oxides, and this is attributed to amorphous iron oxides having higher surface areas (Borggaard, 1983; Parfitt et al., 1975; Wang et al., 2013). o-P adsorption to iron oxides can also differ due to the type and density of surface hydroxyl groups present on the crystal faces, which are the functional groups where o-P adsorption occurs (Cornell and Schwertmann, 2003b). Hematites showed o-P adsorption capacities varying from 0.19 to 3.33 µmol/m^2 due to the differences in their crystal faces (Barron et al., 1988). In contrast, goethites showed a narrower range of o-P adsorption capacities between 2.16 to 2.83 µmol/m^2 owing to their relatively constant crystal face distribution (Torrent et al., 1990). Figure 2-3 shows the o-P adsorption capacities in different iron oxides. The o-P adsorption capacity varies within the same type of iron oxides based on the conditions under which they are synthesized and used (Barron et al., 1988; Cabrera et al., 1981; Guzman et al., 1994).

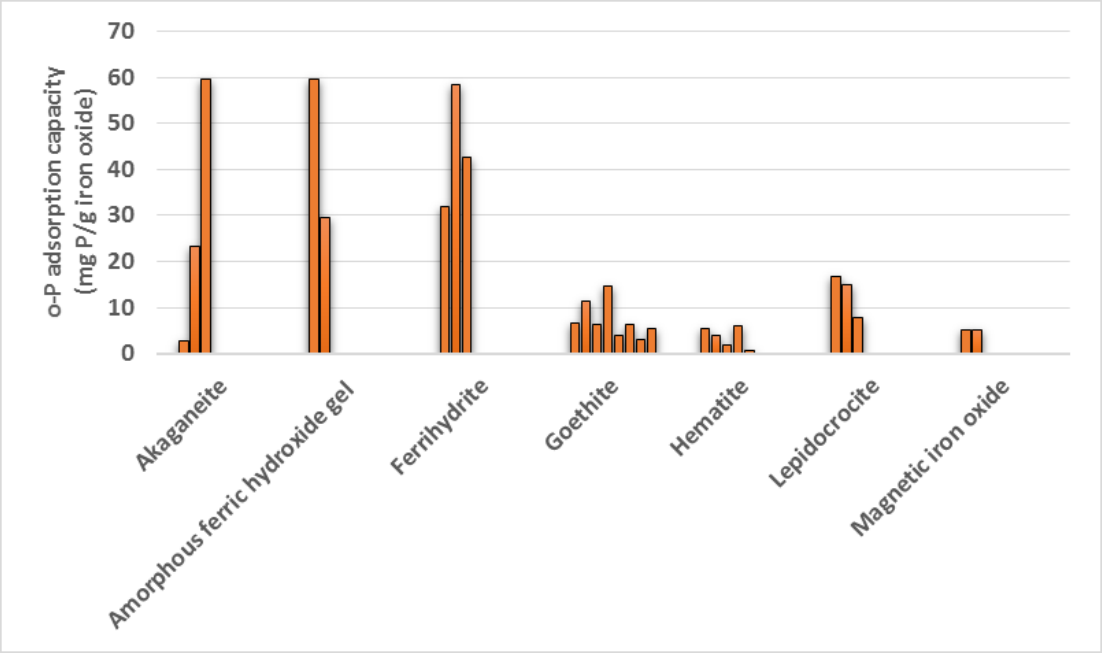


Figure 2-3: o-P adsorption capacities of different iron oxides. Details of conditions used for adsorption are presented in Table S2-4 in supporting information.

o-P adsorption onto iron oxides occurs since the iron beneath the surface hydroxyl acts as a Lewis acid and exchanges the surface OH groups for other ligands (Cornell and Schwertmann, 2003b). When o-P is bound directly to an iron oxide surface through a ligand exchange mechanism, without any water molecules between the o-P and the surface (Figure 2-4 a,b,c), the resulting complex is called an innersphere complex (Goldberg and Sposito, 1985). An innersphere complex can comprise of a single o-P molecule attached through one or two oxygen bonds (mono or bidentate respectively) with either one or two iron atoms (mono or binuclear, respectively, Sparks, 2003). The type of complex formed determines the relative strength at which the o-P is bound. Bidentate complexes have more stable structures than monodentate complexes, which implies that it could be easier to release o-P from monodentate than from bidentate complexes (Abdala et al., 2015).(Abdala et al. 2015a) The types of innersphere complexes differ based on the type of iron oxides and the conditions such as the pH and the initial o-P concentration (Abdala et al., 2015; Arai and Sparks, 2001; Goldberg and Sposito, 1985). Thus, o-P adsorption and desorption properties vary for different iron oxides and for the conditions where the iron oxides are produced and used. This makes adsorption a very versatile process and offers the possibility of engineering specific adsorbents based on iron oxides.

Adsorption is not the only interaction that occurs between o-P and iron oxides. It is possible to have surface precipitation (Figure 2-4 e), which is the formation of three-dimensional entities as opposed to the two-dimensional monolayer coverage during adsorption (Davis and Hayes, 1987; Sparks, 2003). Surface precipitation can lead to the formation of a solid phase from which phosphorus is less readily desorbed because the phosphorus buried in the surface precipitate is no longer in equilibrium with the solution (Li and Stanforth, 2000a). The dissolution of iron from the iron oxide contributes to the formation of the surface precipitate (Jonasson et al., 1988; Li and Stanforth, 2000a). For instance, nano zero-valent iron (nZVI)

particles were shown to have very high o-P adsorption capacities (245 mg P/g) even though their surface area (27.6 m^2/g) was not very high (Wen et al., 2014). This high capacity to remove o-P was explained as being partly caused by the occurrence of precipitation, which was facilitated by the dissolution of iron from the nZVI particles. The initial o-P concentration in the solution influences the type of binding with iron oxide by determining the surface coverage of o-P. Surface complexation tends to dominate at low surface coverages, and surface precipitation becomes dominant as the surface loading increases (Li and Stanforth, 2000a; Sparks, 2003). At a high surface coverage with o-P, goethite and strengite (an iron phosphate mineral) have similar points of zero charge (PZC), suggesting that surface precipitation occurred on goethite (Li and Stanforth, 2000a).

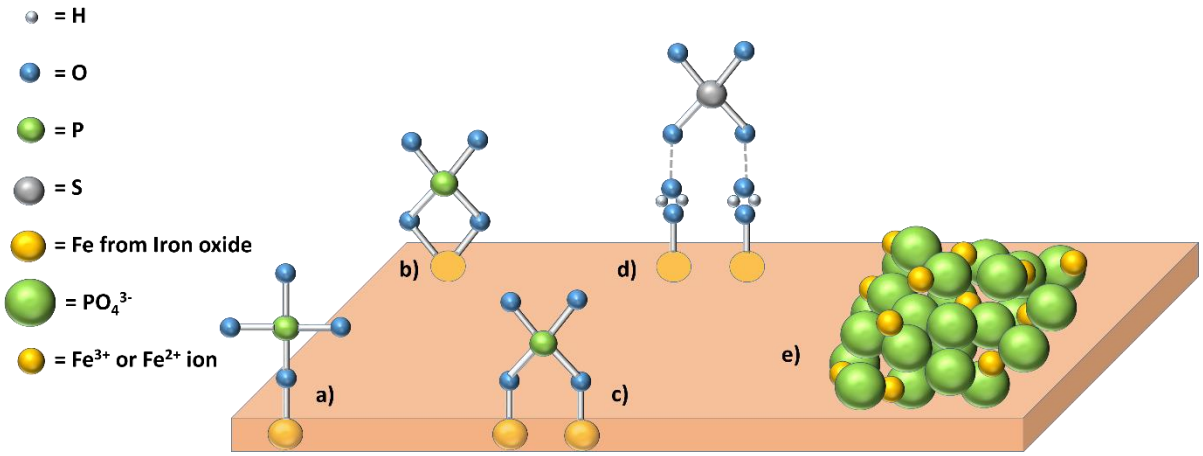


Figure 2-4: Anion binding onto iron oxides. o-P adsorbed as innersphere complexes (Abdala et al., 2015; Arai and Sparks, 2001; Parfitt and Atkinson, 1976): a) mononuclear monodentate b) mononuclear bidentate c) binuclear bidentate. Sulphate adsorption is shown as an example for d) outersphere complex in which water molecules are present between the iron oxide surface and the sulphate (Peak et al., 1999) e) example of surface precipitation in which dissolved iron from the iron oxide surface contributes to the formation of multiple layers of FeP precipitates (Li and Stanforth, 2000a) on the surface of the iron oxide.

2.5.1.3. Iron phosphate minerals

Iron phosphate minerals are polyatomic complexes of iron and phosphate (Moore, 1969, 1970; Stoch et al., 2014). Unlike adsorption complexes where o-P is removed from solution by binding on the surface of a solid (e.g. iron oxide, Sparks, 2003), iron phosphate minerals are usually formed in the presence of o-P and dissolved iron (Bache, 1964; Ming et al., 2011; Roldan et al., 2002). However, the exact mechanisms involved in the formation of iron phosphate precipitates can be complex (Lente et al., 2000; Luedecke et al., 1989). Vivianite ($Fe_3(II)[PO_4]_2 \cdot 8H_2O$) and strengite ($Fe(III)[PO_4] \cdot 2H_2O$) are the common examples of iron phosphate minerals, although there exist several others like lipscombite ($Fe(II)(Fe(III))_2(PO_4)_2(OH)_2$), beraunite ($Fe(II)(Fe(III))_5[(PO_4)_4|(OH)_5] \cdot 6H_2O$) and rockbridgeite ($Fe(II)(Fe(III))_4(PO_4)_3(OH)_5$ (Moore, 1970). The stability of different iron phosphate minerals varies in terms of their formation and solubility with respect to pH and redox conditions (Nriagu and Dell, 1974) which in turn might have implications on the

phosphorus release from these compounds. Vivianite has been found in WWTPs and its formation and role in recovering phosphorus from wastewater will be discussed in detail in later sections.

2.5.2. Iron–Phosphorus compounds in wastewater treatment processes

2.5.2.1. Introduction to chemical phosphorus removal using iron salts

Among other reasons, iron salts are added to wastewater to remove phosphorus (Thomas, 1965; WEF, 2011). The efficiency at which phosphorus is removed in a WWTP by adding iron is influenced by the oxygen concentration (for ferrous salts), the concentrations of competing ions, the presence of organic matter, the pH, the alkalinity, mixing, the age of the iron or iron oxide flocs, the type of phosphorus present, and whether ferric or ferrous iron salts are used (WEF, 2011). FePs are exposed to dramatic changes in ORP and temperature over a period of about one month in a WWTP with an anaerobic digestion process. The following examples will show that adsorption, mineral formation, and recrystallization may occur at different stages in a WWTP (Figure 2-5).

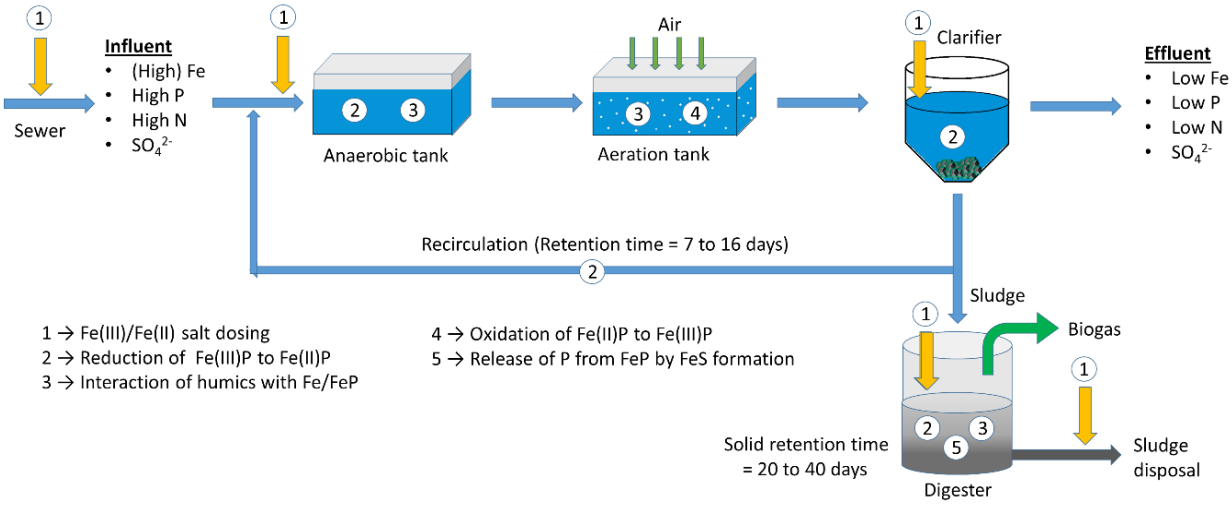


Figure 2-5: WWTP schematic highlighting possible iron and phosphorus interactions at different stages. Iron can be dosed at various stages for reasons like sulphide removal, phosphorus removal, flocculation and to facilitate dewatering of sludge.

2.5.2.2. Dosing ferric versus ferrous iron salts

The exact mechanisms through which ferric or ferrous iron salts initially remove phosphorus are not yet understood. The hydrolysis of ferric iron in an aqueous solution is usually very rapid (Wendt von, 1973). It has been suggested that the adsorption of o-P onto iron oxides is an important (Luedecke et al., 1989; Recht and Ghassemi, 1970a) or even the major mechanism (Smith et al., 2008; Szabo et al., 2008)(Smith et al. 2008, Szabó et al. 2008) involved in the removal of o-P from wastewater when ferric iron salts are dosed.

The situation is even more complex when ferrous iron is added because this can be partly or fully oxidized to ferric iron. The ferrous salts are usually added to aerated stages of the WWTP to allow oxidation to ferric iron. The kinetics of ferrous iron oxidation strongly depend on the oxygen concentration and particularly on the pH (Stumm and Morgan, 1996). Half of the

ferrous iron in water containing 5 mg/L dissolved oxygen has been found to be oxidized to ferric iron within 45 minutes at pH 7 and within 0.5 minutes at pH 8 (Ghassemi and Recht, 1971; Singer and Stumm, 1969). The presence of other ions (e.g., sulphate or o-P) or dissolved organic matter can considerably influence the oxidation kinetics (Pham et al., 2004; Stumm and Morgan, 1996; Theis and Singer, 1974). The kinetics of ferrous iron oxidation and hydrolysis in wastewater are not well established. In a WWTP, about 40 % of the ferrous iron that was added was found to be rapidly oxidized to ferric iron at relatively high pH 8.2 and dissolved oxygen concentration of 4.6 mg/L (Thistleton et al., 2001). Similarly, half of the ferrous iron in activated sludge could be oxidized within minutes but about 10 % of the ferrous iron fraction was not oxidized even after 6 days of aeration (Nielsen, 1996). Measurements on sludge taken from the aeration tank of a WWTP in which ferrous iron was used to remove phosphorus suggest that most of the iron in the sludge was ferric iron (Rasmussen and Nielsen, 1996). In contrast, 43 % of the total iron in activated sludge before anaerobic digestion was found in the form of the ferrous iron phosphate mineral vivianite (Frossard et al., 1997). This data indicates either an extensive reduction of ferric iron during wastewater treatment or incomplete oxidation of the ferrous iron that has been added to the aerated tanks. However, also in the absence of oxygen, o-P could be removed with a ferrous Fe:P molar ratio of 1.5 in batch tests using secondary effluents, a maximum o-P removal efficiency (98 %) was found at pH 8 (Ghassemi and Recht, 1971). It has been suggested that the removal of phosphorus can be made more efficient if ferrous iron is slowly oxidized in situ (Ghassemi and Recht, 1971; Leckie and Stumm, 1970; Svanks, 1971).

2.5.2.3. Vivianite formation in wastewater treatment plants

During wastewater treatment, initially formed FePs may change because of exposure to different ORPs and, therefore, to different microbial and chemical processes (Frossard et al., 1997; Nielsen, 1996; Nielsen et al., 2005; Rasmussen et al., 1994; Rasmussen and Nielsen, 1996). Vivianite can be formed when ferrous iron is added to remove phosphorus (Frossard et al., 1997; Ghassemi and Recht, 1971; Singer, 1972). Mössbauer spectroscopy, scanning electron microscopy (SEM), and X-ray diffraction (XRD) analyses, showed that 43 % of the iron in activated sludge from a WWTP in which ferrous sulphate was used to remove phosphorus, and 60–67 % of the iron in the digested sludge was bound in vivianite (Frossard et al., 1997). Vivianite is sparingly soluble in water ($K_{sp} = 10^{-36}$), and it is stable in the absence of oxygen, at pH 6–9, under non-sulphidic conditions, and in the presence of high ferrous iron and o-P concentrations (Nriagu, 1972). In WWTPs in which ferric salts are used to remove phosphorus or in WWTPs which apply different treatment strategies (e.g., the A-B process), it is not known whether vivianite forms or not and if so to what degree. The microbial reduction of ferric iron in anaerobic treatment stages could initially lead to phosphorus release from FePs (Nielsen, 1996; Rasmussen and Nielsen, 1996). However, the reduced iron could ultimately act as a phosphorus sink by forming vivianite, which has a higher phosphorus content (Fe:P molar ratio of 1.5) than ferric FeP precipitates found in experiments with wastewater (Fe:P molar ratio of 2.5, Luedecke et al., 1989). The formation of ferric phosphate minerals like strengite (Fe:P molar ratio of 1) does not seem to play a significant role in WWTPs. In WWTPs strengite and lipscombite in iron stabilized digested sludge were found after high iron dosing (Fe:P of

6.15) only (Huang and Shenker, 2004). Hence, the formation of vivianite could be the final mechanism for the retention of phosphorus in WWTPs.

2.6. Transforming iron–phosphorus compounds

2.6.1. Oxidizing and reducing conditions

2.6.1.1. Introduction

Iron plays an important role in retaining phosphorus in soil and sediments because of the formation of FePs (Figure 2-6) (Cornell and Schwertmann, 2003b; Froelich, 1988; Schulz and Zabel, 2006; Sundareshwar and Morris, 1999). The mobilization and retention of phosphorus from FePs in these systems, in response to changes of ORPs, is well documented (Caraco et al., 1989; Roden and Edmonds, 1997; Smolders et al., 2006). Similar processes could also occur in WWTPs.

WWTPs require a large range of ORPs to allow different microbial processes to take place. The ORPs in a WWTP will range from less than −300 mV, during anaerobic digestion or the anaerobic period of an EBPR process, to more than +200 mV during the nitrification process. Here, microbial and chemical processes can take place that alter FePs by oxidizing or reducing the iron or by replacing the phosphorus with sulphide or other ions. These modifications can affect the phosphorus removal performance and other parameters, such as the dewaterability of the sludge (Nielsen, 1996). Nevertheless, iron speciation in response to varying ORPs in WWTPs has not received much attention. In a potential phosphorus recovery process, exposing FePs to ORPs that anyway occur in WWTP, could assist in phosphorus mobilization. For instance, at low ORPs iron reducing or sulphate reducing bacteria could mobilize iron bound phosphorus. On the other hand, oxidation can mobilize phosphorus bound in vivianite. The chemical or biological processes that could mobilize phosphorus from FePs could be facilitated by the presence of dissolved organic matter. In this section, we give a short overview on how ORPs can influence phosphorus binding to iron. We will show that changes in the ORPs in both, positive and negative ranges and subsequent changes in microbial processes can assist in either retaining or mobilizing phosphorus from FePs.

2.6.1.2. Iron reduction and iron oxidation

The chemical or biological reductive dissolution of ferric iron can cause iron-bound phosphorus to be released. In general, dissimilatory iron-reducing bacteria are widespread in soil and sediment systems (Lovley et al., 1991a; Lovley, 1997; Weber et al., 2006). These organisms reduce ferric iron in iron oxides or iron phosphate minerals, thereby mobilizing phosphorus (Heiberg et al., 2012; Patrick et al., 1973; Peretyazhko and Sposito, 2005). However, in the absence of sulphate, ferrous iron compounds were formed that bound most of the released phosphorus (Borch and Fendorf, 2007; Roden and Edmonds, 1997). The reducibility of an iron oxide depends on its crystal structure, solubility, and surface area (Bonneville et al., 2009; Larsen and Postma, 2001). Crystalline iron oxides with low surface area (e.g., goethite and hematite) and low solubility are usually less accessible to iron-reducing organisms than amorphous iron oxides, e.g., lepidocrocite and ferrihydrite (Bonneville et al., 2009; Cheng et al., 2015; Munch and Ottow, J. C. G., 1983).

Once formed, ferrous iron can precipitate as secondary iron oxides (e.g., magnetite or green rust) or as ferrous iron phosphate minerals (e.g., vivianite, Weber et al., 2006). In the presence of electron acceptors (e.g., oxygen or nitrate), dissolved or solid ferrous iron compounds may be oxidized. Biogenic iron oxides that can be formed in the presence of iron-oxidizing bacteria include goethite, magnetite, ferrihydrite, and green rust (Weber et al., 2006). Biogenic iron oxides are often amorphous and nanocrystalline (Fortin and Langley, 2005) and thus showed high o-P binding capacities (Rentz et al., 2009). Biologically formed iron oxides can contain organic matter, which disrupts the crystallization process (Cornell and Schwertmann, 2003b; Posth et al., 2014) and makes the iron more accessible and therefore more easily reduced. This reduction process might be assisted by humic substances (Piepenbrock et al., 2014a; Piepenbrock et al., 2014b).

It has been shown that iron-reducing and iron-oxidizing bacteria are very active in WWTPs (Nielsen, 1996; Rasmussen et al., 1994; Rasmussen and Nielsen, 1996). Reduction (presumably enzymatic) of iron has been measured in activated sludge immediately after storage under anaerobic conditions. The ferrous iron produced stayed mainly within the organic matrix of the sludge despite humic substances showing lower affinity to ferrous than ferric iron (Rasmussen and Nielsen, 1996; Stevenson, 1994). The authors hypothesized that the reduction of iron can cause significant phosphorus release from sludge under anaerobic conditions in WWTPs. However, the formation of secondary ferrous iron oxides or vivianite that can bind phosphorus was not taken into account. It has also been shown that the microbial oxidation of ferrous iron in activated sludge using nitrate as an electron acceptor plays a significant role in the denitrification stage in WWTPs (Nielsen, 1996). The authors hypothesized that this anoxic oxidation of ferrous iron could improve sludge dewatering and phosphorus retention. The kinetics of iron oxidation and reduction and the transformation of iron, that is cycled through treatment stages with high and low ORPs, have not been determined yet. Thus, it is not known whether ferrous or ferric, crystalline or amorphous, biogenic or chemogenic iron compounds dominate at different stages of a WWTP. Humic substances also play a role in the redox chemistry of iron. This will be discussed in section 2.6.2.

2.6.1.3. Sulphide and iron–phosphorus compounds

Sulphide can reduce ferric iron compounds (Poulton et al., 2004) and can further react to form various iron sulphide compounds (FeSs) (Morse et al., 1987). It has been hypothesized that this could be the main mechanism through which iron bound phosphorus is released from sediments (Caraco et al., 1989; Roden and Edmonds, 1997; Smolders et al., 2006). The reactivity of an iron oxide toward sulphide (as for iron-reducing bacteria) depends on the crystallinity of the iron oxide (Canfield 1989, Poulton et al. 2004). Reaction times have been found to range from minutes for poorly crystalline iron oxides (e.g., hydrous ferric oxide, ferrihydrite, and lepidocrocite) to days or years for more crystalline iron oxides (e.g., hematite and goethite) (Canfield, 1989; Poulton et al., 2004). The presence of o-P can decrease the reductive dissolution of different iron oxides by sulphide via formation of binculear innersphere complexes (Biber et al., 1994; Stumm, 1997; Yao and Millero, 1996).

Sulphide has already been used to solubilize phosphorus selectively from FePs containing sludge for phosphorus recovery. Sulphide released 75 % of the solid phosphorus into solution

at pH 4 from sludge collected at a water production plant (Likosova et al., 2013). Similarly, 43 % of the total solid phosphorus was found to be released from sludge pre-coagulated with iron by adding sulphide (Kato et al., 2006). In another study, iron sulphate was added to precipitate phosphorus in sludge liquor and the microbial reduction of the added sulphate produced sulphide (Suschka et al., 2001). Subsequently, phosphorus was released (1.5 moles of sulphide released about one mol o-P) over a timescale of days, without gaseous hydrogen sulphide formation.

To our knowledge, it is not known if sulphide induced phosphorus release is influenced by the type of FeP. However, analogous to the difference in reactivity of sulphide to iron oxides, it is likely that the amount of sulphide required to release phosphorus from FePs with different crystal structure varies.

2.6.1.4. Transforming vivianite

Vivianite could be an important ferrous iron phosphate compound in WWTPs (see section 2.5.2.3). Transformation of vivianite by oxidation or by exposing it to sulphide can induce phosphorus release. Chemically, about 5–10 % of the ferrous iron in freshly synthesized vivianite has been found to oxidize within minutes when exposed to air and about two-thirds of the ferrous iron was oxidized after air bubbling for 53 days (Roldan et al., 2002). In this study, oxidation occurred in the presence of a phosphorus sink (an anion exchange membrane). The initial Fe:P ratio (determined by energy dispersive X-ray spectrometry (EDX)) was 1.4 and the final Fe:P ratio was around 6.2. The complete oxidation of vivianite and the formation of an amorphous iron phosphorus compound was much faster (16 days) when the oxidation was microbially induced (Miot et al., 2009). No phosphorus sink was present, but the Fe:P ratio (determined by EDX) increased from 1.3 (vivianite) to 2.8. Due to these properties, vivianite has been used as a slow release iron and phosphorus fertilizer (Diaz et al., 2009; Eynard et al., 1992; Roldan et al., 2002). Accordingly, vivianite may recrystallize when sludge is exposed to air resulting in phosphorus release.

During anaerobic digestion, substantial sulphide formation by sulphate reducing bacteria would most likely result in the release of significant amounts of iron-bound phosphorus, as reported for anoxic sediments (Smolders et al., 2006). The formation of vivianite during anaerobic digestion is not hampered by FeSs formation since the supply of sulphate is limited in digesters (Chen et al., 2008; van den Brand et al., 2014, Nriagu 1972) When considering the recovery of phosphorus from sludge by sulphide, the crystallinity of vivianite should be taken into account. Vivianite could be rather insensitive to sulphide, similar to more crystalline iron oxides (Canfield, 1989; Poulton et al., 2004).

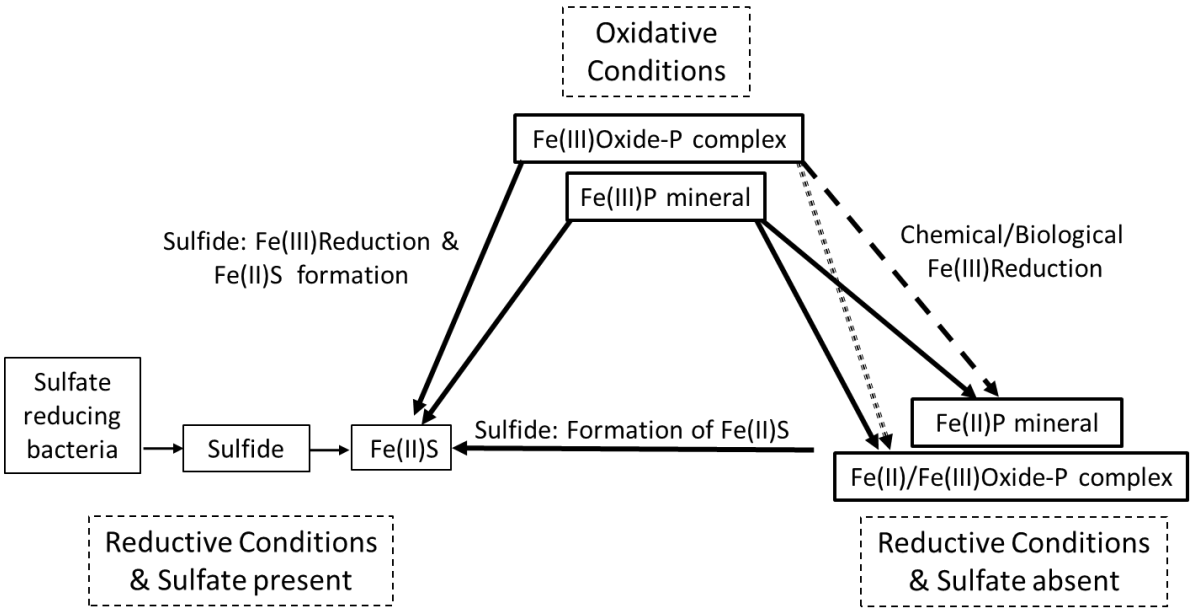


Figure 2-6: Redox processes and the cycling of phosphorus. The arrow keys represent the effect on soluble phosphorus: ⟶ implies phosphorus release, ⟶ implies phosphorus sink, ⟶ implies not clear.

2.6.2. Humic substances

2.6.2.1. Introduction

Organic matter contributes 40–80 wt. % of the total solids in sludge (Tchobanoglous et al., 2013). Organic matter, like humic substances, plays an important role in iron and phosphorus cycling in soil and aquatic systems. Humic substances have received attention because of their omnipresence and relevance to iron and phosphorus chemistry. Humic substances include humic acids, fulvic acids, and humins (Stevenson, 1994). These are relatively large, refractory and complex molecules that are products of organic matter degradation. Humic substances lack well-defined compositions but usually contain large numbers of oxygen-containing functional groups, such as carboxyl and hydroxyl groups (Stevenson, 1994). This characteristic explains some of their interactions with iron and phosphorus. Humic substances contributed about 20 % of the total dissolved organic carbon in the secondary effluent (Frimmel, 1999) and 10–20 % of the total organic carbon in sludge dry matter (Riffaldi et al., 1982). It has been estimated that 22 % of the iron in activated sludge could be bound to organic matter (Rasmussen and Nielsen, 1996). Accordingly, pyrophosphate extractions showed that approximately 30 % of iron in digested sludge could be bound to organic matter (Carliell-Marquet et al., 2009; Ito et al., 2000) Since humic substances are present in abundance in WWTPs, they can considerably affect iron and phosphorus speciation. Hence, their effects need to be considered during research on phosphorus recovery processes from wastewater. Especially, since the effect of humic substances on FePs has shown controversial results (Figure 2-7). In the next section, we will briefly discuss how humic substances interact with iron and the various ways in which they can affect iron and phosphorus interaction.

2.6.2.2. Humic substances interaction with iron and phosphorus

The bond between iron and humic molecules is relatively strong and can prevent the hydrolysis and polymerization of iron (Karlsson and Persson, 2012). Mössbauer spectroscopy (Schwertmann et al., 2005) and synchrotron-based spectroscopy (Karlsson and Persson, 2012) have indicated that ferric iron can occur as oxides and non-oxides together with organic matter. It has also been shown that different bonds between iron and humic substances have different strengths (Senesi et al., 1989) and that mononuclear and polymeric iron humic complexes occur (Karlsson and Persson, 2010, 2012; Morris and Hesterberg, 2012). The type of complex formed influences iron speciation, and the processes that lead to the different species being formed include iron hydrolysis, polymerization, and the binding of arsenate, which has similar structure and reactivity as o-P (Karlsson and Persson, 2012; Mikutta and Kretzschmar, 2011; Puccia et al., 2009; Sjöstedt et al., 2013).

The presence of humic substances decreased the o-P adsorption capacity of goethite (Antelo et al., 2007; Fu et al., 2013; Sibanda and Young, 1986). It has also been suggested that humic substances have either limited or positive effects on the binding of o-P to iron (Borggaard et al., 2005; Gerke, 2010b; Gerke and Hermann, 1992). It has been hypothesized that the o-P adsorption capacity of iron could increase because of the formation of iron–humic–phosphorus complexes (Gerke, 2010b; Weir and Soper, 1963). Such complexes have been found to have about eight times higher o-P adsorption capacities than pure iron oxide phases (Gerke and Hermann, 1992). This could be due to the iron being finely distributed on the organic surfaces (Gerke and Hermann, 1992). In studies using Mössbauer spectroscopy, it has been confirmed that iron oxides can be evenly distributed over the surfaces of humic compounds (Sorkina et al., 2014). Yet, to the best of our knowledge, there is no direct proof for the existence of such iron–humic–phosphorus complexes. However, the binding of arsenic by humic–iron compounds has been proven using extended X-ray absorption fine structure analyses (Mikutta and Kretzschmar, 2011).

The presence of humic substances could increase the o-P adsorption capacity of iron oxides by preventing crystallization of amorphous iron oxides (Gerke, 1993; Schwertmann, 1966, 1970; Schwertmann et al., 2005). However, it has also been shown that organic matter does not have a significant influence on the crystallization of iron oxides and does not affect the adsorption of phosphorus (Borggaard et al., 1990). Ferrous iron can be bound by humic substances, influencing oxidation properties of ferrous iron, the crystallization of iron oxides, and the bioavailability of ferrous iron (Catrouillet et al., 2014; Pédrot et al., 2011). It has been found that humic substances can dissolve phosphorus by chelating iron from ferric FePs (Lobartini et al., 1998). Ferric iron can be kept in solution when it has been complexed with humic acids and may, in that state, bind o-P (Gerke, 2010b; Karlsson and Persson, 2012; Weir and Soper, 1963)

Iron-reducing bacteria can use humic substances as electron acceptors during the oxidation of organic compounds (Lovley et al., 1996). The rate at which iron is reduced may be increased by the presence of humic substances and usually inaccessible iron oxides may be made available (Lovley et al., 1998). The ability of humic substances to transfer or shuttle electrons to ferric iron has led to the hypothesis that even fermenting bacteria, sulphate-reducing bacteria,

or methanogens could reduce ferric iron (Kappler et al., 2004; Piepenbrock et al., 2014a; Piepenbrock et al., 2014b). When humic substances act as electron acceptors, they can be restored after exposure to oxygen (Klüpfel et al., 2014). Figure 2-7 summarizes the possible effect of humics on iron and phosphorus interactions.

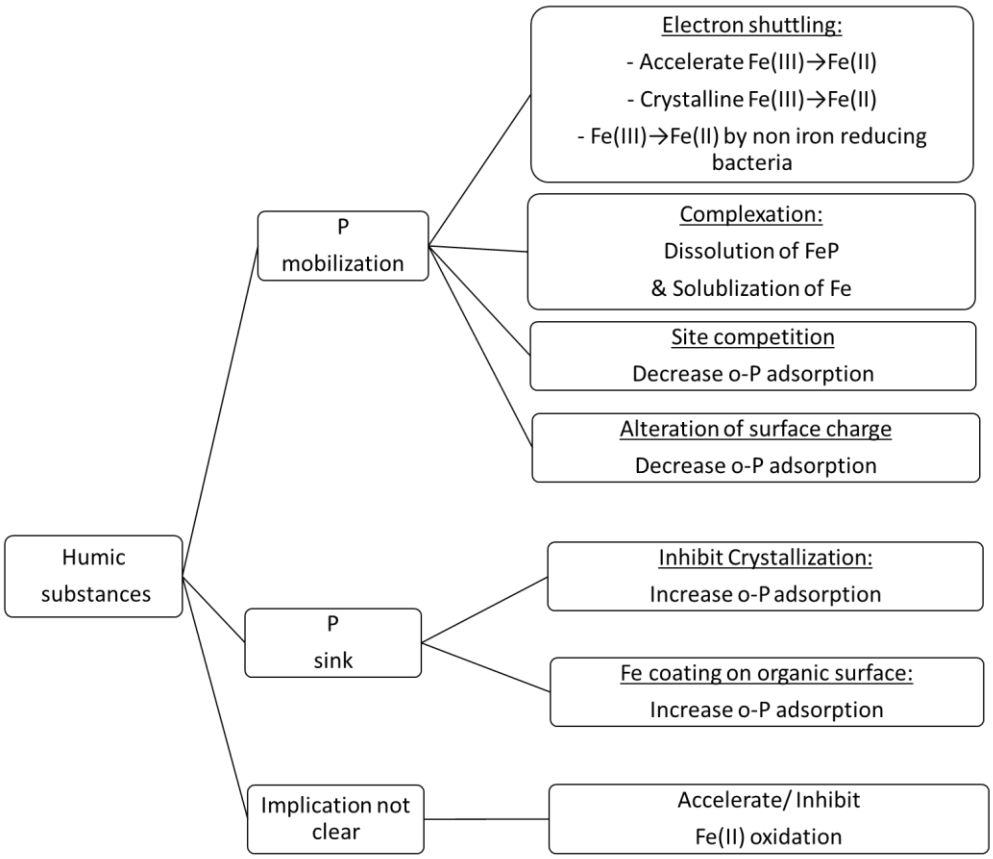


Figure 2-7: Effect of humic substances on iron and phosphorus interaction

2.6.3. The effect of pH

2.6.3.1. Introduction

The pH can have a considerable effect on iron and phosphorus interactions since it affects several factors like the speciation of o-P, the surface charge of iron oxides and the solubility of iron oxides and iron phosphate minerals. We will discuss the effect of pH on iron and phosphorus interactions in two contexts. Firstly, the effect of pH on the adsorption of o-P on and the desorption of o-P from iron oxides respectively. This will be followed by a short discussion on existing techniques to recover phosphorus from FePs in sludge to show controversial experiences that have been made in these studies.

2.6.3.2. Desorption of o-P from iron oxides

The surface potential of the adsorbent, as well as the o-P, becomes more negative as the pH increases (Stumm et al., 1992). Beyond the PZC of the iron oxide, electrostatic repulsion leads to a decrease in o-P adsorption (Yoon et al., 2014). Furthermore, an increase in pH increases the hydroxide ion concentration, which results in o-P desorption. The hydroxide ion is the hardest Lewis base among the common inorganic ions, so it is an effective reagent for desorption (Awual et al., 2011). Desorption of o-P from iron oxides has been studied somewhat less than adsorption. Not all of the adsorbed o-P is easily released by competing ions (Cabrera et al., 1981; Torrent et al., 1990). The proportion of the adsorbate ion that is not easily desorbed could be explained by the formation of surface precipitates, the slow restructuring of the solid, or diffusion limitations related to the porosities of the iron oxides (Cabrera et al., 1981; Chitrakar et al., 2006; Davis and Hayes, 1987; Li and Stanforth, 2000a). XRD measurements have shown that the crystallinity of goethite increased after one adsorption-desorption cycle (with NaOH), and this affected o-P adsorption negatively (Chitrakar et al., 2006). However, no change in crystallinity and reusability (after 10 cycles) was observed after desorption using akaganeite (Chitrakar et al., 2006).

2.6.3.3. Inducing pH changes to recover phosphorus

Wastewater and sludge are usually at pH 6–8 in WWTPs (Tchobanoglous et al., 2013) but much higher or lower pH is applied in some processes to recover phosphorus. It has been suggested that at pH 13, phosphorus may be released from FePs containing sludge using a microbial electrolysis cell (Fischer et al., 2011; Fischer et al., 2015). Phosphorus extraction from FePs containing sludge, taken from a WWTP using iron electrolysis for phosphorus removal, was more selective and greater in alkaline conditions compared to acidic conditions, 92 compared to 70 % of total phosphorus extracted (Sano et al., 2012). In other studies, relatively little phosphorus was released under alkaline extraction conditions from FePs containing sludge (13 % extracted at pH 13) (Maier et al., 2005) and iron-rich sludge ash (3–28 % extracted using 1 M NaOH) (Cornel et al., 2004). These contradictory results further underline the importance of characterizing FePs. The re-precipitation of released phosphorus (as calcium or magnesium phosphorus compounds) could influence its net release. Strong acidification will dissolve and release phosphorus from iron oxides and iron phosphate minerals thereby mobilizing most of the phosphorus in sludge and ash samples (Atienza–Martínez et al., 2014; Biswas et al., 2009; Maier et al., 2005; Petzet et al., 2012; Pinnekamp et al., 2011). Acidification is part of current phosphorus recovery techniques (such as Ecophos, ICL, PHONAX, Seaborne, and Recophos) but can also bring heavy metals and other metals into solution.

2.7. Approaches to recover phosphorus from iron

Future energy producing WWTPs will rely on the removal of phosphorus and COD by iron addition. An economically feasible process for recovering phosphorus from FePs does not yet exist. Many different FePs may be formed in WWTPs because of the wide range of microbial

and chemical processes that occur. The development of processes for recovering phosphorus from FePs demands more research, especially on iron and phosphorus interactions in WWTPs. The generated knowledge will help to identify the best stages for introducing phosphorus recovery processes and will prepare a base for additional focused research. Furthermore, this research will help to better understand and to improve wastewater treatment processes in general. For instance, it may be possible to induce the formation of a specific FeP from which phosphorus is easily extractable. A wide range of processes for releasing phosphorus from FePs in nature exist, these processes depend also on the types of FePs present. The most relevant mechanisms are summarized below:

- The reduction of iron may trigger initial phosphorus release from ferric FePs, but the vivianite subsequently formed can act as a net phosphorus sink. In contrast, the oxidation of iron may cause a net release of phosphorus bound in vivianite. Biological and chemical oxidation and reduction of FePs occur in WWTPs. The use of these processes to develop a phosphorus recovery process remains to be addressed.

- Microbial reduction and oxidation of iron plays an important role in the binding and release of phosphorus. Different iron compounds have different availabilities to the microbes that are responsible for the oxidation or reduction of the iron. These processes may be facilitated (e.g. by the presence of humic substances) or hampered by other parameters (e.g. by the crystal structure of the ferric FePs).

- Sulphide selectively releases phosphorus bound to ferric and ferrous FePs. Sulphide is formed to a limited extent during anaerobic digestion of sludge. However, further stimulation of sulphate reducing activity (e.g. after anaerobic digestion) would require COD input and would reduce the net energy yield of the WWTP. Additionally, sulphide is corrosive and toxic. Therefore, although sulphide addition could be useful to recover phosphorus, the dosing of sulphide needs to be optimized and economic feasibility needs to be considered as well. The reaction mechanisms between sulphide and FePs and the type of FeP in WWTPs have to be investigated in detail to evaluate the potential of sulphide for phosphorus recovery from FePs.

- Under very alkaline or acidic conditions phosphorus is released from most FePs. However, contradictory results have been found under alkaline conditions, suggesting that the release depends on the types of FePs that are present in sludge.

- The presence of high concentrations of organic matter in WWTPs complicates the iron and phosphorus chemistry involved. The role of organic matter in the iron and phosphorus biogeochemistry is not clear. It can, however, be assumed that it significantly influences iron and phosphorus speciation in WWTPs. Thus, organic matter should be included in future research on the development of a biomimetic process to recover phosphorus from FePs.

- Another approach for recovering phosphorus is to simplify the complex FePs interactions by engineering iron-based adsorbents. Iron-based adsorbents are already used to remove phosphorus from WWTP effluent. The regeneration of these adsorbents could be an effective approach for phosphorus recovery. Currently, this aspect receives

insufficient attention. The diversity of FePs chemistry can be used to influence the binding and release characteristics of phosphorus, for example, by varying the crystallinity, pore size distribution or surface area of the iron oxide based adsorbent.

We believe that a process for recovering phosphorus using iron should be developed in two steps. First, suitable FePs should be identified and characterized. Second, specific tools for mobilizing phosphorus from these compounds should be identified. Developing a biomimetic process to recover phosphorus from FePs would be an important step towards WWTPs acting as energy and nutrient factories.

2.8. Supplementary Information

2.8.1. Tables

Table S2-1: Enhanced phosphorus removal methods used in some northern European countries (EBPR = enhanced biological phosphorus removal, CPR = chemical phosphorus removal)

Country	Type of weighting	No tertiary treatment	Mostly EBPR	EBPR with CPR support	CPR	Reference
Germany	People equivalents	2%	6%	31%	61%	DWA, 2005
	No. of plants	20%	16%	21%	43%	DWA, 2005
Netherlands	Sludge production	4%	13%	51%	32%	Korving, 2012
United Kingdom	People equivalents	no data	5%	no data	95%	Carliell-Marquet, 2014
	No. of plants	no data	23%	no data	77%	Carliell-Marquet, 2014
France	No. of plants	no data	17%	36%	47%	Paul et al., 2001

Table S2-2: Iron concentrations that have been found in sewage sludge (in g/kg on a total solids basis)

Country	Lowest Fe concentration	Highest Fe concentration	Average Fe concentration	Comments and reference
Germany	-	-	50	Average of 202 sludge samples (DWA, 2005)
Sweden	4.4	150	49	Based on 47 sludge samples (Eriksson, 2001)
Netherlands	-	-	31	Average of 28 % of Dutch sewage sludge (Schipper and Korving, 2009)

United States	1.6	299	-	Based on 84 biosolid samples (USEPA, 2009)
United States	3.8	84	-	Based on 41 biosolid samples (Brandt et al., 2004)

Table S2-3: Methods used for characterizing iron oxides and FeP interactions

Qualitative	**Quantitative**
Infra-Red (IR)/Fourier Transform Infra-Red spectroscopy (FTIR) - IR studies were used to show the functional groups involved in the o-P binding to iron oxides and to find the type of innersphere complex formed by o-P with the iron oxide surface (Arai and Sparks, 2001; Elzinga and Sparks, 2007; Parfitt and Atkinson, 1976; Persson et al., 1996; Russel et al., 1974).	**N_2 adsorption-desorption experiments** were used to estimate specific surface area and pore size distribution of iron oxides (Cabrera et al., 1981; Colombo et al., 1994; Torrent et al., 1990; Wang et al., 2013). **Water vapor sorption experiments** were also used for estimating the specific surface area of iron oxides (Colombo et al., 1994; Torrent et al., 1990).
X-ray Diffraction (XRD) was used to identify different iron oxides, to identify the crystallinity of iron oxides before and after o-P binding and iron phosphorus minerals (Chitrakar et al., 2006; Colombo et al., 1994; Daou et al., 2007; Frossard et al., 1997; Gálvez, 1999; Patrick et al., 1973; Wang et al., 2013).	**Thermal gravimetry analysis (TGA)** was used to investigate **t**he amounts of physically adsorbed H2O and OH content in the iron oxide structure (Wang et al 2013; Chitrakar et al. 2006).
X-ray photoelectron spectroscopy (XPS) was used to investigate the composition and chemical state before and after phosphonation of nZVI and magnetite by evaluating the binding energies of the surface species (Daou et al., 2007; Wen et al., 2014)	**Electrophoresis measurements and potentiometric titration experiments** were done to determine the zeta potential and PZC of different iron oxides (Antelo et al., 2007; Li and Stanforth, 2000; Parfitt and Atkinson, 1976).

Qualitative	Quantitative
Mössbauer spectroscopy was used for identification of iron oxides (Daou et al., 2007), vivianite in sludge (Frossard et al., 1997), and to show the interaction between organic matter and iron oxide (Schwertmann et al., 2005). **X-ray absorption spectroscopy (XAS) which includes Extended X-ray Absorption Fine Structure (EXAFS) and X-ray Absorption Near Edge Structure (XANES)** studies were used to determine the surface complex by providing information on the local molecular bonding environment / the bonding configuration of the surface species formed by o-P binding to iron oxide surfaces (Abdala et al., 2015; Khare et al., 2007). **Scanning electron microscopy (SEM), Transmission electron microscopy (TEM),** were used to determine the morphology and particle size of iron oxides (Cabrera et al., 1981; Gálvez, 1999; Martin et al., 1988; Torrent et al., 1990; Yoon et al., 2014). **Energy dispersive X-ray spectrometry (EDX)** was used to determines Fe:P molar rations in vivianite (Miot et al., 2009; Roldan et al., 2002).	

Table S2-4: Conditions used for o-P adsorption on different iron oxides

Type of iron oxide	Surface area (m^2/g)	Adsorption capacity (mg P/ g iron oxide)	Initial o-P (mg P/L)	Iron oxide (g/L)	Initial pH	Electrolyte	Time	T (°C)
Goethite (Parfitt et al., 1975)	80	6.5			3.5	0.1 M KCl		
Lepidocrocite (Parfitt et al., 1975)	108	16.72			3.5	0.1 M KCl		

Hematite (Parfitt et al., 1975)	22	5.26			3.5	0.1 M KCl		
Ferric hydroxide gel (Parfitt et al., 1975)	257	29.42			3.5	0.1 M KCl		
Lepidocrocite -1 (Cabrera et al., 1981)	128	14.83	80.52	4.00	3.4	0.1 M NaCl	6 d	25
Lepidocrocite -2 (Cabrera et al., 1981)	85.7	7.71		4.00	3.2	0.1 M NaCl	6 d	25
Goethite-1 (Cabrera et al., 1981)	87.4	11.4	96.01	4.00	3.1	0.1 M NaCl	6 d	25
Goethite-2 (Cabrera et al., 1981)	54.4	6.38		4.00	3	0.1 M NaCl	6 d	25
Fe-Gel (McLaughlin et al., 1981)	280	59.77		1.88	6	0.1 M $NaClO_4$	7 d	23
Hematite (McLaughlin et al., 1981)	18	3.87		1.88	6	0.1 M $NaClO_4$	7 d	23
Goethite (McLaughlin et al., 1981)	17	3.19		1.88	6	0.1 M $NaClO_4$	7 d	23
Akaganeite (McLaughlin et al., 1981)	29.4	2.82		1.88	6	0.1 M $NaClO_4$	7 d	23
Ferrihydrite (Guzman et al., 1994)	266	58.49					16 d	
Hematite-H1 (Guzman et al., 1994)	72	6.02					16 d	

Hematite-H2 (Guzman et al., 1994)	15	0.74					16 d	
Goethite-G1 (Guzman et al., 1994)	169	14.66					16 d	
Goethite-G2 (Guzman et al., 1994)	48	3.87					16 d	
Akaganeite (Genz et al., 2004)	280	23.3			5.5		96 h	20
Ferrihydrite (Borggaard et al., 2005)	264	42.74	49.55	1.00	5	0.2 M NaCl	28 d	22
Goethite (Borggaard et al., 2005)	76	6.41	49.55	2.00	5	0.2 M NaCl	28 d	22
Akaganeite (Deliyanni et al., 2007)	330	59.62	300	0.50	7		24 h	25
Magnetite nanoparticles (Daou et al., 2007)	31	5.2		1.00	3		24 h	
Ferrihydrite (Wang et al., 2013)	348	31.9	250	0.30	4.5	0.01 M KCl	24 h	25
Goethite (Wang et al., 2013)	45	3.13	250	2.35	4.5	0.01 M KCl	24 h	25
Hematite (Wang et al., 2013)(Wang et al. 2013c)	31	1.73	250	3.33	4.5	0.01 M KCl	24 h	25
Goethite (Fu et al., 2013)	30.32	5.48	20	2.00	4.5	0.01 M KNO_3	50 h	22

Magnetic iron oxide nanoparticles (Yoon et al., 2014)	82.2	5.03	20	0.60			24 h	30

2.8.2. Figure

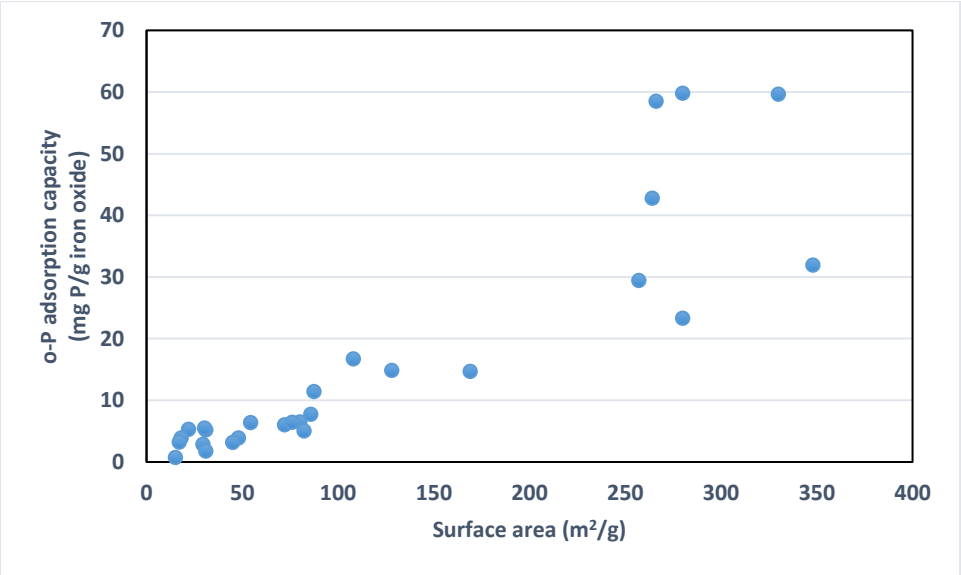
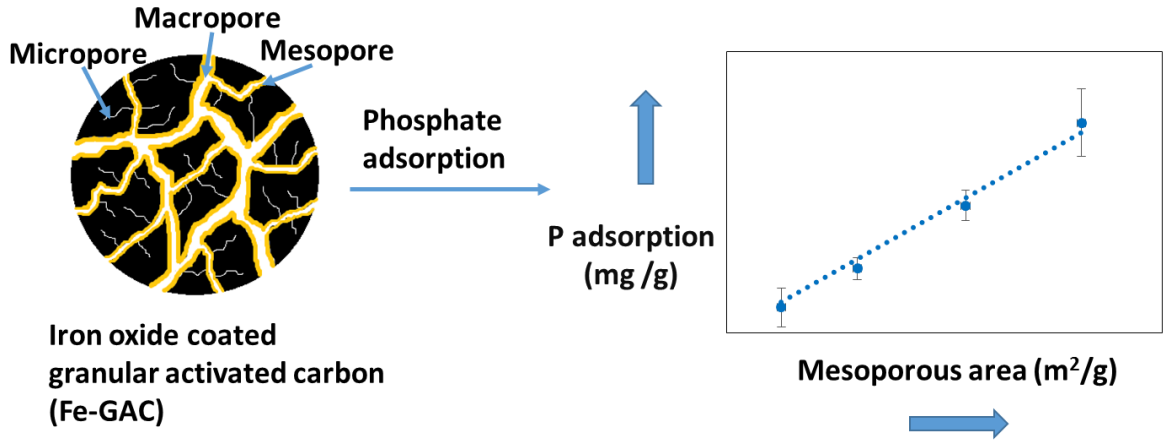


Figure S2-8: o-P adsorption capacity as a function of surface area of different iron oxides

Chapter - 3

Effect of pore size distribution on iron oxide coated granular activated carbons for phosphate adsorption – Importance of mesopores

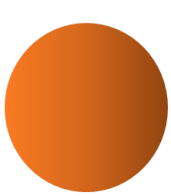
Suresh Kumar, P.; Prot, T.; Korving, L.; Keesman, K. J.; Dugulan, I.; van Loosdrecht, M. C. M.; Witkamp, G.-J., Effect of pore size distribution on iron oxide coated granular activated carbons for phosphate adsorption – Importance of mesopores. Chemical Engineering Journal 2017, 326, 231-239



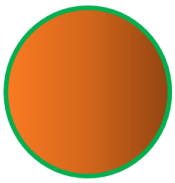
3.1. Prologue

3.1.1. Backdrop

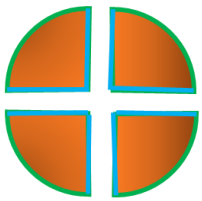
- Increasing an adsorbent's specific surface area (m^2/g) will improve its phosphate adsorption capacity (mg P/g).
- Iron oxides have a good affinity for phosphate and hence are commonly employed as phosphate adsorbents.
- The surface area of a non-porous iron oxide granule comes only from its exterior. Grinding the granule to smaller particles will increase its specific surface area.



Non-porous iron oxide granule



Surface area contributed only by exterior



Grinding exposes additional surface area

- But handling small particles is challenging. It will be more difficult to separate them after use and they cause a higher pressure drop.
- Porous materials like granular activated carbon (GAC) can have a specific surface area that is easily 100 times the specific surface area of non-porous iron oxide.
- A small fraction of iron oxide can result in a high surface area if it can be spread as a thin layer.



- Thus iron oxide can be coated as a thin layer on GAC to result in a high surface area phosphate adsorbent. This should translate to an adsorbent with high phosphate adsorption capacity.



Granular activated carbon

Thin layer of iron oxide

Iron oxide adsorbent of high specific surface area

3.1.2. Research questions

i) Can high surface area backbones like GAC be uniformly coated with iron oxides to improve phosphate adsorption capacity?

ii) If not, why? Is there something else to consider apart from the surface area?

3.2. Abstract

Adsorption is often suggested to reach very low phosphate levels in municipal wastewater effluent and even to recover phosphate. Adsorbent performance is usually associated with the surface area but the exact role of the pore size distribution (PSD) is unclear. Here, we show the effect of the PSD on phosphate adsorption. Granular activated carbons (GACs) with varying PSDs were treated with potassium permanganate followed by reaction with ferric chloride to form iron oxide coated GACs (Fe-GACs). Energy dispersive X-ray and kinetics experiments confirmed that manganese anchored on the GAC is important for subsequent iron attachment. Mössbauer spectroscopy showed the presence of ferrihydrite in Fe-GAC. Transmission electron microscopy showed that the iron oxide particles are not present in the micropores of the GACs. Phosphate adsorption isotherms were performed with the Fe-GACs and adsorption at lower phosphate concentrations correlated with the adsorbent surface area resulting from pores > 3 nm, a high fraction of which is contributed by mesopores. These results show that high surface areas of GACs resulting from micropores do not contribute to adsorption at low phosphate concentrations. This can be explained by the micropores being difficult to coat with iron oxide nanoparticles, but in addition, the diffusion of phosphate into these pores could also be hindered. It is therefore recommended to use backbones having high mesoporous areas. This information is useful for developing adsorbents particularly for applications treating low phosphate concentrations, for e.g. in municipal wastewater effluent polishing.

3.3. Introduction

Phosphorus is an essential nutrient for life. Humans consume phosphorus via food and the excreted phosphorus ends up as phosphate in municipal wastewater treatment plants (Cordell et al. 2009b, Reijnders 2014). In water bodies such as lakes and rivers, the presence of excess dissolved phosphate, especially as inorganic orthophosphate (we refer to this as phosphate henceforth), leads to algal bloom/eutrophication (Jarvie et al. 2006a).This affects the water quality and hence the ecosystem. Adsorption is often suggested as an effluent polishing step to keep the phosphate discharge from municipal wastewater treatment plants down to very low concentrations (Blaney et al. 2007, Loganathan et al. 2014). Iron (hydr)oxides have regularly been used as phosphate adsorbents due to their good binding capacity with phosphate (Lalley et al. 2016, Wilfert et al. 2015). In order to facilitate the recovery of adsorbent particles, increase their stability and enhance the surface area (and hence the adsorption), adsorbents are coated onto granular materials (Blaney et al. 2007, Huang et al. 2014b, Zach-Maor et al. 2011b). One such backbone on to which iron oxide can be coated is granular activated carbon (GAC). Activated carbon is becoming an essential component in water treatment facilities due to its ability to adsorb several contaminants from water. This includes micropollutants, organic compounds, odour, and colour removal (Çeçen and Aktaş 2011, García-Mateos et al. 2015, Gil et al. 2014). Activated carbon has a huge surface area, is relatively cheap, and in the form of granules (GAC) it offers the possibility for regeneration and reuse (Çeçen and Aktaş 2011).

The need for increasing affinity of activated carbon towards specific contaminants has led to studies on its surface modification (Rivera-Utrilla et al. 2011). It is coated with different metal oxides, including iron oxides, to improve specific interaction with phosphate (Liu et al. 2013, Zach-Maor et al. 2011b, Zhang et al. 2011, Zhou et al. 2012).

A key parameter for gauging the performance of an adsorbent is its adsorption capacity. Table S3-3 in supporting information compares adsorption capacity of different iron oxide based adsorbents from literature. Normally adsorbent capacities are expressed in terms of mass of the total adsorbent. However, when the adsorption capacity is expressed in terms of the iron present some adsorbents loaded with iron oxide show very high specific adsorption capacities. For instance, an earlier study(Zach-Maor et al. 2011b) on GAC coated with magnetite (Fe_3O_4), showed a very high maximum adsorption capacity of 141.8 mg P/g Fe indicating the iron oxide (magnetite) was formed as nanoparticles or as a thin layer which is accessible to phosphate. However, a calculation shows that even if monolayer coverage of the iron particles is assumed, less than 10 m^2/g can be covered with iron oxide for the iron content mentioned in the study ((text S1 (c) in supporting information), whereas typically 800-1600 m^2/g is available in GAC's (Table S3-3 and Table S3-5).

This suggests that optimization of the iron distribution may lead to a significantly improved capacity of phosphate adsorption in these adsorbents and this was the objective of our study. To achieve this, we focused on two important aspects. Firstly, we studied the mechanism of coating iron oxide on GAC. Secondly, we evaluated the effect of pore size distribution (PSD) of the GAC in relation to coating iron oxide and adsorbing phosphate. While trying to improve adsorbents, the main focus is usually their surface area and not much attention is given to their PSD. The PSD may however be very important for a good distribution of these nanoparticles, because based on the size of the nanoparticles, not all pores might be available for coating. Also, the pore size could influence the rate of diffusion of the phosphate molecules into the adsorbent. To the best of our knowledge, there are no earlier studies focusing on the effect of PSD of GAC based adsorbents in phosphate adsorption. Our study provides an insight into this aspect and explains how PSD could be key to improving iron based adsorbents for phosphate adsorption.

3.4. Experimental

3.4.1. Chemicals

Five different GACs were evaluated in the study and designated as GAC-1, 2, 3, 4 and 5 (Table S3-5) in supporting information lists their general characteristics). GAC-1 and GAC-2 were obtained from the activated carbon suppliers Norit and Desotech respectively. GAC-3, 4 and 5 were obtained from Mast Carbons (UK). Hydrogen peroxide (H_2O_2), nitric acid (HNO_3), potassium dihydrogen phosphate (KH_2PO_4), and potassium permanganate ($KMnO_4$) were obtained from VWR chemicals. Ferric chloride hexahydrate ($FeCl_3.6H_2O$), hypochloric acid ($HClO_4$) were obtained from Sigma Aldrich, Boom BV (Netherlands), respectively. Manganese (IV) oxide (MnO_2) and nitric acid (HNO_3) were obtained from Merck. Iron color disc test kit (Range: 0 to 5 mg Fe/L) was obtained from Hach.

3.4.2. Characterizing surface area and PSD

About 0.1 g of dried samples were degassed overnight in the presence of nitrogen gas. Subsequently, nitrogen adsorption and desorption cycles were carried out using Micromeritics TriStar 3000. The data from the nitrogen adsorption-desorption profiles were fitted with models included in the analysis software to obtain the Brunauer-Emmett-Teller (BET) surface and Barret-Joyner-Halenda (BJH) PSD, and the pore area and PSD from Non Local Density Functional Theory (NLDFT).

3.4.3. Evaluating mechanism of iron oxide formation on GAC

The iron oxide coating on the GAC was done in two successive steps: first, a reaction with an oxidizing agent then followed by reacting with ferric chloride solution. In between each step, the GAC was thoroughly washed with distilled water and oven dried (105 °C). The GACs treated with $KMnO_4$ were washed till the washed solution turned from pink to colorless. After reacting with ferric chloride, the washing of the GAC was carried out until the iron content of the washed solution reached below the detection limit (0.2 mg Fe/L) when measured by the iron color disc test kit. Unless otherwise mentioned, the solid to liquid ratio was 1 g GAC for 10 ml of solution, and all the reactions were allowed to proceed overnight (~18 h) and at room temperature (22 °C).

3.4.3.1. Effect of different oxidizing agents

Initially, 5 g of GAC-1 was reacted with 5 M aqueous solutions of either H_2O_2, $HClO_4$, HNO_3, or with 0.4 M $KMnO_4$. Subsequently, 3 g of the oxidized GAC-1 was reacted with 20 g Fe/L ferric chloride solution. The resulting iron oxide coated GACs are called Fe-GACs. The Fe-GACs were cross-sectioned and a surface elemental analysis was done at an acceleration voltage of 15 kV using Oxford Instruments x-act SDD Energy Dispersive X-ray Spectrometer (EDX).

3.4.3.2. Role of manganese in iron loading

For profiling the distribution of iron in relation to manganese, 5 g of GAC-1 was mixed with 200 ml of 0.4 M $KMnO_4$ in separate beakers for 15 minutes, 2 hours and 24 hours respectively. Three granules from each batch (after washing and drying) were analyzed for manganese distribution on their cross-section using EDX. The imaging was done using a JEOL JSM-6480 LV Scanning Electron Microscope (SEM). The change in mass of total granules as a result of taking 3 granules from each batch was negligible. The remaining granules from each batch were reacted in three separate beakers with 50 ml of 20 g Fe/L ferric chloride solution for 24 hours. Preliminary experiments showed that iron loading equilibrium was reached within this timeframe. The GAC-1 from the different beakers was washed, oven dried and their cross-sections were analyzed for iron distribution using EDX.

For evaluating the anchorage of iron as a function of manganese released, 5 g of GAC-3 was reacted with a 0.2 M $KMnO_4$ solution and subsequently 3 g of oxidized GAC-3 was treated with 20 g Fe/L solution. 0.1 g of granules were sampled at different intervals of time (10, 30, 60, 120, 240, 375 minutes and 27 hours). These samples were microwave digested using 67 % HNO_3. The iron and manganese concentrations in the digested solution were measured using a Perkin Elmer Optima 5300 DV Inductively Coupled Plasma Optical Emission Spectroscopy

(ICP-OES). As will be explained in the discussion section, the anchorage of iron on manganese was evaluated by replicating the same conditions but in the absence of GAC. To determine this, 710 mg of MnO_2 was added to 50 ml of 20 g Fe/L, and the solution was monitored for iron and manganese concentrations at 15, 30, 60, 180, 360 minutes and 24 hours.

3.4.3. 3. Characterization of Fe-GAC

Fe-GAC based on GAC-3 (which had been produced by treating with 50 ml of 0.4 M $KMnO_4$) was dried and ground. This sample was analyzed using Mössbauer spectroscopy to determine the type of iron oxide. Transmission ^{57}Fe Mössbauer spectra were collected at different temperatures with conventional constant acceleration and sinusoidal velocity spectrometers using a ^{57}Co (Rh) source. Velocity calibration was carried out using an α-Fe foil. The Mössbauer spectra were fitted using the Mosswin 4.0 program (Klencsár 1997). GAC-3, GAC-3 oxidized with $KMnO_4$ (having highest manganese loading), and Fe-GAC from GAC-3 (having highest iron loading) were examined with JEOL JEM 1400 Transmission Electron Microscope (TEM). The GAC-3 oxidized with $KMnO_4$ and corresponding Fe-GAC were also evaluated by X-ray diffraction measurements (XRD). The XRD measurements were carried out using a PANalytical X'Pert pro X-ray diffractometer mounted in the Bragg-Brentano configuration with a Cu anode (0.4 mm x 12 mm line focus, 45 kV, 40 mA). The X-ray scattered intensities were measured with a real-time multi strip (RTMS) detector (X'Celerator). The data were collected in the angle range $5^0<2\theta<90^0$ with a step size of 0.008^0 (2θ); total measuring time was 1h.

3.4.4. Manganese and iron loading on GACs with different PSD

Fe-GACs were produced from GAC-1, 2, 3, 4 and 5 by reacting them with varying amounts of $KMnO_4$. Since $KMnO_4$ is close to its solubility limit at 0.4 M, the amount of $KMnO_4$ available for the GACs was varied by a combination of adjusting the concentration and the solution volume. For GAC-1, 2, 4 and 5, 5 g of GAC was reacted with 25 ml of 0.08, 0.2, 0.4, and with 50 ml, 100 ml and 200 ml of 0.4 M $KMnO_4$. GAC-3 had a low density and 5 g could not be completely submerged in 25 ml solutions. So these solutions were instead replaced with 50 ml of 0.04, 0.1, and 0.2 M $KMnO_4$, so that the amount of $KMnO_4$ exposed per gram of GAC was constant for all GAC's.

3.4.5. Phosphate adsorption

For evaluating adsorption kinetics, Fe-GACs from GAC-1,2 and 3, i.e. Fe-GAC-1, Fe-GAC-2, Fe-GAC-3, were added to 100 ml of 20 mg P/L at different intervals of time (5, 15, 30, 60, 90, 120, 180, 360 minutes, 24, 48, 72 and 96 hours). For determining the adsorption isotherms, Fe-GAC-1, Fe-GAC-2 and Fe-GAC-3 were added to 100 ml aqueous solutions with phosphate concentrations of 1, 5, 10, 25, 50, 75 and 100 mg P/L and the experiment was run for 96 hours. For the adsorption kinetics as well the isotherms, the adsorbent concentration was 2 g/L, with solution pH of 6.5 and at room temperature (22 °C). For Fe-GAC-1 and Fe-GAC-2 the samples with the highest iron loading were used. However, for Fe-GAC-3, the sample with the highest iron loading had become powdered. Hence, for Fe-GAC-3, the sample produced by treating with 50 ml of 0.4 M $KMnO_4$ was used, as this was still granular. To check adsorption of phosphate on $KMnO_4$ treated GAC, the GAC-3 treated with 100 ml of 0.4 M $KMnO_4$ was also

tested at the same adsorbent dose and a phosphate concentration of 100 mg P/L. The phosphate concentration in solutions was measured using Metrohm 761 compact Ion Chromatograph (IC).

3.4.6. Data fitting and error determination

All the experiments were run as duplicates and the average value was reported with the standard deviation unless otherwise indicated. For adsorption kinetics and isotherms, model parameters were fitted by a non-linear regression approach as per Microsoft Excel's Solver program. For determining the errors in fitted model parameters, the standard deviations of the parameter estimates ($\hat{\theta}$) were calculated from the covariance matrix. Here, the 2x2 covariance matrix is calculated as follows:

$$Cov\left(\hat{\theta}\right) = \frac{\varepsilon(\hat{\theta})^T \varepsilon(\hat{\theta})}{n-p} \left(X\left(\hat{\theta}\right)^T X\left(\hat{\theta}\right)\right)^{-1} \quad (1)$$

Where, n denotes the number of samples,

p denotes the number of parameters,

$\varepsilon\left(\hat{\theta}\right)$ denotes the error vector between the experimental and corresponding model output values,

and $X\left(\hat{\theta}\right)$ is the sensitivity matrix, which consists of the partial derivatives of the model output as a function of the estimated parameters.

The standard deviations of the parameter estimates are calculated by taking the square root of the diagonal of the covariance matrix (Keesman 2011). A more elaborate description on determining the sensitivity matrix is provided under text S2 in supporting information.

3.5. Results and discussion

3.5.1. Characterizing the PSD of different GACs

As per the International Union of Pure and Applied Chemistry (IUPAC), porous materials can be classified into three categories based on the pore diameters. These are macropores (pore size > 50 nm), mesopores (2 to 50 nm), and micropores (< 2 nm) (Rouquerol et al. 1994, Sing et al. 2008). The PSD of porous materials can be determined by gas adsorption and desorption profiles (Sing 2001a), for example by a nitrogen adsorption analyzer. The gas adsorption and desorption profiles can be fit with models (inbuilt in the software) to obtain information on the specific surface area, porosity, and PSD of the materials. These include classical, macroscopic models like BJH (Barret-Joyner-Halenda, Barrett et al. 1951) or models like NLDFT (Non Local Density Functional Theory) which connect macroscopic properties to the behavior at molecular scale (Cracknell et al. 1995). The main differences between these models are the underlying assumptions regarding the mechanism of pore filling. BJH models assume that pore filling via pore condensation results in well-defined interfaces in the pores. This assumption works for macropores and large mesopores but fails to accurately describe micropores and small mesopores (Cracknell et al. 1995). The NLDFT model considers the difference in thermodynamic properties of a fluid confined in a pore as opposed to bulk fluid, and is able to

give a more accurate description of micropores and mesopores (Matthias 2004). The NLDFT model is widely used for characterizing materials like activated carbon, which consist of a high fraction of micropores (Landers et al. 2013). For the purpose of our study, we want to characterize the whole PSD (micro, meso, and macropores) of the GACs and hence we evaluate the GACs using both the BJH and NLDFT models as shown in Figure 3-1. The PSD is also shown in terms of pore area instead of pore volume in Figure S3-10 in supporting information. It should be noted that the values obtained from the model are originally provided as a function of pore diameter intervals (graphs of incremental volume will be histograms) which are not equal. The plots are plotted in terms of average diameter (as is often done) for the clarity of the readers.

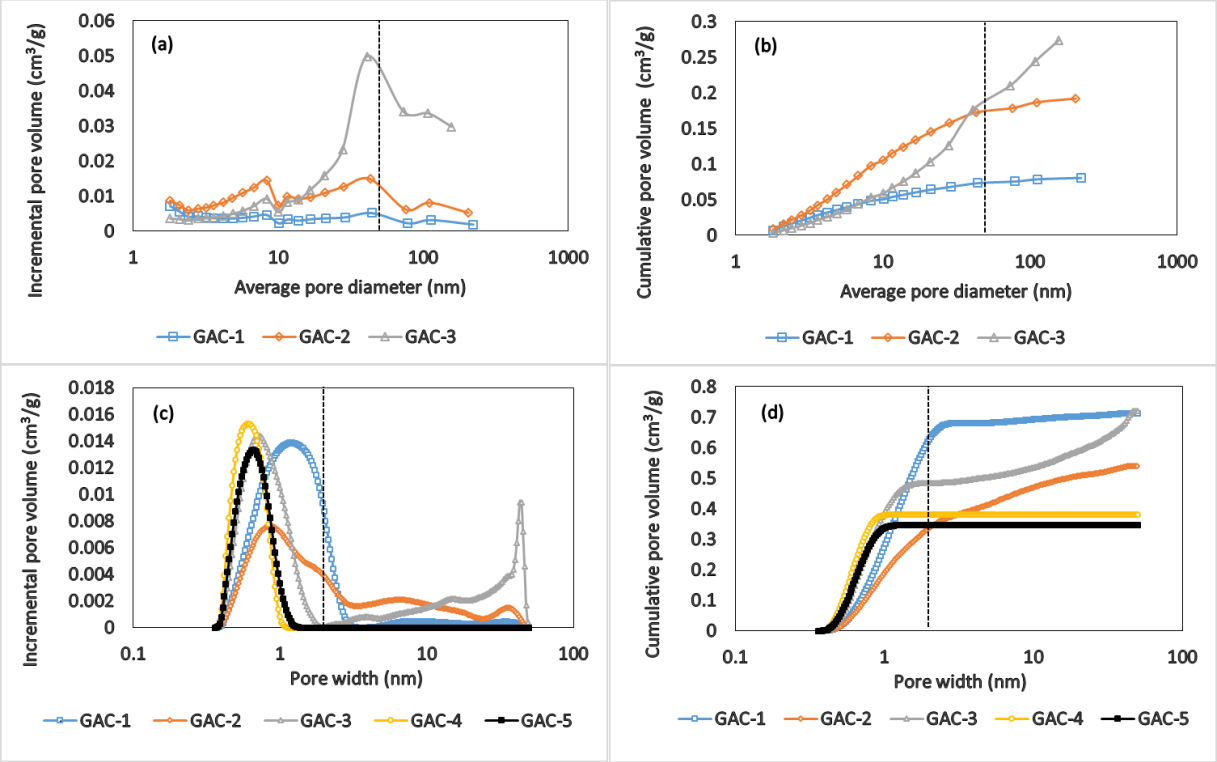


Figure 3-1: Incremental PSD of different GACs using (a) BJH model, (c) NLDFT model. Cumulative PSDs of different GACs using (b) BJH model, (d) NLDFT model. The dashed lines within BJH model plots (a & b) show cut off between meso and macropores (50 nm). The dashed lines within NLDFT model plots (c & d) show cut off between micro and mesopores (2 nm).

Figure 3-1 (a and b) shows that the GACs have a higher fraction of macroporous volume in the following order: GAC-3> GAC-2> GAC-1. GAC-4 and GAC-5 were very microporous and hence could not be fitted by the BJH model. Figure 3-1 (c & d) confirms using the NLDFT model that GAC-4 and GAC-5 are completely microporous. The other GACs have a higher fraction of mesoporous volume in the following order: GAC-3> GAC-2> GAC-1. For all the GACs, more than 90 % of the total pore area is contributed by micropores (Table S3-6 in supporting information).

Figure 3-1 demonstrates that the different GACs have indeed different PSDs. This information is relevant for later discussions where we highlight the importance of PSD for coating iron

oxides onto GAC and subsequently for phosphate adsorption. Other information on the different GACs like BET surface area, particle size and shape are provided in Table S3-5 in supporting information.

3.5.2. Mechanism of coating iron oxide on GAC

3.5.2.1. Iron loading on GAC using different oxidizing agents

Amongst the different methods used for surface modification of activated carbon, the use of oxidizing agents is the most common method (Rivera-Utrilla et al. 2011). We used the same approach for coating of our GACs with iron oxide. Activated carbon has previously been coated with iron oxide by using nitric acid (Wang et al. 2012). The hypothesis is that the surface oxidation of GAC introduces oxidized functional groups to which the dissolved iron reacts to form iron oxides (Wang et al. 2012). We used four commonly used oxidizing agents for surface modification of GAC, namely: H_2O_2, $HClO_4$, HNO_3, and $KMnO_4$. Figure 3-2 describes the effect of the different oxidizing agents on iron loading on GAC-1.

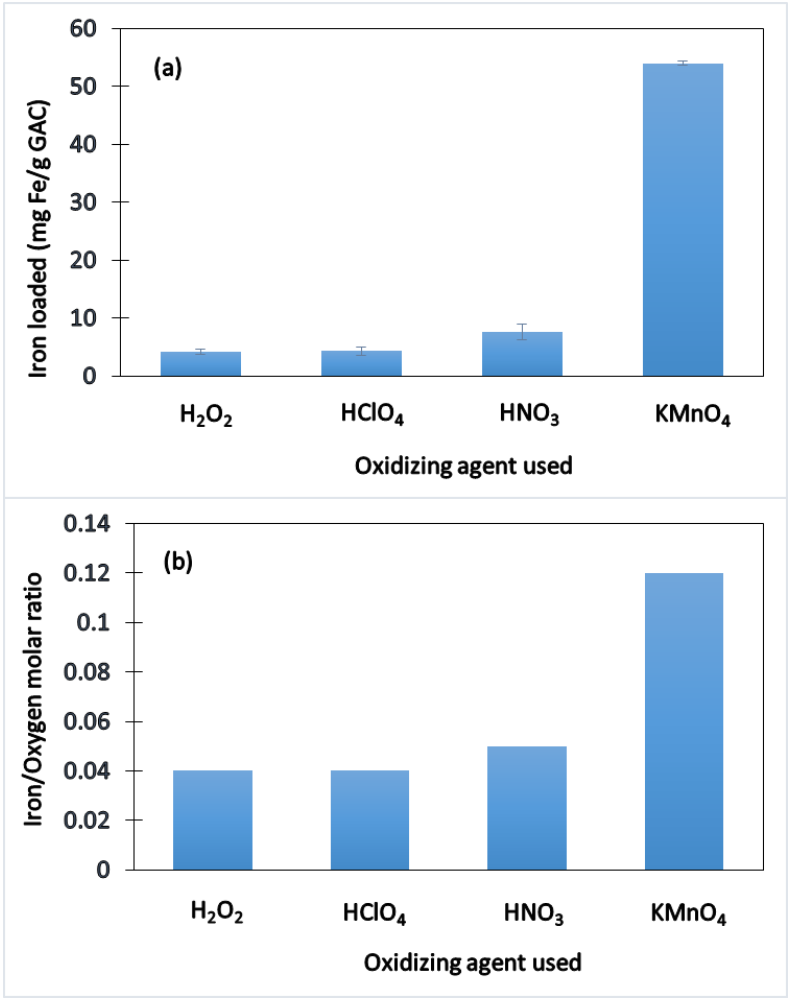


Figure 3-2: (a) Iron loading on GAC-1 via different oxidizing agents, (b) Iron to oxygen molar ratio on the Fe-GAC in relation to the oxidizing agent used (The oxygen used in this calculation is the oxygen added to the GAC after reacting with different oxidizing agents)

Figure 3-2 (a) shows that $KMnO_4$ resulted in maximum iron loading (54 mg Fe/g GAC). This was 7 times better than the next best oxidizer used (HNO_3). Figure 3-2 shows the iron to oxygen molar ratio on the GACs as determined by EDX (Table S3-4 in supporting information shows the oxygen and iron content for the different samples). Although EDX gives a semi-quantitative estimate of the weight percentage of different elements, we only used this ratio for a relative comparison. It can be seen from Figure 3-2 (b) that Fe/O molar ratio for $KMnO_4$ is higher than for other oxidizers, suggesting that oxidation is not the only prerequisite for loading of the iron on the GAC.

3.5.2.2. Role of Manganese in Iron loading

In an earlier study,(Zach-Maor et al. 2011b) the mechanism behind iron loading on GAC using $KMnO_4$ was proposed to be due to the formation of manganese dioxide (MnO_2) on GAC. The hypothesis was that the $KMnO_4$ is reduced to manganese dioxide (MnO_2) on the GAC and that this MnO_2 plays a role in subsequent iron oxide formation. To check for the presence of MnO_2 on the oxidized GAC, the GAC with the highest loading of manganese was examined with XRD. However, there were no distinct peaks obtained that could be attributed to MnO_2 (Figure S3-12 in supporting information). This could be due to the amorphous nature of the GAC backbone. We checked the possible role of manganese in iron loading by mapping the manganese and iron distribution on GAC during the coating process (Figure 3-3).

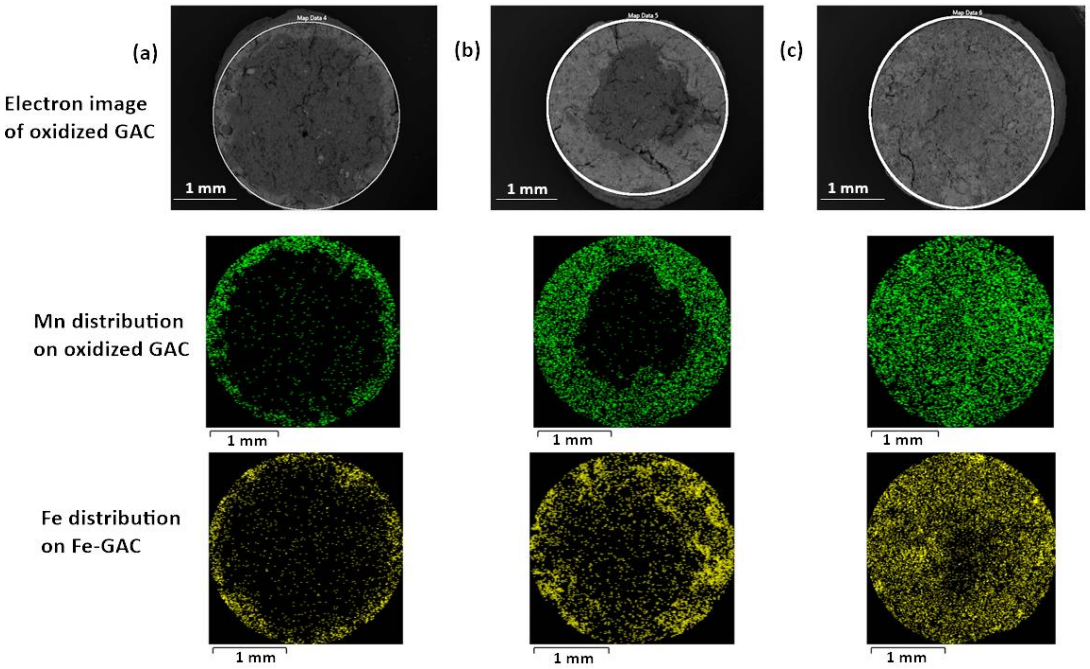


Figure 3-3: Electron image and elemental distribution (using EDX) of GAC-1 cross sections. The GACs were contacted with $KMnO_4$ for the following durations: (a) 15 min (b) 2 h (c) 24 h. The contact time with $FeCl_3$ was 24 h in all cases.

Figure 3-3 shows that Fe distribution follows the Mn distribution on the GAC, which agrees with the hypothesis. We also found that the Fe and Mn distribution overlapped with the oxygen distribution, probably because the manganese and iron are expected to be present in their oxide

forms. Another argument suggested in the earlier study(Zach-Maor et al. 2011b) was that iron oxide formation occurs by displacing the manganese from the MnO_2. To confirm this hypothesis, the amount of manganese and iron on GAC-3 was monitored as a function of time during the reaction of the oxidized GAC in a ferric chloride solution (Figure 3-4).

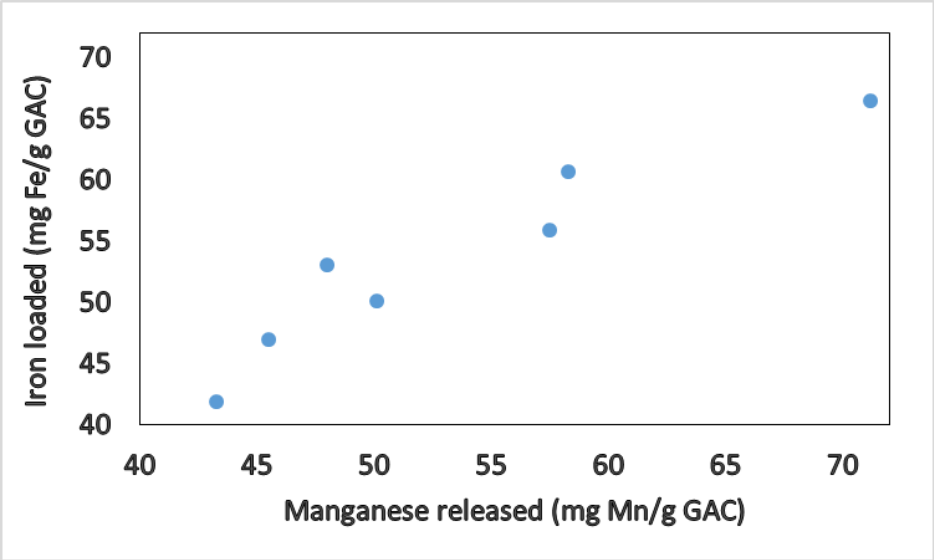


Figure 3-4: Iron loaded as a function of manganese released from GAC-3

Figure 3-4 shows a correlation between iron anchorage and the release of manganese from the GAC. The molar ratio of iron anchored to manganese released was close to 1 under this experimental condition. Along with Figure 3-2 (b) and Figure 3-3, Figure 3-4 confirms the hypothesis that manganese plays a role in the iron anchorage.

3.5.2.3. Characterization of Fe-GAC

To determine the type of iron oxide formed on the GAC, the Fe-GAC on GAC-3 was powdered and analyzed with X-Ray Diffraction (XRD). However, we could not determine the type of iron oxide by XRD (data not shown), implying the iron oxide could be amorphous. Thus Mössbauer spectroscopy was used to determine the type of iron oxide (Figure 3-5 and Table 3-1), with the advantage that even iron oxides with low crystallinity (amorphous) can be detected (Cornell and Schwertmann 2004).

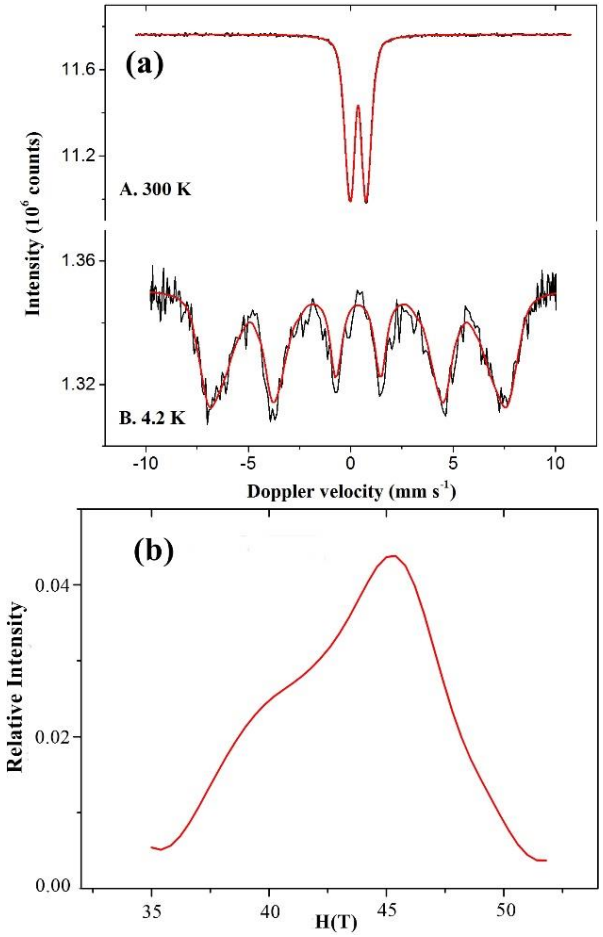


Figure 3-5: (a) Mössbauer spectrum of Fe-GAC (from GAC-3) at 300 K and 4.2 K (b) Magnetic field distribution of the Fe-GAC.

Table 3-1: The Mössbauer fitted parameters of Fe-GAC (from GAC-3)

Sample	**T (K)**	**IS (mm·s^{-1})**	**QS (mm·s^{-1})**	**Hyperfine field (T)**	**Γ (mm·s^{-1})**	**Phase**	**Spectral contribution (%)**
Fe/GAC	*300*	*0.36*	*0.89*	*-*	*0.30*	*Fe^{3+}*	*100*
Fe/GAC	*4.2*	*0.37*	*0*	*42.5**	*0.57*	*Fe^{3+}*	*100*

Experimental uncertainties: Isomer shift: I.S. ± 0.01 mm s^{-1}; Quadrupole splitting: Q.S. ± 0.01 mm s^{-1};

*Line width: Γ ± 0.01 mm s^{-1}; Hyperfine field: ± 0.1 T; Spectral contribution: ± 3%. *Average magnetic field.*

An earlier study (Zach-Maor et al. 2011b) reports the formation of magnetite (Fe_3O_4) when the GAC treated with $KMnO_4$ is reacted with a ferric chloride solution. Using Mössbauer spectroscopy, a doublet formation at 297 K with an isomer shift of 0.36 mm/s and a sextuplet formation at 86 K with a hyperfine field of 44 T was reported (Zach-Maor et al. 2011b). Our Mössbauer spectroscopy measurements (Figure 3-5 and Table 3-1) show a doublet formation at 300 K with an isomer shift of 0.36 mm/s and sextuplet formation at 4.2 K having an average hyperfine field of 42.5 T (maximum value at ~45 T). It is possible that both studies have the same type of iron oxide. However, at 4.2 K the Fe^{3+} ion of magnetite has a hyperfine field around 50 T (Sang Won et al. 2005), whereas the hyperfine field we observed seems closer to ferrihydrite (around 46 T) (Murad 1988a).

Moreover, when the earlier study used 86 K, only 37 % of the spectral contribution was magnetically split, and only 2 % of the spectra were assigned an isomer shift that corresponds to Fe^{2+} ion (Zach-Maor et al. 2011b). In contrast, our measurements at 4.2 K resulted in 100 % of the spectral contribution being magnetically split and all of it being assigned to Fe^{3+} ion. Thus our measurements are more suited to identify the type of iron oxide.

Additionally, the broad magnetic field distribution of our sample (Figure 3-5 b) is a characteristic attributed to low crystallinity (Murad 1988b), which also points out that the Fe-GAC is most likely to have ferrihydrite. This agrees with our XRD observation of not being able to identify the iron oxide (Figure S3-12 in supporting information).

The reaction of $KMnO_4$ on activated carbon backbone to form MnO_2 has been reported multiple times (Deng et al. 2015, Liu et al. 2012, Song et al. 2014). However, the formation of magnetite on the $KMnO_4$ treated activated carbon backbone as per the earlier study (Zach-Maor et al. 2011b) would require the presence of ferrous ion (Fe^{2+}). But the ferric chloride solution used for loading iron consists of ferric ion (Fe^{3+}) and the conditions do not favor the formation of Fe^{2+}. Therefore, magnetite formation would not be possible and this is in line with our Mössbauer results. However, the exact mechanism of ferrihydrite formation has not been studied in our experiments and further study is needed to elaborate on this mechanism. Our studies do establish that manganese loading is a prerequisite for iron loading on the activated carbon backbone.

To determine the size of the MnO_2 and ferrihydrite particles, the oxidized GAC and Fe-GAC formed using GAC-3 was observed with TEM (Figure 3-6).

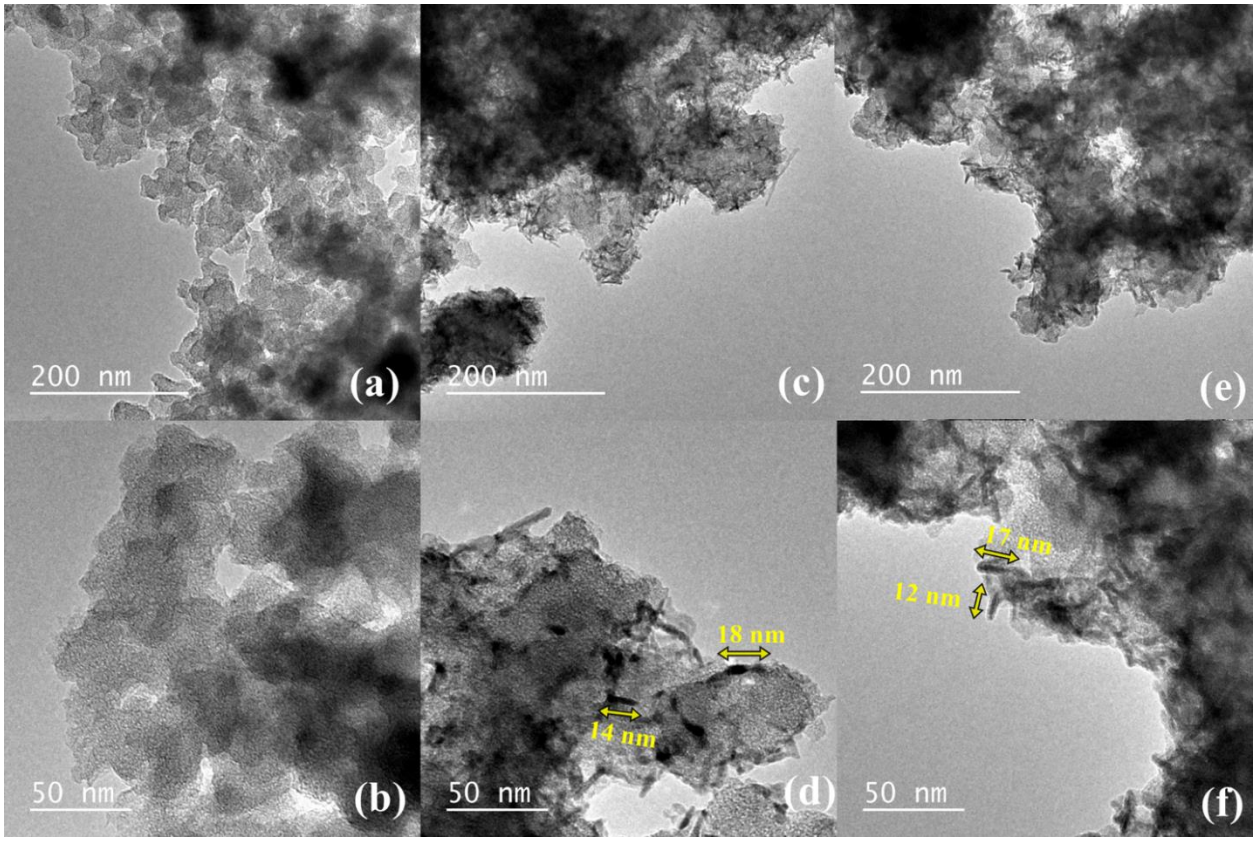


Figure 3-6: TEM images of (a) GAC-3, (b) GAC-3 at higher magnification (c) oxidized GAC-3 (d) oxidized GAC-3 at higher magnification (e) Fe-GAC-3 (f) Fe-GAC-3 at higher magnification

Figure 3-6 shows the formation of needle-like structures in oxidized GAC and Fe-GAC as compared to the GAC backbone. The size of these needle-like structures in the oxidized GAC, as well as the Fe-GAC, are above 10 nm. During the Mössbauer spectroscopy measurements, a blocking temperature of around 25 K was measured for the ferrihydrite particles. As per literature, this indicates that the ferrihydrite particles in the Fe-GAC are around 4 to 5 nm (Murad and Cashion 2004). The observed manganese particles are much bigger than the micropores and therefore it is unlikely that iron oxides are formed in the micropores in the subsequent treatment. Nevertheless, during the coating process, some of the smaller mesopores could be constricted to micropores because of the particles formed inside them. There might still be iron oxides found in such micropores.

3.5.3. Effect of PSD of different GACs

3.5.3.1. Manganese and iron loading on GACs with different PSD

Following the findings from the previous section, different GACs were treated with a varying amount of $KMnO_4$ to find the optimum condition to maximize manganese loading (Figure 3-7 a). The oxidized GACs were subsequently reacted with ferric chloride to determine the highest possible iron loading on the Fe-GACs (Figure 3-7 b).

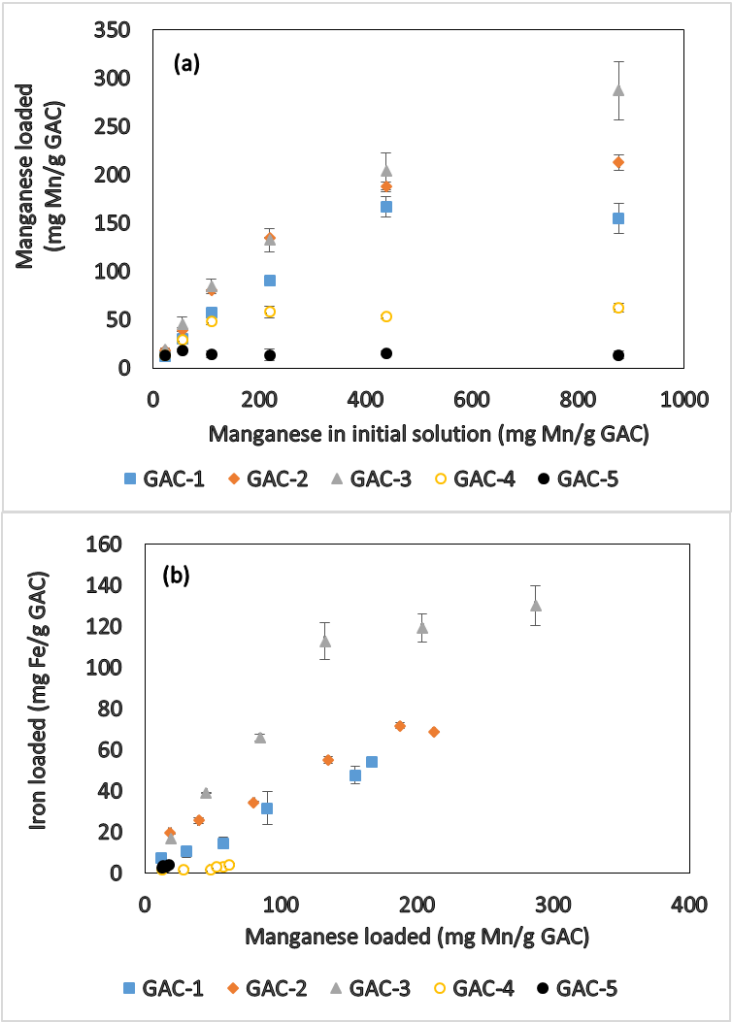


Figure 3-7: (a) Manganese loading onto different GACs as a function of available manganese, (b) Iron loading onto different GACs as a function of manganese loaded

Figure 3-7 (a) shows that the manganese loading onto the GACs increased by using higher concentrations of $KMnO_4$. The overall manganese loading for the different GACs increased in the order: GAC-3> GAC-2 > GAC-1 > GAC-4 > GAC-5. Figure 3-7 (b) shows that the higher the manganese loading per GAC, the higher the iron loading on the GACs. This is in line with the hypothesis in section 3.5.2 that manganese is required for iron anchorage on the GAC.

By comparing the results of Figure 3-7 (a) with Figure 3-1, it can be seen that GACs with a higher portion of mesopores and macropores (or fewer micropores) had higher manganese loadings. Consequently, the iron loading is higher in these GACs. Another observation is the ratio between the iron loading and manganese loading. The iron loaded seems to increase linearly at low manganese loadings. At higher manganese loadings, the amount of iron loaded is much lower than manganese loaded. This suggests that there is residual manganese loaded on the GAC that is not used to anchor iron.

3.5.3.2. P adsorption on adsorbents with different PSD

Adsorption isotherms are a vital tool for characterizing the performance of adsorbents. Adsorption tests were run for 4 days as this is already a long time considering practical

applications. Adsorption kinetics (Figure S3-11 in supporting information) were fitted with pseudo second order model to show that after 4 days we were within 5 % of reaching equilibrium in all cases (Table S3-8 in supporting info). GAC-4 and GAC-5 were not included for P adsorption isotherms since they showed very low iron loading and preliminary experiments showed they could not adsorb P.

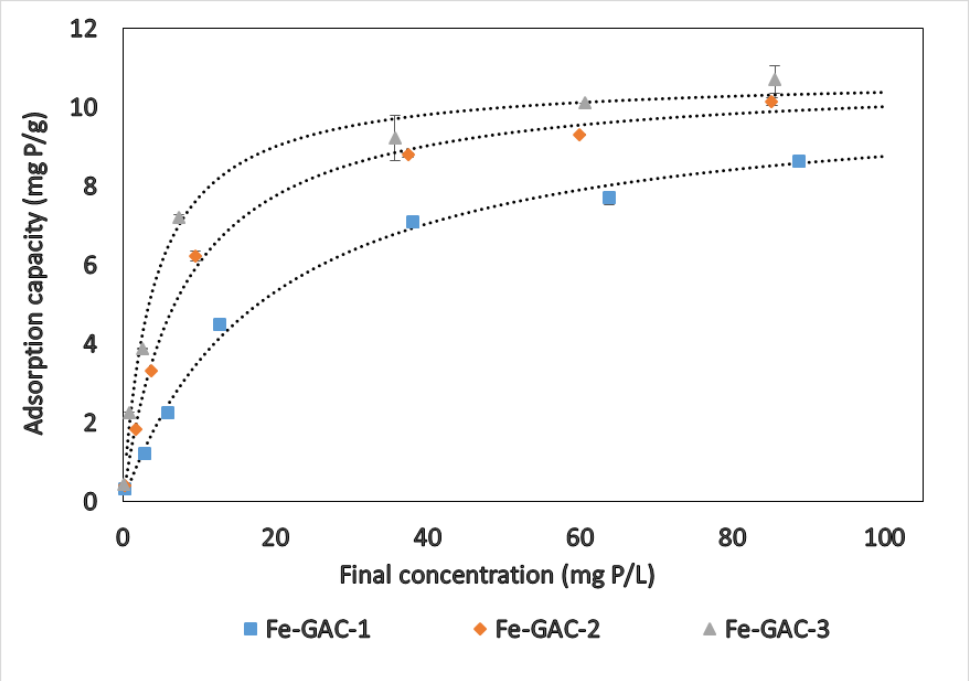


Figure 3-8: P adsorption isotherm (at 22°C) for the different Fe-GACs. The dashed lines represent the Langmuir fit for each adsorbent.

Figure 3-8 shows the adsorption capacities for the different Fe-GACs as a function of the final concentration of phosphate. Phosphate adsorption on iron oxides happens via ligand exchange reaction, in other words via chemisorption (Cornell and Schwertmann 2004). Therefore, the Langmuir isotherm model, which assumes chemisorption at the adsorption mechanism (Langmuir 1918), was used to fit the experimental adsorption data.

The Langmuir expression is:

$$q_e = \frac{q_m K_L C_e}{(1 + K_L C_e)} \quad (2)$$

Where,

q_m = Maximum adsorption capacity (mg P/g),

q_e = Adsorption capacity at equilibrium (mg P/g),

C_e = Concentration at equilibrium (mg P/L),

K_L = Equilibrium constant for the Langmuir adsorption (L/mg P).

Table 3-2: Langmuir model parameters along with BET surface area, iron and residual manganese content of the adsorbents

Sample	BET surface area (m^2/g)	Fe anchored (mg Fe/g)	Residual manganese (mg Mn/g)	q_m (mg P/g adsorbent)	K_L (L/mg P)
Fe-GAC-1	920 ± 5	48 ± 4	76 ± 21	10.4 ± 0.4	0.05 ± 0.01
Fe-GAC-2	441 ± 30	69 ± 0.3	147 ± 8	10.8 ± 0.2	0.13 ± 0.01
Fe-GAC-3	794 ± 1	113 ± 9	31 ± 18	10.8 ± 0.3	0.25 ± 0.04

Table 3-2 compares the Langmuir parameters of the different adsorbents in relation to their surface area, iron anchorage, and residual manganese content. The residual manganese is the remaining manganese after the iron loading process. To determine if the manganese also plays a role in phosphate adsorption, oxidized GAC-3 with a very high manganese loading (200 mg Mn/g) but before iron anchorage was tested. Its adsorption capacity at the maximum phosphate concentration used in isotherms was 3.5 mg P/g. This is about 3 times lower than adsorption capacity of Fe-GACs. Therefore, even though the residual manganese in the Fe-GACs could contribute to phosphate adsorption, the iron contributes for a majority of the phosphate adsorption. Table 3-2 shows that the constant K_L, which is related with the adsorption at lower phosphate concentration, correlates rather to the iron content of the adsorbents than to the manganese content.

For the application of adsorption as a polishing step in municipal wastewater treatment, we are most interested in examining the adsorption at low phosphate concentrations (< 10 mg P/L). Therefore, the initial slopes of the adsorption isotherm curves are most relevant. Figure 3-8 shows that the different GACs vary in their P adsorption capacity especially at a lower concentration, as indicated by the different slopes in the initial part of the curves. To quantify the difference in adsorption of GACs at lower concentrations, we make use of the Langmuir parameters. We define the term adsorption affinity as the constant that relates adsorption capacity to very low adsorbate concentrations. This term is determined by the slope of the Langmuir adsorption curve as the concentration of phosphate tends to zero. As $C_e \rightarrow 0$ (and provided K_L is finite) in the Langmuir equation, the equation becomes:

$$q_e = q_m K_L C_e \quad (3)$$

The term, $q_m K_L$, represents the slope of the initial part of the isotherm curve and denotes the adsorption affinity. The above equation means that at very low concentrations, the equilibrium adsorption capacity depends on the total number of active sites rather than the number of unoccupied active sites.

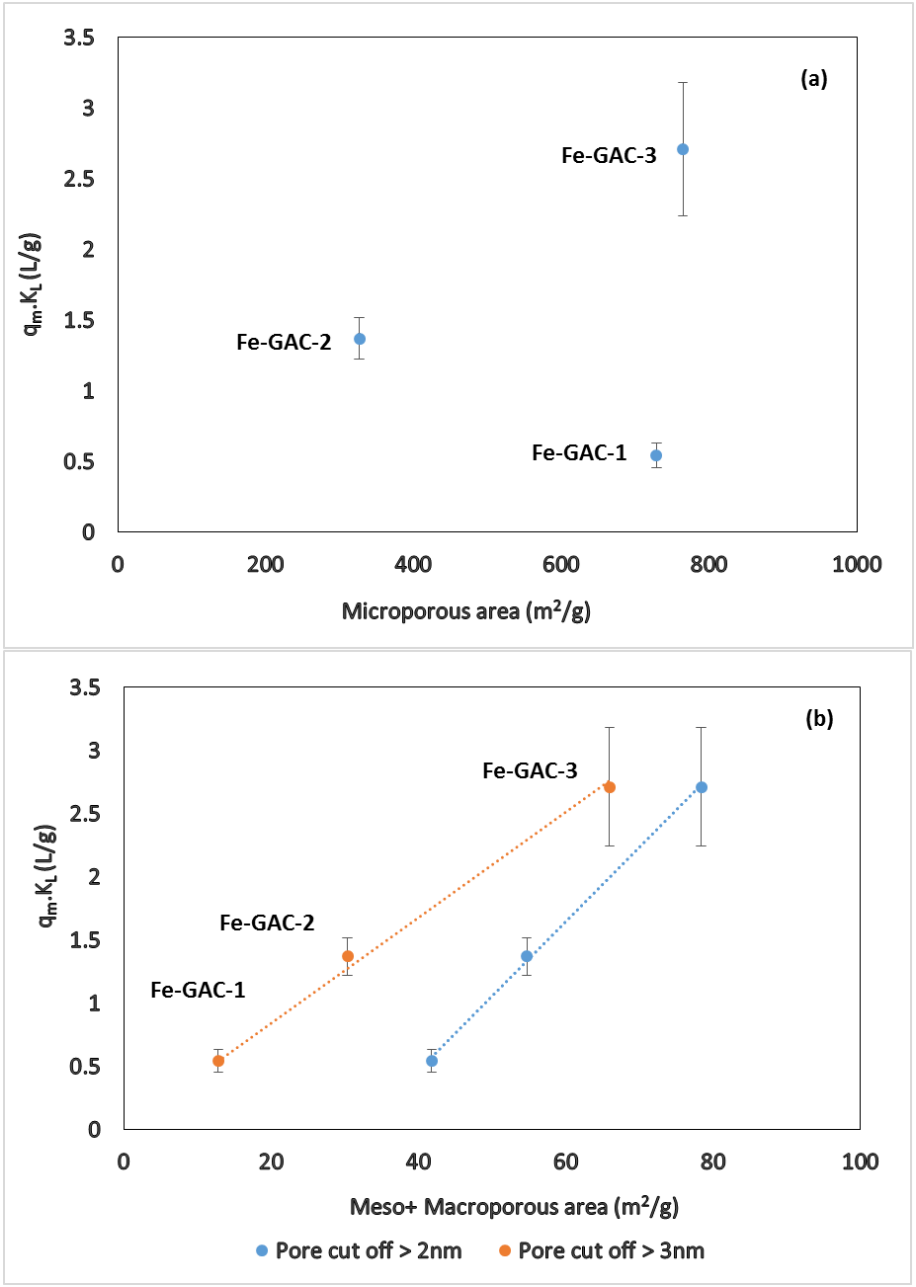


Figure 3-9: Correlation of adsorption affinity of different Fe-GACs to (a) microporous area (b) meso + macroporous area (Pore cut off > 3 nm, correlation coefficient: 0.995) The NLDFT model was used for estimating the microporous and mesoporous area. The BJH model was used for estimating the macroporous area.

Figure 3-9 shows that the adsorption affinity correlated with the porous area of the adsorbents if we assume a cut off pore size of 2 nm. However, if we assume a cut off pore size of 3 nm, we get a correlation with zero intercept which means a completely proportional relation. A majority of this porous area is in the mesopores as compared to the macropores (see Table S3-6 and Table S3-7), which highlights the importance of mesopores. For GAC-3, the mesoporous area increases after iron loading. This is possibly due to the high fraction of macropores in GAC-3, which gets constricted to mesopores during the coating process. One explanation for the microporous area not contributing to P adsorption affinity could be the iron coating process. Figure 3-6 indicates that the MnO_2 particles are much bigger than the

micropores and hence iron oxides would also not be formed in the micropores. Thus the only micropores in the Fe-GAC that contribute to the adsorption would be those that were formed as a result of pore blocking of mesopores. Hence a majority of the micropores would not be contributing to P adsorption. Additionally, the diffusion of phosphate ions in the micropores could be difficult. Phosphate ions have a diameter of about 0.48 nm (Tawfik and Viola 2011a). Thus the adsorbate molecule is in a similar order of magnitude to the micropores and this could lead to hindered diffusion in such pores (Beck and Schultz 1972a). The decrease in diffusion would especially be significant at low concentrations of phosphate where the driving force for diffusion is less. Thus the adsorption affinity would be largely related to mesopores and macropores. But because the surface area is significantly higher for the mesopores compared to the macropores, the mesopores will be the main contributing factor to adsorption.

3.6. Conclusion

High phosphate adsorption capacities can be achieved by coating high surface area backbones (like granular activated carbon) with iron oxide nanoparticles. This study shows that ferrihydrite nanoparticles can be coated on the GAC backbone using $KMnO_4$. Manganese loading on the GAC as an intermediate step is important for this process. However, this study shows that the manganese oxide particles that serve as a precursor for the ferrihydrite formation have needle-like structures with a length of more than 10 nm. This result suggests that only a fraction of the total pore area in the GAC is actually coated with manganese oxide and iron oxide particles because the pore area in GAC is dominated by micropores with a pore size smaller than 2 nm. Testing of GACs with different PSD showed that the adsorption at low P concentrations correlates well with the mesoporous area of the adsorbents.

This result suggests that the applied coating method is best suited for backbones with predominantly mesoporous pore size distributions. Nevertheless, the application on GAC's with predominantly micropores could still be of interest if these micropores can serve another function, for instance, to adsorb micropollutants. Combined removal of phosphate (in the mesopores) and micropollutants (in the mesopores) could be an interesting prospect for polishing of sewage treatment effluents in light of stringent demands and limits to effluent quality.

3.7. Supporting information

3.7.1. Tables

Table S3-3: Maximum phosphate adsorption capacity of different iron oxide based adsorbents (Although conditions like pH, temperature, phosphate concentration, and adsorbent concentration differ in these studies, we expect the adsorbent constituent to be a significant factor for the variation in adsorption)

Adsorbent	**BET surface area (m^2/g)**	**Adsorption capacity (mg P/g adsorbent)**	**Adsorption capacity (mg P/g Fe)**	**Adsorption capacity (mg P/100 m^2 adsorbent)**	**Ref**
Akaganeite	94	13.9			(Kim et al. 2011)
Ferrihydrite	264	42.7	85.4	16.2	(Borggaard et al. 2005b)
Goethite	76	6.4	10.6	8.4	(Borggaard et al. 2005b)
Goethite	63	8.2		13	(Kim et al. 2011)
Granular ferric hydroxide (Akaganeite)	280	23.3	48.5	8.3	(Genz et al. 2004)
Lepidocrocite	85	8.2		9.6	(Kim et al. 2011)
Magnetite	31	5.2	7.2	16.8	(Daou et al. 2007)
Iron coated sand	3.5	0.7	117	20	(Huang et al. 2014c)
Layered iron oxide nanosheets	185	77	124	41.6	(Fang et al. 2015)
Activated carbon doped with Goethite	881	14.1		1.6	(Wang et al. 2012)
Activated carbon doped with Akaganeite	303	8.7		2.9	(Wang et al. 2012)
Granular activated carbon immobilized with nano-sized magnetite	1024	4.8	141.8	0.5	(Zach-Maor et al. 2011b)

Table S3-4: Effect of different oxidizing agents

Oxidizing agent	Oxygen (wt %)*	Iron (wt %)	Iron/Oxygen added (molar ratio)
None	4.23	0	-
HNO_3	8.38	0.76	0.05
$KMnO_4$	17.01	5.28	0.12
$HClO_4$	7.17	0.38	0.04
H_2O_2	5.35	0.17	0.04

*The oxygen content is shown for the GAC-2 and oxidized GAC-2 before the treatment with iron. The iron content is shown for the corresponding Fe-GAC after treatment with iron solution.

Table S3-5: General characteristics of the different GAC's evaluated

Supplier	BET Surface area (m^2/g)	Average size (mm)	Shape	Denoted as
Norit	1616	4 x 2	Cylindrical	GAC-1
Desotec	927	2	Granular	GAC-2
Mast carbon	1307	4	Granular	GAC-3
Mast carbon	982	5 x 2	Cylindrical	GAC-4
Mast carbon	908	5	Granular	GAC-5

Table S3-6: Surface area of different samples as calculated using NLDFT model

Sample	Total pore area (m^2/g)	Microporous area (m^2/g)	Mesoporous area (m^2/g)
GAC-1	1338	1284	54
GAC-2	843	764	79
GAC-3	1365	1329	36
GAC-4	1278	1278	0
GAC-5	1094	1094	0
Fe-GAC-1	770	729	41, 12*
Fe-GAC-2	381	327	54, 30*
Fe-GAC-3	832	765	67, 55*

*Indicates the mesoporous area above pore cut-off of 3nm

Table S3-7: Surface area of different samples as calculated by BJH model

Sample	Total pore area (m^2/g)*	Macroporous area (m^2/g)†
GAC-1	51.8	0.6
GAC-2	109.6	1.3
GAC-3	79.9	8.4
Fe-GAC-1	59	0.3
Fe-GAC-2	87.2	0.4
Fe-GAC-3	118.8	11.2

*Total pore area – It must be noted that the BJH model is not able to describe the microporous area and hence the total pore area is much lower than that estimated by NLDFT model.

†Macroporous area (Since cutoff values from exactly 50 nm were not available, the closest available average pore diameters were considered. For GAC-3 and Fe-GAC-3 this was around 40 nm. For all other samples this was around 44 nm).

Table S3-8: Rate constants from pseudo second order kinetic model

Sample	q_e (mg P/g) - experimental	q_e (mg P/g) - fitted	k (g/mg min)
Fe-GAC-1	4.5 ± 0.1	4.6 ± 0.3	$4 \times 10^{-4} \pm 1 \times 10^{-4}$
Fe-GAC-2	6.2 ± 0.1	6.5 ± 0.4	$2.8 \times 10^{-4} \pm 7 \times 10^{-5}$
Fe-GAC-3	7.2 ± 0.1	7.1 ± 0.2	$8.8 \times 10^{-4} \pm 9 \times 10^{-5}$

3.7.2. Figures

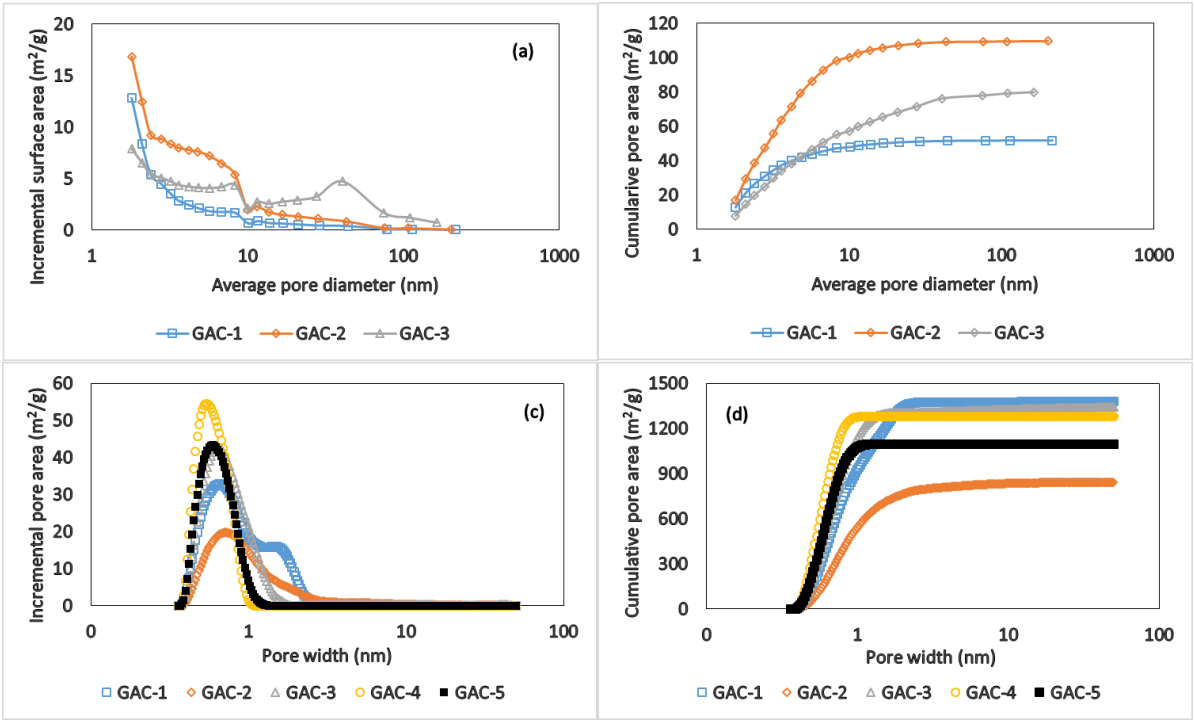


Figure S3-10: Incremental PSD of different GACs in terms of the pore area using (a) BJH model, (c) NLDFT model. Cumulative PSDs of different GACs in term of the pore area using (b) BJH model, (d) NLDFT model.

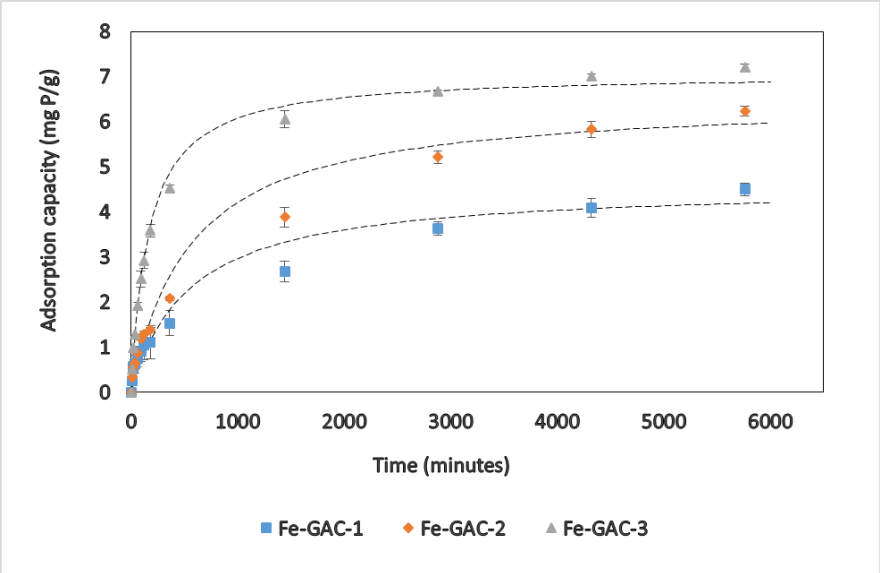


Figure S3-11: Adsorption kinetics of the Fe-GACs. Dashed lines represent the pseudo second order kinetic model fit. (Initial phosphate concentration = 20 mg P/L, Adsorbent concentration = 2 g/L, pH ≈6.5)

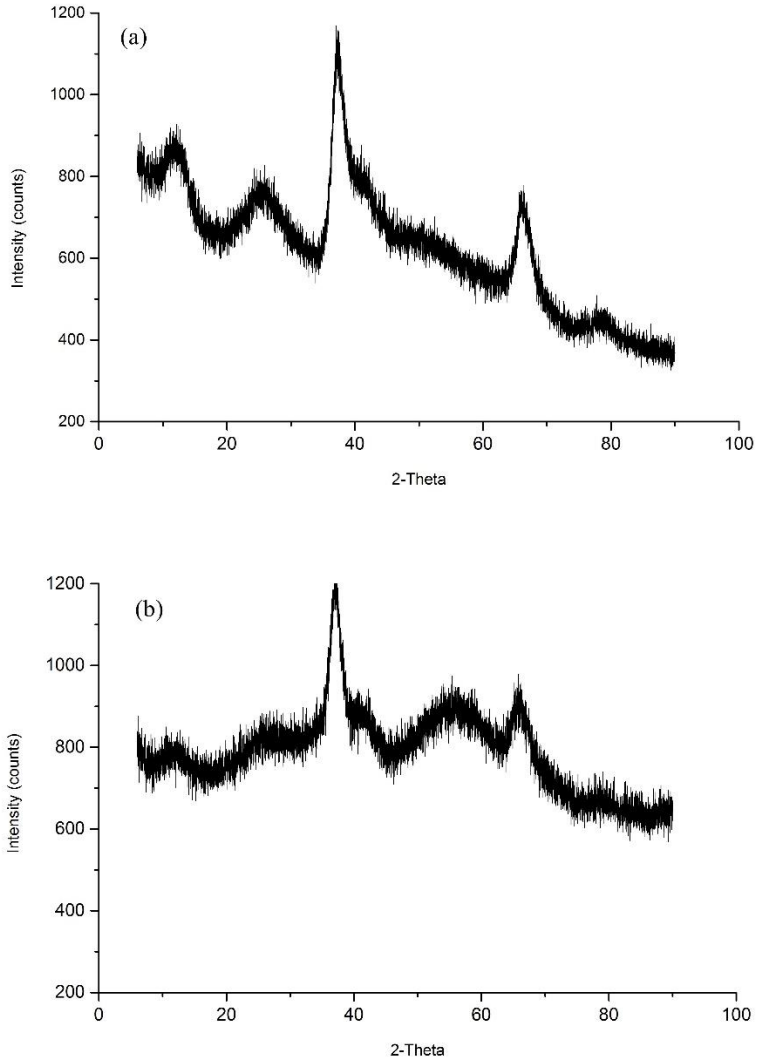


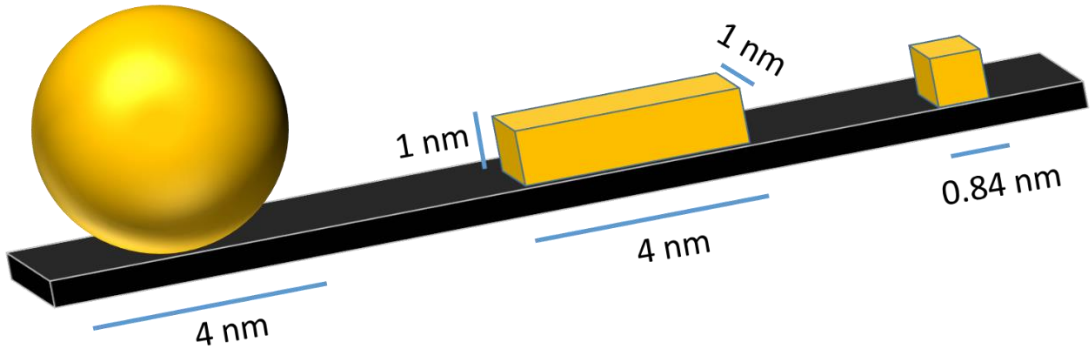
Figure S3-12: XRD spectra of (a) GAC-3 oxidized with $KMnO_4$ (b) Fe-GAC (GAC-3 with highest iron loading)

3.7.3. Text

Text S1: Surface area covered by monolayer coating

The monolayer coverage on the GAC surface has been estimated for 3 different scenarios as depicted in the following schematic:

(a) Spherical particle (b) Cuboid particle (c) Cubic unit cell



The surface coverage was estimated by the following formula

$$A_{Fe} = \frac{A_{unit}}{V_{unit}} * \frac{C_{Fe}}{\rho_{unit} X_{Fe/Fe_xO_y}}$$

Where:

A_{Fe} = Area coated by Fe per gram of adsorbent (m^2/g)
A_{unit} = Surface area covered by a unit particle (m^2/particle)
V_{unit} = Volume of a unit particle
ρ_{unit} = density of a unit particle (g/m^3, 5.18 g/m^3 for Fe_3O_4 (Cornell and Schwertmann 2004))
C_{Fe} = Iron content of the Fe coated adsorbent (g Fe/g adsorbent)
$X_{Fe/FexOy}$ = mass fraction of Fe in a certain iron oxide (0.72 g/g for Fe_3O_4)

(a) For spherical magnetite (Fe_3O_4) particle of diameter 4 nm,

Cross-sectional area (m^2) = 1.25 x 10^{-17},

Volume (cm^3) = 3.35 x 10^{-20},

Thereby, area coated by 34 mg Fe / g adsorbent = 3.40 m^2/ g adsorbent

(b) If the 4 nm magnetite particle were cuboid shaped (assuming length 4 nm, width 1 nm, and height 1 nm), the area coated by 34 mg Fe is estimated in a similar way to be 9.07 m^2/g

(c) If we consider coverage by unit cells of magnetite (cubic structure),

Length of unit cell (nm) = 0.84 (as mentioned in (Cornell and Schwertmann 2004))

Cross-sectional area (m^2) = 7.05 x 10^{-19},

Volume (cm^3) = 5.92 x 10^{-22},

Using the above formula, area coated by 34 mg of Fe (m^2) = 10.80 m^2/g

Text S2: Sensitivity matrix

Let us consider the Langmuir model that was fitted to the adsorption data. The Langmuir equation is given by:

$$q_e = q_m K_L/(1 + K_L C_e)$$

Where, q_m and K_L are the model parameters that will be estimated from the data and q_e is the model output. The predicted model output ($\widehat{q_e}$) is determined by substituting the C_e values from the experiment and replacing the parameters by the parameter estimates ($\hat{\theta}$).

In this case, the sensitivity matrix (X) is an n x 2 matrix with rows:

$X_i := [\ (\partial q_{e,i}/\ \partial q_m)\ \ (\partial q_{e,i}/\partial K_L)]$, for i = 1, 2,…n

Where,

$$(\partial q_{e,i}/\ \partial q_m) = 1 - 1/(C_{e,i}K_L + 1),$$

$$(\partial q_{e,i}/\ \partial K_L) = (C_{e,i}q_m)/(C_{e,i}K_L + 1)^2,$$

After substituting the parameter estimates ($\widehat{q_m}$ and $\widehat{K_L}$) and the measured C_e values (n in total), the sensitivity matrix $X(\hat{\theta})$ is obtained which is used in the calculation of the covariance matrix. In this case, the covariance matrix is a 2 x2 matrix where the square root of the diagonal elements give the standard deviations of the estimated parameters ($\widehat{q_m}$ and $\widehat{K_L}$), respectively.

Text S3: kinetic model

The pseudo second order kinetic model is described by the following equation:

$$q_t = \frac{(k{q_e}^2 t)}{(1 + (kq_e t))}$$

where,

q_t is the adsorption capacity at time t,

k is the rate constant of adsorption (g/mg min),

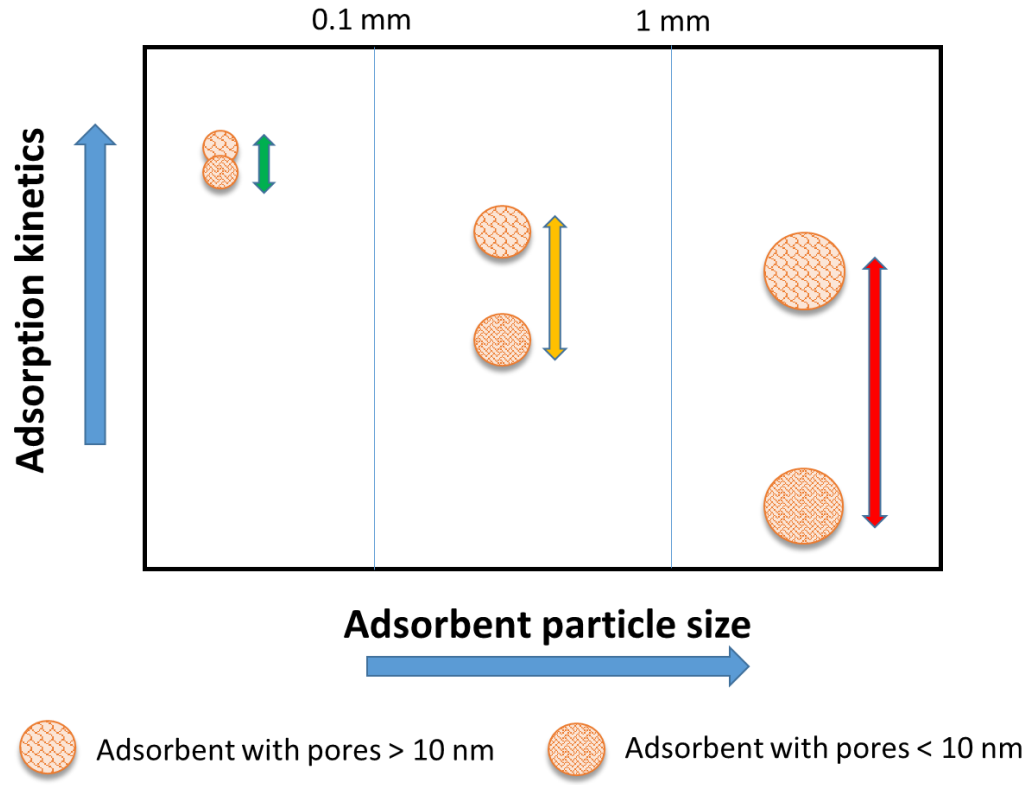
q_e is the adsorption capacity at equilibrium.

The pseudo second order kinetic model predicts the adsorption capacity when equilibrium is reached as indicated by the fitted adsorption capacities in Table S3-8. The difference between the fitted and experimental adsorption capacities after 4 days were less than 5 %. This shows that the experimental conditions had reached close to equilibrium by 4 days.

Chapter - 4

Effect of pore size distribution and particle size of porous metal oxides on phosphate adsorption capacity and kinetics

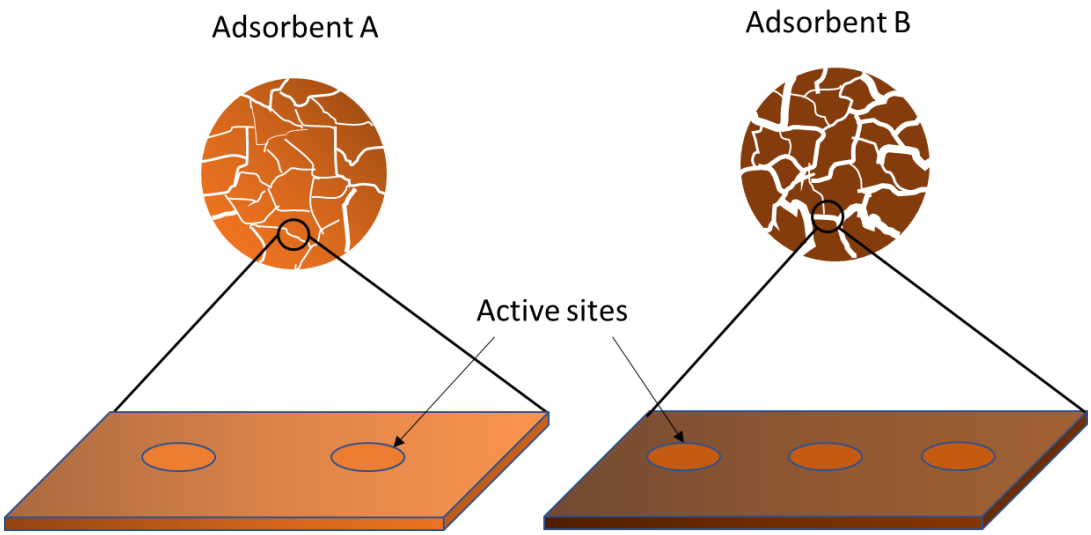
Suresh Kumar, P., Korving, L., Keesman, K.J., van Loosdrecht, M.C.M. and Witkamp, G.-J. (2019) Effect of pore size distribution and particle size of porous metal oxides on phosphate adsorption capacity and kinetics. Chemical Engineering Journal 358, 160-169.



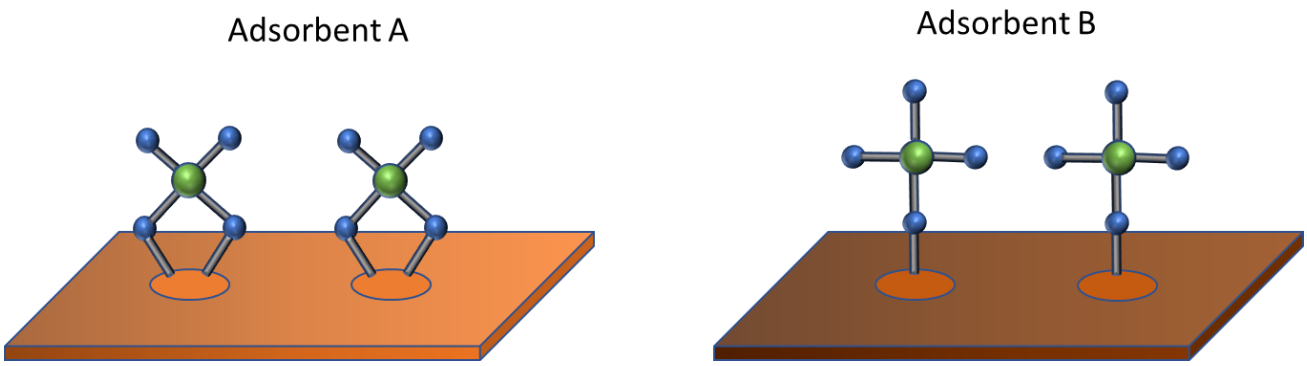
4.1. Prologue

4.1.1. Backdrop

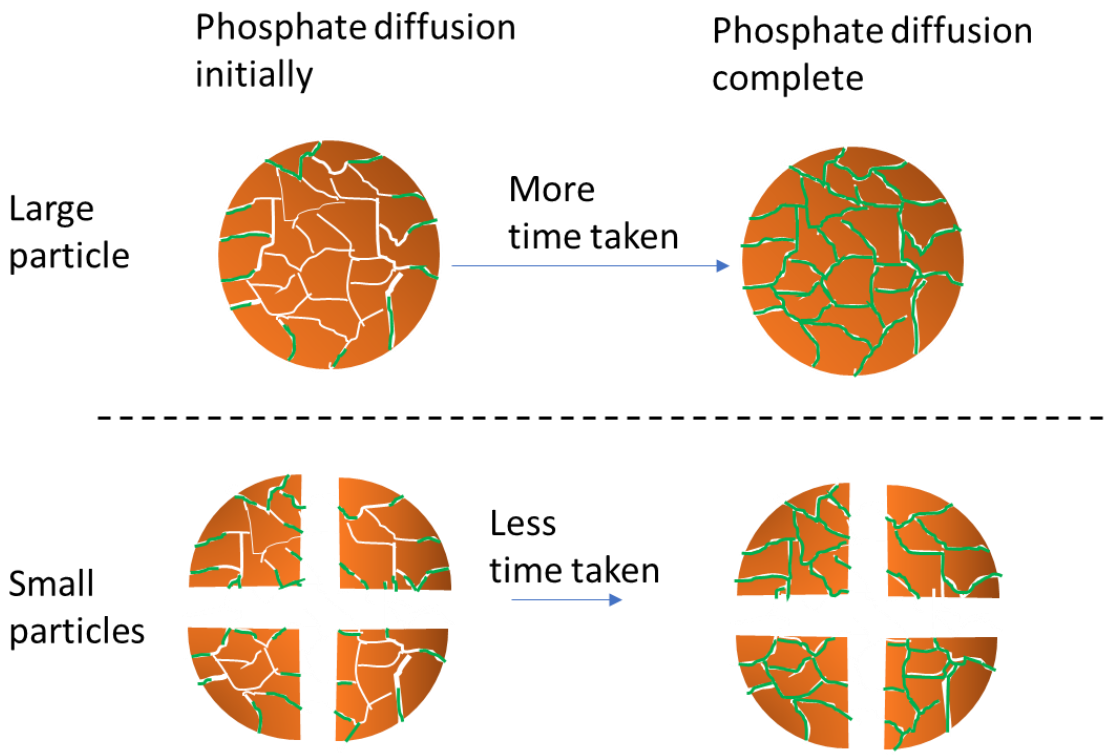
- Granular porous metal oxides offer high specific surface area.
- The specific surface area increases in the presence of small pores like micropores (pore size < 2 nm). But if the pores are very small the transport kinetics of phosphate molecule, which has a diameter of 0.48 nm, will reduce significantly.
- Thus it is important to determine the optimum pore size distribution (PSD) for a phosphate adsorbent.
- Granular porous metal oxides with different PSD are commercially available. But they also have different metal oxide composition, which will also affect their phosphate adsorption.
- For instance, different metal oxides can have different amounts of active sites per unit area.



- Or the surface chemistry can be different, leading to different types of interactions of the phosphate molecule with the active sites.



- Hence for a fair comparison of the effect of PSD on phosphate adsorption, the variation in chemistry needs to be excluded.
- This can be done by grinding the adsorbent into particles of different size. For porous adsorbents, grinding will not result in a significant increase of surface area since the pore sizes are way smaller than the particle sizes.
- For a fixed mass (and hence fixed surface area), smaller particles will have more ports of entry than a larger particle. Thus the time taken for phosphate to diffuse and reach inside all the pores for a given adsorbent mass will be less for smaller particles.



- This difference in time taken for smaller particles as compared to the larger particle is purely based on the effect of PSD and is not influenced by the chemistry.
- The adsorbents with optimum PSD will show the least difference in time taken as a function of particle sizes.

4.1.2. Research questions

i) What will be the pore size that allows for optimum adsorption kinetics?

ii) Can the smallest classification of pores, i.e. micropores (< 2 nm), adsorb phosphate?

iii) How long can it take for a phosphate molecule to diffuse inside the pores and access all the pores of an adsorbent?

4.2. Abstract

Phosphate is a vital nutrient but its presence in surface waters even at very low concentrations can lead to eutrophication. Adsorption is often suggested as a step for reducing phosphate down to very low concentrations. Porous metal oxides can be used as granular adsorbents that have a high surface area and hence a high adsorption capacity. But from a practical point of view, these adsorbents also need to have good adsorption kinetics. The surface area of such adsorbents comes from pores of varying pore size and the pore size distribution (PSD) of the adsorbents can affect the phosphate adsorption kinetics. In this study, the PSD of 4 different adsorbents was correlated with their phosphate adsorption kinetics. The adsorbents based on iron and aluminium (hydr)oxide were ground and the adsorption performance was studied as a function of their particle size. This was done to identify diffusion limitations due to the PSD of the adsorbents. The phosphate adsorption kinetics were similar for small particles of all the adsorbents. For larger particles, the adsorbents having pores larger than 10 nm (FSP and DD6) showed faster adsorption than adsorbents with smaller pores (GEH and CFH). Even though micropores (pores < 2 nm) contributed to a higher portion of the adsorbent surface area, pores bigger than 10 nm were needed to increase the rate of adsorption.

4.3. Introduction

Phosphate is a vital nutrient that is essential for life. It is a key component added in fertilizers for food production and has no substitute (Ashley et al. 2011a, Cordell et al. 2009a). But concentrations of phosphate in surface waters even in the range of 0.01 to 0.1 mg P/L can lead to eutrophication (Carvalho et al. 2013, Richardson et al. 2007). This can happen via discharge from diffuse sources such as agricultural run-offs or point sources such as municipal wastewater treatment plants (Maccoux et al. 2016, Mekonnen Mesfin and Hoekstra Arjen 2017). Eutrophication poses a large risk to the ecosystem resulting in environmental as well as economical damage (Hoagland et al. 2002, Pretty et al. 2003, Smith et al. 1999). Hence there is a need for technology that can effectively reduce the phosphate to concentrations in the sub-microgram levels.

Adsorption is often suggested as polishing technology for reducing contaminants to such low concentrations (Blaney et al. 2007, Genz et al. 2004, Midorikawa et al. 2008). A chief characteristic while developing adsorbents is to improve the adsorption capacity, i.e. the amount of phosphate removed per mass of adsorbent. Since adsorption is a surface reaction, a high surface area is often seen as an important characteristic to improve the adsorption capacity (Deliyanni et al. 2007, Huang et al. 2015). Some studies report high capacity phosphate adsorbents by using nanoparticles which have a high surface area (Moreira et al. 2017, Recillas et al. 2012, Su et al. 2013). But such adsorbents are difficult to apply from a practical viewpoint due to difficulty in recovery or pressure drop related problems. These problems are overcome by immobilizing adsorbent particles in high surface area granular backbones (Chubar et al. 2005, Suresh Kumar et al. 2017, Zach-Maor et al. 2011b). Another way is to use granular

porous metal oxides, where the pores give rise to a high surface area (Boels et al. 2012, Genz et al. 2004, Lalley et al. 2015). The surface area of such porous metal oxides is contributed by pores of varying size. Depending on the size of the pores as well as their arrangement, their accessibility by phosphate molecules could be affected. Moreover, the diffusion of phosphate into such pores could also get affected, which in turn will affect the adsorption kinetics. In this study, we address the effect of adsorbent pore size distribution (PSD) on the accessibility as well as diffusion of phosphate ions.

Four different granular porous metal oxide adsorbents were tested for phosphate adsorption. Three of them are based on iron oxides, namely: granular ferric hydroxide (GEH), FerroSorp Plus (FSP), compacted ferric (hydr)oxides (CFH). The other adsorbent, called DD6, is based on aluminium oxides. These adsorbents have been studied due to their varying PSD and because iron and aluminium (hydr)oxides are known for their good phosphate adsorption properties. These adsorbents have different chemical properties owing to the difference in their metal oxide composition. The type of metal oxide varies its properties like crystallinity, type and amount of surface functional groups, surface charge (Barrón and Torrent 1996, Chitrakar et al. 2006, Cornell and Schwertmann 2004a). Hence the differences in phosphate adsorption from such adsorbents cannot be related directly to the PSD. To overcome this challenge, the different adsorbents were ground to varying particle sizes of 0 to 0.1 mm, 0.4 to 0.5 mm and 1 to 1.25 mm. Grinding porous adsorbents does not significantly influence their surface area since a majority of their area comes from pores smaller than 50 nm, which are way smaller than the particle size (Table S4-5 in supporting information). In such a case, reducing the particle size will mainly reduce the path length for diffusion inside the adsorbent (Karau et al. 1997, Liese and Hilterhaus 2013). Hence by comparing adsorption performance between the different particle sizes of the same adsorbent, the effect due to chemical properties and surface area is excluded and the difference in adsorption is only due to diffusion limitation, which can be directly correlated with the PSD.

The aim of this study is to give insights on the optimum PSD that can provide accessible surface area and faster diffusion for phosphate adsorption. This will thus help in designing an adsorbent that has a high phosphate adsorption capacity along with good adsorption kinetics.

4.4. Materials and methods

4.4.1. Chemicals

Potassium dihydrogen phosphate (KH_2PO_4), hydrochloric acid (HCl) and sodium hydroxide (NaOH) were obtained from VWR chemicals. MOPS (3-(N-morpholino)propanesulfonic acid) was purchased from Sigma Aldrich. Granular ferric hydroxide (GEH), Ferrosorp Plus (FSP), compacted ferric hydroxide (CFH) were provided by GEH Wasserchemie Gmbh, HeGO Biotech Gmbh, and Kemira, respectively. DD6 was purchased from BASF.

4.4.2. Phosphate adsorption kinetic experiments

The different adsorbents were ground and sieved to give 3 particle size ranges: 0 to 100 µm, 400 to 500 µm, 1 to 1.25 mm. An aqueous solution of phosphate with a concentration of 25 mg P/L was prepared in MilliQ water. MOPS has been known to be a non-chelating agent and

hence was used as the buffering agent (Mao et al. 2012). A concentration of 20 mM of MOPS was used and the solution pH was adjusted to 7.2 with HCl and/or NaOH. The adsorbent dose was 0.2 g (dry weight) in 100 ml phosphate solutions, resulting in an adsorbent concentration of 2 g/L. The adsorption process happened in a shaking incubator at 21 °C and 250 rpm. The kinetics were determined by measuring the phosphate concentrations at time intervals of 30 mins, 1, 3, 6 h, 1, 2, 3, 4, 7 days, and 1, 2, 3 months. The shaking speed (or stirring rate) affects the external transfer from the bulk solution to the adsorbent boundary layer but not the internal diffusion to the adsorbent pores (Corma et al. 1990, Liese and Hilterhaus 2013, Urano and Tachikawa 1991). Thus it is enough to use a shaking speed that overcomes external mass transfer resistance. The shaking speed used here was based on the range provided by other studies involving porous phosphate adsorbents (Shin et al. 2004, Urano and Tachikawa 1991, Zach-Maor et al. 2011b).

4.4.3. Phosphate adsorption isotherm experiments

The different adsorbents of the aforementioned particle size ranges were added to 100 ml solutions with phosphate concentrations of 1, 5, 10, 15, 25, 50, 75 and 100 mg P/L. MOPS buffer of 20mM concentrations was used to buffer the pH which was adjusted to 7.2. The adsorbent concentration was 2 g/L. The adsorption process happened in a shaking incubator at 21 °C and 250 rpm. The adsorption process was continued till 7 days after which the phosphate concentrations were measured.

4.4.4. Analysis

Phosphate concentration was measured by ion chromatography (Metrohm Compact IC Flex 930). All samples were filtered by 0.45 µm membrane before analysis. The types of iron oxide in GEH, FSP, and CFH were determined using Mössbauer spectroscopy. Transmission ^{57}Fe Mössbauer spectra were collected at different temperatures with conventional constant acceleration and sinusoidal velocity spectrometers using a ^{57}Co (Rh) source. Velocity calibration was carried out using an α-Fe foil. The Mössbauer spectra were fitted using the Mosswin 4.0 program. The type of aluminium oxide in the adsorbent DD6 was measured by X-Ray Diffraction (XRD). The XRD measurements were carried out using a PANalytical X'Pert pro X-ray diffractometer mounted in the Bragg-Brentano configuration with a Cu anode (0.4 mm x 12 mm line focus, 45 kV, 40 mA). For determining the surface area of the adsorbents, nitrogen adsorption and desorption cycles were carried out using Micromeritics TriStar 3000. The data from the nitrogen adsorption-desorption profiles were fitted with models included in the analysis software to obtain the pore area from Non Local Density Functional Theory (NLDFT).

4.4.5. Data fitting and error analysis

All the adsorption experiments were run as duplicates and the average value was reported with standard deviation. For adsorption isotherms and pseudo second order kinetic models, model parameters were fitted with non-linear regression using Microsoft Excel's solver program. The standard deviation of the parameter estimates ($\hat{\theta}$) were calculated using the covariance matrix, which is expressed as follows:

$$Cov\left(\hat{\theta}\right) = \frac{SSE\left(\hat{\theta}\right)}{n-p}\left(X\left(\hat{\theta}\right)^{T}X\left(\hat{\theta}\right)\right)^{-1}$$

Where,

n denotes the number of samples, p denotes the number of parameters, SSE ($\hat{\theta}$) denotes the sum of squared error between the experimental data and fitted model output, X($\hat{\theta}$) denotes the sensitivity matrix. The sensitivity matrix is calculated by analyzing the sensitivity of each parameters separately by ± 10% of their optimum value and quantifying the change in model output. The standard deviation of the parameter estimates are calculated by taking squathe re root of the diagonal of the covariance matrix.

The Root Mean Square Error (RMSE) is used as a measure of goodness of fit and is calculated as follows:

$$\text{RMSE } \hat{\theta} = \sqrt{\frac{SSE(\hat{\theta})}{n-p}}$$

Where SSE ($\hat{\theta}$), n and p denote the same parameters as used in the covariance matrix.

Non-linear regression was used for the isotherm and kinetic models to avoid inaccuracies that occur due to the linearization of such models (Osmari et al. 2013, Subramanyam and Das 2009). While the coefficient of determination (R^2) can be used as a measure for the goodness of fit of linear models, they are not suitable for non-linear regression (Spiess and Neumeyer 2010). Hence, in this case, the RMSE, which is the standard deviation of residuals (the difference between observed and fitted value) is used as a goodness of fit, with a lower RMSE value indicating a better fit. Moreover, the covariance matrix indicates the uncertainty in the parameter estimates and thus is also indicative of the nature of the fit (Keesman 2011).

4.5. Results and discussion

4.5.1. Adsorbent characteristics

Table 4-1 shows the different characteristics of the adsorbents used. The type of metal oxide for iron based adsorbents was determined using Mössbauer spectroscopy (Mössbauer parameters shown in Table S4-6 in supporting information). The type of metal oxide for the aluminium based adsorbent DD6 was determined using XRD (Figure S4-8 in supporting information shows the spectrogram).

Table 4-1: *Adsorbent characteristics*

Adsorbent	Type and proportion of constituent metal oxide(s)	Total pore area (m^2/g)[a]
GEH	Hematite – 11 %	244
	Ferrihydrite – 89 %	
FSP	Ferrihydrite – 100 %	179
CFH	Goethite/Hematite – 43 %	119
	Ferrihydrite/Lepidocrocite – 57 %	
DD6	Aluminium oxide hydroxide – 34 %	235
	Aluminium oxide – 66 %	

[a]- The total pore area shown here is for the adsorbents of size 1 to 1.25 mm. However, the area of the adsorbents showed little change (a maximum change of < 5 %) when the particle sizes were reduced (Table S4-5 in supporting information).

As can be seen from Table 4-1, FSP and GEH predominantly comprised of ferrihydrite, although GEH had a small fraction of hematite. For CFH, the hyperfine fields could not be exactly assigned to a specific iron oxide and hence it could be a combination of iron oxides that include lepidocrocite as well as goethite. The XRD spectra of DD6 included peaks that corresponded to aluminium oxide as well as aluminum oxide hydroxide. The result shows that most of the adsorbents had a mixture of metal oxide types. This would lead to having heterogeneous sites for adsorption.

The total pore area was determined using the Non-Linear Density Functional Theory (NLDFT) model, incorporated within the software of the Micrometric nitrogen adsorption analyzer. The International Union of Pure and Applied Chemistry (IUPAC) classifies porous materials into 3 categories based on the pore diameters; namely, micropores (< 2 nm), mesopores (2 to 50 nm) and macropores (> 50 nm) (Rouquerol et al. 1994, Sing 1985). Gas adsorption and desorption profiles can be fitted with different models (inbuilt within the Micrometric software) to obtain information like the specific surface area, pore volume and pore size distribution (Sing 2001b). While meso and macropores can be described by the classic/macroscopical models like BJH (Barret-Joyner-Halenda), the accurate description of micropores requires more modern models like NLDFT (Barrett et al. 1951, Cracknell et al. 1995). The mechanism of pore filling constitutes the main difference between these models. BJH model assumes that pore filling via pore condensation constitutes well-defined interfaces in the pores. While this works for macropores and to the larger mesopores, the adsorptive potential between adsorbate and adsorbent plays a major influence in the condensation and evaporation from smaller mesopores and micropores (Cracknell et al. 1995). The NLDFT model takes into account the differences in thermodynamic properties of a bulk fluid vs a fluid confined in pores (Thommes 2004). Thus, it is able to give a more accurate description of the micro and mesopores.

To get a complete picture of micro, meso and macropores, the adsorbents used were characterized using both the NLDFT and the BJH model (Figure S4-9 in supporting information). The pore size distribution (PSD) of the adsorbents as determined by the NLDFT method is shown in Figure 4-1. Henceforth, the term surface area actually implies the pore area.

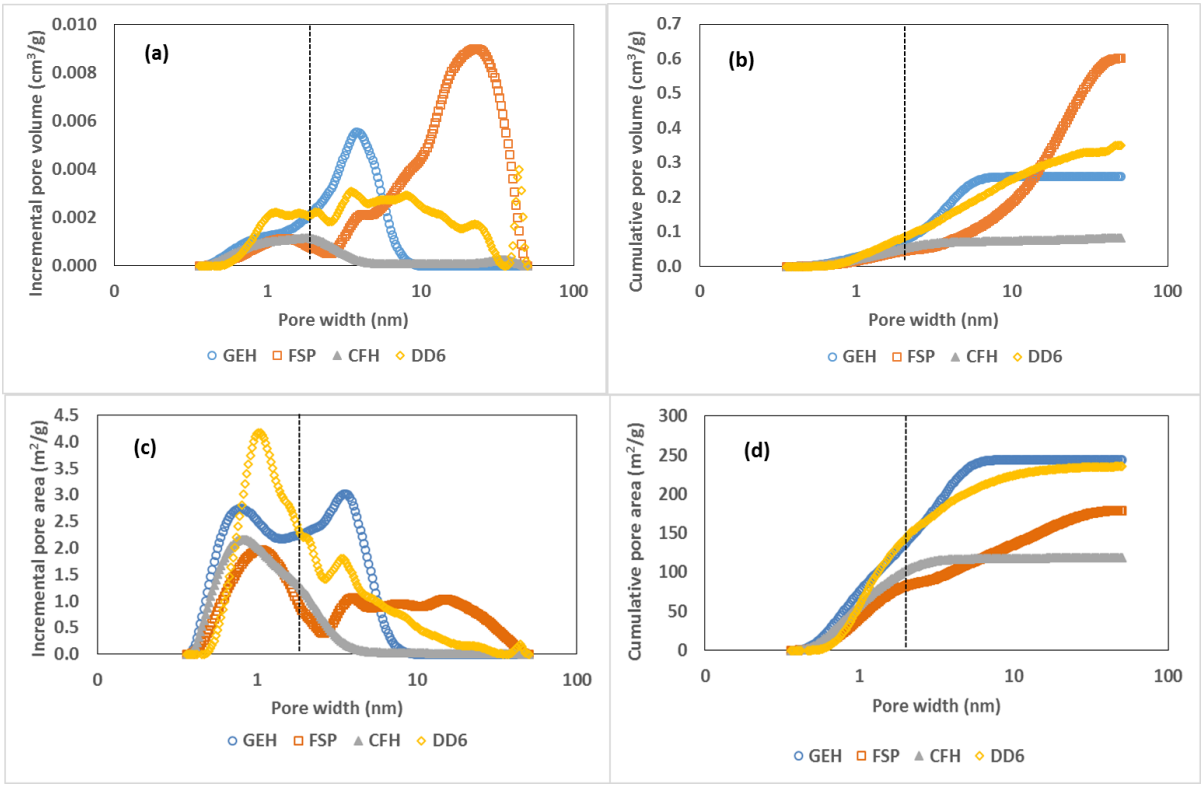


Figure 4-1: (a) Incremental and (b) Cumulative pore volume of different adsorbents as determined by the NLDFT method. (c) Incremental and (d) Cumulative pore area for the corresponding adsorbents. The dashed lines within the plots show the cut off (2 nm) between micro and mesopores.

As seen in Figure 4-1, the adsorbents had very different PSD. Figure 4-1 (a and b) show that the GEH and CFH had pores smaller than 10 nm. FSP and DD6, on the other hand, had a significant fraction of pore volume resulting from pores bigger than 10 nm. Figure 4-1 (c and d) show the area resulting from the corresponding pores in the adsorbent. This shows that GEH had significant pore area resulting from micropores as well as mesopores smaller than 10 nm, whereas CFH had a majority of pore area from the micropores. FSP and DD6 had pore area resulting from pores greater than 10 nm as well. Figure 4-2 shows the relative fraction of micropore area, and mesopore areas that are between 2 and 10 nm, and between 10 and 50 nm.

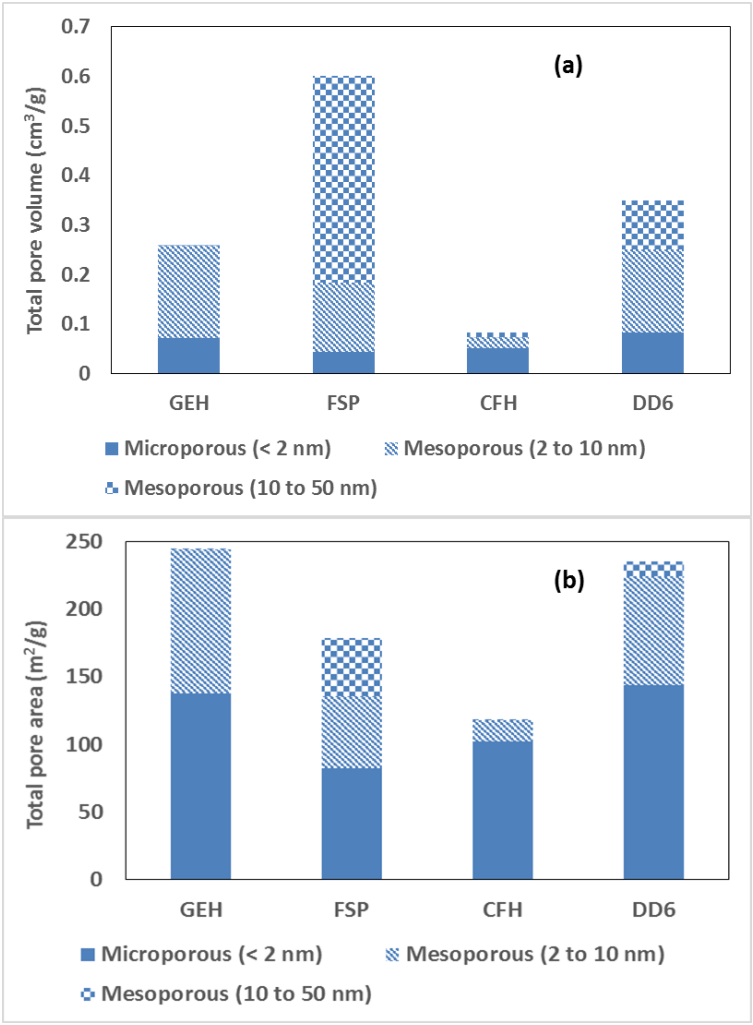


Figure 4-2: Relative fractions for microporous, mesoporous (a) pore volume and (b) pore area in the different adsorbents. The mesoporous fraction is split further at the cut-off of 10 nm.

Figure 4-2 shows that even though the pore volume resulting from micropores is lower than that from the mesopores for all adsorbents, the pore area of micropores has a significantly higher fraction. This was to be expected since smaller pores will have the highest area to volume ratio. Figure 4-2 also shows that FSP has the highest amount of surface area resulting from pores bigger than 10 nm, followed by DD6. CFH and GEH have little to no surface area resulting from such pores. The area contributed by macropores was also negligible (Figure S4-9 in supporting information). Since adsorption is a surface phenomenon depending on the area, very little phosphate adsorption will happen in macropores compared to micropores and mesopores. Nevertheless, macropores can still play a role by allowing faster diffusion of phosphate (Végh et al. 1990).

4.5.2. Adsorption kinetics for varying particle sizes and correlation with the PSD

The adsorption kinetics were done with varying particle sizes to understand how phosphate diffusion through the pores is affected by varying path lengths for diffusion. All the adsorbents were ground between 3 particle size ranges: 1 to 1.25 mm, 0.4 to 0.5 mm, and 0 to 0.1 mm, henceforth called large, medium and small, respectively. Figure 4-3 shows the adsorption kinetics for the different particle sizes of all adsorbents.

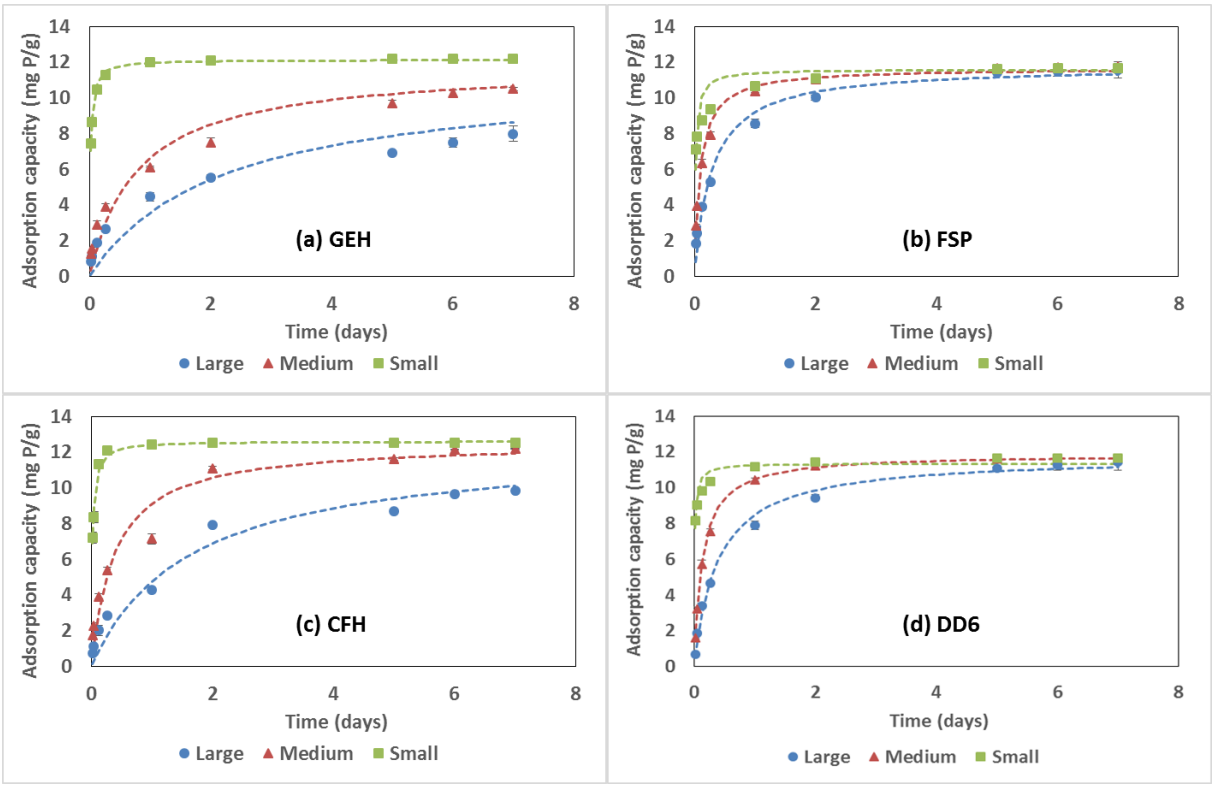


Figure 4-3: Adsorption kinetics for different sizes of adsorbents (a) GEH (b) FSP (c) CFH (d) DD6. Dashed lines represent fit by the pseudo second order kinetics.

As seen in Figure 4-3, the small particles of all adsorbents reached equilibrium by 7 days. For FSP and DD6, the large particles also almost reached equilibrium in 7 days. However, this was not the case for the large particles of GEH and CFH. To find out the time required to reach equilibrium for these particles, the adsorption kinetic experiments were prolonged. It was found that it took between 60 to 90 days for the large particles of GEH and CFH to reach equilibrium (see Figure 4-4). This is a significantly longer time than reported in most phosphate adsorption studies and shows that these adsorbents show severe diffusion limitation. As will be elaborated in the following sections, this is related to the PSD of these adsorbents.

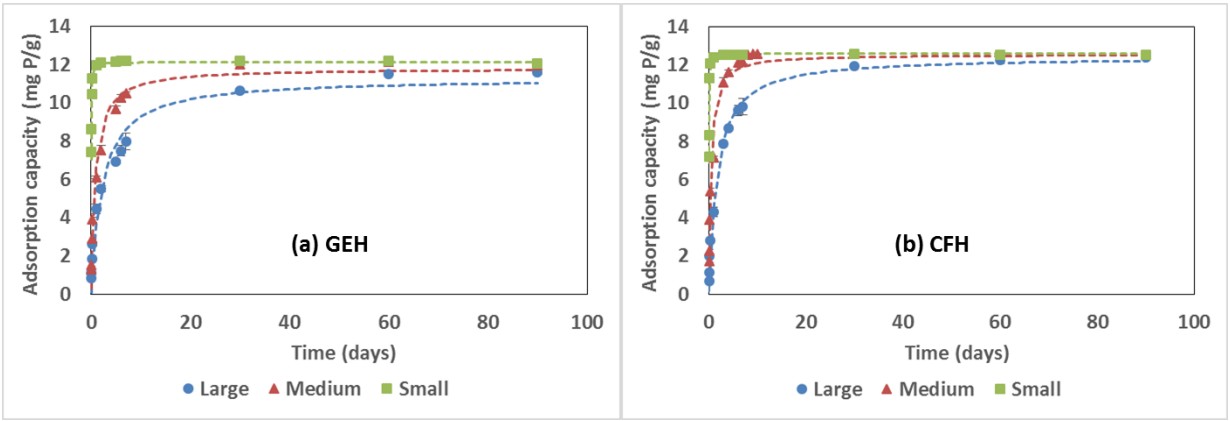


Figure 4-4: Adsorption kinetics performed up to 90 days as a function of different particle sizes for (a) GEH (b) CFH

To correlate these differences with the pore size distribution, the adsorption kinetics needed to be modeled. A pseudo second order kinetic model was chosen due to its basic nature and it has been commonly used for fitting phosphate adsorption kinetics (Drenkova-Tuhtan et al. 2017, Jung et al. 2017, Park et al. 2017). It is described by the following expression:

$$q_t = \frac{(kq_e{}^2 t)}{(1 + (kq_e t))}$$

where q_t is the adsorption capacity at time t, k is the adsorption rate constant (g/mg min),

q_e is the adsorption capacity at equilibrium.

The parameters estimated from the pseudo second order kinetic model are shown in Table 4-2. The rate constant obtained from the pseudo second order model for different adsorbents was plotted as a function of the adsorbent particle size (Figure 4-5).

Table 4-2: Pseudo second order kinetic model fitted parameters

Adsorbent/ Particle Size	**Large**	**Medium**	**Small**
GEH	q_e(mg P/g) = 11.3 ± 2.1 k (g/mg min) = 2.8 x 10^{-5} ± 2.6 x 10^{-6} RMSE = 0.9	q_e(mg P/g) = 11.8 ± 0.9 k (g/mg min) = 7.5 x 10^{-5} ± 9.6 x 10^{-6} RMSE = 0.8	q_e(mg P/g) = 12.1 ± 0.1 k (g/mg min) = 3.8 x 10^{-3} ± 1.8 x 10^{-4} RMSE = 0.2
FSP	q_e(mg P/g) = 11.8 ± 0.4 k (g/mg min) = 2.1 x 10^{-4} ± 9.5 x 10^{-6} RMSE = 0.6	q_e(mg P/g) = 11.7 ± 0.3 k (g/mg min) = 6.2 x 10^{-4} ± 5 x 10^{-5} RMSE = 0.4	q_e(mg P/g) = 11.6 ± 0.4 k (g/mg min) = 3.1 x 10^{-3} ± 2.1 x 10^{-4} RMSE = 0.9
CFH	q_e(mg P/g) = 12.4 ± 1.2 k (g/mg min) = 3.4 x 10^{-5} ± 1.7 x 10^{-6} RMSE = 0.6	q_e(mg P/g) = 12.6 ± 0.5 k (g/mg min) = 1.5 x 10^{-4} ± 2.1 x 10^{-5} RMSE = 0.8	q_e(mg P/g) = 12.6 ± 0.1 k (g/mg min) = 3.1 x 10^{-3} ± 4.7 x 10^{-4} RMSE = 0.2
DD6	q_e(mg P/g) = 11.8 ± 0.5 k (g/mg min) = 1.5 x 10^{-4} ± 3.5 x 10^{-6} RMSE = 0.4	q_e(mg P/g) = 11.9 ± 0.2 k (g/mg min) = 4.4 x 10^{-4} ± 3.1 x 10^{-5} RMSE = 0.2	q_e(mg P/g) = 11.3 ± 0.2 k (g/mg min) = 6.3 x 10^{-3} ± 2.9x 10^{-4} RMSE = 0.4

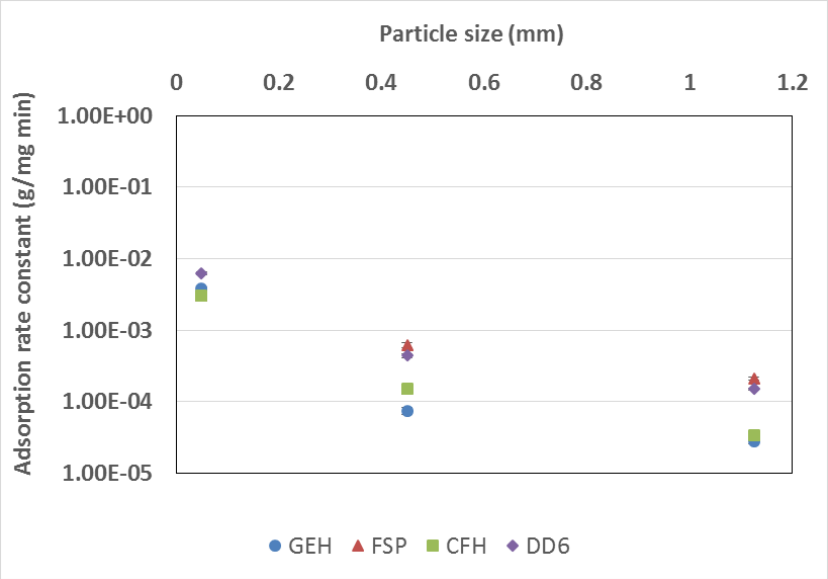


Figure 4-5: rate constants as a function of particle size of different adsorbents. Particle sizes were considered as 0.05 mm, 0.45 mm, 1.125 mm since they represented the average values between the particle size ranges of 0 t 0.1, 0.4 to 0.5 and 1 to 1.25 mm. The adsorption rate constant is presented on a log scale.

As can be seen from Table 4-2 and Figure 4-5, the rate constants for the small particle size of all adsorbents were in the same order of magnitude. However, as the particle size increased (> 0.4 mm) the rate constants for the different adsorbents varied as much as by an order of magnitude. For the large adsorbent particles, FSP and DD6 had rate constants that were higher by one order of magnitude compared to GEH and CFH. This implied the adsorption rate was higher for the large particles of FSP and DD6 compared to GEH and CFH, which can be seen from Figure 4-3.

A ratio of the rate constant of the small (K_{Small}) to the large adsorbent (K_{Large}) can be used as an indication of the extent of diffusion limitation in this case. If this ratio of K_{Small}/K_{Large} is lower, this implies the adsorption kinetics is less affected by varying the particle size. To correlate this effect with the PSD, the ratio of the rate constant of small to the large adsorbent particles (K_{Small}/K_{Large}) was plotted against the pore area resulting from micropores (< 2 nm), pores between 2 to 10 nm, and pores greater than 10 nm, as shown in Figure 4-6.

As can be seen from Figure 4-6, GEH and CFH had a significantly higher K_{Small}/K_{Large} value than FSP and DD6, which correlates with the observation in Figure 4-3 regarding the adsorption kinetics. Also, Figure 4-6 (a and b) shows that no clear correlation could be made between the K_{Small}/K_{Large} values of the different adsorbents and the microporous area and the area resulting from pores between 2 to 10 nm. For instance, GEH had a higher microporous area as well as the area from pores between 2 to 10 nm, but still showed a higher variation in the adsorption kinetic constants. This implies that the adsorption kinetics are not dominated by the pores in the size ranges that are smaller than 10 nm.

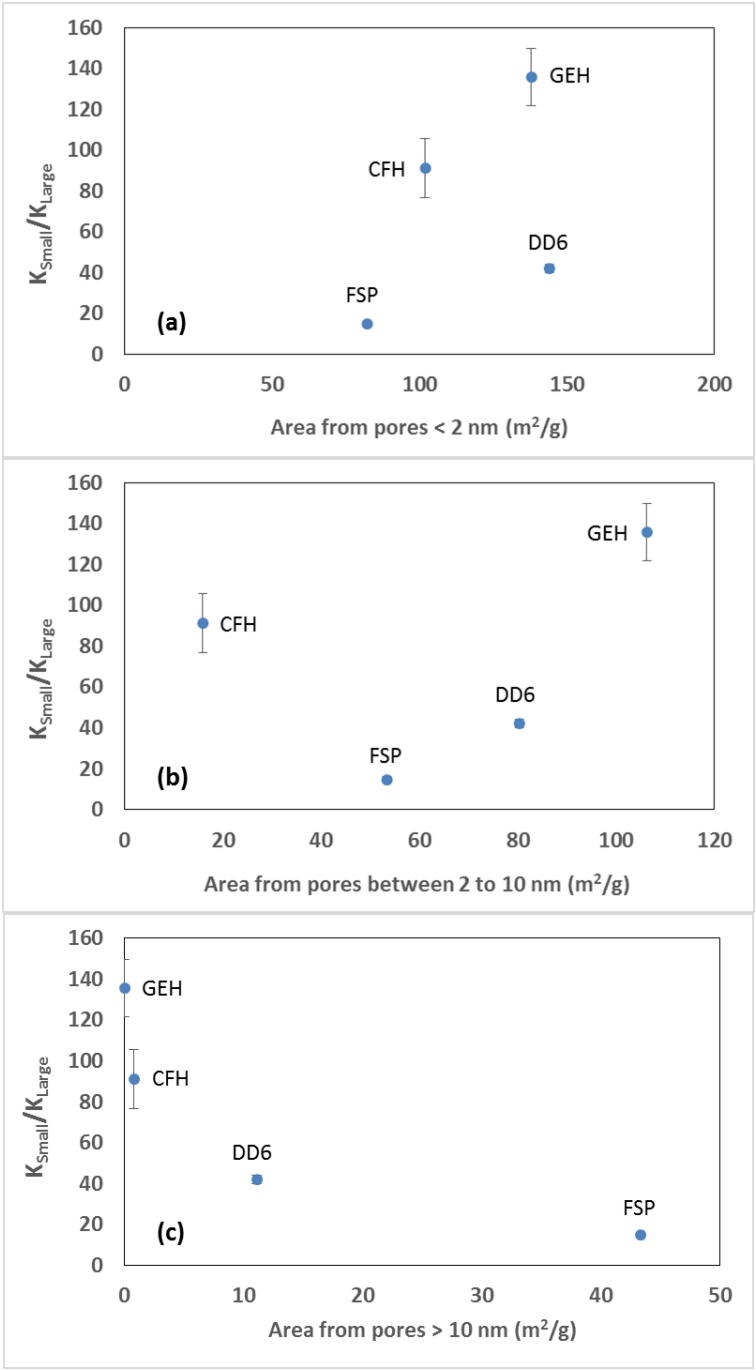


Figure 4-6: Ratio of rate constants from pseudo second order kinetic model of small (0 to 0.1 mm) to large particles (1 to 1.25 mm) for the different adsorbents as a function of (a) Area by pores less than 2 nm (b) Area by pores between 2 to 10 nm (c) Area by pores greater than 10 nm.

However, a correlation could be observed between K_{Small}/K_{Large} values of the adsorbents and the area resulting from pores bigger than 10 nm (Figure 4-6 c). The K_{Small}/K_{Large} values varied inversely with the area resulting from pores bigger than 10 nm. In practice, the rate constant for a smaller particle will always be higher than the rate constant for a larger particle of the corresponding adsorbent. Thus K_{Small}/K_{Large} value will always be higher than 1. The plot in Figure 4-6 (c) is in line with this expected asymptote at value 1 as the area from pores bigger than 10 nm keeps increasing. This correlation was also observed with the pore volume from

such mesopores (Figure S4-10 in supporting information). This shows that having pores bigger than 10 nm is crucial for improving the phosphate adsorption kinetics of granular porous metal oxides.

4.5.3. Adsorption isotherms for varying particle sizes

Adsorption isotherms are an important tool that provide phosphate adsorption capacities over a wide range of phosphate concentration. The adsorption kinetics experiment showed that the small sized particles of all adsorbents reached equilibrium by 7 days. Thus the adsorption isotherms were run for 7 days for all the particle sizes to see the effect of diffusion limitation over different phosphate concentrations. Figure 4-7 shows the adsorption isotherms of the different adsorbents of the varying particle sizes after allowing adsorption for 7 days.

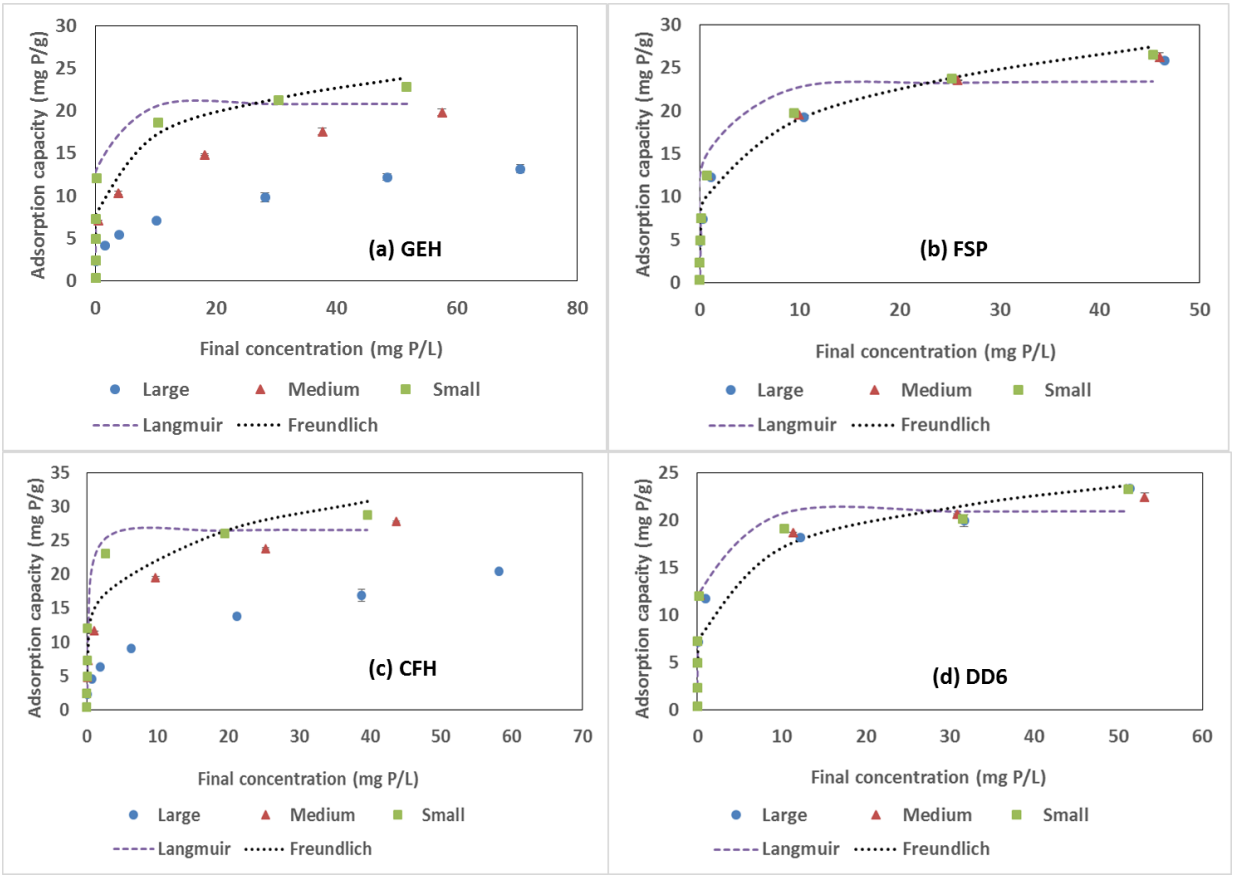


Figure 4-7: Adsorption capacities as a function of final concentration after 7 days for different sizes of adsorbents (a) GEH (b) FSP (c) CFH (d) DD6. The dashed plot shows the fits with Langmuir and Freundlich models of the small adsorbent particles.

Figure 4-7 shows that for the small particles of all adsorbents, similar experimental adsorption capacities around 25 mg P/g were observed at final concentrations of 40 to 50 mg P/L. Moreover the adsorption isotherms for the different adsorbents correlated with the observations in the adsorption kinetic studies. That is, varying particle sizes of FSP and DD6 showed similar

adsorption profiles. This agrees with the fact that these adsorbents reached equilibrium by 7 days for all particle sizes. GEH and CFH, on the other hand, showed differences in the adsorption profiles between the varying particle sizes. This agrees with the fact that the medium and larger sized granules of such adsorbents need a much longer time for reaching equilibrium. Modeling the equilibrium adsorption data allows the prediction of adsorption capacities at different phosphate concentrations. As seen earlier, the small particles had reached equilibrium by 7 days for all the adsorbents. Hence the isotherms from the small sized adsorbent particles were chosen to be modeled.

The Langmuir and Freundlich adsorption isotherm models are commonly used for describing phosphate adsorption (Deliyanni et al. 2007, Genz et al. 2004, Guzmán et al. 1994, Wang et al. 2013a).

The Langmuir expression is:

$$q_e = \frac{q_m K_L C_e}{(1 + K_L C_e)}$$

Where, q_m = Maximum adsorption capacity (mg P/g),

q_e = Adsorption capacity at equilibrium (mg P/g),

C_e = Concentration at equilibrium (mg P/L),

K_L = Langmuir isotherm constant (L/mg P).

The Freundlich expression is: $q_e = K_F {C_e}^n$

Where, q_e = Adsorption capacity at equilibrium (mg P/g),

C_e = Concentration at equilibrium (mg P/L),

n = Adsorption intensity (heterogeneity factor),

K_F = Freundlich isotherm constant ((mg P/g)/(mg P/L)^n)

Since phosphate adsorption onto metal oxides happens by ligand exchange/chemisorption (thus excluding multilayer adsorption), the main difference between the assumptions of Langmuir and Freundlich models, in this case, lies in the nature of the active sites for adsorption. Langmuir model assumes homogenous active sites, whereas the Freundlich model assumes heterogenous active sites (Foo and Hameed 2010, Freundlich 1907, Langmuir 1918). Thus the Freundlich model implies that phosphate will bind on the adsorbent at active sites having the different heat of adsorption and affinities (Foo and Hameed 2010). Table 4-3 shows the fitted values of the parameters from these models and the corresponding Root Mean Square Error (RMSE).

Table 4-3: Isotherm parameters for small particles of different adsorbents

Adsorbent/ Isotherm model	Freundlich	Langmuir
GEH	K_F ((mg P/g)/(mg P/L)^n) = 10.8 ± 3.7 n = 0.2 ± 0.1 RMSE = 2.8	K_L (L/mg P) = 7.6 ± 1 q_m (mg P/g) = 20.9 ± 1.8 RMSE = 1.7
FSP	K_F ((mg P/g)/(mg P/L)^n) = 10.9 ± 1.8 n = 0.2 ± 0.05 RMSE = 2	K_L (L/mg P) = 2.3 ± 1.7 q_m (mg P/g) = 23.6 ± 1 RMSE = 2.7
CFH	K_F ((mg P/g)/(mg P/L)^n) = 13.9 ± 4.2 n = 0.2 ± 0.09 RMSE = 4	K_L (L/mg P) = 7.6 ± 1.1 q_m (mg P/g) = 26.6 ± 1.5 RMSE = 1.9
DD6	K_F ((mg P/g)/(mg P/L)^n) = 10.8 ± 4.2 n = 0.2 ± 0.1 RMSE = 2.9	K_L (L/mg P) = 8.4 ± 0.9 q_m (mg P/g) = 20.9 ± 1.7 RMSE = 1.6

As can be seen from the RMSE values in Table 4-3, the Langmuir model gave a better fit than the Freundlich model for all adsorbents except FSP. However, it can be seen from Figure 4-7 that neither adsorption model fitted the experimental data perfectly over the complete range of phosphate concentrations. The Langmuir model gave a better fit over the lower concentration ranges and the Freundlich model gave a better fit over the higher concentration ranges. Since most of the adsorbents comprised of multiple phases/types of metal oxides, it could be that at

lower phosphate concentrations one of the metal oxides were preferred for phosphate adsorption thus resembling the Langmuir fit better. At higher phosphate concentration, the fraction of active sites occupied by other metal oxide phases might become important as well. This would lead to a heterogeneous nature of adsorption and thereby resemble the Freundlich fit better at such concentrations.

Another explanation could be the formation of surface precipitates at higher phosphate concentration (Li and Stanforth 2000). Even though the adsorbents were washed with MilliQ (deionized) water before the adsorption experiments, during the course of 7 days, some soluble components of the adsorbent (e.g. iron and aluminium) inside the pores might result in surface precipitation with phosphate. Surface precipitation will follow a reaction mechanism that will be different than adsorption (Li and Stanforth 2000). This will show an increased removal and hence might lead to a higher apparent adsorption capacity than the monolayer adsorption predicted by the Langmuir model.

The adsorption isotherms can help get an estimate of the fraction of the adsorbent surface area covered by phosphate at different equilibrium concentrations. The phosphate molecule has a diameter of about 0.48 nm (Tawfik and Viola 2011b), and assuming a monolayer, this approximately translates to a cross-sectional area of 3.5 m^2/mg P. Table 4-4 shows the fractions of adsorbent surface area occupied at the maximum adsorption capacity and the adsorption capacity at an equilibrium phosphate concentration of 0.1 mg P/L ($q_{0.1}$) as estimated from the Langmuir equation. $q_{0.1}$ is relevant considering the need for achieving very low concentrations of phosphate via adsorption.

Table 4-4: Fraction of adsorbent surface area occupied at maximum adsorption capacity and adsorption capacity at an equilibrium concentration of 0.1 mg P/L, i.e. $q_{0.1}$. The fraction of the surface area occupied is calculated assuming monolayer coverage, and the $q_{0.1}$ is calculated using the Langmuir equation.

Adsorbents	**q_m (mg P/g)**	**Fraction of surface area occupied at q_m (%)**	**$q_{0.1}$ (mg P/g)**	**Fraction of surface area occupied at $q_{0.1}$ (%)**
GEH	20.9	30	9	13
FSP	23.6	46	4.4	9
CFH	26.6	78	11.5	34
DD6	20.9	31	9.5	14

Table 4-4 shows that CFH had the highest fraction of adsorbent surface coverage for both q_m as well as $q_{0.1}$. In all other cases, less than $1/7^{th}$ of the adsorbent surface area is occupied at $q_{0.1}$. This shows that only a small fraction of the adsorbent surface area is covered at equilibrium

phosphate concentrations of 0.1 mg P/L. Another conclusion that can be drawn from this observation is regarding the contribution of micropores. CFH has about 85 % of its surface area coming from micropores (Figure 4-2 b) and the occupancy by phosphate is between 34 to 78 % of the surface area of CFH. Thus, it can be concluded that the micropores do contribute to phosphate adsorption.

4.5.4. Possible explanations for diffusion limitation

The severe diffusion limitation shown by larger adsorbent particles for GEH and CFH can be seen from the adsorption kinetics (Figure 4-3 and Figure 4-4). By modeling with the pseudo second order kinetic model, it could be shown that pores bigger than 10 nm are essential for allowing fast transport of phosphate through the adsorbent. While the pseudo second order kinetic model was useful in correlating the adsorption kinetics to the PSD, it is an empirical model and does not give an insight into the mechanism of phosphate adsorption kinetics (Russo et al. 2017). The adsorption kinetics were thus also modeled by a pore diffusion model (PDM), which is a more mechanistic model considering Fick's laws of diffusion for estimating the effective pore diffusivity and external film mass transfer coefficient (Boels et al. 2012). However, this model gave a poorer fit than the pseudo second order model and hence was not considered further. Amongst the major limitations from the current PDM is the fact that it considers the adsorbent particle size to be all the same. In practice, the adsorbents will have a particle size distribution. Moreover, it takes into account the adsorbent particle porosity, but it does not differentiate between the porosity contributed by micro, meso or macropores. Also, adsorption could be happening via a combination of pore and surface diffusion (Russo et al. 2015), in which case pore diffusion alone will not be able to give a sufficient description.

Moreover, it is not just the PSD, but also the 3-dimensional arrangement of the pores that would play a key role in the diffusion of an adsorbate ion through the adsorbent (Zhou et al. 2011). Techniques such as focused ion beam scanning electron microscopy (FIBSEM) can be used to obtain 3D information of porous structures (Prill and Schladitz 2013). A phosphate molecule has a size of 0.48 nm and once they are adsorbed in micropores (pore width < 2 nm), they could hinder the subsequent transport of other phosphate molecules through the micropores. This will also depend on the arrangement of micropores, i.e. if they are highly branched or exist as long isolated cylinders. In the latter case, the adsorbed phosphate molecule has to diffuse along the surface before a subsequent phosphate molecule can travel through the pore and adsorb. The diffusion could also be affected by the formation of hydration shells (B. et al. 2008). Such factors would lead to hindered diffusion through small pores which would slow down the rate of phosphate adsorption (Beck and Schultz 1972b). More detailed models considering all these parameters can give a better insight into the adsorption mechanism. The downside with such models could be the complexity involved in solving such models accurately to estimate the mass transfer coefficients or adsorption rate constants. It would be practical to study such models in conjunction with column studies and model the kinetic data based on realistic hydraulic retention times.

4.6. Conclusion

This study determined the effect of pore size distribution (PSD) on phosphate adsorption. Varying the adsorbent particle size allowed the difference in adsorption to be correlated directly with the diffusion into the pores. Adsorption kinetic experiments showed that equilibrium was reached within 7 days for all particle sizes of FSP and DD6, whereas the large particles (1 to 1.25 mm) of GEH and CFH required 60 to 90 days to reach equilibrium. The adsorption kinetics were fitted by a pseudo second order model and the ratio of rate constants of the large to small particles, i.e. K_{Small}/K_{Large} was used as an indication to understand the diffusion limitation. This ratio was correlated with the adsorbent PSD to show that pore sizes greater than 10 nm are required for good adsorption kinetics.

The insights from this study will help to design granular porous phosphate adsorbents with an appropriate PSD. This is necessary to obtain high phosphate adsorption capacities in relatively short contact times. Future studies should include modeling the adsorption kinetics in a column mode at more realistic contact times. More holistic studies on the pore structure of adsorbent must include the 3-dimensional arrangement of the pores apart from the PSD.

4.7. Supporting information

4.7.1. Tables

Table S4-5: Specific surface area of varying particle sizes for different adsorbents

Adsorbents	Particle size	Total pore area (m^2/g)	Micropore area (m^2/g)	Mesopore area (m^2/g)
GEH	**Large**	244	138	106
	Medium	243	141	102
	Small	239	143	96
FSP	**Large**	179	82	97
	Medium	174	78	96
	Small	174	81	93
CFH	**Large**	119	102	17
	Medium	113	98	15
	Small	113	97	16
DD6	**Large**	235	144	91
	Medium	238	147	91
	Small	240	153	87

Large, medium and small refers to adsorbent particle sizes of 1 to 1.25 mm, 0.4 to 0.5 mm, and 0 to 0.1 mm, respectively.

Table S4-6: Mössbauer fitted parameters for the different iron based adsorbents

Sample	***T (K)***	***IS (mm·s^{-1})***	***QS (mm·s^{-1})***	***Hyperfine field (T)***	***Γ (mm·s^{-1})***	***Phase***	***Spectral contribution (%)***
GEH	4.2	0.35	0.06	51.6	0.45	Fe^{3+} (*Hematite*)	11
		0.35	-0.08	47.5*	0.44	Fe^{3+} (*Ferrihydrite*)	89
FSP	4.2	0.33	-0.01	44.6*	0.53	Fe3+ (Ferrihydrite)	100
CFH	4.2	0.36	-0.17	50.3	0.47	Fe^{3+} (*Goethite/Hematite*)	43
		0.35	-0.10	46.2*	0.39	Fe^{3+} (*Ferrihydrite/ Lepidocrocite*)	57

Experimental uncertainties: Isomer shift: I.S. ± 0.01 mm s^{-1}; Quadrupole splitting: Q.S. ± 0.01 mm s^{-1}; Line width: Γ ± 0.01 mm s^{-1}; Hyperfine field: ± 0.1 T; Spectral contribution: ± 3%. *Average magnetic field.

4.7.2. Figures

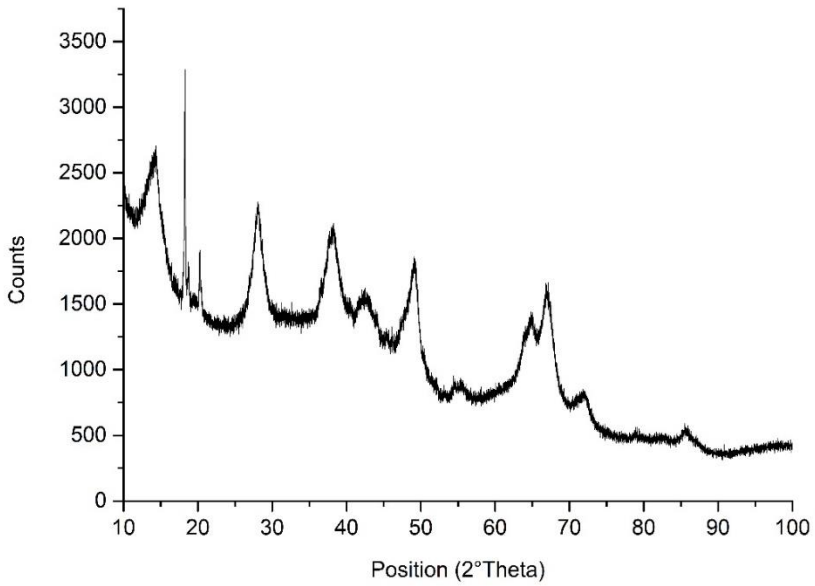


Figure S4-8: XRD spectrum of DD6. The peaks at position 18.2, 18.7, 20.3 correspond with aluminium oxide ($Al_{2.67}O_4$), whereas the peak at 13.9 corresponds with aluminium oxide hydroxide (AlO(OH)). Peaks at positions 28.1, 32.6, 38, 42.8, 48.9, 54.8, 64.4, 67, 71.8, 85.6 correspond with both aluminium oxide and aluminium oxide hydroxide.

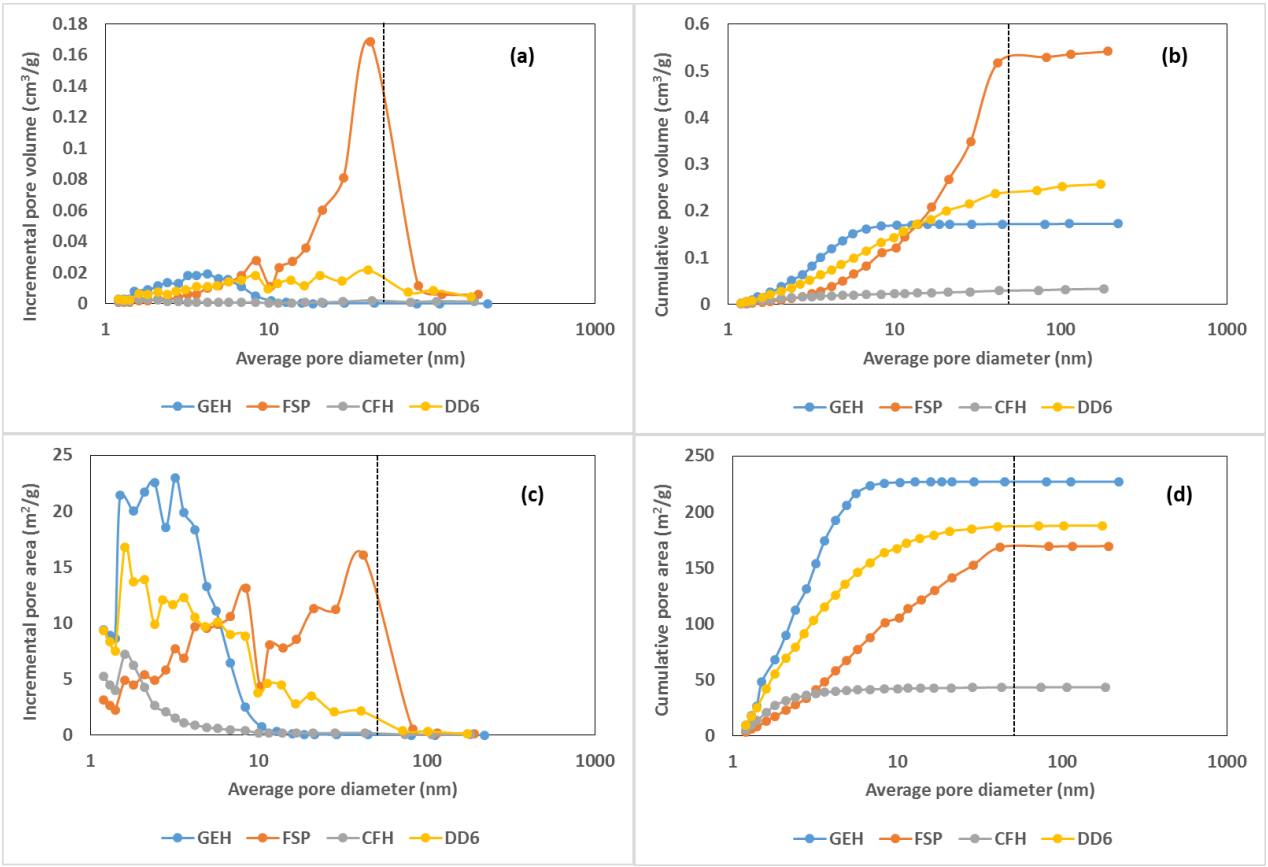


Figure S4-9: (a) Incremental and (b) Cumulative pore volume of different adsorbents as determined by the BJH method. (c) Incremental and (d) Cumulative pore area for the corresponding adsorbents. The dashed lines within the plots show the cut off (50 nm) between meso and macropores.

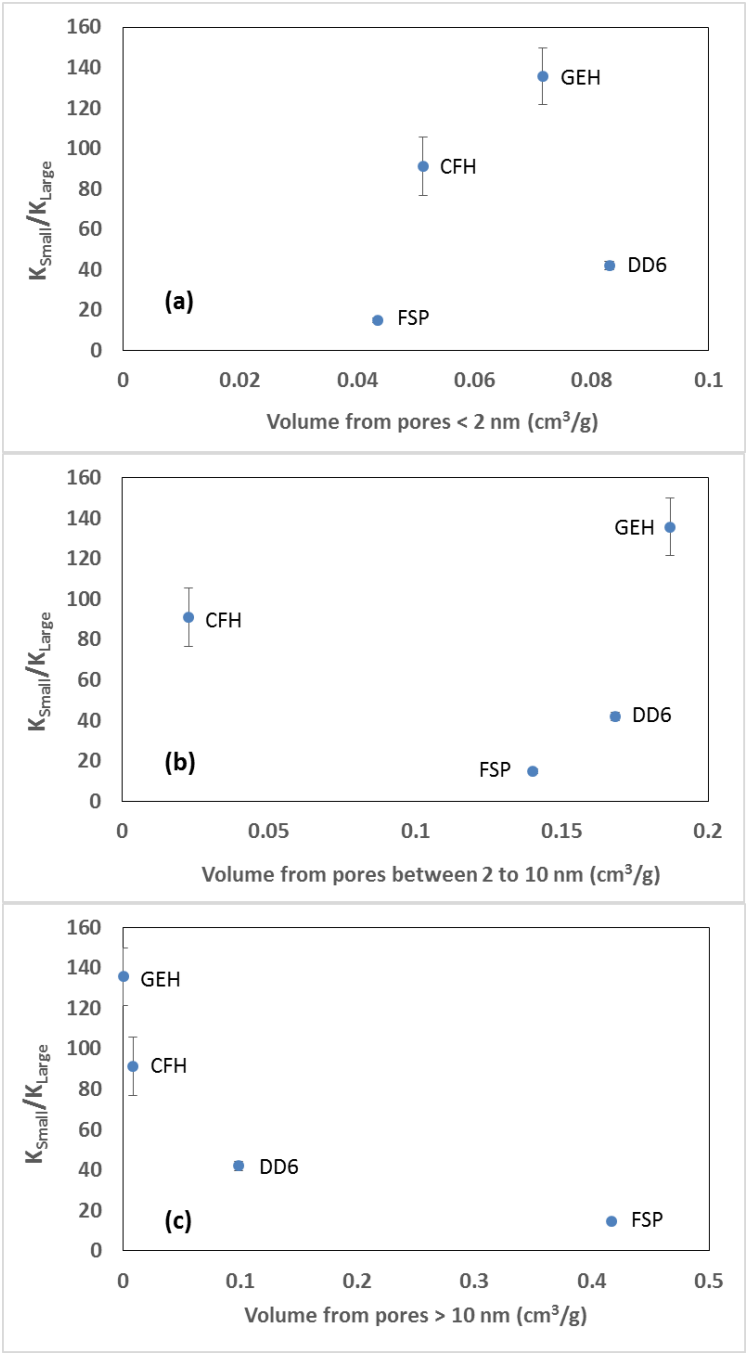
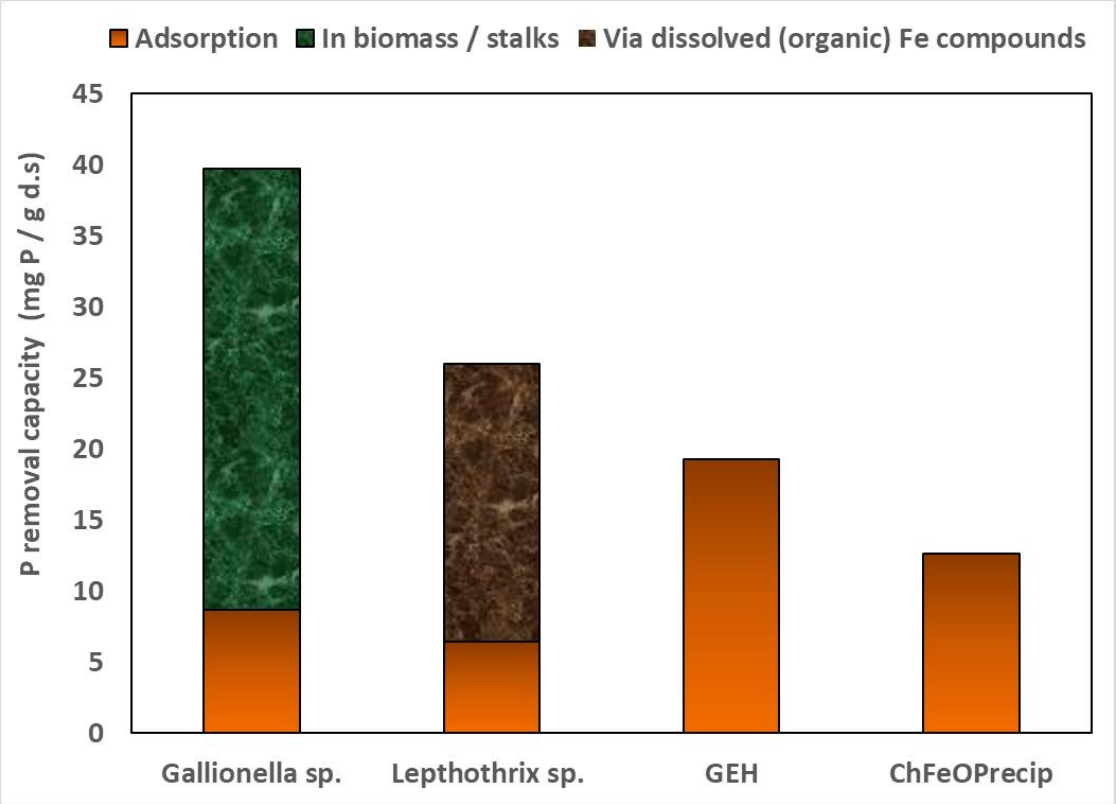


Figure S4-10: Ratio of rate constants from pseudo second order kinetic model of small (0 to 0.1 mm) to large adsorbent particle (1 to 1.25 mm) for the different adsorbents as a function of (a) Volume by pores less than 2 nm (b) Volume by pores between 2 to 10 nm (c) Volume by pores greater than 10 nm.

Chapter - 5

Biogenic Iron Oxides for Phosphate Removal

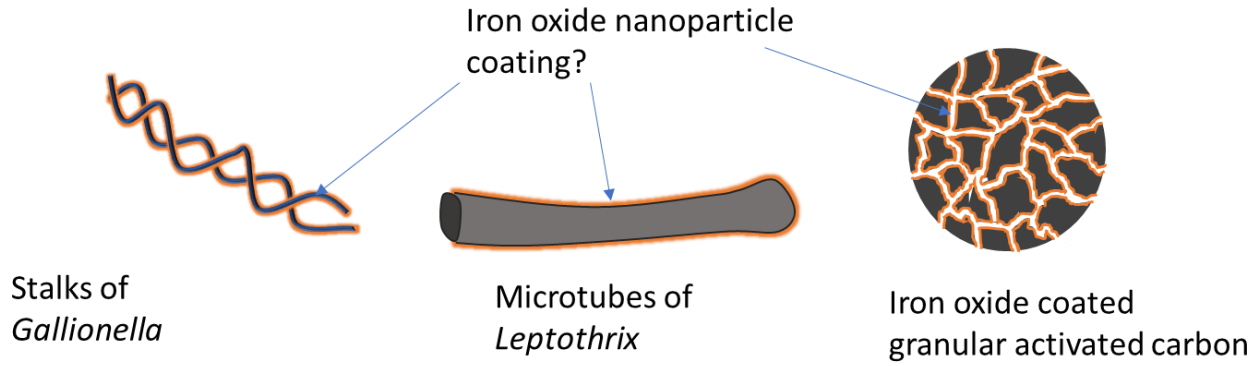
Buliauskaitė, R., Wilfert, P., Suresh Kumar, P., de Vet, W.W.J.M., Witkamp, G.-J., Korving, L. and van Loosdrecht, M.C.M. (2018) Biogenic iron oxides for phosphate removal. Environmental Technology, 1-7.



5.1. Prologue

5.1.1. Backdrop

- *Gallionella* and *Leptothrix* are two iron oxidizing bacterial genera that form extracellular biogenic iron oxides.
- Biogenic iron oxides have been shown to remove phosphate to very low concentrations.
- This very high affinity for phosphate could be due to the structure and distribution of these biogenic iron oxides.
- For instance, biogenic iron oxides are sometimes distributed as nanocrystals forming a thin layer which would result in a high specific surface area.



5.1.2. Research questions

i) Do biogenic iron oxides really show very high phosphate removal?

ii) Is the removal purely via adsorption or are there multiple mechanisms involved?

iii) Can these bacteria achieve the type of iron oxide coating that was envisioned in the earlier study coating granular activated carbons?

iv) Can biogenic iron oxides be used for reversible adsorption of phosphate?

5.2. Abstract

Biogenic iron oxides (BioFeO) formed by *Leptothrix* sp. and *Gallionella* sp. were compared with chemically formed iron oxides (ChFeO) for their suitability to remove and recover phosphate from solutions. The ChFeO used for comparison included a commercial iron based adsorbent (GEH) and chemical precipitates. Despite contrary observations in earlier studies batch experiments showed that BioFeO do not have superior phosphate adsorption capacities compared to ChFeO. However, it seems multiple mechanisms are involved in phosphate removal by BioFeO which make their overall phosphate removal capacity higher than that of

ChFeO. The overall phosphate removal capacity of *Leptothrix* sp. was 26.3 mg P/g d.s. of which less than 6.4 mg P/g d.s. was attributed to adsorption. The main removal is likely due to the formation of organic iron phosphate complexes (19.6 mg P/g d.s.). *Gallionella* sp. had an overall phosphate removal capacity of 39.6 mg P/g d.s. Significant amounts of phosphate were apparently incorporated into the *Gallionella* sp. stalks during their growth (31.0 mg P/g d.s.) and only one-fourth of the total phosphate removal can be related to adsorption (8.6 mg P/g d.s.). Their overall ability to immobilize large quantities of phosphate from solutions indicate that BioFeO could play an important role in environmental and engineered systems for the removal of contaminants.

5.3. Introduction

Adsorption has the potential to reduce phosphate levels in wastewaters to as low as 20 µg P/L (Zelmanov and Semiat 2011), which could help to prevent eutrophication, and even to substitute iron salts dosing for phosphate removal during wastewater treatment (Wilfert et al. 2015). Achieving very low phosphate concentrations (0.3 µg P/L) may restrict biofouling in drinking water production and distribution systems (Vrouwenvelder et al. 2010). An ideal adsorbent has good adsorption capacity, high affinity, and selectivity towards phosphate and can be produced at relatively low cost. Adsorption is also a reversible process which allows for the adsorbent reuse via regeneration and thereby allowing for phosphate recovery (Loganathan et al. 2014).

Biogenic iron oxides (BioFeO) are complex aggregates of organic material, bacterial cells, and iron (oxyhydr)oxides, which contain impurities, such as sorbed or structural phosphate, Si, SO_4, Mn, Al, etc. Extracellular BioFeO can be formed by iron-oxidizing bacteria (FeOB) such as *Gallionella* sp. or *Leptothrix* sp. (Fortin and Langley 2005) BioFeO are widespread in the environment, have large surface areas and reactive surface properties, which would have a positive effect on phosphate adsorption (Fortin and Langley 2005, Suzuki et al. 2012). Accordingly, *Leptothrix* sp. deposits showed relatively high adsorption capacities between 10.8 to 39.9 mg P/g d.s. (Rentz et al. 2009) comparing to the values of ChFeO (Wilfert et al. 2015). The adsorption capacities of *Leptothrix* sp. deposits were high when expressed in terms of iron, with adsorption capacities between 46.9 to 165.0 mg P/g iron (Rentz et al. 2009) which corresponds with a molar phosphate/iron ratio of up to 0.3. This implies that the iron on the BioFeO is efficiently used to bind phosphate. Additionally, (de Vet et al. 2012) showed that in the presence of *Gallionella* sp., phosphate levels were reduced to such an extent that growth of autotrophic bacteria was minimized. In contrast, in the presence of ChFeO these bacteria could grow. This observation indicates that BioFeO can be applied to reduce dissolved phosphate to levels where even biofouling is diminished (de Vet et al. 2012, Emerson D 2015). BioFeO have also been used for removal of arsenic (Ahoranta et al. 2016, Bai et al. 2016, Katsoyiannis 2016, Pokhrel and Viraraghavan 2009) and other heavy metals (Katsoyiannis 2016) remediation. The aim of this study was to investigate if and why BioFeO have superior phosphate adsorption characteristics compared to ChFeO. We studied the differences in phosphate binding capacity, the morphology and chemical composition between BioFeO and ChFeO, which included a commercial iron based adsorbent (GEH) with

large surface area and high phosphate adsorption capacity (Genz et al. 2004) and chemical precipitates from groundwater.

5.4. Material and methods

5.4.1. Biogenic iron oxides of Leptothrix sp. and Gallionella sp.

Leptothrix sp. deposits were collected between December 2015 and February 2016 from ditches with groundwater seeps in Earnewâld (53.145270, 5.954955), Beetsterzwaag (53.053125, 6.118824) and Lettelbert (53.192624, 6.425097). The water overlaying the deposits had a neutral pH, temperatures between 277-281K and dissolved oxygen concentration between 4-6 mg/L. The loosely accumulated deposits were collected using sterile 100 ml plastic syringes and stored at 277K (Earnewâld's sample was kept for 27 days and *Leptothrix* sp. from Beetsterzwaag and Lettelbert were kept for 3 days) until the experiments started. *Gallionella* sp. stalks originated from a set-up designed for biological iron oxidation (de Vet et al. 2011).

Light microscopy and scanning electron microscopy (SEM) were used to identify *Leptothrix* sp. and *Gallionella* sp. and to check if the characteristic shape of the BioFeO was intact (Figure S5-3 in supporting information). Samples for SEM analyses were rinsed with PBS before dehydration in an ethanol series (Heim et al. 2015). Samples for XRD analyses were air-dried.

TS and VS were determined according to the standard methods (Clesceri 1998). The elemental composition of the samples was determined using ICP-OES after a microwave-assisted acid digestion (15 minutes at 180°C) using concentrated HNO_3 (Table S5-1).

5.4.2. Chemically formed iron oxides

Granulated ferric hydroxide (GEH) is a commercially available adsorbent, which consists of akageneite (Genz et al. 2004). For experiments, ground GEH was used (≤ 100 µm) to allow a fair comparison with the BioFeO which were in powdered form. Additionally, chemical iron oxide precipitates (ChFeOPrecip) were used, which were formed by bubbling oxygen trough raw groundwater.

5.4.3. Phosphate adsorption experiments

Leptothrix sp. and *Gallionella* sp. deposits were washed with MilliQ (MQ) until total iron in the supernatant (0.45 µm polycarbonate filtered) was < 0.2 mg Fe/L (Hach Lange disc kit and ICP-OES).

Preliminary experiments showed no significant difference between dry and wet samples. For all experiments, MQ washed and vacuum dried (25 °C) precipitates of *Gallionella* sp. were used. To prevent structural changes in iron oxides, the drying temperature was kept below 40°C (Schwertmann and Cornell 2000). However, for the experiments with *Leptothrix* sp. wet samples were used for better comparison with the earlier study (Rentz et al. 2009).

The adsorption experiments were carried out in batch mode (initial conditions: 5-6 mg P/L, pH 6.5 ± 0.2, 25 °C, stirred manually once per day) in duplicates. For determining phosphate adsorption kinetics, an adsorbent concentration of 0.5 g/L was used and the solutions were sampled after 1, 2, 3, 4 and 7 (or 8) days. The data were fitted with the non-linear form of a pseudo second order kinetic model. This model is based on the assumption of chemisorption (Ho and McKay 1999) as is the case with phosphate adsorption onto iron oxides (Cornell and Schwertmann 2006). For isotherm experiments, the adsorbent concentrations used were 2, 1, 0.5, 0.25, 0.125, 0.062 or 0.031 g/L. Phosphate adsorption studies with ChFeO showed that time taken to reach adsorption equilibrium can vary between 1 to 28 days (Borggaard et al. 2005, Chitrakar et al. 2006, Genz et al. 2004, Yoon et al. 2014). From an application point of view, it is not practical to run adsorption on a very long time scale and hence it was decided that 4 days were enough to perform all isotherm experiments. Samples were filtered (0.45 µm polycarbonate membrane filter), phosphate concentrations were determined by IC and total phosphorus using ICP-OES (Table S5-2).

5.5. Results and discussion

5.5.1. Washing of BioFeO and ChFeO prior to phosphate adsorption experiments

During experiments with non-washed deposits of *Leptothrix* sp. dissolved iron was detected, therefore, it was decided to wash the deposits. Also (Rentz et al. 2009) washed *Leptothrix* sp. deposits once with a saline solution (100 mM NaCl) prior to adsorption experiments to remove background phosphate. We have not performed experiments with deposits of *Leptothrix* sp., which have been washed just once, because significant amounts of soluble iron were still in the supernatant after a single washing step. This indicates that the sample preparation in this previous study was not optimal. Iron release for *Leptothrix* sp. deposits washed with saline solution was greater compared to MQ washed samples. Perhaps due to a higher solubility of Na-organic linkages, which can cause an increase in organically complexed metals in solution (Nelson and Oades 1998). Thus, it was decided to wash BioFeO and ChFeO with MQ before the adsorption experiments.

Our study showed that *Leptothrix* sp. required more intensive washing to remove soluble iron then *Gallionella* sp. deposits, ChFeOPrecip and GEH. *Leptothrix* sp. normally occurs in waters rich in organic matter (Harder 1919). It is well known that dissolved organics have the ability to retain iron (as ferrous and ferric iron) in solution/suspension (Lobartini et al. 1998). Thus, organically complexed iron could be the reason for the high concentration of iron in solution (up to 19.4 mg Fe/L when deposits were washed with saline solution) measured during washing of *Leptothrix* sp. and explains why intensive washing was necessary.

5.5.2. Phosphate adsorption kinetics of BioFeO and ChFeO

Adsorption capacities of MQ washed *Leptothrix* sp. from Beetsterzwaag and Lettelbert were similar to adsorption capacity of MQ washed *Leptothrix* sp. from Earnewâld, therefore, only kinetics with non-washed vs MQ washed for *Leptothrix* sp. from Earnewâld were performed. Figure 5-1 shows the adsorption kinetics for phosphate on ChFeO and Leptothrix sp E.

According to the pseudo second order kinetic model, more than 95 % of the adsorption equilibrium was reached within 4 days for the non-washed BioFeO of *Leptothrix* sp. E and ground GEH (Table S5-3: Kinetic parameters for the adsorption of phosphate by BioFeO, ChFeOPrecip and GEH). For ChFeOPrecip and MQ washed BioFeO of *Leptothrix* sp. E 90 % and 76 % of the adsorption equilibrium was reached respectively. In adsorption experiments by the earlier study (Rentz et al. 2009) the equilibrium was reached within 1 day using deposits of *Leptothrix* sp. This might be due to the less intense washing and the use of the saline solution for washing which causes more intensive iron release which precipitates with the phosphate thereby accelerating the phosphate removal. The slow kinetics in experiments with washed BioFeO of *Leptothrix* sp. E could be related to the complex nature of BioFeO (Fortin and Langley 2005). The organics in the BioFeO structure could slow down the phosphate diffusion and adsorption to the adsorption sites.

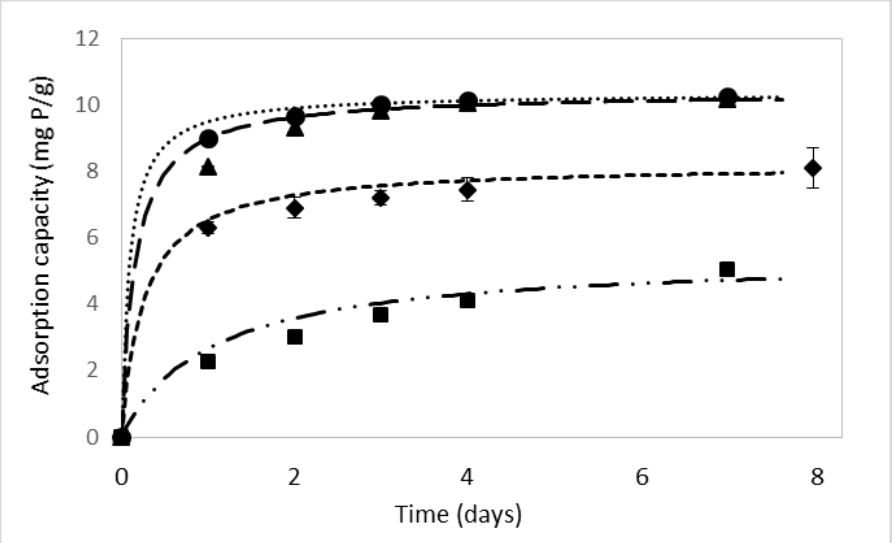


Figure 5-1: Phosphate adsorption kinetics for different adsorbents. Markers represent the actual adsorption capacities (n = 2) and dashed lines represent the corresponding fitting using the pseudo second order kinetic model. ● Leptothrix sp E: non-washed; ▲ GEH; ♦ ChFeOPrecip; ■ Leptothrix sp E: MQ washed.

5.5.3. Phosphate adsorption isotherms of BioFeO and ChFeO

Figure 5-2 shows the adsorption isotherms of BioFeO and ChFeO. The Langmuir adsorption model was only fitted for GEH and non-washed BioFeO of *Leptothrix* sp. E since adsorption to these two samples reached most close to equilibrium (Table S5-3). Maximum phosphate adsorption of non-washed *Leptothrix* sp. E obtained with Langmuir model was 24.7 ± 0.2 mg P/g d.s. and it is in the 10.8-39.9 mg P/g d.s. range reported earlier (Rentz et al. 2009) (q_e is in the range of 12-19 mg P/L) (Table S5-4). The maximum experimentally observed adsorption capacities for all the adsorbents are listed in Table S5-5 in mg P/g d.s. and mg P/g iron.

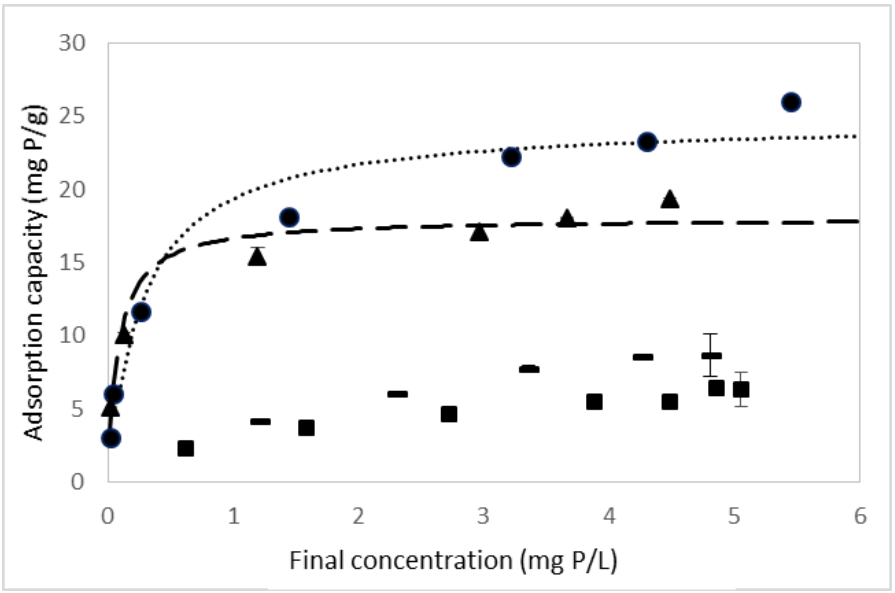


Figure 5-2: Isotherms fitted according to Langmuir adsorption model for phosphate adsorption to 5 different iron based adsorbents after 4 days, mgP/g d.s (n = 2)

• Leptothrix sp E: non-washed; ▲ GEH; ▬ Gallionella sp: MQ washed; ■ Leptothrix sp E: MQ washed.

The adsorption capacity of MQ washed *Leptothrix* sp. E was 6.4 mg P/g d.s., which is about 4 times lower compared to non-washed *Leptothrix* sp. E. Isotherms of MQ washed BioFeO of *Leptothrix* sp. from all three origins showed the same pattern with adsorption capacities between 6.4-8.4 mgP/g d.s. Also, dissolved iron (up to 2.2 mg Fe/L) was measured for the MQ washed *Leptothrix* sp. samples in the supernatant of the adsorption experiments. This indicates continuous release of dissolved iron from *Leptothrix* sp. deposits, which implies that even in washed samples, the phosphate removal could be a combination of adsorption and precipitation. Dissolved iron concentrations in the supernatant correlated well (R^2=0.949-0.987) with DOC (Figure S5-4). Organic matter is a potent complexing agent for iron (Lobartini et al. 1998). (Rentz et al. 2009) showed that *Leptothrix* sp. deposits have very high phosphate adsorption capacity. However, the results they report are most likely a combination of adsorption and precipitation of phosphate by organic-iron complexes (Gerke 2010, Weir and Soper 1963). It is important to distinguish between these two mechanisms. Adsorption enables phosphate release and recovery as well as reusability of the adsorbent. When the phosphate precipitates, it can only be partly released and recovered. Furthermore, precipitation is not as selective as adsorption (Li and Stanforth 2000, Loganathan et al. 2014). Therefore, biogenic iron oxides produced by *Leptothrix* sp. are not a suitable material for phosphate recovery via reversible adsorption.

Phosphate was apparently immobilized by sorption and/or co-precipitation during the growth of *Gallionella* sp. stalks. The phosphate in the stalks before adsorption experiments amounted to 31.0 mgP/g d.s., which gives iron:phosphorus molar ratio of 7 (Table S5-1). Similar iron:phosphorus molar ratio of 10 was reported in the literature for *Gallionella* sp. sampled from drinking water systems with low phosphate concentrations (Ridgway et al.

1981). Our *Leptothrix* sp. samples had an iron:phosphorus molar ratio of 39.6. Studies on *Leptothrix* sp. samples from freshwater purification system showed an iron:phosphorus molar ratio of 80 (Hashimoto et al. 2007). This high phosphate content of the *Gallionella* sp. precipitate could not only explain strongly reduced phosphate in the residual water (de Vet et al. 2012) but also the retardation of the heterogenic (autocatalytic) chemical iron oxidation observed (van der Grift et al. 2016). For *Gallionella* sp., living cells and thus in situ production of iron stalks are required to reduce phosphate levels to a very low concentration that could even prevent biofouling.

During isotherm experiments, the pH of the solution containing *Gallionella* sp. increased up to 7.5, whereas the pH for *Leptothrix* sp. and GEH remained stable (6.5±0.3). Additional experiments showed that even when the pH was kept constant for all adsorbents at 7.5, the adsorption capacity for the biogenic adsorbents was lower than GEH (Figure S5-5). XRD measurements showed that no crystalline material was present in the samples and thus that the iron structures of *Gallionella* sp. and *Leptothrix* sp. were amorphous. The difference in adsorption capacity (mg P/g d.s.) between MQ washed *Gallionella* sp. stalks, and *Leptothrix* sp. sheats is not high (Table S5-5). Therefore, it is also concluded that the structure of BioFeO tested does not have an influence on phosphate adsorption capacity.

The overall phosphate removal capacity of BioFeO is high, with *Gallionella* sp. and *Leptothrix* sp. *E* removing 39.6 and 26.3 mg P/g d.s., respectively. The phosphate removal attributed to adsorption is significantly lower, with 8.7 and less than 6.4 mg P/g d.s, for *Gallionella* sp. and *Leptothrix* sp. *E*, respectively. Table S5-5 shows that the adsorption capacity of washed biogenic adsorbents was much lower than the chemical adsorbent GEH (19.3 mg P/g d.s.) and ChFeOPrecip (12.6 mg P/g d.s., not shown in the figure).

Based on our measurements we hypothesize that both *Gallionella* sp. and *Leptothrix* sp. remove phosphate via multiple mechanisms. This study shows, in contrast to earlier reports, that the adsorption capacities of biogenic adsorbents are in general lower than the one of ChFeO (Wilfert et al. 2015). However, the overall ability to immobilize large quantities of phosphate from solutions indicate that BioFeO could play an important role in environmental and engineered systems, which focus on removal rather than recovery. Besides efficient removal of phosphate to prevent bacterial growth and fouling, these BioFeO are also good candidates for removing arsenate, which has similar structure and reactivity to phosphate (Antelo et al. 2005, Violante and Pigna 2002) and preventing its leakage from sediments of marine and freshwater ecosystems (Bai et al. 2016), groundwater (Katsoyiannis 2016, Pokhrel and Viraraghavan 2009) and mine drainage systems (Ahoranta et al. 2016). Further research is needed to explore and confirm the removal mechanisms and stability of produced compounds and the interaction of BioFeO with contaminants such as phosphate, arsenate, heavy metals and others.

5.7. Supplementary information

5.7.1. Tables

Table S5-1: Characteristics of BioFeO, ChFeOPrecip and GEH

	***Leptothrix* sp. E non-washed**	***Leptothrix* sp. E saline-washed**	***Leptothrix* sp. E, A, L MQ washed**	***Gallionella* sp. MQ washed**	**ChFeOPrecip MQ washed**	**GEH MQ washed**
Fe, mgFe/g	237.4 ± 4.0 (n=2)	204.7 ± 0.4 (n=2)	235.7 ± 13.0 (n=6)	390.8 ± 10.3 (n=2)	339.2 ± 4.3 (n=2)	566.1 ± 4.9 (n=2)
P, mgP/g	<0.3 ± 0.1 (n=2)	<0.4 ± 0.0 (n=2)	3.3 ± 2.6 (n=6)	31.0 ± 0.3 (n=2)	10.4 ± 0.4 (n=2)	<0.4 ± 0.0 (n=2)
Ca, mgCa/g	25.0 ± 0.2 (n=2)	3.3 ± 0.1 (n=2)	10.3 ± 3.4 (n=6)	31.7 ± 0.4 (n=2)	35.6 ± 0.2 (n=2)	<0.4 ± 0.0 (n=2)
VS, g/kg d.s.	365.8 ± 34.6 (n=9)	476.3 ± 8.2 (n=4)	447.1 ± 69.6 (n=12)	–	–	–
Fe/P molar ratio	>337.6	>291.1	39.6	7.0	18.1	>805.1
XRD	–	–	amorphous	amorphous	–	–

Table S5-2: P_{ortho} and P_{total} concentrations in the supernatant after adsorption experiments with BioFeO, $P_{initial}$=5-6 mgP/l (Leptothrix sp. from Earnwalds after 7 days, Leptothrix sp. from Alddjp and Lettelbert after 4 days)

TS, g/l	***Leptothrix* sp. E non-washed**		***Leptothrix* sp. E MQ washed**		***Leptothrix* sp. E saline washed**		***Leptothrix* sp. A MQ washed**		***Leptothrix* sp. L MQ washed**		***Gallionella sp.* MQ washed**	
	$P_{ortho, mg/l}$	**$P_{total, mg/l}$**	**$P_{ortho, mg/l}$**	**$P_{total, mg/l}$**	**$P_{ortho, mg/l}$**	**$P_{total, mg/l}$**	**$P_{ortho, mg/l}$**	**$P_{total, mg/l}$**	**$P_{ortho, mg/l}$**	**$P_{total, mg/l}$**	$P_{ortho, mg/l}$	$P_{total, mg/l}$
0.2	-	-	0.3 ± 0.0	0.4 ± 0.0	0.1 ± 0.0	-	0.1 ± 0.0	0.2 ± 0.0	0.1 ± 0.0	0.2 ± 0.0	-	-
0.1	0.0 ± 0.0	-	1.0 ± 0.0	1.2 ± 0.0	0.5 ± 0.0	-	0.6 ± 0.1	0.7 ± 0.1	0.7 ± 0.3	0.8 ± 0.4	-	-
0.05	0.1 ± 0.0	0.2 ± 0.0	2.2 ± 0.2	2.2 ± 0.2	1.4 ± 0.0	1.8 ± 0.0	1.8 ± 0.1	1.9 ± 0.1	1.5 ± 0.0	1.7 ± 0.0	1.2 ± 0.0	1.2 ± 0.0
0.025	1.1 ± 0.1	-	3.5 ± 0.1	3.4 ± 0.1	2.4 ± 0.1	3.0 ± 0.1	3.1 ± 0.0	3.2 ± 0.0	2.9 ± 0.0	3.0 ± 0.0	2.3 ± 0.0	2.2 ± 0.0
0.0125	2.6 ± 0.1	2.8 ± 0.0	4.2 ± 0.1	4.0 ± 0.1	3.3 ± 0.0	4.0 ± 0.0	4.0 ± 0.0	4.0 ± 0.1	3.8 ± 0.0	3.9 ± 0.0	3.4 ± 0.0	3.1 ± 0.0
0.00625	3.6 ± 0.2	-	4.7 ± 0.0	4.4 ± 0.0	3.7 ± 0.0	4.5 ± 0.1	4.4 ± 0.0	4.4 ± 0.0	4.2 ± 0.2	4.3 ± 0.2	4.3 ± 0.0	4.0 ± 0.2
0.00313	4.8 ± 0.1	-	4.9 ± 0.0	4.6 ± 0.0	4.0 ± 0.0	5.0 ± 0.0	4.6 ± 0.0	4.5 ± 0.0	4.6 ± 0.0	4.6 ± 0.0	4.8 ± 0.1	4.5 ± 0.2

The pseudo second order kinetic model is described by the following equation:

$$q_t = \frac{(kq_e{}^2 t)}{(1 + (kq_e t))}$$

where,

q_t is the adsorption capacity at time t,

k is the rate constant of adsorption (g/mg min),

q_e is the adsorption capacity at equilibrium.

The difference between q_e determined by fitting with model and q_e reached experimentally is a measure of how close the samples were to adsorption equilibrium.

Table S5-3: Kinetic parameters for the adsorption of phosphate by BioFeO, ChFeOPrecip and GEH

Sample	**q_e, mgP/g (fitted)**	**q_e, mgP/g (experimental, after 4 days)**	**k, µgP/g min**	**q_e reached experimentally in comparison to q_e estimated with model (%)**
***Leptothrix sp.* E non-washed**	10.3 ±0.0	10.1 ±0.0	$7.5 \times 10^{-1} \pm 1.1 \times 10^{-1}$	98.0
***Leptothrix sp.* E MQ washed**	5.4 ± 0.1	4.1 ±0.0	$1.3 \times 10^{-1} \pm 1.7 \times 10^{-3}$	75.9
ChFeOPrecip MQ washed	8.2 ± 0.6	7.4 ±0.4	$3.3 \times 10^{-1} \pm 1.1 \times 10^{-1}$	90.2
GEH grinded, ≤100 µm	10.4 ± 0.0	10.0 ±0.05	$4.3 \times 10^{-1} \pm 2.1 \times 10^{-2}$	96.1

The Langmuir adsorption model is expressed as follows:

$$q_e = \frac{q_m K_L C_e}{(1 + K_L C_e)}$$

Where,

q_m = Maximum adsorption capacity (mg P/g),

q_e = Adsorption capacity at equilibrium (mg P/g),

C_e = Concentration at equilibrium (mg P/L),

K_L = Equilibrium constant for the Langmuir adsorption (L/mg P).

Table S5-4: Langmuir isotherms constants for the adsorption of phosphate by Leptothrix sp and GEH

Sample	q_m, mgP/g dried solids	q_m, mgP/g Fe	K_l, L/mgP	RMSE[1]
***Leptothrix sp*, (Rentz et al. 2009) saline washed (once) non-dried**	10.8 - 39.9	46.9 -165.0	-	-
***Leptothrix sp* E non-washed non-dried**	24.7 ± 0.2	109.6 ± 1.0	3.6 ± 0.1	1.7 ± 0.0
GEH grinded, ≤100 µm	18.0 ± 0.3	31.8 ± 0.5	12.1 ± 0.8	1.3 ± 0.2

[1]RMSE - Root-mean-square error for the fit of experimental data to the isotherms model using non-linear regression.

Table S5-5: Actual maximum phosphate adsorption capacities observed after 4 days adsorption by BioFeO and GEH

Sample	Actual adsorption capacities, mg P/g dried solids	Actual adsorption capacities, mg P/g Fe	Final P concentration in the solution, mg P_{ortho} /l
***Leptothrix sp.* E non-washed non-dried**	26.0 ± 0.3	115.3 ± 1.4	5.4 ± 0.0
***Leptothrix sp.* E MQ washed non-dried**	6.4 ± 1.2	27.5 ± 5.2	5.1 ± 0.0
***Leptothrix sp.* E, A, L MQ washed non-dried**	7.3 ± 0.7	31.0 ± 3.1	4.8 ± 0.3
***Gallionella sp.* MQ washed dried**	8.7 ± 1.5	22.1 ± 3.8	4.8 ± 0.1
GEH grinded (≤100 µm) dried	19.3 ± 0.1	34.1 ± 0.2	4.5 ± 0.0
ChFeOPrecip MQ washed dried	12.6 ± 0.3	37.2 ± 0.9	3.6 ± 0.1

5.7.2. Figures

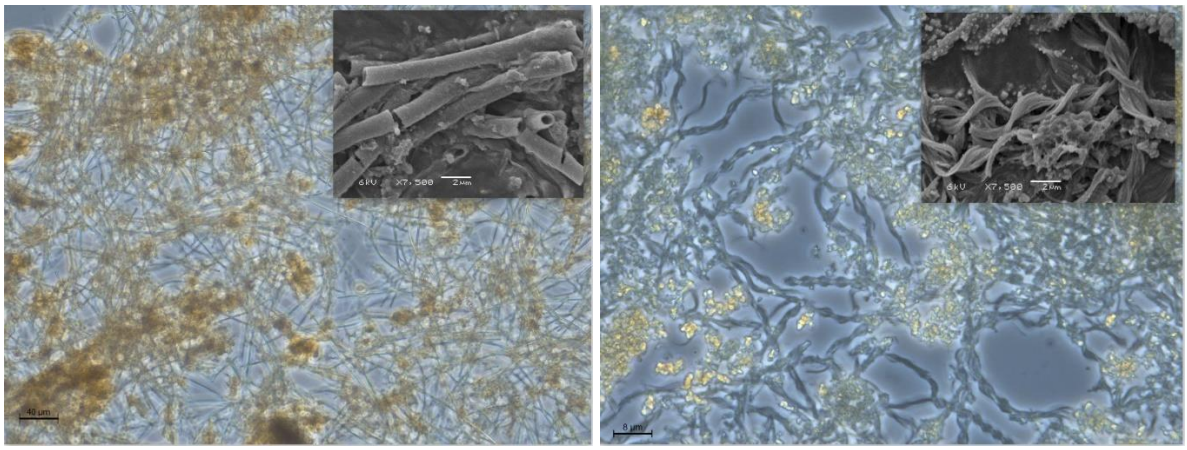


Figure S5-3: Light microscopy and SEM images of Leptothrix *sp. sheats (left) and* Gallionella *sp. stalks (right).* Leptothrix *sp. is a sheathed filamentous bacterium and form oxyhydroxides as hollow microtubes.* Gallionella *sp. produce iron oxides, which have the shape of twisted stalks. The photo on the left: bar equals 40 µm, on the right – equals 8 µm*

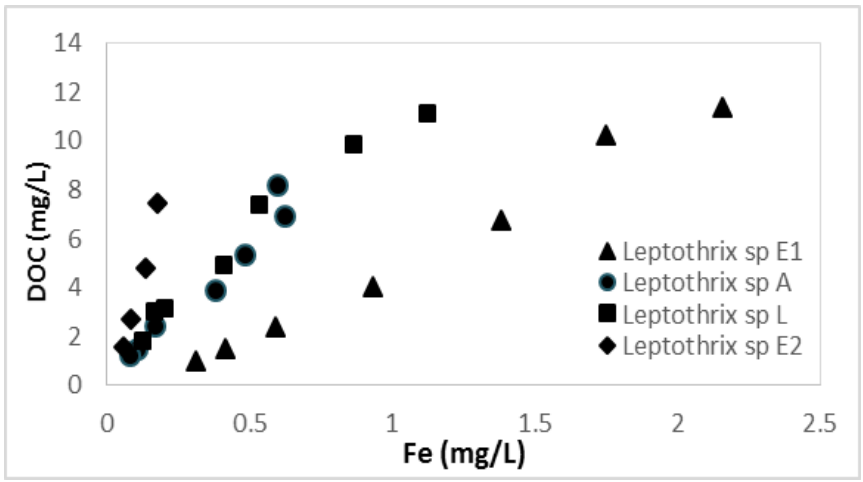


Figure S5-4: Correlation of DOC and Fe concentrations in the supernatant after isotherms with MQ washed BioFeO of Leptothrix sp., where E, A and L letters refer to the sampling locations.

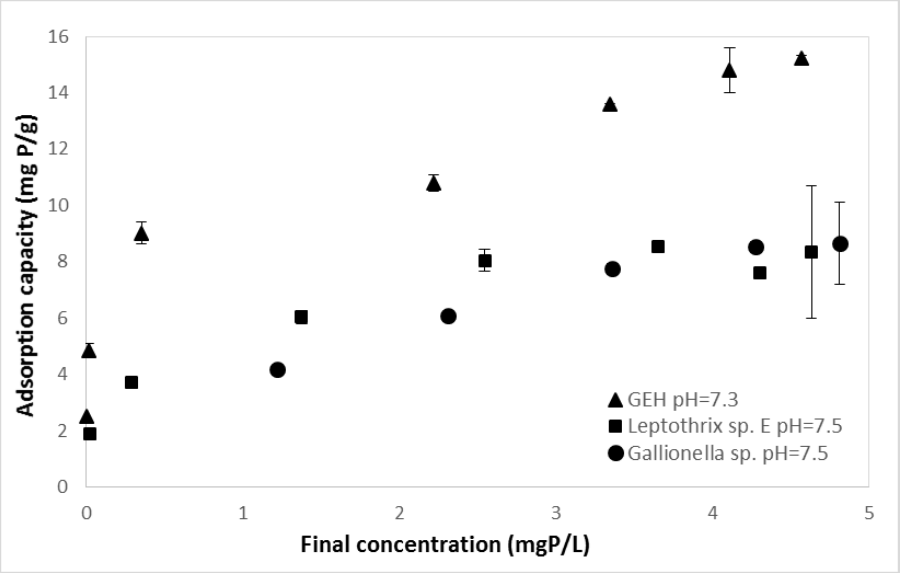
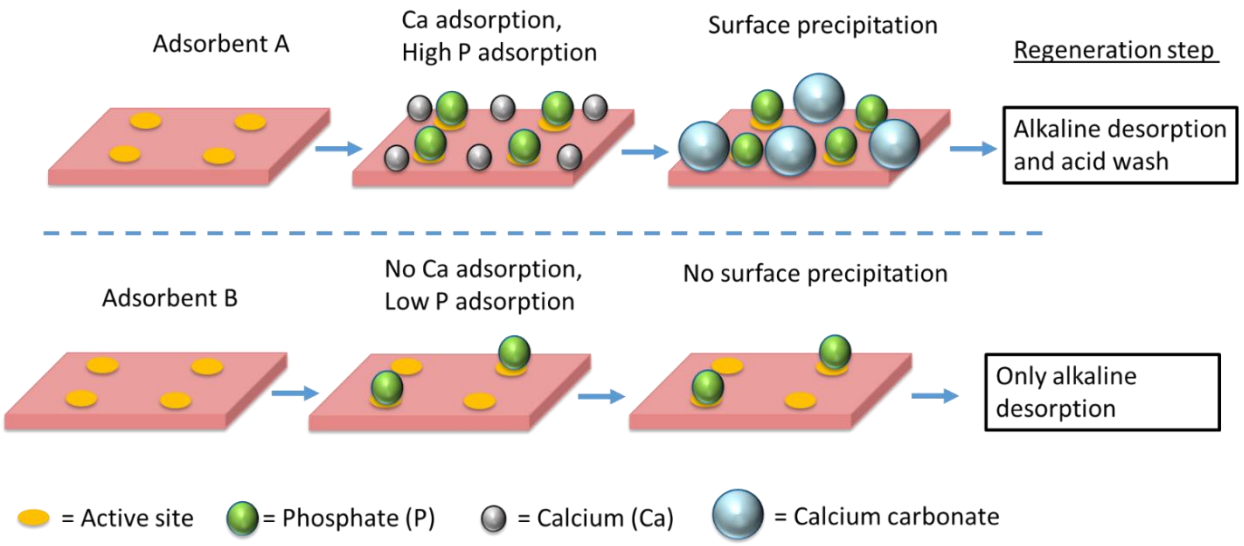


Figure S5-5: Isotherms for GEH and Leptothrix sp. and Gallionella sp. at around pH = 7.5

Chapter – 6

Understanding and improving the reusability of phosphate adsorbents for wastewater effluent polishing

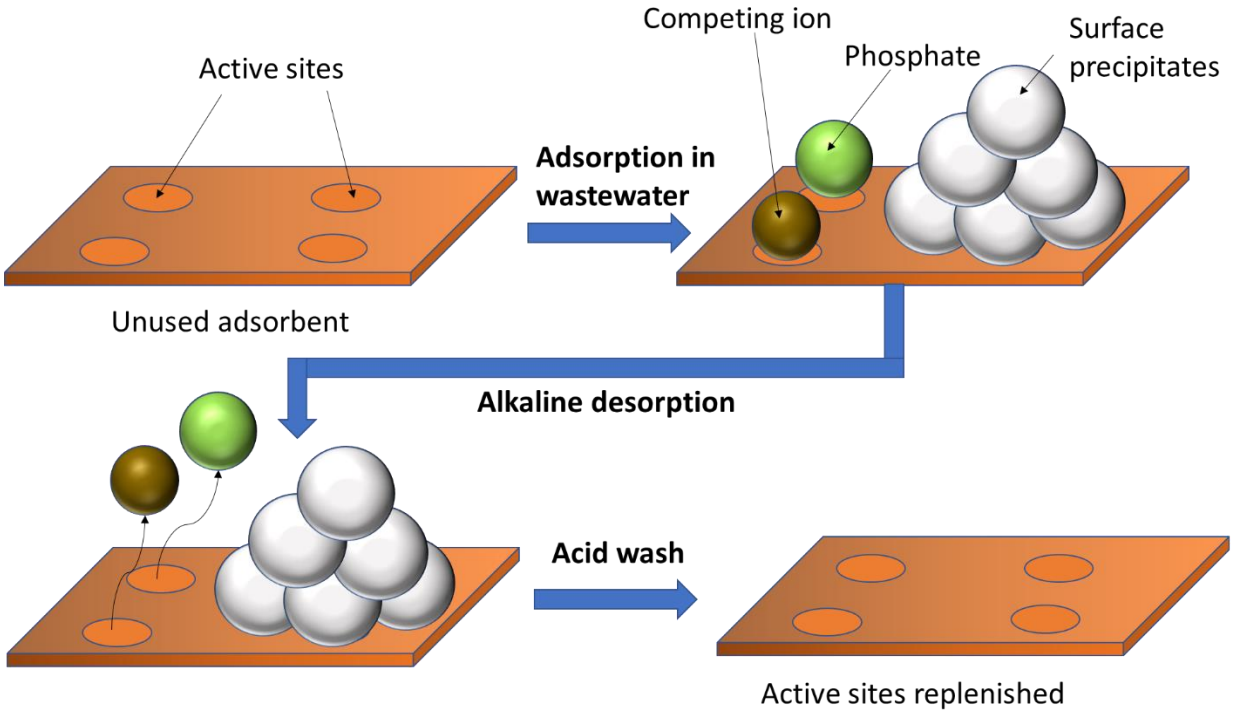
Suresh Kumar, P., Ejerssa, W.W., Wegener, C.C., Korving, L., Dugulan, A.I., Temmink, H., van Loosdrecht, M.C.M. and Witkamp, G.-J. (2018) Understanding and improving the reusability of phosphate adsorbents for wastewater effluent polishing. Water Research 145, 365-374.



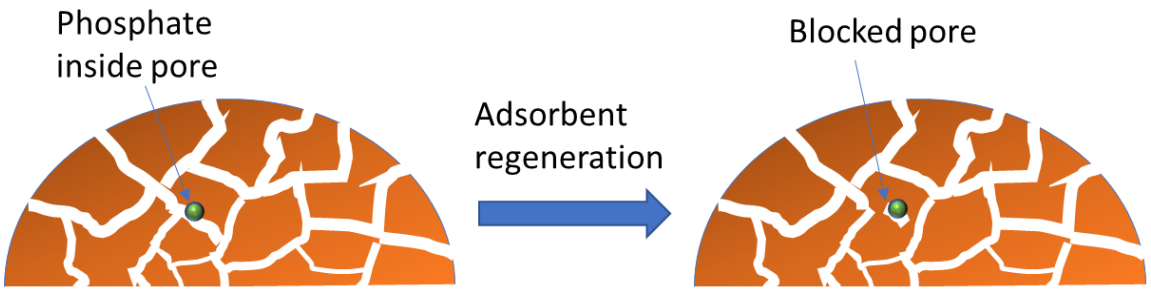
6.1. Prologue

6.1.1. Backdrop

- Adsorbent reusability is essential from an environmental as well as economic perspective.
- Wastewater contains several ions that can interact with the adsorbent and affect its reusability. These interactions include phosphate adsorption, adsorption of competing ions, surface precipitation.
- An alkaline treatment will desorb ions bound directly on the active sites via ligand exchange. However, surface precipitates would need an additional acid treatment step.



- Additionally, the adsorbent might undergo dissolution and reprecipitation during the regeneration process. This might change the adsorbent properties like the crystallinity or pore size distribution.
- For instance, the old pores might get blocked trapping adsorbed phosphate and decreasing specific surface area. Alternatively, new pores can form which might increase the surface area for phosphate removal.



- Thus, monitoring the mass balance of all the competing ions and the adsorbent properties during reuse cycles would give insight into the most significant factors affecting reusability.

6.1.2. Research questions

i) Which factor has the most significant effect on adsorbent reusability?

ii) Is there an adsorbent property can be modified to improve its reusability?

iii) What are the different strategies to regenerate the adsorbent?

6.2. Abstract

Phosphate is a vital nutrient for life but its discharge from wastewater effluents can lead to eutrophication. Adsorption can be used as effluent polishing step to reduce phosphate to very low concentrations. Adsorbent reusability is an important parameter to make the adsorption process economically feasible. This implies that the adsorbent can be regenerated and used over several cycles without appreciable performance decline. In the current study, we have studied the phosphate adsorption and reusability of commercial iron oxide based adsorbents for wastewater effluent. Effects of adsorbent properties like particle size, surface area, type of iron oxide, and effects of some competing ions were determined. Moreover, the effects of regeneration methods, which include an alkaline desorption step and an acid wash step, were studied. It was found that reducing the adsorbent particle size increased the phosphate adsorption of porous adsorbents significantly. Amongst all the other parameters, calcium had the greatest influence on phosphate adsorption and adsorbent reusability. Phosphate adsorption was enhanced by co-adsorption of calcium, but calcium formed surface precipitates such as calcium carbonate. These surface precipitates affected the adsorbent reusability and needed to be removed by implementing an acid wash step. The insights from this study are useful in designing optimal regeneration procedures and improving the lifetime of phosphate adsorbents used for wastewater effluent polishing.

6.3. Introduction

Phosphate, the common form of inorganic phosphorus, is a vital nutrient for life and an essential component of food. Humans consume phosphate as food which subsequently ends up in municipal wastewater plants (Cordell et al. 2009). Discharge of phosphate from the wastewater effluent even in the range of micrograms per liter can cause eutrophication of surface water (L. Correll 1998). Adsorption is often suggested as a polishing step but for the process to be economically feasible, either the adsorbent needs to be extremely cheap or be reusable (Li et al. 2016, Loganathan et al. 2014). Effective reusability means the adsorbent can be regenerated and used again for several cycles without diminishing its adsorption capacity. The reusability of the adsorbent via regeneration also enables phosphate recovery and contributes to a circular economy.

Many studies focus on producing phosphate adsorbents with high adsorption capacity but fewer studies touch on the reusability aspect (Li et al. 2016). An adsorbent's performance can decrease over time due to multiple reasons. These include incomplete desorption of adsorbate, surface precipitation, loss of active sites due to adsorbent wear and tear, and changes in adsorbent properties like surface area, porosity, crystallinity during adsorption and regeneration (Cabrera et al. 1981, Chitrakar et al. 2006, Kunaschk et al. 2015). The reusability of the adsorbents becomes an issue especially in a complex matrix like wastewater effluent where several ions can bind simultaneously on the adsorbent. Thus the choice of regeneration procedure is important in ensuring the proper release of the bound ions. For instance, metal oxides like iron (hydr)oxides bind phosphate via a ligand exchange mechanism with their surface hydroxyl groups (Cornell and Schwertmann 2004). Their regeneration requires using

an alkaline solution to reverse the reaction and release the bound phosphate (Kalaitzidou et al. 2016). However, an earlier study showed surface precipitation on iron oxide adsorbents used in a drinking water matrix and an additional step using acidic solution was required to regenerate the adsorbents (Kunaschk et al. 2015). Moreover, regeneration first with an acidic solution before using alkaline solution improved the adsorbent reusability compared to the reverse order. This was attributed to surface precipitates blocking the adsorbed phosphate and hence the need to first remove the surface precipitates before desorbing the phosphate.

In the current study, we use a similar regeneration approach to optimize phosphate adsorbents in municipal wastewater effluent. We used commercially available iron (hydr)oxide based adsorbents since iron oxides have been known for their good phosphate adsorption properties (Cornell and Schwertmann 2004). These were granular ferric hydroxide (GEH), Ferrosorp (FSP), and an ion exchange resin impregnated with iron oxide (BioPhree). GEH and FSP are porous iron oxides chosen for their high surface area. The BioPhree (henceforth referred as IEX) is similar to a hybrid ion exchange resin where the iron oxide is responsible for the phosphate adsorption and the resin acts as a backbone matrix (Blaney et al. 2007). Two principal factors of an adsorbent govern the process economics: i) Its adsorption capacity (at a given effluent concentration and under a given operation time) ii) its reusability. During the course of the experiments, we focused on improving both these properties. The regeneration procedure used included an alkaline solution to desorb phosphate as well as an acidic solution to remove surface precipitates. The order of using these solutions was also varied during regeneration to understand the effect on reusability. Moreover, adsorbent properties (like surface area and crystallinity) and mass balances of competing ions were monitored during the different adsorption-regeneration cycles. Finally, to test adsorbent regeneration from a practical viewpoint, a regeneration process with a minimal number of steps and chemical consumption was done. The methods were aimed at monitoring the adsorbents to develop the best practices to regenerate and reuse the adsorbents.

6.4. Materials and methods

6.4.1. Chemicals

Potassium dihydrogen phosphate (KH_2PO_4), hydrochloric acid (HCl) and sodium hydroxide (NaOH) were obtained from VWR chemicals. The adsorbents: granular ferric hydroxide (GEH), Ferrosorp (FSP) and ion exchange resin impregnated with iron oxide (commercially called BioPhree, but referred to as IEX henceforth) were provided by GEH Wasserchemie Gmbh, HeGO Biotech Gmbh, and Green Water Solution, respectively.

6.4.2. Methods

6.4.2.1. Wastewater effluent

Wastewater effluent was sampled from Leeuwarden wastewater treatment plant and spiked using KH_2PO_4 to get an initial phosphate concentration around 2 mg P/L. No other chemicals were spiked. The particulates in the wastewater effluent were separated by sedimentation and only the supernatant was used for the adsorption runs. Phosphorus analysis of filtered (using 0.45 µm membrane filter) and unfiltered supernatant showed that there was no particulate phosphorus larger than 0.45 micron present in the supernatant.

6.4.2.2. Adsorbent columns

Adsorbents GEH and FSP were ground and sieved to reach particle size ranges of 1 to 1.25 mm and 0.25 to 0.325 mm, respectively. IEX was by default delivered (in its wet state) in the particle size range between 0.25 to 0.325 mm. The adsorbents were filled inside a glass column (height = 20 cm, diameter = 1.8 cm) to get an adsorbent bed volume of 10 ± 0.5 ml. The adsorbent bed was packed by using glass wool and glass beads to fill the remaining volume of the column (Figure S6-9 in supporting information shows the adsorbent column).

6.4.2.3. Adsorption and regeneration experiments

For the adsorption experiments, the wastewater effluent was pumped to the adsorbent columns in an up-flow mode with a flowrate of 2 ml/min. This gave an empty bed contact time (EBCT) of 5 minutes. The treated solution from the outlet of the column was collected in an automated fraction collector every 3 to 5 hours. These were analyzed for phosphate and the adsorption process was stopped when the outlet phosphate concentration reached 0.1 mg P/L.

Adsorbent regeneration was done in different ways. The first method, designated as alkaline-acid regeneration, used an alkaline solution followed by an acidic solution. The second method, designated as acid-alkaline regeneration, used acidic solution followed by an alkaline solution. In both these methods, the acid wash was done until the pH coming out of the column matched the initial pH of the acid solution. Moreover, the pH in the adsorbent column was neutralized with distilled water or HCl solution of pH 4 prior to subsequent adsorption cycles. Finally, in another method, the adsorbent was regenerated only with an alkaline solution and the pH in the adsorbent column was not neutralized prior to subsequent adsorption cycles. Table 6-1 summarizes the different regeneration methods used. For all methods, 3 adsorption and regeneration cycles were done. The GEH and FSP adsorbent particle sizes were varied to check the influence on the adsorption capacity, whereas the IEX was only available in the size range of 0.25 to 0.325 mm. The rationale for varying the acid wash conditions in different regeneration cycles was to improve the reusability. The terms alkaline desorption and acid wash are used in the text to imply the release of ions from the adsorbent using alkaline and acidic solution respectively.

Table 6-1: Differences in the regeneration methods

Regeneration method	**Adsorbents used**	**Particle size (mm)**	**Regeneration conditions**
Alkaline-acid regeneration	GEH, FSP	1 to 1.25	Alkaline desorption – For all 3 cycles: 100 ml of 1 M NaOH, Recirculation mode for 24 h, Flowrate = 5 ml/min; Acid wash - For all 3 cycles: Single pass mode with HCl (pH = 4) till outlet pH reached 4, Flowrate= 2 ml/min
Acid-alkaline regeneration	GEH, FSP, IEX	0.25 to 0.325	Acid wash – 1st cycle: Recirculation mode with 1L HCl (pH = 4), HCl was added to the acid reservoir till pH stabilized at 4. 2nd and 3rd cycle: HCl (pH = 2.5), Single pass mode till outlet pH reached 2.5, Flowrate = 2ml/min; Alkaline desorption – For all 3 cycles: 100 ml of 1 M NaOH, Recirculation mode for 24 h, Flowrate = 5 ml/min
Alkaline regeneration	FSP	0.25 to 0.325	Alkaline desorption For all 3 cycles: 100 ml of 1 M NaOH, Recirculation mode for 24 h, Flowrate = 5 ml/min

6.4.2.3. Analysis of wastewater samples

Calcium, magnesium, nitrate, nitrite, phosphate and sulphate ions were analyzed by ion chromatography (Metrohm Compact IC Flex 930). Soluble phosphorus, silicon, and iron were measured using inductively-coupled plasma optical emission spectroscopy (Perkin Elmer, Optima 5300 DV). Dissolved organic carbon and inorganic carbon (carbonate ion) were measured using combustion catalytic oxidation method with TOC analyzer (Shimadzu, TOC-L CPH). Table 6-2 shows the composition of the wastewater effluent used.

Table 6-2: Wastewater effluent (from Leeuwarden) characteristics:

Components/Parameters	**Average value/concentration**
Temperature (during adsorption)	21 °C
pH	7.9 ± 0.2
Conductivity	1.8 ± 0.2 mS/cm
Calcium	66 ± 5 mg Ca/L
Magnesium	17 ± 0.5 mg Mg/L
Nitrate	5.5 ± 1 mg NO_3^-/L
Nitrite	2.5 ± 2 mg NO_2^-/L
Phosphate (after spiking)	2 ± 0.2 mg P/L
Soluble silicon	12 ± 1.5 mg Si/L
Sulphate	31 ± 1 mg SO_4^{2-}/L
Dissolved organic carbon	18 ± 1 mg C/L
Inorganic carbon	106 ± 3 mg C/L

6.4.2.4. Adsorbent characterization

The types of iron oxide in the adsorbents were determined using Mössbauer spectroscopy. Transmission ^{57}Fe Mössbauer spectra were collected at different temperatures with conventional constant acceleration and sinusoidal velocity spectrometers using a ^{57}Co (Rh) source. Velocity calibration was carried out using an α-Fe foil. The Mössbauer spectra were fitted using the Mosswinn 4.0 program.

For determining the surface area of the adsorbents, nitrogen adsorption and desorption cycles were carried out using Micromeritics TriStar 3000. The data from the nitrogen adsorption-

desorption profiles were fitted with models included in the analysis software to obtain the pore area from Non Local Density Functional Theory (NLDFT) (Cracknell et al. 1995).

The elemental composition of the adsorbents was quantitatively measured by microwave digestion with 67 % HNO_3. The elemental distribution on the adsorbent surface was monitored using a scanning electron microscope coupled energy dispersive X-Ray (SEM-EDX). The imaging was done using a JEOL JSM-6480 LV scanning electron microscope. Elemental analysis was done at an acceleration voltage of 15 kV using Oxford Instruments x-act SDD energy dispersive X-ray spectrometer. The composition of the surface precipitates on the adsorbent was determined using Raman Spectroscopy (LabRam HR Raman spectrometer).

Point of zero charge (PZC) of the adsorbents was determined by using the salt addition method (Mahmood et al. 2011); 0.2 g of adsorbents (particle size < 0.35 mm) were added to aqueous solutions of 0.1 M $NaNO_3$ with initial pH varying from 4 to 11. The $NaNO_3$ solution was bubbled with N_2 gas prior to the adsorbent addition, and the experiment was conducted in a glovebox with a N_2 atmosphere to avoid the effect of carbon dioxide on the pH. The adsorbents were allowed to mix for 48 hours and the final pH was measured. The difference in initial and final pH was plotted against the initial pH values and the PZC was defined by the pH where the difference in pH was zero. Table 6-3 shows the characteristics of the adsorbents used.

Table 6-3: Adsorbent characteristics

Adsorbent	**Type of adsorbent**	**Bulk density (g/cm^3)**	**Surface area (m^2/g)**	**Point of zero charge**	**Major constituents (wt%)[a]**
GEH	Porous iron oxide	1.1	244	6.1	Fe – 51 %
FSP	Porous iron oxide	0.7	179	9.1	Fe – 47 %, Ca – 8 %
IEX[b]	Iron oxide impregnated in resin	0.7	58	6.6	Fe – 22 %, TOC – 25 %

[a]- Shows constituents comprising more than 5 wt % of adsorbent as measured after microwave digestion of the samples

[b] – For the IEX the bulk density was measured in its default wet state, whereas for FSP and GEH the bulk density was estimated in their dry forms.

6.4.2.5. Estimation of adsorption capacity

The phosphate adsorption capacity was calculated by evaluating breakthrough curves for the different adsorbents. The breakthrough point was considered to be the point when the outlet phosphate concentration from the columns reached 0.1 mg P/L. The detection limit for phosphate was 0.02 mg P/L. The amount of phosphate adsorbed was calculated by plotting the

concentration of phosphate removed versus the volume of solution passed and estimating the area under the curve using trapezoidal rule (Atkinson 1989).

6.5. Results and discussion

6.5.1. Optimization of phosphate adsorption and reusability by varying adsorbent particle size and regeneration conditions

Figure 6-1 shows the phosphate adsorption capacities of GEH and FSP for 3 consecutive cycles using alkaline-acid regeneration. The adsorption capacity was estimated from the breakthrough curves when the phosphate concentration from the column outlet reached 0.1 mg P/L (Figure S6-10 in supporting information shows an example of such a breakthrough curve).

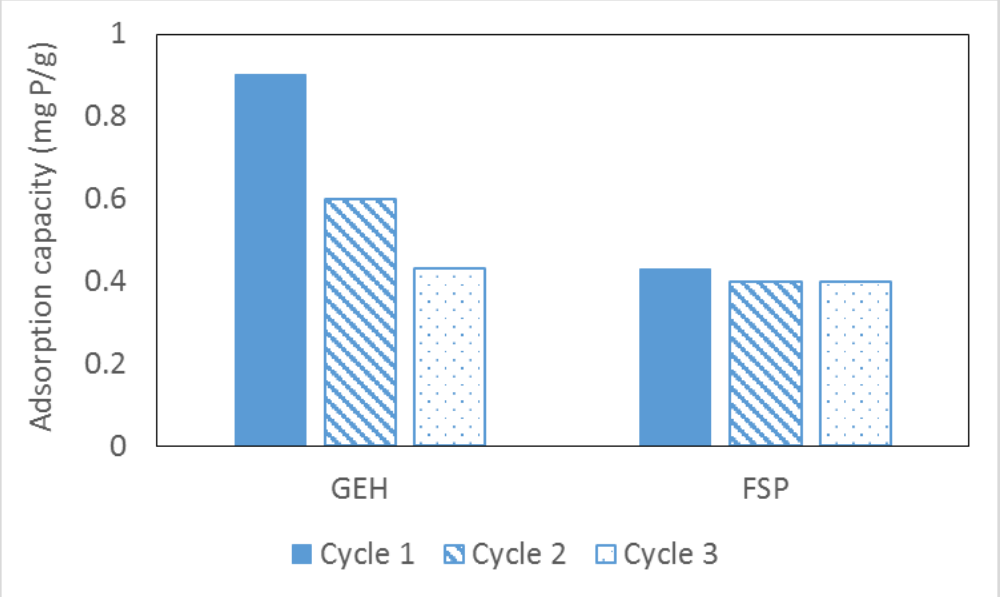


Figure 6-1: Adsorption capacities of 1 to 1.25 mm sized GEH and FSP for breakthrough at 0.1 mg P/L using alkaline-acid regeneration

Figure 6-1 shows that for the 1st cycle, the adsorption capacity of GEH and FSP at an effluent concentration of 0.1 mg P/L was around 0.9 and 0.4 mg P/g, respectively. A phosphate molecule has a diameter of 0.48 nm (Tawfik and Viola 2011). Assuming a monolayer coverage, these adsorption capacities correspond to an area of 3.1 m^2 for GEH and 1.4 m^2 for FSP. This implies only around 1 % of the overall surface area is covered in both these adsorbents. It must be noted that the values shown in Figure 6-1 are not equilibrium adsorption capacities, but adsorption capacities estimated under the given EBCT of 5 minutes. The reason for such a low adsorption capacity corresponding to a very low area coverage fraction is likely due to the diffusion limitation in these porous adsorbents.

Moreover, the reusability of GEH was also affected significantly during these 3 cycles. The adsorption capacity for GEH dropped by 50 % by the 3rd cycle, whereas for FSP the adsorption capacity dropped by about 7 %.

To improve the reusability of the adsorbents, the regeneration order was reversed by first doing an acid wash followed by alkaline desorption as suggested elsewhere (Kunaschk et al. 2015).

To improve the adsorption capacity of the adsorbents, GEH and FSP were ground to a particle size of 0.25 to 0.325 mm, which was similar to the particle size of the IEX adsorbent. Figure 6-2 shows the phosphate adsorption capacities of GEH, FSP, and IEX for 3 consecutive cycles using acid-alkaline regeneration.

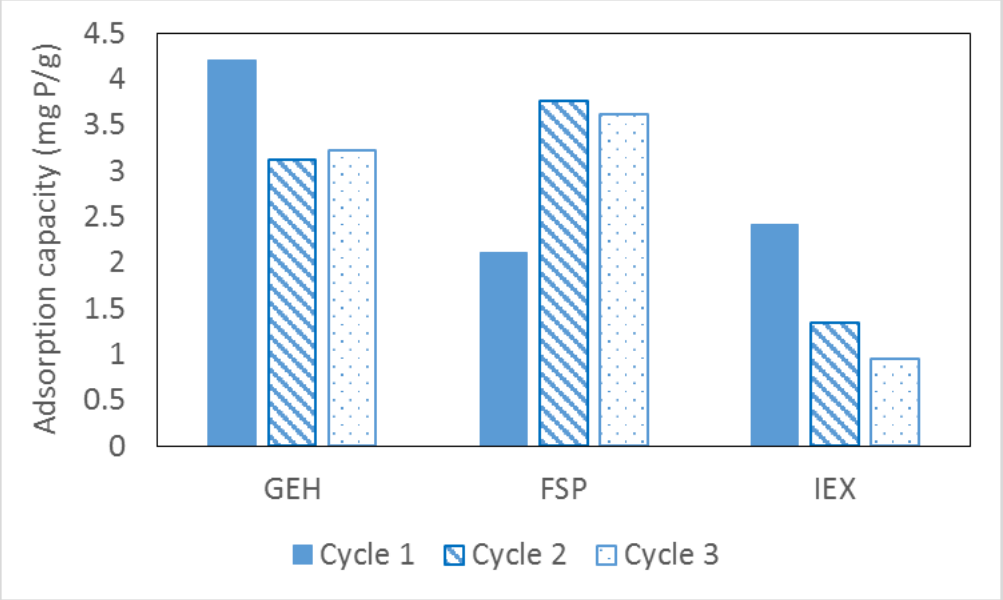


Figure 6-2: Adsorption capacities of 0.25 to 0.325 mm sized GEH, FSP, and IEX for breakthrough at 0.1 mg P/L using acid-alkaline regeneration

Phosphate adsorption capacities for the 1st cycle of GEH and FSP were more than 4 times higher for the 0.25 to 0.325 mm sized particles as compared to the 1 to 1.25 mm sized particles. The specific surface areas of the large (1 to 1.25 mm) and small (0.25 to 0.325 mm) sized adsorbents were similar (Table S6-7). GEH and FSP are porous adsorbents where the measured surface area is related to micropores (< 2 nm) and mesopores (2 to 50 nm) as calculated by the NLDFT method (Cracknell et al. 1995). Thereby grinding them in the mm range does not change their overall area. Porous adsorbents offer the advantage of high surface area even in granular form, thereby allowing for easier handling and operation. However, the porous nature of such adsorbents implies that the adsorption is limited by diffusion. Thereby, under non-equilibrium conditions, decreasing their particle size increases the phosphate adsorption even though their surface area stays the same (Figure 6-1 and Figure 6-2). This shows the need to consider the accessibility of the pores properties while designing such adsorbents, especially for operations with short contact times.

The reusability of the GEH and FSP adsorbents were enhanced for the smaller particle sizes. The decrease in adsorption capacity of GEH for the 2nd and 3rd cycles in Figure 6-2 was less than the decrease seen in Figure 6-1. The adsorption capacity of FSP increased for the 2nd and 3rd cycles by a factor 2 as compared to cycle 1. The adsorption capacity of IEX decreased by 50 % by the 3rd cycle.

Usually, the reusability of adsorbents in lab scale experiments is demonstrated for 5 to 10 cycles (Chitrakar et al. 2006, Kim et al. 2017, Wan et al. 2016). However, as can be seen from Figure 6-1 and Figure 6-2, we see interesting trends in reusability of the adsorbents already by 3 cycles.

This is also due to the complex nature of the wastewater effluent as opposed to the cleaner solutions spiked with phosphate that are often used to demonstrate successful reusability. Thus the focus of this study henceforth was to understand the reason for these differing trends in reusability. By understanding what factors exactly contribute to adsorbent reusability, the optimal procedures for regeneration can be designed. Even if 5 to 10 cycles of successful reuse can be demonstrated via the optimal regeneration methods and if it can be shown that the adsorbent characteristics do not change over this period, then the adsorbent lifetime can be extrapolated to longer reuse cycles.

6.5.2. Understanding phosphate adsorption and reusability by monitoring different parameters

6.5.2.1. Effect of surface (porous) area

During the regeneration process, the acid and alkaline treatment might cause the iron oxides to solubilize and recrystallize. In such a case the physical, as well as chemical properties of the iron oxide, can change, such as the change in surface area or the crystallinity/type of iron oxide. A change in surface area could lead to a loss of active sites which would thus affect the adsorbent reusability. Table 6-4 shows the overall change in the adsorbent surface area along with the change in adsorption capacity for cycle 1 and cycle 3 (surface areas are given in Table S6-7 in supporting information).

Table 6-4: Overall change in surface area (between 1st and 3rd cycles) for adsorbents regenerated using the alkaline-acid and acid-alkaline methods. The + and – signs imply increase or decrease.

	Regeneration using alkaline-acid method		**Regeneration using acid-alkaline method**	
Adsorbents	**Change in surface area**	**Change in adsorption capacity**	**Change in surface area**	**Change in adsorption capacity**
GEH	- 10 %	- 52 %	- 8 %	- 23 %
FSP	+ 25 %	- 7 %	+ 56 %	+ 71 %
IEX			+ 20 %	- 60 %

In general, except for FSP regenerated using the acid-alkaline method, the change in the surface area did not show a correlation with the change in adsorption capacity. This implies that the adsorbent reusability is also affected by other parameters.

6.5.2.2. Effect of the type of iron oxide in the adsorbent

Phosphate adsorption happens on iron oxides via a ligand exchange mechanism with the surface hydroxyl groups (Parfitt et al. 1975). The change in the crystallinity/type of iron oxide during regeneration will lead to exposure of differing types and amount of surface hydroxyl groups which in turn will affect the phosphate adsorption (Cornell and Schwertmann 2004). In an earlier study, a decrease in crystallinity of goethite decreased the adsorbent reusability within 2 cycles (Chitrakar et al. 2006). The crystallinity of akaganeite stayed intact in the same study and the adsorbent could be reused successfully for 10 cycles. Apart from the regeneration

chemicals, the binding of ions like silicate and organics from the wastewater can also influence the crystallinity of the adsorbents (Schwertmann et al. 1984).

To measure if the type of iron oxide changes during the adsorbent usage, the adsorbents were measured with Mössbauer spectroscopy in their unused states and used state (after 3 adsorption cycles). During these cycles, the adsorbents were regenerated using the acid-alkaline method which involved acid wash at pH 2.5 and alkaline desorption at pH 14. Table 6-5 shows the Mössbauer fitted parameters for the different adsorbents.

Table 6-5: The Mössbauer fitted parameters of different adsorbents in their unused and used states. Used state refers to the adsorbent after 3 adsorption cycles.

Sample	**T (K)**	**IS ($mm \cdot s^{-1}$)**	**QS ($mm \cdot s^{-1}$)**	**Hyperfine field (T)**	**Γ ($mm \cdot s^{-1}$)**	**Phase**	**Spectral contribution (%)**
GEH	4.2	0.35	0.06	51.6	0.45	Fe^{3+} (*Hematite*)	11
		0.35	-0.08	47.5*	0.44	Fe^{3+} (*Ferrihydrite*)	89
GEH used	4.2	0.36	0.02	51.9	0.45	Fe^{3+} (*Hematite*)	10
		0.35	-0.07	47.8*	0.45	Fe^{3+} (*Ferrihydrite*)	90
FSP	4.2	0.33	-0.01	44.6*	0.53	Fe^{3+} (*Ferrihydrite)*	100
FSP used	4.2	0.34	-0.01	48.0*	0.44	Fe^{3+} (*Ferrihydrite*)	100
IEX	4.2	0.36	-0.15	50.6	0.39	Fe^{3+} (*Goethite/Hematite*)	21
		0.36	0.11	52.8	0.45		7
		0.35	-0.10	46.3*	0.42	Fe^{3+} (*Hematite*)	72
						Fe^{3+} (*Ferrihydrite*)	
IEX used	4.2	0.36	-0.10	50.2	0.49	Fe^{3+} (*Goethite/Hematite*)	31
		0.35	0.01	52.0	0.36		8
		0.35	-0.08	46.7*	0.45	Fe^{3+} (*Hematite*)	61
						Fe^{3+} (*Ferrihydrite*)	

Experimental uncertainties: Isomer shift: I.S. ± 0.01 mm s^{-1}; Quadrupole splitting: Q.S. ± 0.01 mm s^{-1}; Line width: Γ ± 0.01 mm s^{-1}; Hyperfine field: ± 0.1 T; Spectral contribution: ± 3%. *Average magnetic field.

Based on the fitted parameters (Murad 1988), Table 6-5 shows that ferrihydrite is present in all the samples. GEH and IEX comprised of more than one type of iron oxide. The spectral contribution of the different iron oxide phases shows the transformation between used and unused adsorbents.

For instance, GEH does not undergo significant changes in its composition before and after adsorption. It must be noted that GEH has previously been reported as akaganeite when analyzed using X-ray diffraction (XRD)(Kolbe et al. 2011). But XRD detects only the crystalline part of the adsorbent whereas Mossbauer spectroscopy can detect even the amorphous/nanocrystalline iron oxides making it a more suitable method.

For FSP even though the iron oxide phase is ferrihydrite in both the used and unused samples, there is a change in the hyperfine field. The unused FSP has a hyperfine field that is lower than the usual value for ferrihydrite (Murad 1988, Murad; and Schwertmann 1980). It could be that the FSP transformed from an adsorbent having a highly disordered to a more ordered ferrihydrite species. Usually, the surface area is higher for more amorphous iron oxides (Borggaard 2006). However, in this case, the used FSP, i.e. the adsorbent having more crystalline ferrihydrite, showed a higher surface area (Table S6-7). The surface area of the used FSP increased by more than 56 % compared to the unused FSP. This could be the reason for the increased adsorption capacity of the FSP after regeneration by the acid-alkaline method. But this increase in the surface area need not have been due to the transformation of iron oxide species but rather due to the removal of surface precipitates as will be discussed later.

For IEX, the content of ferrihydrite decreased and the overall content of goethite/hematite increased by 10 %. This higher transformation of the iron oxide phase in the IEX compared to GEH and FSP could be due to the nature of iron distribution in the adsorbent. FSP and GEH are bulk iron oxides, whereas IEX is a resin impregnated with iron oxide nanoparticles. This means that the iron oxide particles in IEX have a higher surface area to volume ratio. Thus, the fraction of the total iron oxide that is accessible to phosphate adsorption will be much higher in the IEX as compared to FSP and GEH. Hence, even if the active sites in all the adsorbents underwent a similar extent of transformation during regeneration, the overall change in the iron oxide phase will be higher for the IEX. Goethite and hematite have lower phosphate adsorption per unit area compared to ferrihydrite (Wang et al. 2013). So it is possible that this transformation in the IEX contributes to a decrease in its reusability. However, the decrease in ferrihydrite content is only 11 % whereas the decrease in adsorption capacity is about 60 %. Thus, it can be understood that transformation of the iron oxides alone is not affecting the reusability.

6.5.2.3. Effect of competing ions

To make the adsorbent reusable, it is necessary to regenerate the adsorbent properly, whereby the adsorbate molecules are desorbed, and the active sites are replenished. The phosphate adsorption experiments with 1 to 1.25 mm sized GEH and FSP granules were used to optimize the adsorption and regeneration procedure. Apart from phosphate, different competing ions

were monitored during adsorption cycle 1. Based on these observations (shown in Figure S6-11), selected ions were screened to be included in a mass balance while using adsorbents with particle size of 0.25 to 0.325 mm. These included calcium, organic carbon, inorganic carbon, silicon (Figure S6-12).

Values of the mass balance for the 0.25 to 0.325 mm sized adsorbents are shown in Table S6-8 in the supporting information. The mass balances could not be closed in several cases. For e.g. for GEH, the silicon released during regeneration was always lower than the amount adsorbed, and for IEX, the dissolved organic carbon released was always lower than amount adsorbed (shown in Figure S6-13).

Calcium was monitored since it can form surface precipitates (Kunaschk et al. 2015). The release of calcium from the different adsorbents regenerated using the acid-alkaline regeneration is shown in Figure S6-12. For GEH, the calcium release was less than 50 % in cycle 1. Thus the acid wash was switched from a pH of 4 to pH of 2.5 for cycles 2 and 3, based on the earlier protocol (Kunaschk et al. 2015). This improved the calcium release significantly amounting to 98 and 88 % for cycles 2 and 3. Iron concentration was monitored in the acid wash to check if the adsorbent was leaching iron. Even using a pH as low as 2.5, the amount of iron released per cycle for all the adsorbents was less than 0.01 % of the adsorbent mass packed in the column. For FSP, the calcium release during cycle 1 and 2 was higher than 100 % since FSP by default consists of calcium (see Table 6-3). For IEX, only around 20 % of calcium could be released during cycles 2 and 3.

In this study, the alkaline desorption step was used to desorb ions like phosphate that bind with the surface hydroxyl groups on the iron oxide. The acid wash step, on the other hand, was used to release the surface precipitates. Thus the release of a competing ion in either the acid wash step or during alkaline desorption gives information about its mechanism of binding on the adsorbent.

Figure 6-3 shows the average relative release percentages of different ions for FSP during the acid wash and alkaline desorption while using the acid-alkaline regeneration. The adsorbents GEH and IEX exhibited similar release patterns for the different ions (Figure S6-13).

From Figure 6-3, it can be seen that calcium is released exclusively during acid wash whereas phosphate is released exclusively via alkaline desorption. This was the case for all adsorbents (Figure S6-13). This shows that there is no formation of calcium phosphate precipitate and these ions bind via different mechanisms.

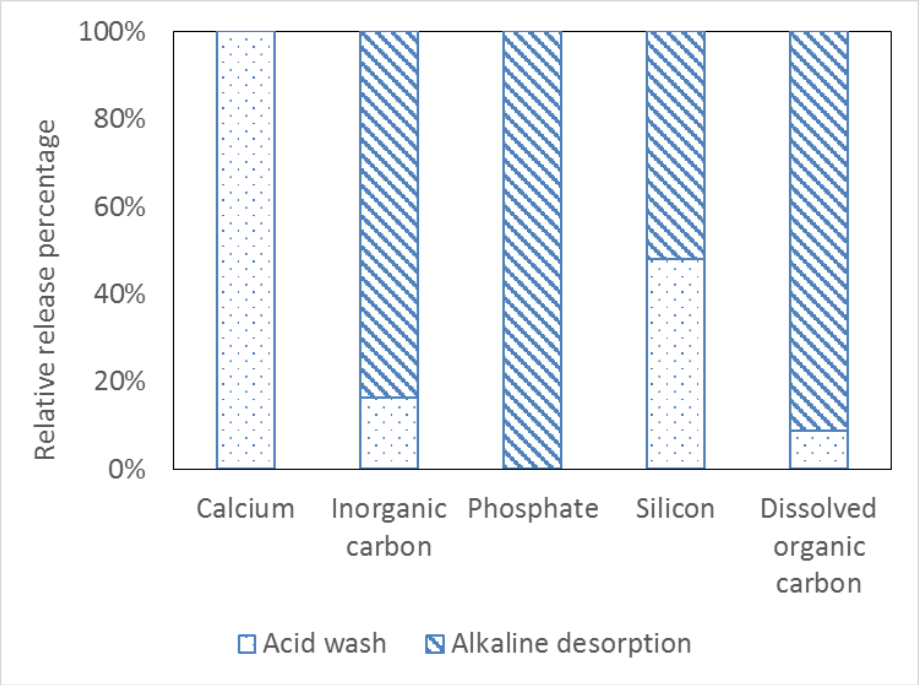


Figure 6-3: Relative release percentage of different ions from FSP in acid wash and alkaline desorption (for acid-alkaline regeneration)

A majority of the inorganic carbon, which at this pH would represent (bi)carbonate ions, was released during alkaline desorption. While it is possible that carbonate ions can sometimes adsorb via ligand exchange on iron oxides (Chunming Su and Suarez 1997), it was expected that in this case carbonate forms surface precipitates with calcium. But in these experiments, the acid wash was done in an open system. Therefore, if there were carbonate ions that were released during the acid wash, they would have mostly escaped as carbon dioxide (Hey et al. 1994).

Soluble silicon was about equally released in the acid wash as well as in alkaline desorption. Silicon present as orthosilicates can bind as innersphere complexes that would be desorbed during alkaline desorption, but could also form calcium silicate based precipitates that would dissolve in the acid wash (Lothenbach and Nonat 2015, Sigg and Stumm 1981). Organic carbon was mostly released by alkaline desorption. This is expected since organics like humics also bind to iron oxides via the ligand exchange with their surface functional groups (Antelo et al. 2007, Ko et al. 2005).

These results show that different ions bind on the adsorbent via different mechanisms and not all of them are completely released. More regeneration cycles would show how this affects the adsorbent reusability over time.

6.5.2.4. Effect of calcium based surface precipitation

The reason for using acid wash in the regeneration methods was based on the premise of removing calcium based surface precipitates (Kunaschk et al. 2015). Figure 6-4 shows the SEM-EDX observations on the unused FSP, FSP that had been used for 3 adsorption cycles using acid-alkaline regeneration, and FSP that been used for 3 adsorption cycles but

regenerated only using alkaline desorption. The color codes for the elemental maps are stated in the figure caption.

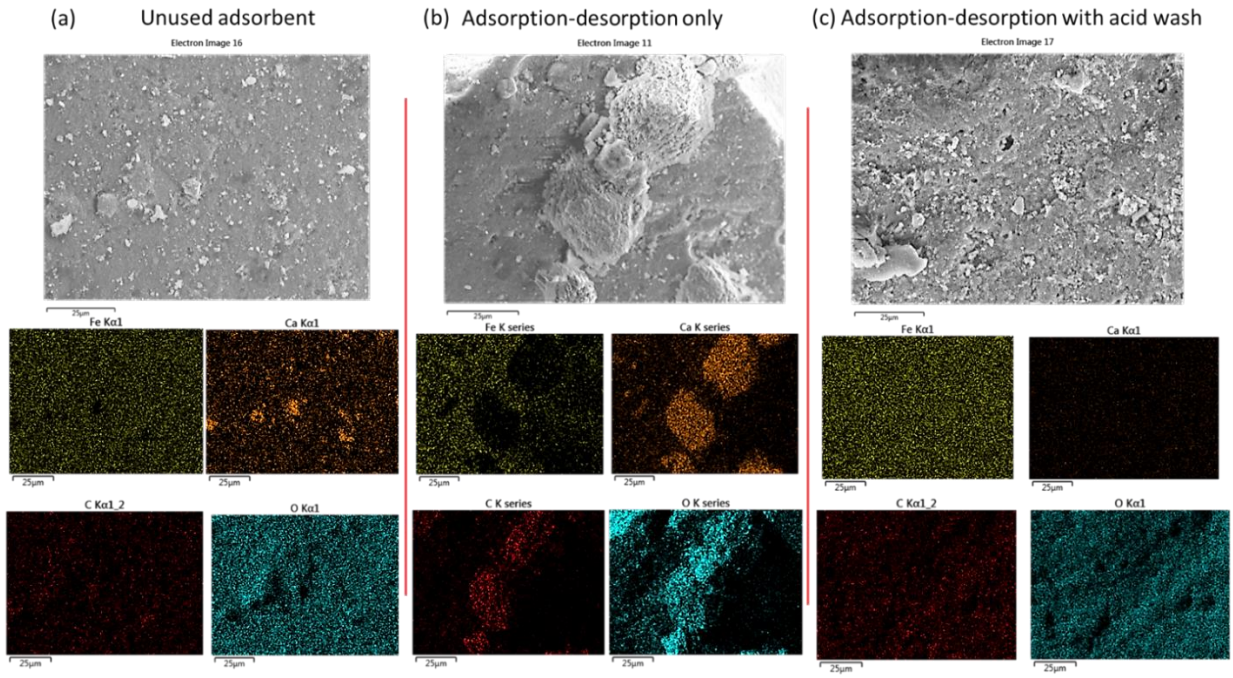


Figure 6-4: SEM-EDX observations of FSP adsorbent for (a) unused content (Ca content as per EDX = 5 wt %), (b) FSP regenerated without acid wash (Ca content = 15 wt %), (c) FSP regenerated with acid wash ash (Ca content = 0 wt %). Scalebar represent 25 µm. Color code for elemental maps- Yellow = Iron, Orange = Calcium, Red = Carbon, Blue = Oxygen.

It can be seen from Figure 6-4 (a), that unused FSP has calcium by default. But the elemental map of calcium and carbon do not overlap implying there is no observable calcium carbonate. Figure 6-4 (b) shows the FSP that was regenerated only with alkaline desorption and no acid wash. There are large areas in the elemental distribution where calcium, carbon and oxygen overlap. This implies the presence of calcium carbonate. The observable calcium carbonate particles are about 25 µm in size. Figure 6-4 (c) shows that the acid washed FSP (using acid-alkaline regeneration) has no calcium left and thus the surface precipitates are removed via acid wash. This was confirmed by Raman spectroscopy where the FSP regenerated without acid wash showed Raman shift characteristics of calcium carbonate (shown in Figure S6-14).

This result is in line with the observations in Figure 6-3 and Figure S6-13 that the calcium was released exclusively via the acid wash and hence must be present in the form of surface precipitates. While calcium carbonate was the only precipitate that was observable, some silicon was also released during the acid wash (Figure 6-3), indicating the possibility of calcium silicate precipitates. However, the molar ratio of inorganic carbon to silicon present in the wastewater was more than 20 (as seen from Table 6-2), and the solubility product for calcium carbonate is lower than calcium silicate (Benjamin 2010, Greenberg et al. 1960). Thus calcium carbonates are likely the dominant precipitates formed on the adsorbent surface.

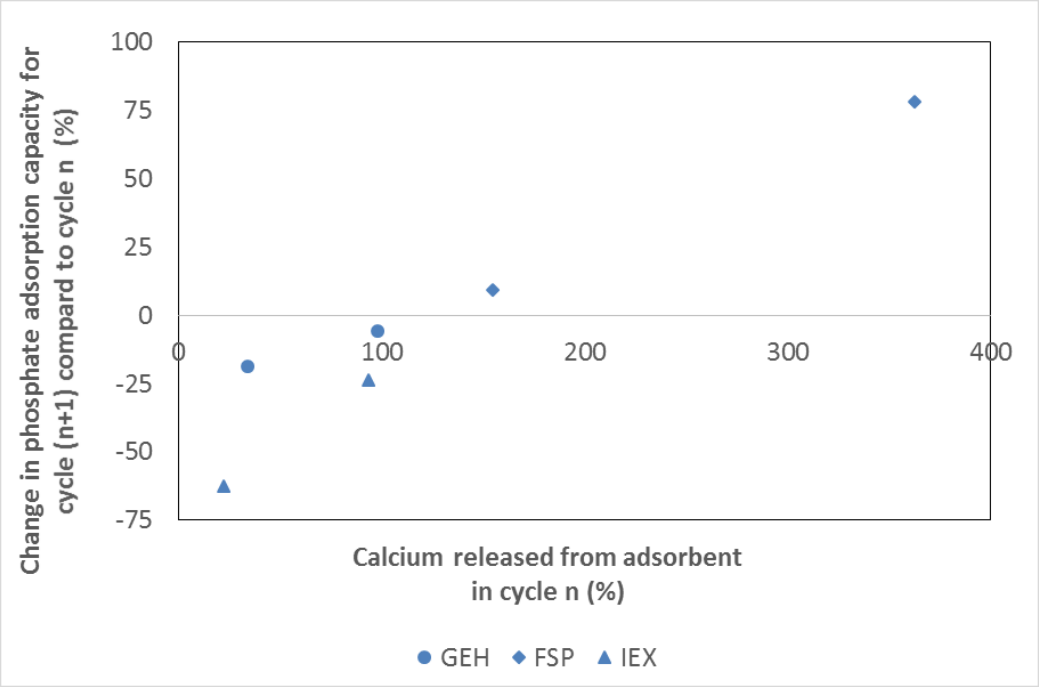


Figure 6-5: Change in phosphate adsorption capacity for a given cycle compared to the calcium release in the previous cycle (using acid-alkaline regeneration). n+1 is used to denote the current cycle and n denotes the previous cycle. n = 1,2. A negative change in the phosphate adsorption capacity implies the adsorbent reusability decreases whereas a positive change implies the reusability is enhanced.

To test for the effect of calcium based surface precipitates on the adsorbent reusability, the extent of calcium release from the adsorbents was correlated with the adsorption capacities. Figure 6-5 shows the change in phosphate adsorption capacity for a given cycle compared to the calcium released from the previous cycle. n+1 denotes the current cycle and n denotes the previous cycle.

Figure 6-5 includes data points from all the adsorbents regenerated using the acid-alkaline method. The data points showing more than 100 % calcium release are from FSP since it contained calcium by default. The general trend observed is that the change in phosphate adsorption capacity is negative, i.e. the adsorbent reusability decreases if not all the calcium from the adsorbent is released. This agrees with the reasoning that the calcium carbonate precipitates affect the adsorbent reusability and needs to be removed via an acid wash.

6.5.3. Mechanism of decrease in adsorbent reusability via surface precipitation

6.5.3.1. Hypothesis based on desorption of phosphate

The above results show the need for an acid wash step to remove the calcium based surface precipitates. As per the earlier study, having an acid wash step before alkaline desorption

resulted in better adsorbent reusability than the other way around (Kunaschk et al. 2015). The explanation provided in that study was that adsorbed phosphate was blocked by surface precipitates. Thus the surface precipitates need to be first released before the phosphate can be released via alkaline desorption (a depiction of this hypothesis is shown in Figure S6-15). This hypothesis was tested in our study by reversing the order of regeneration and checking the extent of phosphate released during regeneration. If the hypothesis is correct, then having an acid wash step after alkaline desorption should lead to a lower desorption of phosphate. Figure 6-6 (a) and (b) show phosphate released during alkaline desorption for the adsorbents used in the experiments corresponding to Figure 6-1 and Figure 6-2, respectively. The release percentage was calculated by measuring the amount desorbed in relation to the amount adsorbed.

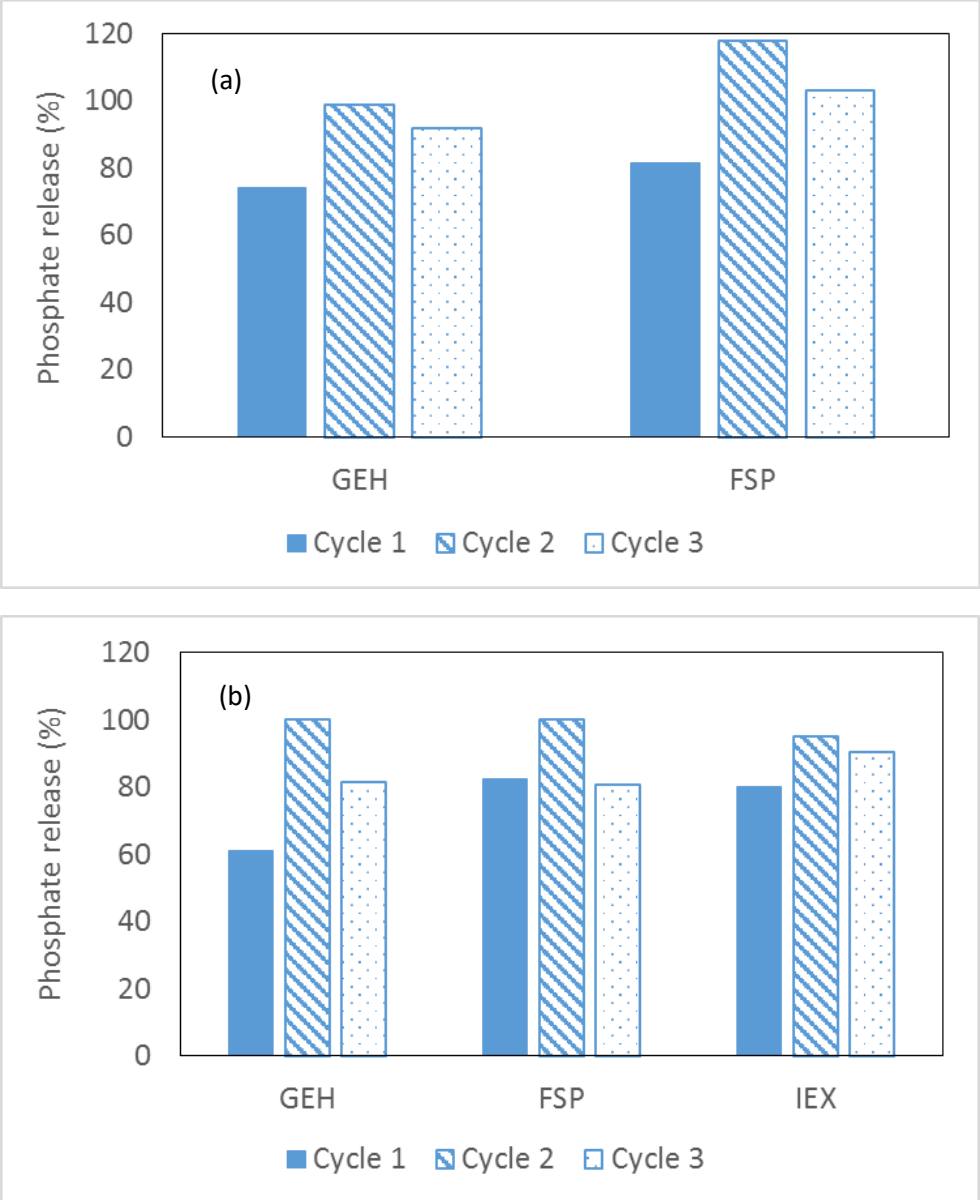


Figure 6-6: Percentage of phosphate released during alkaline desorption step using (a) alkaline-acid regeneration (b) acid-alkaline regeneration.

The phosphate release from all adsorbents mostly varied between 80 to 100 % using both regeneration methods. From Figure 6-6 (a) it can be seen that FSP released more than 100 % phosphate for the 2nd cycle. This could have come from the phosphate that was not released during the 1st cycle. Comparing Figure 6-6 (a) and (b), there was no significant difference in the phosphate released by the two different regeneration methods. Thus, we conclude the differences in reusability as seen in Figure 6-1 and Figure 6-2 are apparently not due to blockage of adsorbed phosphate molecules as suggested in the earlier hypothesis.

This implies that the reason for differences in reusability for GEH and FSP between the two regeneration methods (as seen in Figure 6-1 and Figure 6-2) was due to the differences in the acid wash conditions. In the alkaline-acid regeneration, a pH of 4 was used for the acid wash step. This was to make sure iron dissolution from the iron oxides does not happen. In the acid-alkaline regeneration, we tried to improve the reusability by having stronger acid wash conditions. This was done by first having longer exposure time with pH 4. However, the calcium release from GEH was still less than 50 % (Table S6-8 and Figure S6-12). Thus a stronger acidic pH of 2.5 was used as suggested previously (Kunaschk et al. 2015). We noticed that no significant iron was leached from the acid wash implying that the acid was consumed primarily for breaking the surface precipitates. Thus the enhanced reusability was due to the release of surface precipitates. But apparently, the surface precipitates do not hinder reusability by just blocking the adsorbed phosphate. This implies that there could be some additional mechanism by which surface precipitation affects reusability.

6.5.3.2. Possible role of calcium adsorption

It could be that the calcium based surface precipitates block the actives sites for phosphate on the adsorbent. However, as seen from Figure 6-3 and Figure S6-13, calcium binds on the adsorbent via a different mechanism to phosphate and hence should not directly block the active sites. In the case of FSP, the adsorbent already contains calcium in its unused state. If this calcium was present as precipitates blocking the adsorbent pores or covering the iron oxide, the removal of this calcium during washing would expose active sites on the adsorbent that were previously inaccessible. This could be a reason for the increase in the surface area and the adsorption capacity of FSP for the 2nd and 3rd cycle when using acid-alkaline regeneration (Figure 6-2).

Another possible way that calcium carbonate precipitates can affect the adsorbent reusability is by changing the point of zero charge (PZC) of the adsorbent and affecting the adsorption of calcium on them. Calcium ions are known to bind to iron oxide surfaces and enhance phosphate adsorption by making the surface electropositive (Antelo et al. 2015, Han et al. 2017, Rietra et al. 2001). A study testing GEH for adsorption of phosphonate, which binds to iron oxides in a similar mechanism as phosphate, reported that phosphonate adsorption at equilibrium doubled in a solution having a Ca:P molar ratio of 2 as compared to a solution without any calcium (Boels et al. 2012). This implies calcium adsorption onto GEH could result in a favorable equilibrium shift for phosphate adsorption as well.

Figure 6-7 shows the calcium and phosphate adsorption for all the adsorbents during all adsorption cycles for acid-alkaline regeneration. This includes only the calcium that was adsorbed during the adsorption process and does not consider the calcium that is by default in the FSP adsorbent. A positive correlation was observed between overall adsorption of calcium and phosphate ions.

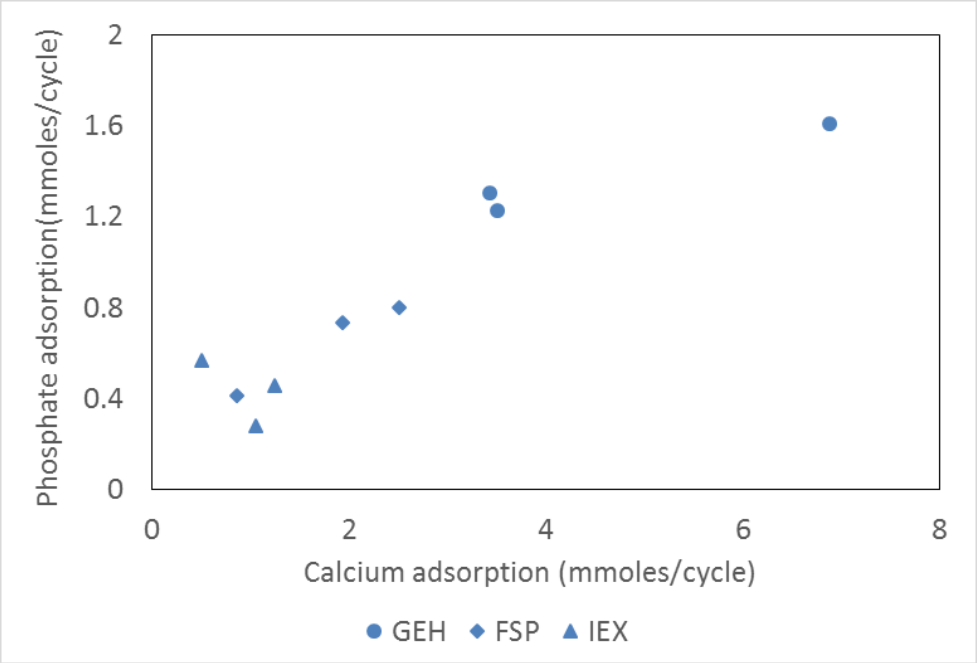


Figure 6-7: Correlation of Ca vs P adsorption (including all cycles for all adsorbents using acid-alkaline regeneration)

Calcium likely first physisorbs on the adsorbent surface before it forms calcium carbonate precipitates. Physisorption of calcium would enhance phosphate adsorption by making the surface electropositive (Antelo et al. 2015). Studies show that significant calcium binding happens only at a pH higher than the PZC of the adsorbent (Antelo et al. 2015, Rietra et al. 2001). At pH higher than PZC, the adsorbent surface is electronegative which will enhance calcium binding. Thus, if an adsorbent has lower PZC than the pH of wastewater effluent, more calcium would bind to the adsorbent, which in turn would enhance the P adsorption. The pH of the wastewater effluent was 7.9 and the PZC for GEH and FSP was 6.1 and 9.1, respectively. This could be the reason why more calcium binds to GEH in cycle 1 compared to FSP (Table S6-8 and Figure S6-11). Hence GEH shows a higher phosphate adsorption capacity for cycle 1 than FSP.

However, the PZC on the adsorbent could shift upon the binding of calcium. Calcium carbonates have often shown PZC that are higher than 9 (Al Mahrouqi et al. 2017). The formation of calcium carbonate precipitates could thus increase the PZC of the adsorbent. This would usually be more favourable for phosphate adsorption since the adsorbent surface is more electropositive at a given pH. However, a higher PZC would mean less calcium adsorption, which in turn would imply less phosphate adsorption.

PZC measurements (Figure S6-16) supported the above speculation. FSP with calcium carbonate had a higher PZC (PZC = 9.8), than the unused FSP which had some calcium (PZC = 9) and the acid-washed FSP which had no calcium (PZC = 7.5). These PZC's were determined using the salt addition method which depends on the pH measurements (Mahmood et al. 2011). This commonly used method can however have a shortcoming when measuring PZC of porous materials because impurities/unwashed ions (like hydroxide ions) in the pores can affect the measurement. Thus, to prove/disprove this hypothesis, more accurate methods like zeta potential measurements should be used to determine the surface charge.

For IEX, the correlation with calcium is not as strong. In the case of IEX, the decrease in reusability could thereby be due to multiple reasons like the transformation of iron oxide phase and incomplete release of adsorbed organics. The incomplete release of organics from IEX could be related to the nature of regeneration. Hybrid ion exchange resins have been shown to remove anions via a combination of mechanisms involving ligand exchange on the iron oxide as well as coulombic interaction on the functional groups of the resin backbone. (Sengupta and Pandit 2011) used a combination of sodium chloride (NaCl) and NaOH solutions for regeneration and reported ten successful regeneration cycles. However, the adsorption was studied for solutions containing only phosphate and sulphate ions, unlike the wastewater effluent which also contains organics. Organics like humic acids also bind to hybrid ion exchange resins via the functional groups on the resin backbone as well as the iron oxides impregnated within them (Shuang et al. 2013). Hence regeneration with only NaOH might not release the organics bound on the functional groups of the resin. Although such organics might not compete with the active sites for phosphate directly, the binding of humics might confer a negative charge to the adsorbent (Antelo et al. 2007). This would be similar to a Donnan ion exclusion effect which would hinder the transport of anions into the resin and hence reduce phosphate adsorption in subsequent cycles (Cumbal and SenGupta 2005).

6.5.4. Adsorbent regeneration from a practical point of view

In regeneration methods involving acid wash, the pH in the adsorbent column was neutralized after the regeneration process. In some of these cases, when the alkaline desorption was the last step, more than 1000 bed volumes of distilled water were required to neutralize the column. To reduce the bed volume needed to neutralize the pH in these cases, the distilled water was spiked with HCl solution of pH 4.

In practice, a regeneration method producing a minimal amount of waste and consuming the least chemicals should be employed. Moreover, we also wanted to check if an acid wash was necessary prior to every adsorption cycle. In the current experiment, after alkaline desorption, the column was rinsed with 50 bed volumes of distilled water but the pH in the pores was still not neutralized. Subsequent adsorption runs were performed as such. Figure 6-8 shows the reusability of FSP when this regeneration strategy was used.

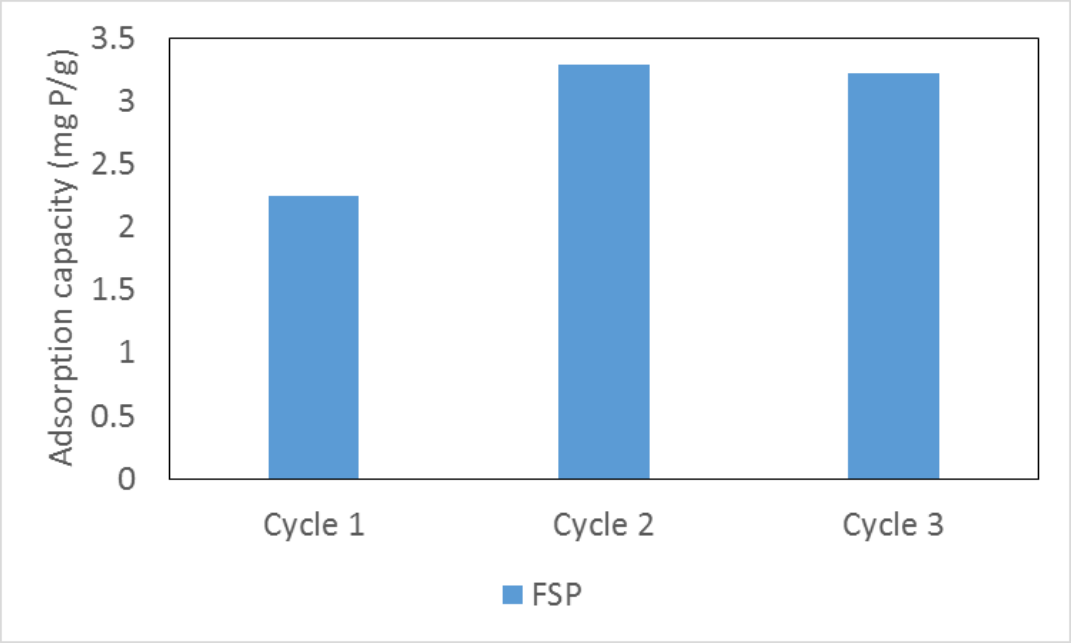


Figure 6-8: Adsorption capacity at an effluent concentration of 0.1 mg P/L for FSP regenerated using only alkaline desorption. Adsorbent particle size was 0.25 to 0.325 mm.

Figure 6-8 shows that the phosphate adsorption capacity increased for cycle 2 and cycle 3. From mass balances (Table S6-9), it was seen that the amount of calcium bound to the adsorbent increased by a factor of about 7 times for cycles 2 and 3 compared to cycle 1. When comparing the pH profile from the column effluent with the calcium removal by the adsorbent, it was seen that the increase in calcium uptake coincided with higher effluent pH (Figure S6-17).

The increase in calcium binding is likely because the pH inside the pores of the regenerated adsorbent is higher than the PZC. Thus, a high amount of calcium could bind to the adsorbent in such cases, which could also enhance phosphate adsorption. During such a regeneration method there is also a possibility of calcium phosphate precipitation. This would happen in the initial bed volumes of the adsorption run where the pH is high. Results from mass balance calculations (Table S6-9) show that the average phosphate release via alkaline desorption during this regeneration method is about 1.5 times lower than regeneration methods 1 and 2. This implies that some phosphate is bound as surface precipitates and hence this would be released only via acid wash. Thus, an acid wash would probably be needed after some adsorption cycles.

Based on our observations, we can envision 3 different strategies for adsorbent regeneration as listed in Table 6-6.

Table 6-6: Different regeneration strategies with their advantages and disadvantages

Regeneration method	Advantages	Disadvantages
Alkaline desorption with acid wash during every cycle	Adsorption capacity is retained for each cycle	Neutralization of adsorbent bed required after every cycle
	No buildup of surface precipitates after every cycle	More chemical consumption during regeneration than other methods
Alkaline desorption each cycle, with intermittent acid wash in between some cycles	Neutralization of adsorbent bed is not required after every cycle	Calcium phosphate precipitation occurs
	Adsorption capacity will be retained for some cycles before adsorbent needs acid wash	Part of phosphate will be released in acid wash
Alkaline desorption with no acid wash at all	No acid consumption	This is a viable option only if calcium carbonate precipitation does not happen
	Least chemical consumption compared to other regeneration methods	Phosphate adsorption capacity will be lower in the absence of calcium adsorption

In our study, we have used fresh acid and alkaline solutions for every regeneration step. In practice, the regenerate solutions would need to be reused to make the process more cost-effective. We noticed that more than 250 bed volumes of acid wash solution of pH 2.5 were consumed while regenerating the FSP adsorbent. This would thus be attributed to waste generated during the regeneration process unless the solution can be reused over many cycles by only replenishing the acid consumed. One way to overcome this problem is to prevent surface precipitation in the first place and hence prevent an acid wash step, which is the 3rd type of regeneration strategy we highlight in Table 6-6. To prevent/minimize surface precipitation, the mechanism of calcium binding needs to be understood better. Understanding this mechanism could help modify adsorbent properties such that calcium binding could be moderated. This can be used to enhance phosphate adsorption due to co-adsorption of calcium but minimize surface precipitation to lower acid consumption. For e.g. changing the adsorbent surface charge could be a strategy to moderate calcium binding.

Moreover, we have only shown 3 adsorption-regeneration cycles in our study. The adsorbent would need to last several adsorption cycles in practice. Hence future studies should also test the reusability over more adsorption-regeneration cycles.

6.6. Conclusion

This research has monitored various aspects that could affect the phosphate adsorption and reusability of adsorbents in a wastewater effluent.

- Despite having a similar surface area, smaller adsorbent particles (0.25 to 0.325 mm) exhibited more than 4 times higher phosphate adsorption capacities than larger adsorbent particles (1 to 1.25 mm). This points at the importance of diffusion in porous adsorbents.
- In most cases, only minor changes were noticed for the adsorbents in the type of iron oxide and surface area after 3 cycles of reuse. These changes were not significant to explain changes in reusability of the adsorbent.
- Reversing the order of acid wash and alkaline desorption steps during regeneration did not affect the desorption of phosphate during the 3 cycles.
- Calcium enhanced phosphate adsorption but also formed calcium carbonate based precipitates on the adsorbent which need to be removed to maintain reusability.
- Future studies should focus on understanding the mechanism of calcium binding and monitoring the reusability for more cycles.

6.7. Supporting information

6.7.1. Tables

Table S6-7: Change in adsorption capacity of the adsorbents with respect to change in pore area

		GEH		FSP		IEX*	
Regeneration method		**Total pore area (m2/g)**	**Adsorption capacity (mg P/g)**	**Total pore area (m2/g)**	**Adsorption capacity (mg P/g)**	**Total pore area (m2/g)**	**Adsorption capacity (mg P/g)**
Alkaline-acid	**Cycle 1**	244.0	0.90	178.9	0.43	-	-
	Cycle 3	219.8	0.43	224.1	0.40	-	-
Acid-alkaline	**Cycle 1**	243.5	4.2	174.5	2.1	58.2	4.8
	Cycle 3	224.9	3.2	271.8	3.6	69.9	1.9
Only alkaline desorption	**Cycle 1**	-	-	174.5	2.2	-	-
	Cycle 3	-	-	220.7	3.2	-	-

*For IEX dry weight was used in these calculations since the pore area was measured for the dry adsorbents.

Note that for method 1, the adsorbent particle sizes used in the column were 1 to 1.25 mm, whereas for method 2 and 3, the adsorbent particle sizes used in the column were 0.25 to 0.325 mm.

Table S6-8: Mass balance[a] during acid-alkaline regeneration for

(a) GEH

		Calcium (mg Ca)	Inorganic carbon (mg C)	Phosphate (mg P)	Silicon (mg Si)	Dissolved organic carbon (mg C)
Cycle 1	**Adsorption**	275	368	50	197	25
	Acid wash	94	0	0	5	0
	Alkaline desorption	0	40	30	10	39
Cycle 2	**Adsorption**	137	100	40	124	98
	Acid wash	134	4	0	54	4
	Alkaline desorption	0	16	40	21	23
Cycle 3	**Adsorption**	141	66	38	97	87
	Acid wash	124	6	0	29	2
	Alkaline desorption	0	17	31	13	25

(b) FSP

		Calcium (mg Ca)	Inorganic carbon (mg C)	Phosphate (mg P)	Silicon (mg Si)	Dissolved organic carbon (mg C)
Cycle 1	**Adsorption**	35	79	13	19	-3[b]
	Acid wash	125	0	0	6	0
	Alkaline desorption	0	36	10	18	22
Cycle 2	**Adsorption**	78	66	23	41	31
	Acid wash	120	6	0	40	3

	Alkaline desorption	0	16	23	21[c]	23
Cycle 3	**Adsorption**	101	31	25	67	68
	Acid wash	78	3	0	17	1
	Alkaline desorption	0	9	20	15	24

(c) IEX

		Calcium (mg Ca)	**Inorganic carbon (mg C)**	**Phosphate (mg P)**	**Silicon (mg Si)**	**Dissolved organic carbon (mg C)**
Cycle 1	**Adsorption**	20	137	18	34	46
	Acid wash	19	0	0	6	0
	Alkaline desorption	0	22	14	12	30
Cycle 2	**Adsorption**	50	16	14	18	46
	Acid wash	11	11	0	21	4
	Alkaline desorption	0	9	13	12	22
Cycle 3	**Adsorption**	42	31	9	25	31
	Acid wash	7	10	0	11	4
	Alkaline desorption	0	13	8	6	20

a- Note that in some cases, by the time the adsorption process was stopped, the outflow concentration was higher than 0.1 mg P/L. In these cases, for the estimation of adsorption capacity, only the amount adsorbed till 0.1 mg P/L was considered. However, in the overall mass balances, the amount adsorbed from the complete run is considered.

b- For the 1st cycle of GEH and FSP, the dissolved organic carbon released was higher than adsorbed. For FSP, there was some release of dissolved organic carbon during the adsorption. Perhaps some organics might have remained in the column from the previous runs (regeneration method 1) that were not washed away.

c- Silicon release was also higher than adsorbed in some cases. A reason could be that 24 h exposure to 1M NaOH solution during the alkaline desorption. This might have leached silica from the glass material like the column, glass beads, and glass wool.

Table S6-9: Mass balance for FSP regenerated only using alkaline desorption.

		Calcium (mg Ca)	**Inorganic carbon (mg C)**	**Phosphate (mg P)**	**Silicon (mg Si)**	**Dissolved organic carbon (mg C)**
Cycle 1	**Adsorption**	21	0	14	24	36
	Alkaline desorption	0	12	7	13	2
Cycle 2	**Adsorption**	145	63	20	53	41
	Alkaline desorption	0	45	14	18	6
Cycle 3	**Adsorption**	150	70	19	31	35
	Alkaline desorption	0	46	11	18	18

6.7.2. Figures

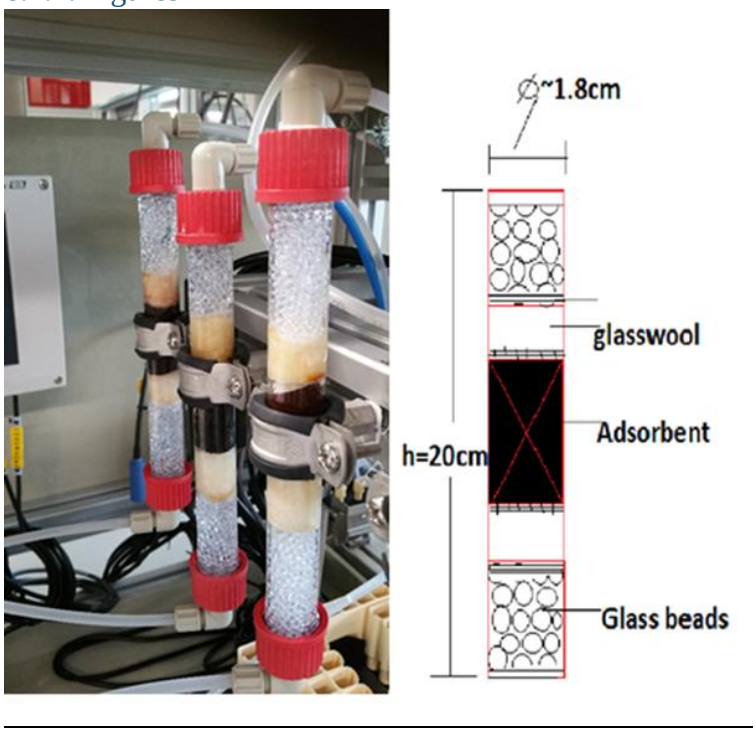


Figure S6-9: Adsorption column used for the experiments

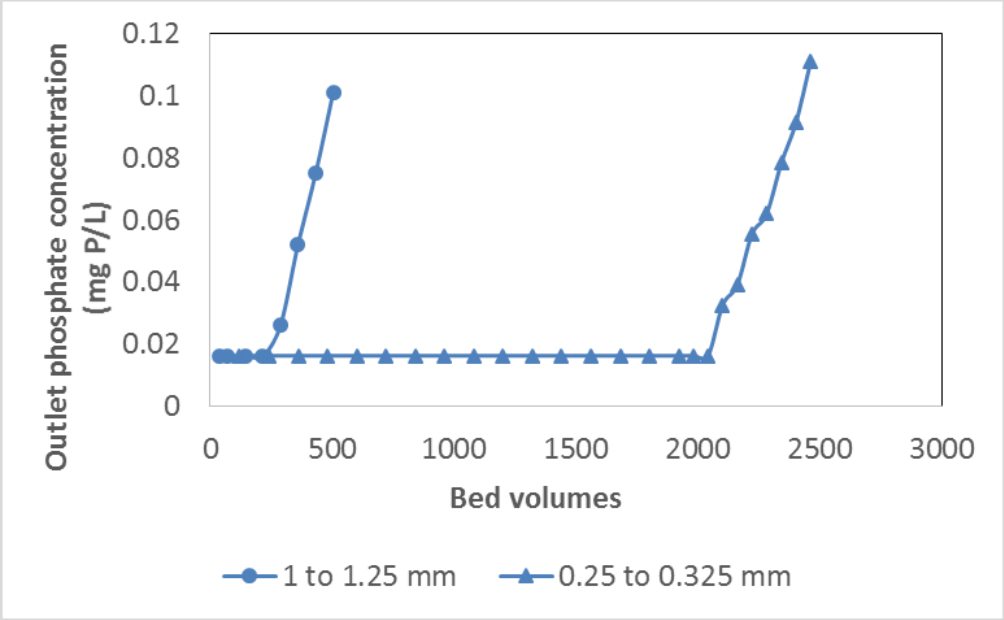


Figure S6-10: Breakthrough curve for 1st cycle of GEH of varying particle sizes. Inlet concentration was 2 ± 0.2 mg P/L.

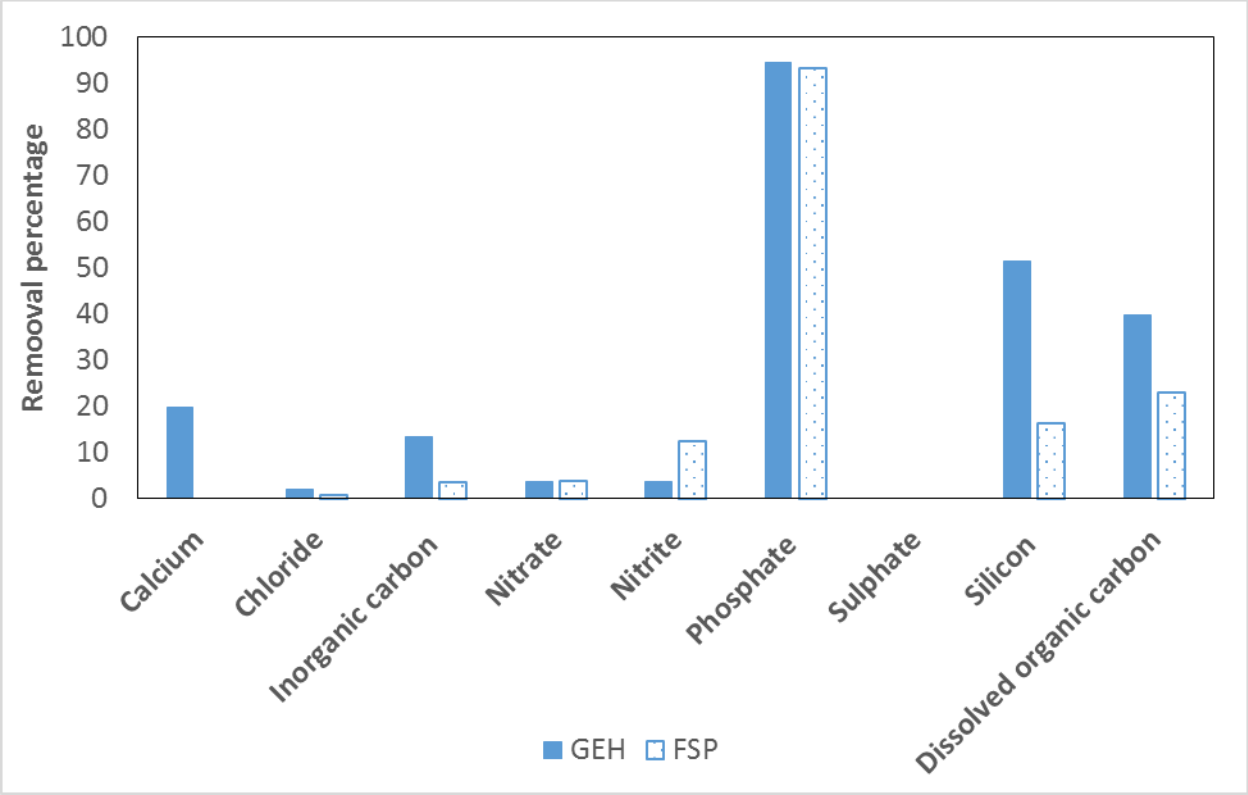
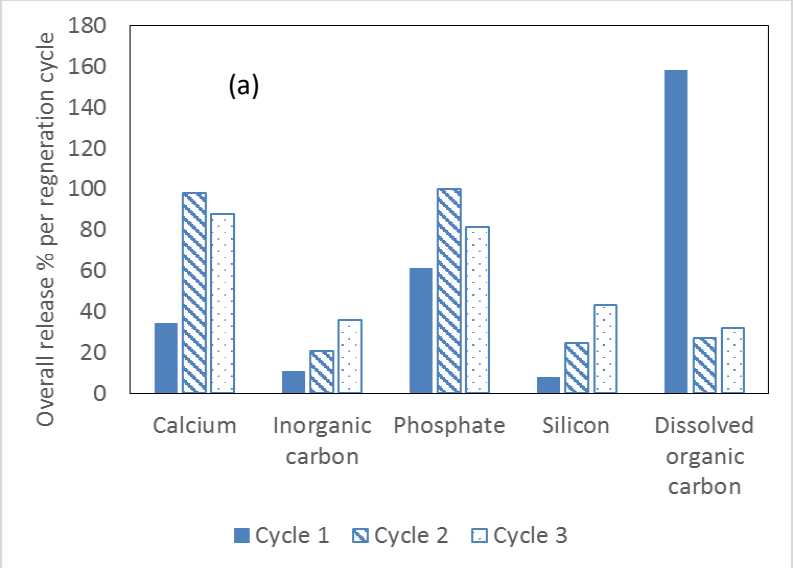
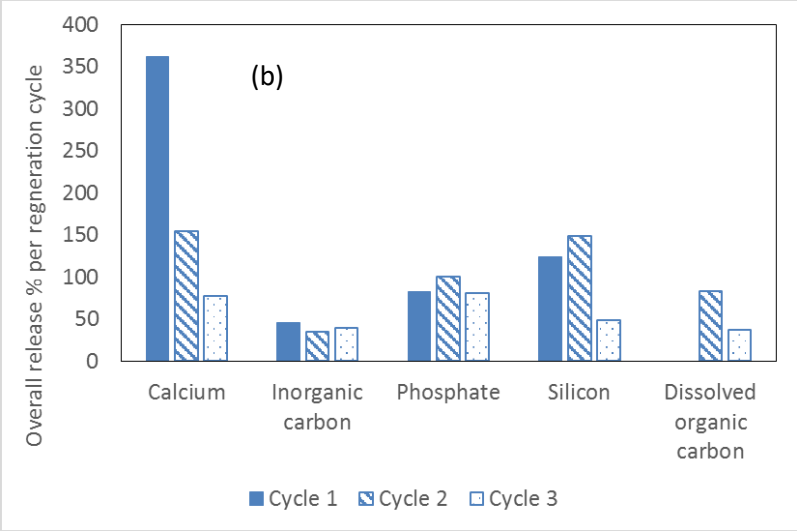


Figure S6-11: Removal percentage of various ions that were tested for competing effects during cycle 1 of alkaline-acid regeneration. The plot represents the removal percentage when the effluent concentration from the outflow reaches 0.1 mg P/L.





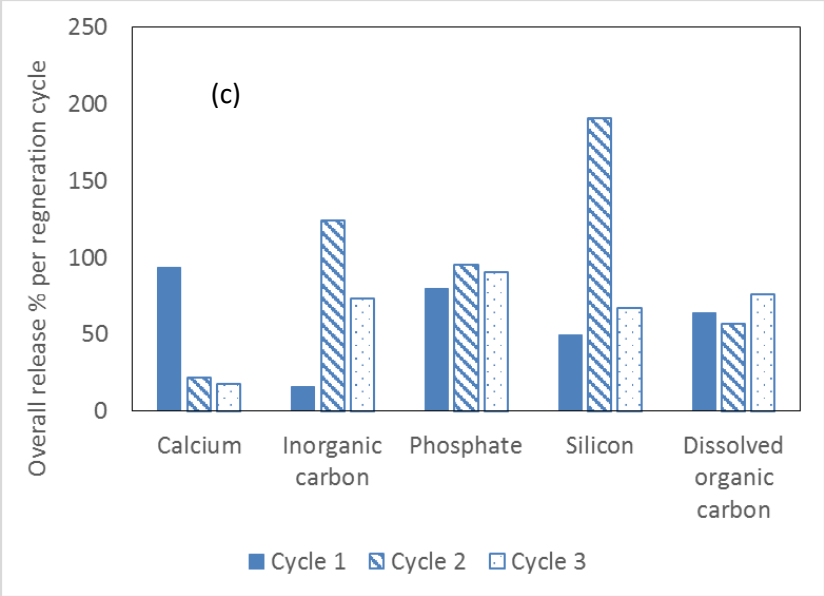
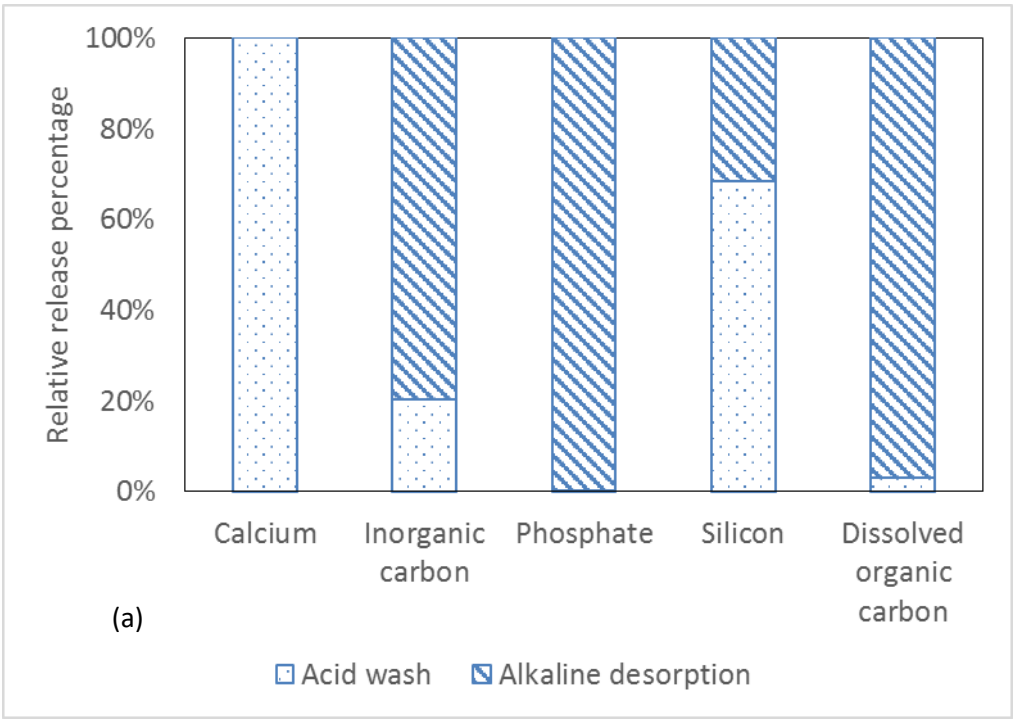


Figure S6-12: Release percentage of different ions during acid-alkaline regeneration. Plots are based on values from table S2 for (a) GEH (b) FSP (c) IEX



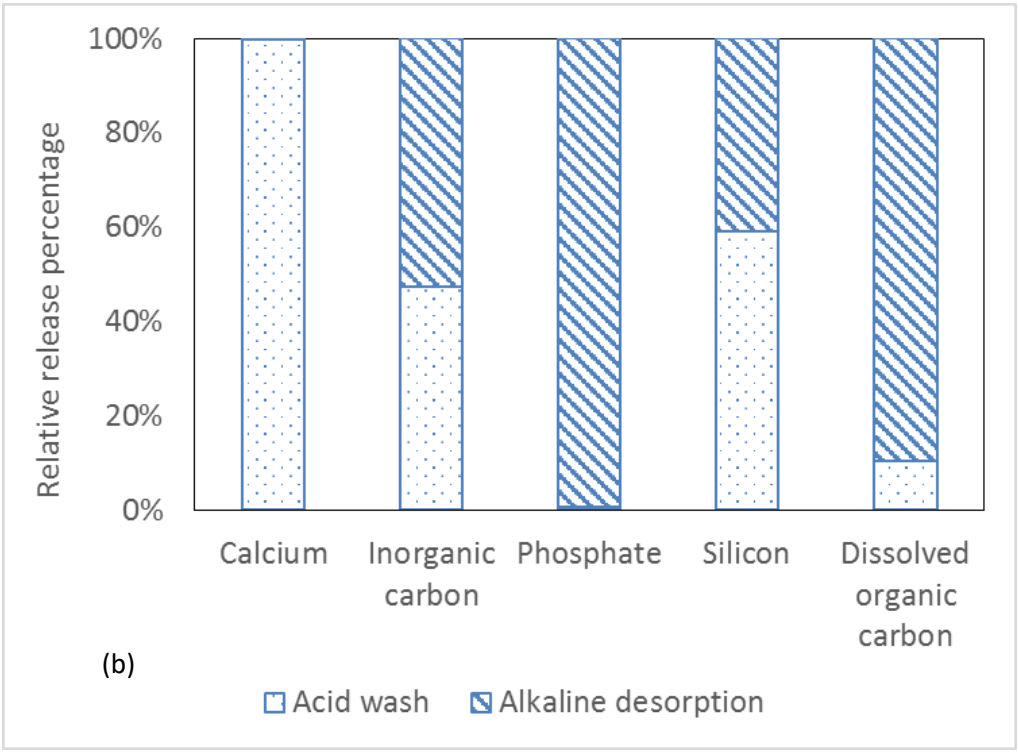
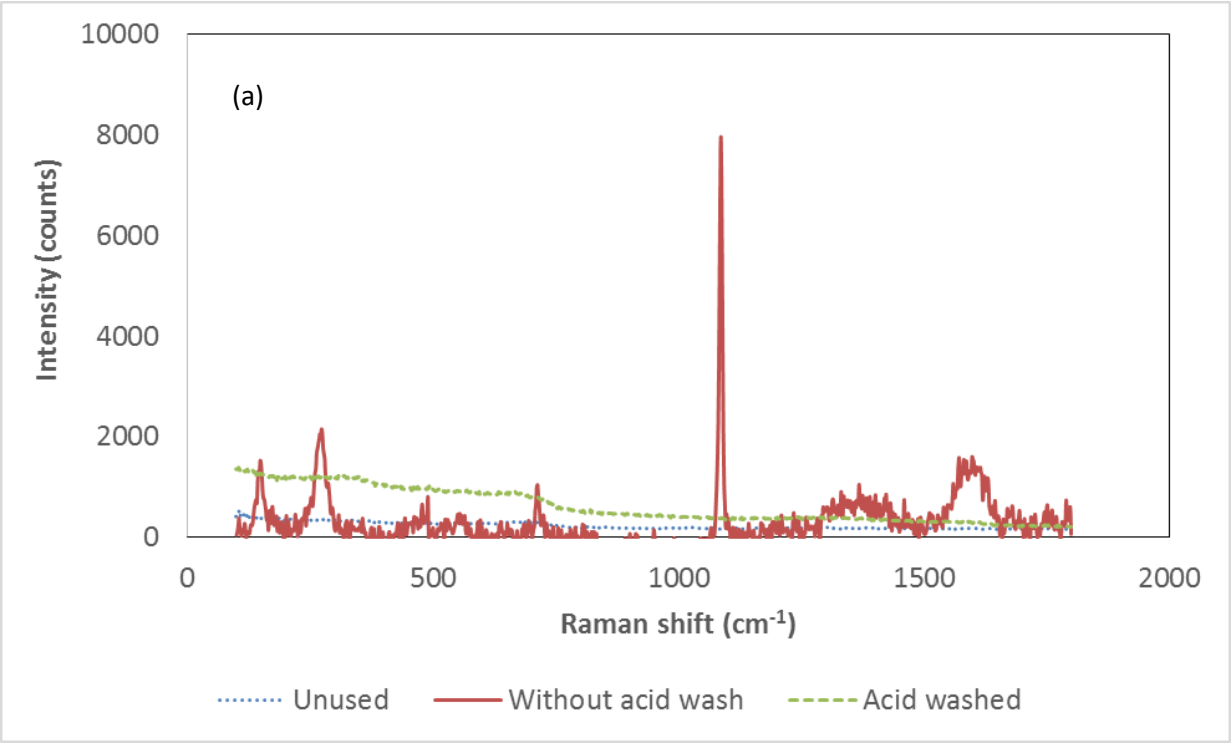


Figure S6-13: Relative release of different molecules in acid wash and alkaline desorption during acid-alkaline regeneration for (a) GEH and (b) IEX



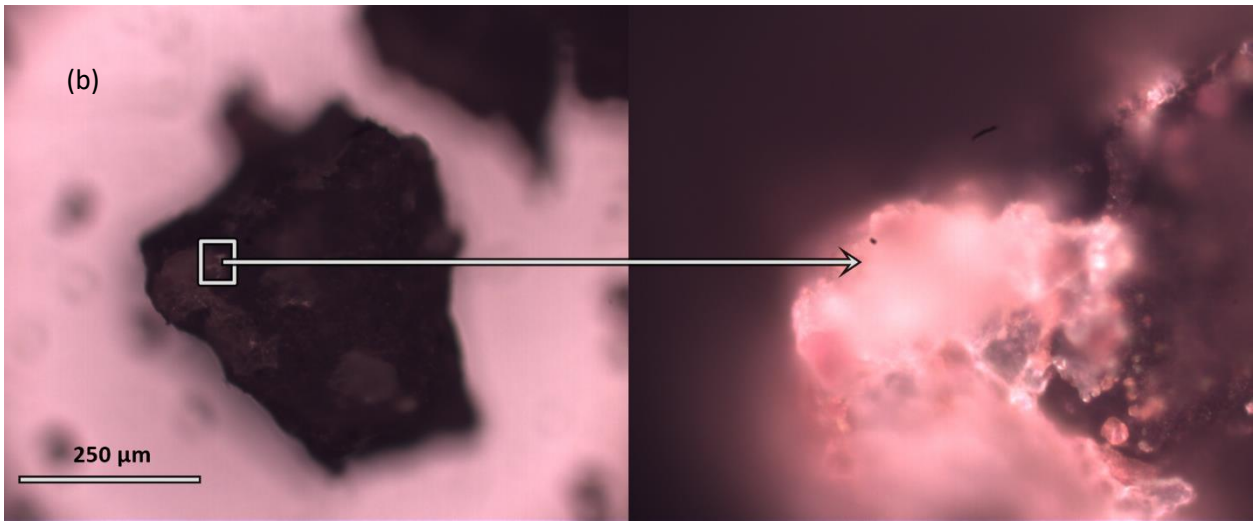


Figure S6-14:(a) Raman spectra for the unused FSP, and FSP regenerated with and without an acid wash. The sharp peak at 1086 cm^{-1} corresponds to calcium carbonate (M et al. 2016). (b) Image of a FSP adsorbent granule which was regenerated without an acid wash. The picture on the right shows the spot where the calcium carbonate was spotted for the corresponding spectra in (a).

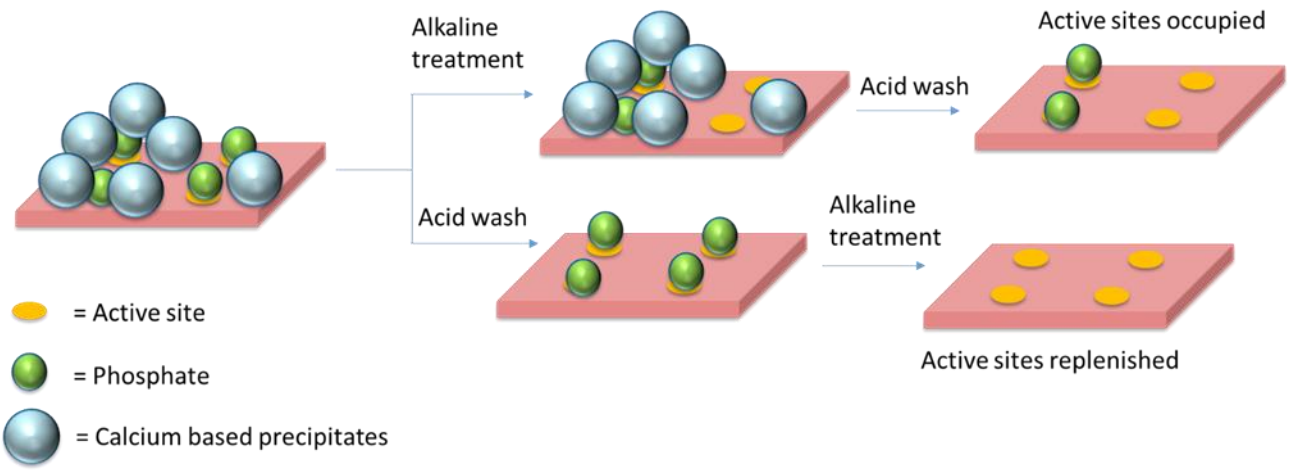


Figure S6-15: Schematic for explanation of the regeneration method as proposed by an earlier study (Kunaschk et al. 2015).

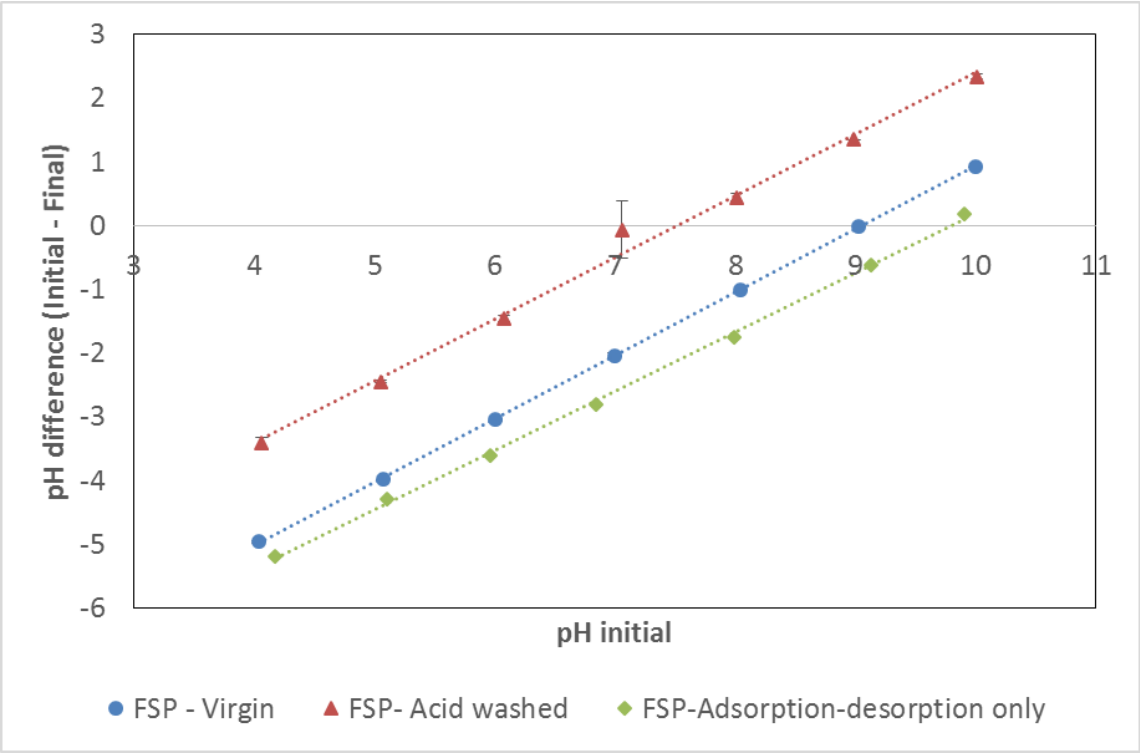


Figure S6-16: Point of zero charge (PZC) determination for unused FSP, and FSP regenerated with and without acid wash.

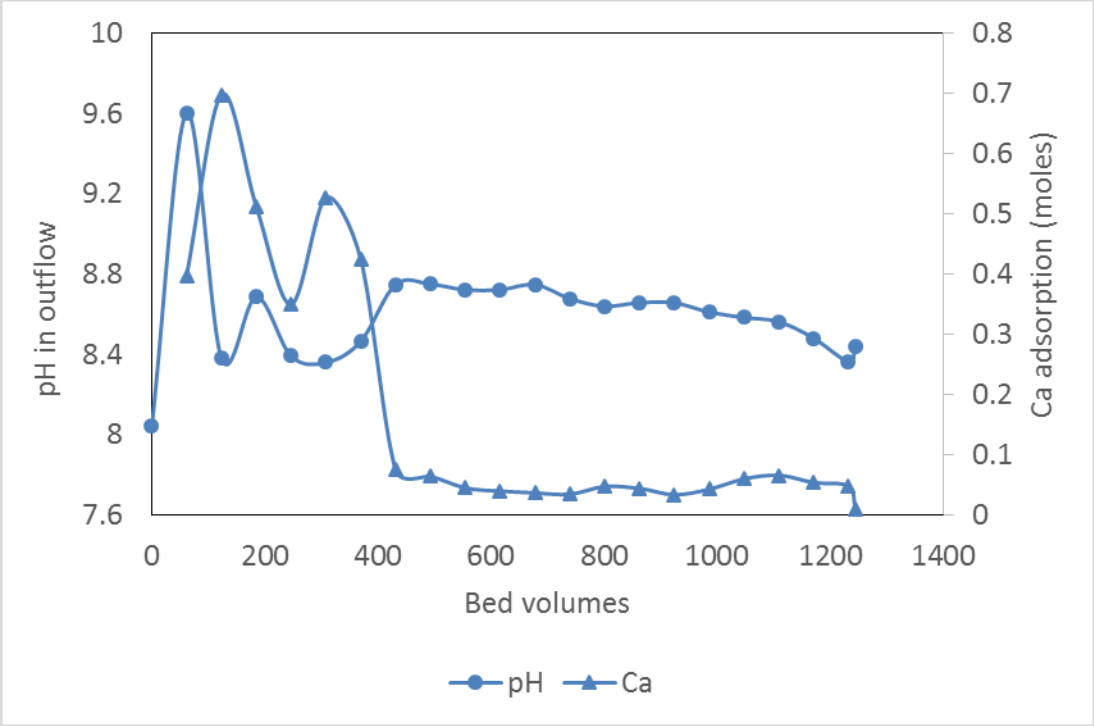


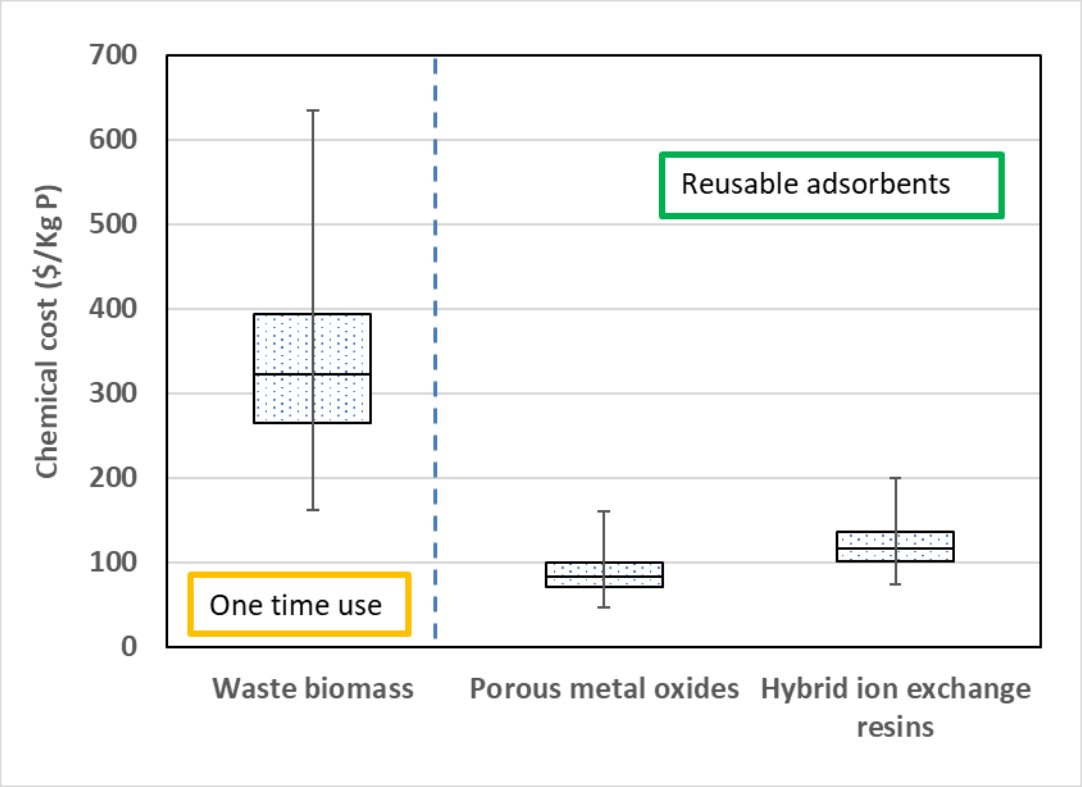
Figure S6-17: pH and Ca adsorption profile for the 2nd cycle of FSP regenerated using method 3.

Chapter - 7

Adsorption as a technology for achieving ultra-low concentrations of phosphate: Research gaps and economic analysis

Submitted to Water Research

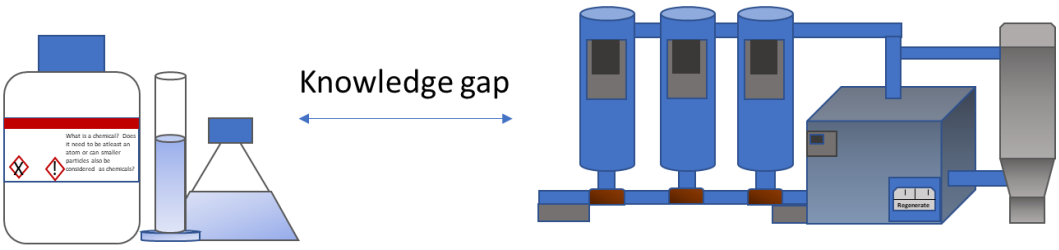
Authors: Prashanth Suresh Kumar, Leon Korving, Mark van Loosdrecht, Geert-Jan Witkamp



7.1. Prologue

7.1.1. Backdrop

- Several studies show that adsorption is able to reduce phosphate to very low concentrations and also enable its recovery. But little information is available on its full-scale application.
- An economic assessment is needed as a first step to evaluate the benefit of phosphate adsorption in large scales.
- An economic assessment helps identify the main parameters influencing the cost of the technology. This will also highlight the research gaps pertaining to the application of phosphate adsorption.



- Studies report on low-cost adsorbents that can be used directly as fertilizers after one-time use. A scenario analysis highlights the difference of such adsorbents in comparison with engineered adsorbents that are more expensive but have a longer lifetime.



- Moreover, chemical precipitation, i.e. dosing of metal salts is cheaper compared to adsorption at high phosphate concentrations. Hence adsorption is favourable only below a certain phosphate concentration.

7.1.2. Research questions

i) Which parameters need to be researched better to improve the economics of the phosphate adsorption?

ii) What is the potential of low-cost adsorbents compared to engineered adsorbents that have a higher cost but also longer lifetime?

iii) Which technologies exist that can reach ultra low phosphate concentrations?

iv) When is it favourable to apply adsorption as compared to other technologies?

7.2. Abstract

Eutrophication and the resulting formation of harmful algal blooms (HAB) cause huge economic and environmental damages. Phosphorus (P) has been identified as a major limiting nutrient for eutrophication. A phosphorus concentration greater than 100 µg P/L is usually considered high enough for causing eutrophication. The strictest regulations, however, aim to restrict the concentration below 10 µg P/L. Orthophosphate (or phosphate) is the bioavailable form of phosphorus. Adsorption is often suggested as technology to reduce phosphate to concentrations less than 100 and even 10 ppb with the advantages of a low-footprint, minimal waste generation and the option to recover the phosphate. Although several studies report on phosphate adsorption, there is insufficient information regarding parameters that are necessary to evaluate its application on a large scale. This review discusses the main parameters that affect the economics of phosphate adsorption and highlights the research gaps. A scenario and sensitivity analysis shows the importance of adsorbent regeneration and reuse. The cost of phosphate adsorption using reusable porous metal oxide is in the range of $ 100 to 200/Kg P for reducing the phosphate concentration upto 0.016 mg P/L. Future research needs to focus on adsorption capacity at low phosphate concentrations, regeneration and reuse of both the adsorbent and the regeneration liquid.

7.3. Introduction

7.3.1. Need to achieve very low concentrations of Phosphorus

Eutrophication is the process wherein water bodies receive an excessive supply of nutrients which in its most excessive form leads to the formation of harmful algal blooms (HABs) (Anderson et al. 2002, Smith et al. 1999). This has been recognized as a global concern for several decades (Nixon 1995) and has led to huge economic and environmental damages (Dodds et al. 2009, Hoagland et al. 2002, Pretty et al. 2003, Smith et al. 1999). Apart from posing health risks for humans and other organisms in the ecosystem eutrophication causes economic losses by affecting industries such as fishing, water treatment, housing, recreation and tourism (Ingrid Chorus 2000, Pretty et al. 2003, USEPA 2015, Wu 1999). The annual damage costs due to freshwater eutrophication were estimated to be between $ 105 to 160 million in England and Wales (Pretty et al. 2003). The overall annual costs incurred as a result of eutrophication in US freshwaters was estimated at $ 2.2 billion (Dodds et al. 2009).

The reduction of phosphorus (P) concentrations in the water bodies has been a dominant theme to combat freshwater eutrophication (L. Correll 1998, Schindler et al. 2016). Orthophosphate (o-P), also called soluble reactive phosphorus (SRP), is the only form of P that can be assimilated by autotrophs and the microbes present in the water (Correll 1999). But factors such as varying redox conditions, mineralization of organic matter, and an equilibration with dissolved P can cause the release of o-P from the settled as well as suspended particulates (Boström et al. 1988, Froelich Philip 1988, Hupfer and Lewandowski 2008). This has led to total phosphorus (TP), which includes dissolved and particulate P, to be used as an assessment

for controlling eutrophication. There is no clear consensus yet on the concentration of TP that is acceptable for preventing eutrophication, although most studies consider a concentration above 100 µg P/L to be too high (Vollenweider RA 1980, Dodds et al. 1998, Richardson et al. 2007, Lurling and Oosterhout 2013, Carvalho et al. 2013). The United States Environmental Protection Agency suggested a mean TP concentration of 10 µg P/L in its nutrient criteria guidelines for lakes and reservoirs (USEPA 2000). This value has often been promoted as the lowest concentration of TP to be reached to keep clear of eutrophication.

Sewage effluent and agricultural run-offs are chief sources for P loading in surface waters (White and Hammond 2009, Hendriks and Langeveld 2017). Management of P from diffuse sources like agricultural run-off includes practices that monitor fertilizer usage, livestock numbers and P input from manure (Knowlton et al. 2004, Sharpley 2016). Regulation of non-point/diffuse sources can nonetheless be difficult since they arise due to activities distributed over wide areas and are more variable over time due to changes in weather (Carpenter et al. 1998). Point sources of P like sewage effluent are easier to monitor and regulate (Dodds and Whiles 2010). Moreover, P loads from sewage effluent have been shown to have a higher fraction of SRP/bioavailable P compared to nonpoint sources (Gerdes and Kunst 1998, Maccoux et al. 2016).

Given the risk of P pollution from sewage effluent, regulations regarding the P discharge limits are getting stricter. The National Pollution Discharge Elimination System (NPDES) regulates the discharge of pollutants from point sources in the United States. The NPDES permit limitation for P has already been stringent in different municipalities with required values often ranging from 0.1 to 0.5 mg P/L (USEPA 2007). In the European Union, the standard for quality of water bodies is set by the Water Framework Directive (WFD) and an effluent value of 0.15 mg P/L is sometimes taken to be in line with the WFD (P.M.J. Janssen 2006). The current effluent regulations of individual EU member states need to meet either 1 or 2 mg P/L depending on the population equivalence, with the more stringent value for facilities with higher population equivalence and sensitive areas (Jan Oleszkiewicz 2015, EuropeanCommission 2017). China has municipal/domestic wastewater discharge limits ranging from 0.5 to 1 mg P/L (Li et al. 2012, Liu 2005). Discharge standards for Brazil, on the other hand, are not applied in all the states with effluent concentrations from domestic sewage generally higher than 4 mg P/L (Sperling 2016). This shows there is a discrepancy between the allowed effluent P discharge levels between different countries. But the rising concern over eutrophication could pose stricter values of 0.1 mg P/L or lower for WWTP effluents in the future (Ashekuzzaman and Jiang 2017, CanadianWaterNetwork 2018).

7.3.2. Technologies to achieve ultra-low P concentrations

The terms ultra-low level/advanced removal of P have often been used to denote achieving very low P concentrations. But they do not refer to an established value yet and can imply P concentrations lower than those achieved by conventional treatment methods. Such terms usually refer to a concentration range between 0.01 to 0.15 mg P/L (Bolton & Menk 2016, Genz et al. 2004, Langer et al. 2017, USEPA 2007, Whalley 2013).

P removal techniques can broadly be classified as physical, chemical and biological. Physical methods include separation of the P based on size exclusion and include sand filtration or membrane filtration (Erickson et al. 2007, Leo et al. 2011, Wathugala et al. 1987, Yildiz 2004). Chemical methods that have been used for P removal include precipitation, flocculation or adsorption (Clark et al. 1997, Drenkova-Tuhtan et al. 2017, Langer et al. 2017, Laridi et al. 2005). Precipitation involves the usage of metal salts to react with dissolved P to result in insoluble precipitates (Sedlak 1991). Flocculation uses metals or organic polymers to destabilize colloidal particles and to result in aggregates (Jiang and Graham 1998, Ngo and Guo 2009). Adsorption is the removal of dissolved P by using a solid material (Loganathan et al. 2014). Biological methods involve P uptake/assimilation by plants, microorganisms. This involves using halophytes in wetlands, polyphosphate accumulating organisms (PAO) for enhanced biological P removal (EBPR) and the use of microalgae (Boelee et al. 2011, Buhmann and Papenbrock 2013, Oehmen et al. 2007).

The use of a single method is often ineffective to reach ultra-low P concentrations and several studies use a combination of these methods to achieve the desired P concentration (Bolton & Menk 2016, Kim et al. 2008, Mitchell and Ullman 2016, P.M.J. Janssen 2006). For instance, conventional treatments in WWTP's include chemical precipitation with metal salts and can generally achieve P levels between 0.5 to 1 mg P/L in the effluent depending on the salt dosage (Clark et al. 1997, Sedlak 1991). Reducing the P concentrations further by increasing the salt dosing can lead to significant increase in sludge production(Sedlak 1991). But a study using a combination of chemical precipitation along with a series of sand filtration and ultra-filtration units was able to achieve TP values of less than 0.015 mg P/L (Mitchell and Ullman 2016). Another study used a reactive filter where iron salts were dosed along with sands to form a hydrous iron oxide coated sand (Newcombe et al. 2008). The soluble P was removed by co-precipitation with iron or adsorption onto the iron-coated sand whereas particulate P was removed by a moving bed sand filter. An average effluent concentration of 0.011 mg P/L was observed.

Phoslock is a lanthanum modified bentonite that removes SRP by forming lanthanum phosphate precipitates (Lürling et al. 2014). Even though Phoslock has been used for P remediation in lakes, a high solid dosage of 200:1 Phoslock:P weight ratio has been shown necessary to bring down concentrations to less than 0.01 mg P/L (Reitzel et al. 2013). Moreover, the presence of humic substances can release the lanthanum from Phoslock which would cause ecotoxicity issues in the surface water (Herrmann et al. 2016, Lürling et al. 2014)

The use of EBPR can lead to effluent P concentrations lower than 0.5 mg P/L depending on the extent of readily biodegradable organics present (Gu et al. 2008). A pilot study used a combination of EBPR with membrane bioreactor to reach average effluent values of 0.3 mg P/L (Smith et al. 2014). It has been suggested that EBPR can reduce effluent TP concentrations to 0.1 to 0.2 mg P/L under ideal conditions (Blackall et al. 2002). EBPR is however sensitive to several factors like the extent of organics, dosing of metal salts, nitrate, ammonium and heavy metal content that can inhibit the process (Zheng et al. 2014). This makes the ideal conditions rather narrow. Microalgae based biofilm reactors have been used to reach P concentrations less than 0.15 mg P/L (Boelee et al. 2011, Sukačová et al. 2015). The optimal

performance of microalgae, however, depended on parameters like the nutrient loading and illumination condition.

Wetlands offer another way of removing P by using a combination of different processes. Plants and microbes can uptake P whereas some fractions of P can also bind to minerals (Buhmann and Papenbrock 2013, Lüderitz and Gerlach 2002, Vohla et al. 2011). The use of submerged aquatic based vegetation wetlands was shown to reduce mean inflow TP concentration of 107 µg P/L to as low as 23 µg P/L (Dierberg et al. 2002). A limitation of wetlands though is the need for very high areas and hence they can be land intensive (R. Kadlec 1996).

Thus even though certain technologies or combinations can achieve very low P concentrations, each has its own limits. Based on the above observations, this could be a high dependence on physicochemical conditions, the need for membranes which can potentially lead to fouling issues, production of chemical precipitates which might not be recoverable, the requirement for large areas. Hence there is a need for technology that can reduce P consistently to ultra-low levels, with less reliance on having ideal conditions, a high throughput without fouling issues, with a low footprint, minimum waste generation and where the P is recoverable.

7.3.3. Adsorption as a polishing technology

Adsorption is a technology that has often been reported for achieving very low concentrations of o-P. Several studies in literature report on consistently reaching o-P concentrations less than 0.1 mg P/L and even lower than 0.01 mg P/L (Awual et al. 2014, Genz et al. 2004, Luo et al. 2016, Midorikawa et al. 2008, Sengupta and Pandit 2011). One of the limitations of adsorption is its ability to only remove dissolved P. This usually implies o-P (henceforth referred to as phosphate) however studies also show the removal of organic phosphates like phosphonates using adsorption (Boels et al. 2012, Kumar et al. 2010). This limitation can be overcome by combining adsorption with another step that can target particulate P, for instance with flocculation.

Apart from removing soluble P to very low concentrations, adsorption also offers the possibility to recover the P by regeneration of the adsorbent (Drenkova-Tuhtan et al. 2017, Kalaitzidou et al. 2016b, Kuzawa et al. 2006). This contributes to a circular economy. Despite several existing literature sources showcasing the potential of adsorption to reach low P concentrations, there is little information regarding their implementation at larger scales. A major reason could be that the process is not economical yet or there is a lack of understanding regarding the parameters affecting the economics. The objective of the following sections is hence to highlight what are the main parameters that affect the economics of phosphate adsorption, the existing research gaps for understanding these parameters and to give a sensitivity analysis of how these parameters affect the cost. Moreover, the need for adsorbent regeneration is also considered by making a scenario analysis. This analysis includes low-cost adsorbents that cannot be regenerated along with more expensive adsorbents that can be regenerated several times.

7.4. Factors governing the chemical costs of phosphate adsorption

The chemical costs of phosphate adsorption are governed by three important parameters, namely, the adsorbent cost, the practical loading and the costs during regeneration (seen in Figure 7-1). The following sections will discuss the research gaps for these parameters.

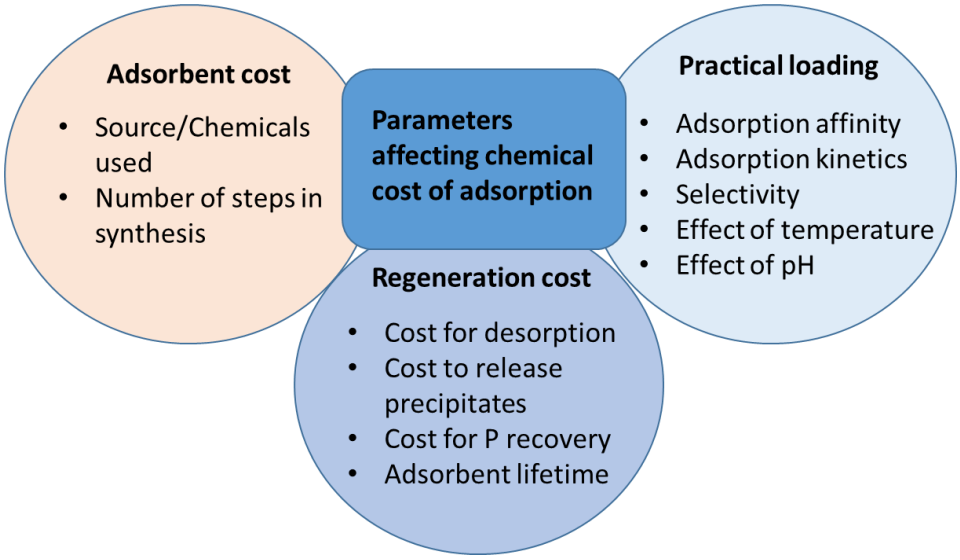


Figure 7-1: Summary of factors governing the chemical costs of phosphate adsorption

7.4.1. Adsorbent cost

A wide variety of phosphate adsorbents have been synthesized or studied regularly. These range from using waste materials or byproducts like food residue or slag to using engineered adsorbents based on metal-organic-frameworks or layered nanosheets (Abbas 2015, Fang et al. 2015, Sellner et al. 2017, Xie et al. 2017). However, information on the cost of these adsorbents is seldom provided and is often difficult to deduce. Without providing an estimate on the adsorbent cost it is not possible to have an economic evaluation of these adsorbents.

A way to classify the adsorbents into different cost categories would be to consider the number of steps/chemicals required to produce/modify the adsorbent. For example, despite no information on costs being provided, adsorbents are reported as low-cost due to the usage of waste materials or byproducts with or without further modification(Mezenner and Bensmaili 2009, Xue et al. 2009, Yuan et al. 2015, Zeng et al. 2004). In a similar way, composite adsorbents having active sites immobilized/impregnated on a backbone involve more chemicals/steps to produce or modify the adsorbent; hence these approaches can be associated with more expensive adsorbents (Fang et al. 2017b, Ge et al. 2016, Huang et al. 2015). Synthesized adsorbents comprising chiefly of metal oxides with no additional backbones can be considered in the intermediate cost category and include granular iron oxide based adsorbents (Genz et al. 2004, Kunaschk et al. 2015).

Based on the above rationale we classified adsorbents into 3 cost categories. i) Low cost – These include waste biomass and cost significantly lower than $ 1 per Kg. ii) Intermediate cost – These include granular porous metal oxides which generally cost between $ 3 to 6 per Kg

(based on the information provided for the granular ferric hydroxide GEH and FerroSorp). iii) High cost – These include hybrid ion exchange resins like BioPhree® which cost between $ 15 to 20 per Kg. Classifying adsorbents into these different categories helps in cost analysis with respect to different scenarios as will be discussed later. Studies reporting the synthesis of novel adsorbents must estimate the cost regarding chemicals consumed which would indicate which of these 3 cost categories it will be closer to.

7.4.2. Practical loading

Adsorption capacity denotes the removal capacity of an adsorbent and is expressed as the amount of phosphate that can be removed per mass of adsorbent. Even though it is the most studied property of adsorbents, it is also the property that is most variable. Phosphate adsorption capacity is a function of the adsorbent properties like the surface area, surface charge, surface functionality as well as the physicochemical properties of the solution like phosphate concentration, temperature, pH, presence of other ions/molecules (Mia et al. 2017, Weng et al. 2012, Zhu et al. 2013). Since different studies are conducted under varying conditions it makes it very difficult to compare the adsorption capacities between different adsorbents.

To simply state adsorption capacity could be confusing and misleading since it can imply the maximum adsorption capacity or the adsorption capacity at equilibrium. The term practical loading is used here to denote the phosphate adsorption capacity that will be realized in practice for a given set of conditions. For instance, this term can be used to differentiate the adsorption capacity realized at short contact times from the adsorption capacity under equilibrium conditions or at different phosphate concentrations.

7.4.2.1. Affinity

Phosphate adsorption capacity varies as a function of the equilibrium phosphate concentration and this relationship is given by an adsorption isotherm. The adsorption isotherm is a very valuable characterization because modeling it allows estimating the adsorption capacity at different concentrations (Foo and Hameed 2010). For instance, the Langmuir equation is a commonly used adsorption isotherm model given by the following expression (Langmuir 1918):

$$q_e = \frac{q_{max} K_L C_e}{(1 + K_L C_e)}$$

Where q_{max} is the maximum adsorption capacity and K_L is the Langmuir isotherm constant (Foo and Hameed 2010). In the context of effluent polishing, it is desirable to have a high equilibrium adsorption capacity (q_e) even at lower equilibrium phosphate concentrations (C_e). This property is referred to as the affinity of the adsorbent (Tran et al. 2017, Volesky 2007). This depends both on the maximum adsorption capacity as well as the Langmuir isotherm constant (Suresh Kumar et al. 2017). However, studies usually focus only on the maximum adsorption capacity of the adsorbent. Such capacities are often observed at equilibrium concentrations much greater than 10 mg P/L, which are rather unrealistic when applying in the context of effluent polishing.

Figure 7-2 uses data of Langmuir modeling from adsorption studies over the past 5 years (references in Table S7-4 in supporting information) and predicts the q_e at an equilibrium concentration of 0.1 mg P/L, denoted as $q_{0.1}$. The ratio between q_{max} and $q_{0.1}$ is shown to point out the wide range of discrepancy between the maximum adsorption capacity and the adsorption capacity that will be achieved at lower phosphate concentrations.

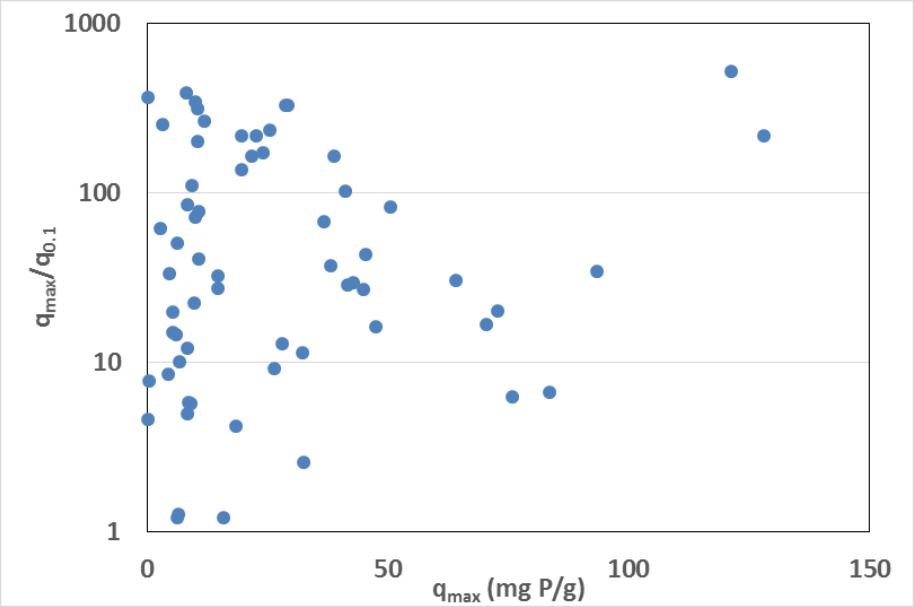


Figure 7-2: Ratio of q_{max} to adsorption capacity at an equilibrium concentration of 0.1 mg P/L as a function of q_{max} (references to the data points shown in Table S7-4 in supporting information)

The ratio of $q_{max}/q_{0.1}$ shows that the maximum phosphate adsorption capacity can decrease even by a factor of more than 100 times at equilibrium concentrations of 0.1 mg P/L. Figure 7-2 also shows there is no correlation with the q_{max} value. This suggests that for the application of effluent polishing the maximum adsorption capacity is irrelevant. Instead, it is more important to consider the affinity (for instance expressed as the constant K_L in the Langmuir equation) when developing phosphate adsorbents for this application.

The affinity of adsorbents varies with the type of metal oxides. Lanthanum based adsorbents often show a high affinity towards phosphate (Wang et al. 2016, Wu et al. 2007, Zhang et al. 2012). This is attributed to Lanthanum's hard Lewis acidic property which promotes its Lewis acid-base interaction with phosphate. Iron oxides also show a good affinity towards phosphate although the adsorption properties vary between the different types of iron oxides (Cornell 2004, Mc et al. 1981, Parfitt et al. 1975). A study comparing different iron oxides found that ferrihydrite had a higher maximum adsorption capacity per unit area than hematite and goethite (Wang et al. 2013). However, goethite had a much higher value for the affinity constant and this amounted to a higher adsorption capacity at lower phosphate concentrations. This is in line with another study that reports similar trends with ferrihydrite and goethite (Borggaard et al. 2005). This reiterates the need to focus on the adsorption capacity at the relevant concentrations rather than the maximum adsorption capacity.

7.4.2.2. Kinetics

The phosphate adsorption capacities estimated from adsorption isotherms are based on equilibrium conditions. However, the time taken to reach equilibrium can range from some minutes to several days, with some adsorbents even taking a timescale of weeks (He et al. 2017, J. Torrent 1992, Wan et al. 2016). The pseudo second order adsorption kinetic model is a commonly used model that has been used in a wide range of adsorbent studies (Ho and McKay 1999). Figure 7-3 shows the time taken to reach 90 % (t_{90}) of equilibrium adsorption capacity based on the pseudo second order model for adsorption studies over the past 5 years (references to the data points shown in Table S7-5 of supporting information). The value of t_{90} is considered because most of these experiments are also only done for this duration, likely due to the fact that experimentally any change in adsorption is very slow after this time. This can also be understood from the mathematical expression of the pseudo second order model that it takes 11 times longer to reach 99 % of equilibrium adsorption capacity (t_{99}) as compared to t_{90}.

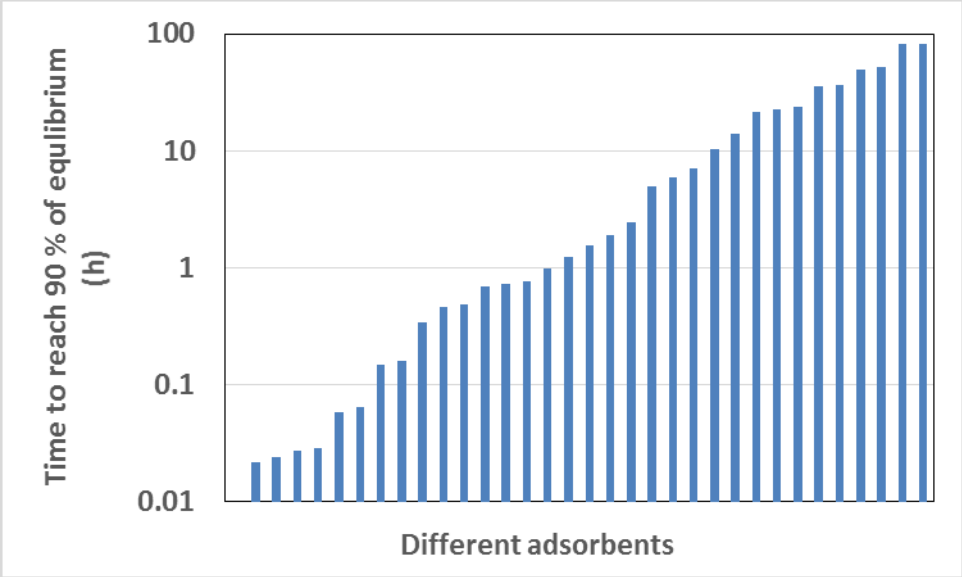


Figure 7-3: Estimated time for reaching 90 % of equilibrium for different adsorbents based on pseudo second order kinetic model (References shown in Table S7-5 in supporting information)

Even if t_{90} is considered as the indicator of adsorption kinetics, Figure 7-3 shows that in several cases it is in the timescale of several hours to days. From a practical point of view, time is money and hence an adsorbent with superior kinetics is highly preferable. Especially, when running in a column mode, the contact times (measured as empty bed contact time or space velocity) are usually in the order of several minutes to less than an hour (Kalaitzidou et al. 2016a, Midorikawa et al. 2008, Yamashita et al. 2013).

Porous adsorbents offer a high surface area in combination with a particle size big enough to avoid pressure drop problems while using them in column mode. For instance, granular activated carbon provides a very high surface area (in excess of 1000 m^2/g) and has been used for coating iron oxide nanoparticles to enhance phosphate adsorption (Zach-Maor et al. 2011b). However, a majority of its surface area comes from micropores (pore width < 2 nm), and phosphate adsorption in such adsorbents via pore diffusion takes place in the order of several

days (Suresh Kumar et al. 2017, Zach-Maor et al. 2011b). On the other hand, 96 % of phosphate removal was achieved within 30 minutes in a macroporous (pore size > 50 nm) adsorbent (Yang et al. 2012). In a study comparing phosphate adsorption onto different porous metal oxides, it was determined that pores bigger than 10 nm are required to enhance phosphate adsorption kinetics (Suresh Kumar et al. 2019). This shows the need to characterize the pore structure of the adsorbents along with their surface area to ensure good phosphate adsorption kinetics.

7.4.2.3. Selectivity

The ability of an adsorbent to remove phosphate preferentially amidst the competing ions is called its selectivity. The adsorbent selectivity depends on the type of interaction formed by the competing ion with the adsorbent surface. In general, ions like chloride, nitrate show little or no competition whereas ions like arsenate and silicate show high competition (Ge et al. 2016, Lǔ et al. 2013, Xie et al. 2014a, Zhang et al. 2016). Arsenate, phosphate, and silicate are all tetrahedral ions that form innersphere complexes with metal (hydr)oxides like iron oxides (Parfitt 1979, Su and Puls 2001, Tuutijärvi et al. 2012). Nitrate and chloride form outersphere complexes which are weaker interactions (Parfitt 1979). Sulphate and carbonate, on the other hand, vary in competing effects although carbonate often has a higher competing effect (Ge et al. 2016, He et al. 2017, Rashid et al. 2017, Xie et al. 2014a). Sulphate can exist as both inner or outersphere complexes on metal oxide surfaces (Wijnja and Schulthess 2000). Carbonate can bind via electrostatic attraction but can also form calcium carbonate surface precipitates (Chitrakar et al. 2006, Kunaschk et al. 2015). Dissolved organic matter like humic acids and fulvic acids can also compete with phosphate adsorption via direct competition with the active sites as well as steric hindrance (Fu et al. 2013, Antelo et al. 2007, Weng et al. 2008)

Apart from ions and molecules that directly compete for active sites, certain cations like calcium and magnesium can also influence phosphate adsorption. The binding of these ions can enhance phosphate adsorption by making the surface more electropositive or by forming intermediate ternary complexes (Antelo et al. 2015, Han et al. 2017, Lin et al. 2017, Talebi Atouei et al. 2016). Thus depending on the type of ions present in the water matrix, the adsorption of phosphate can get enhanced or reduced (Suresh Kumar et al. 2018). Adsorbent selectivity is often tested in the presence of separate competing ions with varying concentrations (Antelo et al. 2007, Gu et al. 2018, Sengupta and Pandit 2011). But in realistic conditions several competing ions will exist together and can interact to form different complexes or precipitates. To test the selectivity, it is hence best to mimic the conditions that will be representative of the solution in which the adsorbent is applied.

7.4.2.4. Effect of temperature

The effect of temperature on an adsorbent's performance is governed by its thermodynamic properties. An endothermic process will lead to improved adsorption at higher temperatures, while an exothermic process will lead vice versa (Huang et al. 2014, Jung et al. 2017). The extent of effect of temperature also varies with adsorbents. Phosphate adsorption on an adsorbent formed by thermal decomposition of alunite and potassium chloride mixture was found to be endothermic (Akar et al. 2010). But the maximum adsorption capacity only increased by 5 % when the temperature increased from 20 to 40 °C. On the other hand, a magnesium ferrite biochar composite which also had an exothermic adsorption, showed a

66 % increase in maximum adsorption capacity when the temperature increased from 15 to 35 °C (Jung et al. 2017). Similar variations also exist between adsorbents showcasing exothermic property (Huang et al. 2014, Qian et al. 2017).

It is also important to consider the effect of temperature on adsorption kinetics. This is especially relevant for performance in continuous modes where contact times are short. Kinetic constants for different adsorbents mostly increased with an increasing temperature (Table S7-6 in supporting information). This could be due to improved phosphate diffusion at higher temperatures, indicating practical loading will decrease at lower temperatures for such adsorbents.

7.4.2.5. Effect of pH

Phosphate has pKa values of 2.15, 7.2 and 12.33, and depending on the solution pH it can thus exist in the form of H_3PO_4, $H_2PO_4^-$, HPO_4^{2-} or PO_4^{3-} (Xiong et al. 2017). Phosphate adsorption usually reaches an optimum when the pH favours its electrostatic attraction with the adsorbent. This happens when the pH of the solution is less than the adsorbent PZC so that the adsorbent is electropositive and the phosphate is in its anionic form. Since several adsorbents have their point of zero charge close to neutral pH, the phosphate adsorption optimum is often in the acidic range (Fang et al. 2017b, He et al. 2017, Wen et al. 2014).

While the effect of pH on phosphate adsorption is well documented, the effect of competing ions must also be considered. For example, it was reported that for similar concentrations of humic acid, phosphate adsorption on goethite reduced by 45 % at pH 4.5 compared to a 25 % reduction at pH 7 (Antelo et al. 2007). (Sibanda H and Young S 1986) observed similar effects of higher humic acid adsorption on goethite and gibbsite at lower pH. Similarly, even though phosphate adsorption is enhanced at pH < PZC of the adsorbent, calcium adsorption happens at pH > PZC, which would in turn enhance phosphate adsorption. (Antelo et al. 2015) observed this while monitoring calcium and phosphate adsorption on ferrihydrite nanoparticles. Even though phosphate adsorption decreased significantly at higher pH in the absence of calcium, increasing the concentrations of calcium increased the phosphate adsorption at the same pH.

7.4.3. Cost for regeneration

Regeneration is the process by which the molecules bound on the loaded adsorbent are released. This might include phosphate as well as other competing ions. Regeneration is done for two reasons i) To recover the separated molecule of interest, i.e. phosphate. ii) To replenish the active sites of the adsorbent so that the adsorbent can be reused. The reuse of the adsorbent as well as any excess chemicals from the regeneration makes the overall process economic and environmental friendly. The sections below discuss the factors associated with the chemical costs for regeneration.

7.4.3.1. For replenishing adsorbent active sites

a) Releasing adsorbed complexes

Phosphate binds to metal (hydr)oxides by a ligand exchange mechanism (innersphere complex) with the surface hydroxyl groups. This includes a range of metal oxides that include metals like aluminium, iron, lanthanum, zirconium, and sometimes even a mixture of different metal oxides (Awual et al. 2011, Fang et al. 2017a, Liu and Hesterberg 2011, Sibanda H and Young

S 1986, Zhang et al. 2009). In such a case, desorption of phosphate is done by an alkaline solution like sodium hydroxide (NaOH), since the hydroxide ions acts as a hard Lewis base (Awual et al. 2011). From an economic point of view, it is important to know how much chemical is consumed for the desorption of phosphate. Phosphate adsorption as innersphere complex happens as a monodentate or bidentate complex (Abdala et al. 2015, Connor and McQuillan 1999, Fang et al. 2017a). This means stoichiometrically, only one or two molecules of hydroxide ion should be consumed for desorption of each phosphate molecule. However, an excess amount of hydroxide ions are required to provide a driving force. Thus, high concentrations of NaOH solutions are used for phosphate desorption, often ranging from 0.1 to 1 M (Drenkova-Tuhtan et al. 2017, Fang et al. 2017b, Genz et al. 2004, Sun et al. 2014). But the actual amount of hydroxide ions consumed will be less and the excess of the hydroxide ions in the regenerate solution can be reused. For instance, the NaOH solution was replenished and reused for desorption of phosphate for 60 cycles in a pilot study (Drenkova-Tuhtan et al. 2017).

When the adsorbent is used in a water matrix consisting of several competing ions, the actual consumption of hydroxide ion during desorption will also depend on the other ions that bind via the same mechanism. Having a selective adsorbent will decrease the overall consumption of hydroxide ions per mole of phosphate desorbed. However, having a highly selective adsorbent also implies that it will have a high affinity to phosphate and the binding could be too strong to facilitate easy desorption. For example, although lanthanum based adsorbents are known for their strong affinity towards phosphate, the recovery of phosphate from these adsorbents is not always discussed (Wang et al. 2016, Zhang et al. 2012). (Xie et al. 2014c) showed that very high concentrations of upto 12.5 M NaOH along with temperatures in excess of 100 °C are required for optimum desorption of phosphate from lanthanum hydroxide. Similar requirements of high concentrations of NaOH or a combination with thermal steps are reported for desorbing phosphate from other adsorbents based on rare earths like lanthanum and yittrium (Dong et al. 2017, Xie et al. 2014b, Kim et al. 2017).

b) Releasing surface precipitates

While NaOH can be used to release molecules adsorbed on the surface, adsorption is not the only interaction that can happen on the adsorbent. Depending on the adsorbent properties and physicochemical properties of the solution, sometimes surface precipitation might also occur. Surface precipitation leads to formation of multilayered structures (/three dimensional molecular arrangement) as opposed to the monolayer coverage during chemisorption (Sparks 2003, Sposito 1987). In such a case the precipitate can bury the adsorbed phosphate and hence prevent it from getting desorbed (Li and Stanforth 2000). Surface precipitation can form either from the dissolution and re precipitation of ions from the adsorbent or due to the binding of competing ions from the solution. For instance, the dissolution of iron from goethite has been reported to contribute to surface precipitation (Li and Stanforth 2000). (Kunaschk et al. 2015) studied phosphate adsorption from a drinking water matrix, where calcium based surface precipitates were reported to block effective desorption of phosphate. In such a case, an acid treatment with a HCl solution of pH 2.5 was recommended to release the surface precipitates and effectively regenerate the adsorbent. Similarly, calcium carbonate precipitation was observed while using adsorbents in a wastewater matrix and an acidic treatment was required

to improve the adsorbent reusability (Suresh Kumar et al. 2018). The chemical consumption of acid needs to be monitored in such scenarios.

c) Neutralization of excess NaOH in the adsorbent

In the case of porous adsorbents, some of the NaOH used during desorption will be retained in the pores. The removal of such NaOH will be necessary prior to a subsequent reuse cycle to allow for efficient adsorption and to prevent unwanted precipitation inside the pores during the next adsorption cycle. While the excess NaOH can be rinsed by water, an acid neutralization step can be used to speed up the process (Suresh Kumar et al. 2018, Zach-Maor et al. 2011a). Neutralizing such columns purely with water could result in high consumption of water and result in large amounts of waste stream (Suresh Kumar et al. 2018). In case of using an acid neutralization step, the acid consumption needs to be considered.

7.4.3.2. For phosphate recovery

Phosphate concentrated in the regenerate stream (NaOH) can be recovered as a form of calcium phosphate or magnesium ammonium phosphate/struvite (Drenkova-Tuhtan et al. 2017, Kalaitzidou et al. 2016b, Kuzawa et al. 2006, Midorikawa et al. 2008). Recovery as struvite needs addition of magnesium and ammonium and a pH around 9 was suggested as the optimum pH for obtaining compact structures and maximum yield (Drenkova-Tuhtan et al. 2017, Ye et al. 2014). Recovery as calcium phosphate only needs the addition of a calcium source and has been suggested as the better choice due to the high pH of the regenerate solution (Kuzawa et al. 2006).

The composition of the regenerate stream will affect the consumption of the chemicals used for precipitation of phosphate. For example, after phosphate adsorption from secondary wastewater effluent, the molar ratio of magnesium:ammonium:phosphate required to form struvite in the regenerate stream was 1.5:1.5:1 (Drenkova-Tuhtan et al. 2017). This was higher than the stoichiometric ratio of 1:1:1 and was attributed due to competing parallel reactions. Similarly, a molar ratio of Ca to P between 2 to 2.5 was required for optimum calcium phosphate formation (Kuzawa et al. 2006, Kalaitzidou et al. 2016b, Midorikawa et al. 2008). This is higher than the stoichiometric molar ratio of 1.5 and 1.67, required for forming tricalcium phosphate and hydroxyapatite, respectively (Song et al. 2002b). Excess requirement of calcium could be due to the presence of carbonates in the regenerate solution which will lead to the formation of calcium carbonate (Song et al. 2002a) A pilot study recovering calcium phosphate from the regenerate found that about 40 % of their recovered product consisted of calcium carbonate (Kalaitzidou et al. 2016b). This was attributed to CO_2 adsorption from the atmosphere since the regeneration solution was maintained in an open tank.

Thus the amount of chemicals consumed for phosphate recovery will be dependent on the conditions during regeneration as well as the selectivity of the adsorbent. Moreover, more studies are needed to show the potential for reusing the regenerate solution, especially the effect on desorption due to the accumulation of phosphate in the regenerate. This will give essential

information on when and how often the phosphate needs to be recovered to enable effective reuse of the regenerate solution.

7.4.3.3. Adsorbent lifetime

The adsorbent lifetime is increased by reusing it multiple times. Many studies test the adsorbent reusability between 5 to 10 cycles (Fang et al. 2017b, Ju et al. 2016, Jung et al. 2017, Kim et al. 2017, Luo et al. 2017, Wan et al. 2016). Adsorbent attrition during the adsorption or regeneration process is the common reason for reusability getting affected. For example, zirconium oxide particles confined in mesoporous carbon showed a drop in adsorption capacity from 17 to 13 mg P/g over the first 4 cycles whereas the capacity remained stable over the next 3 cycles (Ju et al. 2016). This was attributed to the leaching of zirconium oxide particles located on the external surface or pore mouth region of the adsorbent composite. Adsorption capacity of calcined LDH decreased by about 50 % over 5 cycles which was attributed to destruction of the layered structure (Sun et al. 2014). The structure or active sites of amino-functionalized clay adsorbent composites was considered damaged during regeneration with NaOH (Unuabonah et al. 2017). This led to a decrease in adsorption performance over every consecutive adsorption cycle. (Drenkova-Tuhtan et al. 2017) tested nanocomposite magnetic particles in wastewater effluent over 20 adsorption-desorption cycles. Effluent concentrations less than 0.05 mg P/L could only be achieved for the first few runs after which the adsorption efficiency decreased. This was attributed to a consistent loss of adsorbent particles at a rate of about 5 % per cycle.

Incomplete desorption of phosphate has also been found to decrease the reusability. For instance, (Kunaschk et al. 2015) reasoned that calcium based surface precipitation blocked adsorbed phosphate. This would lead to a decrease in available active sites during the next adsorption cycle and thus affect the reusability. Presence of phosphate into micropores of iron oxides has also been reported to affect desorption (Cabrera et al. 1981). Additionally, the adsorbent crystallinity or type of metal oxides can change during regeneration which would affect their surface functional groups. For instance, the crystallinity of goethite was observed to increase after regeneration with NaOH and was correlated to a decrease in adsorption capacity after the very first cycle (Chitrakar et al. 2006). In contrast, the crystallinity of akaganeite did not change even after 10 cycles and the reusability was also intact. (Suresh Kumar et al. 2018) monitored the adsorbent characteristics such as a change in surface area, crystallinity, as well mass balance of competing ions for 3 adsorption - regeneration cycles in a real wastewater effluent. Amongst all the other parameters, calcium based surface precipitation was shown to have the highest influence on adsorbent reusability. However, the surface precipitates were not found to affect phosphate desorption, but rather affect calcium adsorption which in turn affects phosphate adsorption. Understanding the mechanism of surface precipitation was suggested as an important step to enhance adsorbent reusability.

There are also studies where the reusability is intact for the studied duration (Fang et al. 2017b, Wan et al. 2016, Wu et al. 2017, Zong et al. 2013). This could be related to the stability of the adsorbent but it could also be due to the fact that not enough regeneration cycles were done. For instance, nanocomposites based on lanthanum hydroxide and iron oxide showed stable adsorption capacities during 5 adsorption cycles (Wu et al. 2017). However, the phosphate

desorption efficiency varied between 70 to 80 % during each regeneration cycle. This incomplete desorption could affect the reusability in the long run.

From a practical viewpoint, the adsorbent lifetime needs to be much higher than 5 to 10 reuse times. But rather than performing endless regeneration cycles, studies should focus on developing a better understanding of the parameters that affect reusability. In that way, optimal regeneration methods can be developed. If with such methods it can be shown that the adsorbent characteristics do not change over a certain number of reuse cycles, then the adsorbent lifetime can be extrapolated to longer reuse cycles with more certainty.

7.5. Economic analysis for phosphate adsorption

The economics of the adsorption process can be divided between the operating costs and capital costs. The operating costs mainly include the chemical costs as well as the costs due to energy consumption. The following sections describe the sensitivity and scenario analysis for the chemical costs, followed by a brief overview of the energy and capital costs.

7.5.1. Scenario and sensitivity analysis for chemical costs

The chemical costs are the costs that can be addressed by phosphate adsorption studies. A simple schematic of the adsorption process applied in a column mode is shown below (Figure 7-4). However, the evaluation used for these chemical costs will also apply for a batch mode.

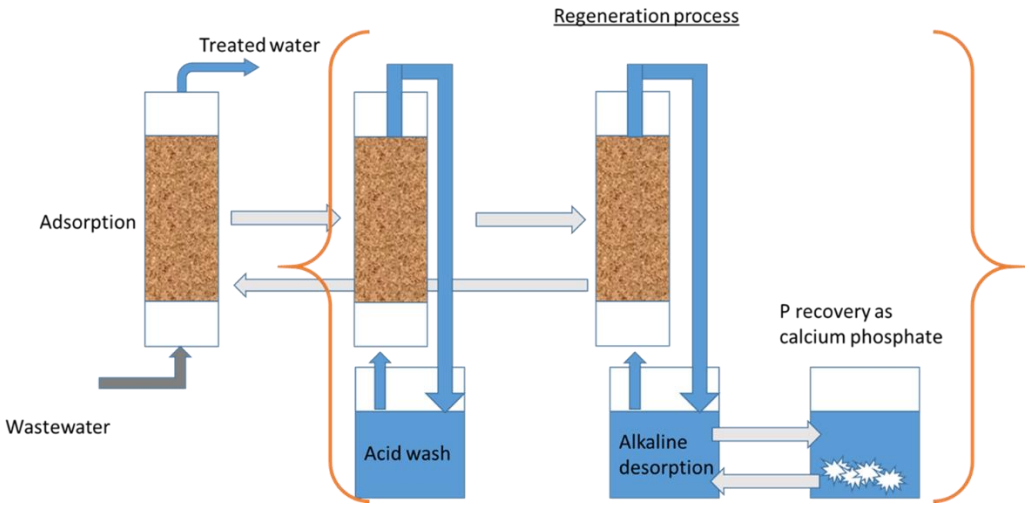


Figure 7-4: Scheme of adsorption process. The acid wash step serves to remove surface precipitates.

Based on the scheme shown in Figure 7-4, the chemical cost for phosphate adsorption can be expressed as follows:

$$Chemical\ cost\ of\ adsorption\left(\frac{\$}{mole\ P}\right)=\frac{[A+(B*n)]}{(n+1)}$$

Where, A = Cost for 1st adsorption cycle ($/mole P), B = Cost per regeneration cycle ($/mole P/cycle), n = Number of regeneration cycles. The denominator in the formula denotes the total number of cycles and is n+1 since the regeneration begins after the 1st cycle. The term A is a function of the adsorbent cost and adsorption capacity. It can be expressed as:

$$A = a_1/a_2$$

Where, a_1 = adsorbent cost ($/Kg adsorbent), a_2 = Practical loading (moles P/Kg adsorbent).

The cost per regeneration cycle can be further split as:

$$B = (C + D + E)/a_2$$

Where, C = Cost per cycle of desorption ($/Kg adsorbent/cycle), D = Cost per cycle of acid wash ($/Kg adsorbent/cycle), E = Cost per cycle of P recovery ($/Kg adsorbent/cycle). Table 7-1 shows the split up of the variables used in calculating the cost of each of these steps.

Certain assumptions have been made to arrive at these derivations. The following points discuss these assumptions and their limitations:

- The adsorption capacity stays same throughout the n regeneration/reuse cycles. In reality, the adsorption capacity will vary depending on the change in the physicochemical characteristics of the incoming solution as well as the amount of wear and tear the adsorbent undergoes.

- The excess of chemicals used during regeneration can be reused. Hence, only the cost for the chemicals actually consumed per cycle is considered. Studies show the possibility to reuse the regenerate solution by replenishing only the spent chemicals (Kalaitzidou et al. 2016a, Kuzawa et al. 2006). The phosphate recovery from the regenerate stream allows reusing the regenerate stream effectively.

- Complete desorption of phosphate is achieved using NaOH solution. This assumption was necessary to relate the OH consumption to the phosphate adsorption capacity. Complete desorption might not be achieved in the first couple of cycles for porous adsorbents due to phosphate diffusion into inner pores. But once such sites are saturated near complete desorption can be expected (Zach-Maor et al. 2011a). Moreover, the extent of desorption also depends on the affinity of the adsorbent.

- Surface precipitation happens primarily via calcium binding. This allows establishing a relationship between calcium binding and amount of acid required to remove surface precipitates. Calcium based surface precipitation has been reported before on phosphate adsorbents (Kunaschk et al. 2015, Suresh Kumar et al. 2018). Given its ubiquitous nature in surface and wastewaters, it can be the chief component to cause a precipitate. However, precipitates based on adsorbent dissolution are also possible (Li and Stanforth 2000).

Table 7-1: Parameters and formulas used for calculating the chemical costs of phosphate adsorption

Variables involved	**Steps with formulas**
For adsorption step: a_1 = Adsorbent cost ($/Kg) a_2 = Practical loading (Moles P/Kg)	$A = a_1/a_2$ $B = (C + D + E)/a_2$
For desorption step: c_1 = OH consumed to desorb (Moles OH/mole P) c_2 = Adsorbent pore volume (L/Kg) c_3 = Concentration of NaOH (Moles OH/L) c4 = Cost of NaOH ($/mole NaOH)	$C = ((c_1 * a_2) + (c_2 * c_3)) * c_4$
For acid wash step: d_1 = Acid consumption to release surface precipitate (Moles H/mole Ca) d_2 = Practical loading for calcium (Moles Ca/Kg adsorbent) d_3 = Cost of HCl ($/mole HCl)	$D = ((d_1 * d_2) + (c_2 * c_3)) * d_3$ $E = (e_1 * a_2 * e_2) + (e_3 * a_2 * c_4) - (a_2 * e_4)$
For recovery step: e_1 = Calcium consumed for calcium phosphate precipitation (Moles Ca/mole P) e_2 = Cost of calcium ($/mole $CaCl_2$) e_3 = Hydroxide consumed during calcium phosphate precipitation (Moles OH/mole calcium phosphate) e_4 = Cost of calcium phosphate ($/mole calcium phosphate)	$Chemical\ cost\ of\ adsorption\ \left(\frac{\$}{mole\ P}\right) = \frac{[A + (B * n)]}{(n+1)}$
For reusability: n = Number of reuse cycles	

The overall formula for calculating the chemical cost can be used to show the importance of reusing the adsorbent several times. Figure 7-5 shows the decrease in chemical cost as a function of the regeneration cycles.

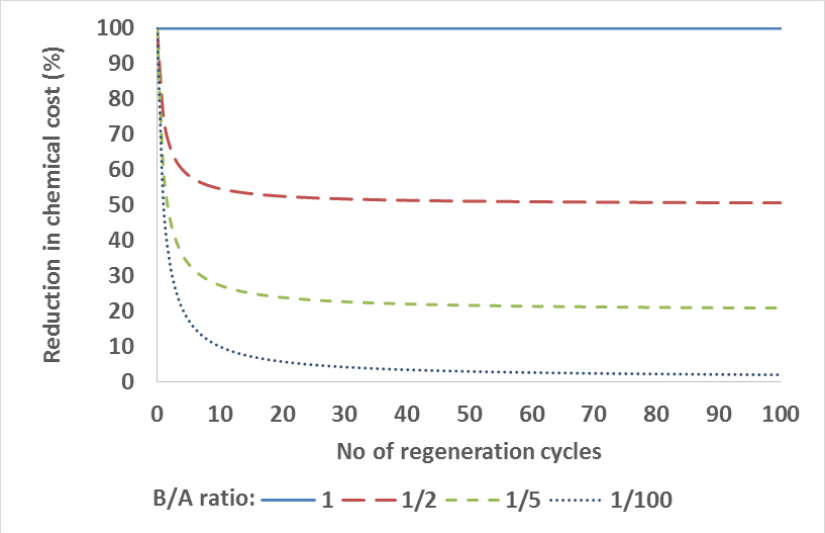


Figure 7-5: The decrease in chemical cost of adsorption as a function of the number of regeneration cycles. The legends show the ratio of the terms B/A, i.e. the cost per regeneration cycle as compared to the cost of the 1st adsorption cycle.

The reduction in chemical cost is both a function of the number of regeneration cycles as well as the ratio of cost per regeneration cycle to the cost of the 1st adsorption cycle. For scenarios where the cost per regeneration cycle is at least 5 times cheaper than the cost of 1st adsorption cycle, about 80 % or more of the reduction in chemical costs is reached by 30 regeneration cycles. However, the number of regeneration cycles that can be implemented relates to the adsorbent lifetime which in turn depends on the composition of the adsorbent. This includes how stable the adsorbent material is to abrasion and structural modification over the adsorption and the regeneration cycles. There are several studies which specify low-cost phosphate adsorbent alternatives which are normal or modified products of industrial waste or biomass (Biswas et al. 2008, Ismail 2012, Karthikeyan et al. 2004, Namasivayam and Sangeetha 2004). However, most of these adsorbents are either not resistant to the conditions used in regeneration (alkaline or acidic pH) and are suggested for direct application as fertilizers (Nguyen et al. 2014).

To compare how their adsorption costs fare with reversible adsorption (i.e. reusable adsorbents), we consider a scenario analysis for 3 different categories of adsorbent: Waste biomass-based adsorbents, porous metal oxides, hybrid ion exchange resins. The main criteria for categorizing this way is based on the adsorbent cost as discussed in section 7.4.1, but the other important differences to consider include the adsorption capacity and the lifetime of the adsorbents. Table 7-2 summarizes these aspects.

Table 7-2: Differences in adsorbent categories

	Low cost	Intermediate cost	High cost
Example	**Waste biomass** (Nguyen et al. 2014)	**Porous metal oxide** (Genz et al. 2004)	**Hybrid ion exchange resins** (Sengupta and Pandit 2011)
Composition	Waste biomass which can be used as such, but often modified with metal salts to increase selectivity towards phosphate adsorption	Bulk metal oxides like iron or aluminium oxides with high specific surface area due to the porous structure	Include ion exchange resins that are impregnated with metal oxides like iron oxide to increase selectivity towards phosphate adsorption
Phosphate adsorption	Low adsorption capacity due to low specificity and surface area	Higher adsorption capacity due to the high surface area, but adsorption kinetics is limited by diffusion into the pores and hence practical loading depends on contact time in continuous mode	Lower surface area than the porous metal oxides but adsorption kinetics is faster and hence displays high adsorption capacity with relatively low contact times
Lifetime	One time usable	Reusable but mechanically less stable than resins. Hence might undergo breakdown during regeneration which would result in the development of very fine particles. These fines can lead to an increase in pressure drop or can also escape into the effluent carrying the adsorbed phosphate onto them.	High lifetime due to mechanically superior/abrasion resistant properties.

A Monte Carlo simulation was used to account for the uncertainty in calculating the chemical costs for the 3 categories of adsorbents. A lower and upper range was provided for each parameter used in estimating the chemical cost and 10,000 random variables were generated using a uniform distribution. The range for the main parameters used for calculating the chemical costs are shown in Table 7-3 (values for complete parameters shown in Table S7-7 in supporting information). These parameter values will of course depend on the operating

conditions and the type of water matrix being treated. But at least in the case of porous metal oxides and the ion exchange resin, they have been estimated from adsorption in a wastewater effluent matrix (Suresh Kumar et al. 2018). Hence these provide a more realistic value than phosphate solutions prepared using clean water.

Table 7-3: Main parameters used for simulating the chemical cost for reaching 0.1 mg P/L

Parameters/Adsorbent type	**Waste biomass**	**Porous metal oxide**	**Hybrid ion exchange resin**
Example used	Rice husk	FerroSorp (FSP)	BioPhree®
Adsorbent cost ($/Kg)	Minimum = 0.1 Maximum = 0.2	3 to 6	15 to 20
Practical loading (moles P/Kg adsorbent)	0.01 to 0.02	0.05 to 0.1	0.04 to 0.08
Reuse cycles	None	27 to 33	90 to 110

The main assumption made is the lifetime/number of regeneration cycles for porous metal oxides and the hybrid ion exchange resin. Rice husk was considered as the waste biomass and the adsorbent was considered for a one-time use. Hence for this adsorbent regeneration costs were not considered. For porous metal oxide, FerroSorp (FSP) which is a granular iron oxide was used as the example. The average lifetime was considered as 30 regeneration cycles since around 80 % reduction in chemical costs is achieved by this lifetime in line with the explanation provided by Figure 7-5. For the hybrid ion exchange resin, BioPhree® which is an ion exchange resin impregnated with iron oxide was used as the example. The lifetime of ion exchange resins depends on the process conditions and can vary between 7 to 15 years. In our case, we considered an average lifetime of 100 regeneration cycles. The lower and upper range for the FSP and BioPhree® were thus taken as ± 10 % of 30 and 100 cycles, respectively.

Figure 7-6 shows the box plot for the chemical costs of these 3 categories of adsorbents as estimated by the Monte-Carlo simulation. The error bar shows the spread of possible chemical costs as per the range provided for the different parameters.

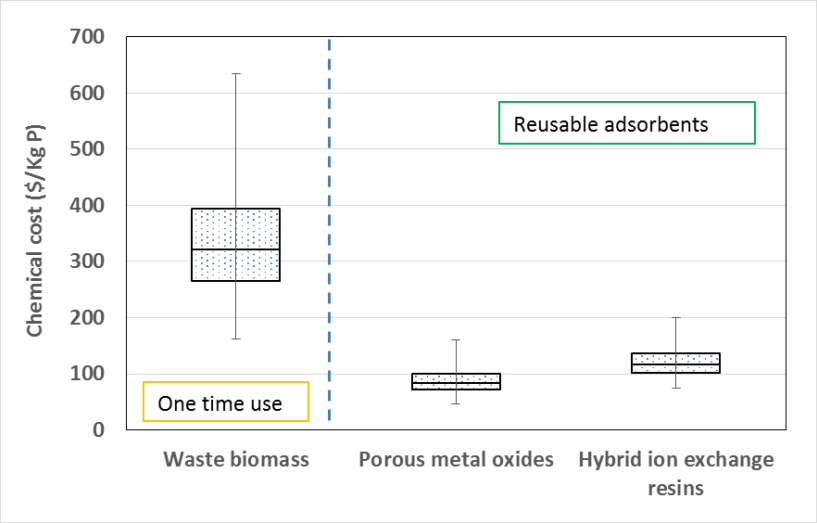


Figure 7-6: Scenario analysis for the chemical costs of 3 types of phosphate adsorbents

It can be seen from Figure 7-6 that despite considering a very low cost for the waste biomass-based adsorbents, reversible adsorption with porous metal oxides and hybrid ion exchange resins are more cost effective due to their higher adsorption capacity and longer lifetime. The median value for the chemical cost was around $ 100/Kg P for both the porous metal oxide and the hybrid ion exchange resin.

Figure 7-6 shows the sensitivity for different parameters towards the chemical cost for the porous metal oxide. Figure S7-11 in supporting info shows a similar graph for the ion exchange resin.

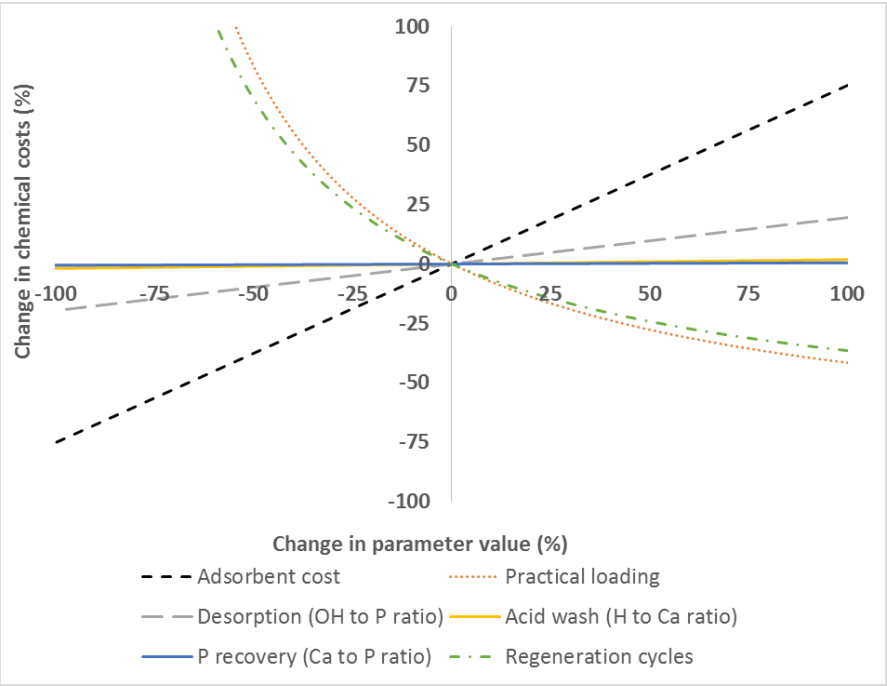


Figure 7-7: Sensitivity of different parameters to chemical costs of porous metal oxide

Figure 7-7 shows that amongst all parameters, the adsorbent cost, the practical loading, and number of regeneration cycles had the most significant effect. An increase in practical loading

and regeneration cycles reduced the chemical cost non-linearly, whereas a decrease in adsorbent cost reduced the chemical cost linearly at a higher slope than the other parameters. Thus the optimization of these parameters would be essential for making the process economically feasible.

The chemical costs calculated here are for an effluent concentration of 0.1 mg P/L. For an effluent concentration of 0.01 mg P/L, these costs will be higher depending on how the adsorption capacity decreases corresponding to that concentration. If an adsorbent has a high affinity, this decrease in adsorption capacity will be minimal. For the example for the porous metal oxide used, the practical loading at an effluent concentration of 0.016 mg P/L capacity was 60 % of the loading observed at 0.1 mg P/L. Assuming all other parameters to be constant, the change in chemical cost can be deduced from the sensitivity analysis as shown in Figure 7-7. In this case, the chemical cost increased only by 50 % even though the effluent concentration was reduced by a factor 6. Moreover, the practical loadings used in this analysis are based on a relatively short empty bed contact time (EBCT) of 5 minutes. Depending on the adsorption kinetics increasing the EBCT can significantly increase the practical loading. This will hence lower the chemical costs.

7.5.2. Energy and capital costs

Energy consumption costs will vary based on the mode of operation. Stirred tank batch systems will consume energy primarily due to the stirring, whereas fixed bed column studies will consume energy primarily due to pumping. For the current scenario, a fixed bed continuous mode of operation is considered. The regeneration would be simpler for the fixed adsorbent bed compared to a stirred tank reactor where the adsorbent needs to be first recovered after the adsorption process. A continuous mode can also lead to a more efficient use of the adsorption capacity because the adsorbent is always exposed to the same influent concentration rather than the decreasing concentrations in batch mode (Loganathan et al. 2014). The energy cost in terms of P removed can be given by the following formula:

$$Energy\ cost\ (\$/Kg\ P)\ =\ \frac{(F\ *\ G)}{(Q\ *\ (C_{in}\ -\ C_{out})\ *\ 10^{-3})}$$

Where, F = Hourly power consumption (kWh/h), G = Electricity cost ($/kWh), Q = Volumetric flow rate (m3/h), C_{in} = Phosphate concentration at inlet (mg P/L), C_{out} = Phosphate concentration at outlet (mg P/L).

The power consumption is related to the pressure drop over the adsorbent column as follows:

$F = (Q * \Delta P)/36\ \eta$

Where, ΔP = Pressure drop (bar), η = Pump efficiency (%). The pressure drop can be calculated by the Ergun equation (Equation S1 in supporting information).

The capital costs will chiefly include the cost of the adsorbent column(s), the regeneration tanks (one for desorption with an alkaline solution and other for acid washing), and a crystallizer for recovering the desorbed phosphate as calcium phosphate. The process can use two adsorbent columns in series so that when one is getting regenerated the other adsorbent column can still be in operation. A simplified way to estimate the capital cost would be to assume that the equipment will operate effectively for a fixed lifetime, in which case the capital cost in terms of P will be:

$$Capital\ cost\ (\$/Kg\ P)\ =\ \frac{(H)}{I * Q\ *\ (C_{in}\ -\ C_{out})\ *\ 10^{-3}}$$

Where, H = Total investment cost ($), I = Lifetime of equipment (h)

It is difficult to establish the capital costs since the cost of equipment will vary with scale and the specific costs will usually reduce at bigger scales due to the economy of scale. In this case, the costs were based on pilot scale experiments at a scale of 1.5 m^3/h (Figure S7-12 and Table S7-8 in supporting information show). However, these were scaled up to determine the costs for treating at a full-scale flowrate of 500 m^3/h. This was done by using the scaling coefficient which relates the capacity increase (in this case denoted by the increase in volumetric flowrate) to the increase in equipment cost (Tribe and Alpine 1986). A scaling coefficient value of 0.6 was used in this case, which is in line with common practice (Tribe and Alpine 1986). Moreover, to consider the installation charges, the Lang factor was considered in the calculation (Wain 2014). Since adsorption is used for treating liquids, a Lang factor of 4.8 was used and multiplied with the full-scale equipment cost (Wain 2014). Thus the total investment cost, denoted by the term H, includes the installation cost as well. The calculated value for the total investment cost for a capacity of handling 500 m^3/h amounted to $ 970,000. Considering the equipment has a lifetime of 10 years, an influent concentration (C_{in}) of 1 mg P/L, and the desired effluent concentration (C_{out}) of 0.1 mg P/L, the capital cost expressed in terms of P amounts to about $ 25/Kg P. The energy cost for these conditions (parameters used are listed in Table S7-9 of supporting information) amounts to about $ 10/Kg P. Thus the overall cost including capital, energy and chemical costs for reducing phosphate from 1 to 0.1 mg P/L using reversible adsorption on porous iron oxides is about $ 120/Kg P. Figure 7-8 shows the distribution of the different costs.

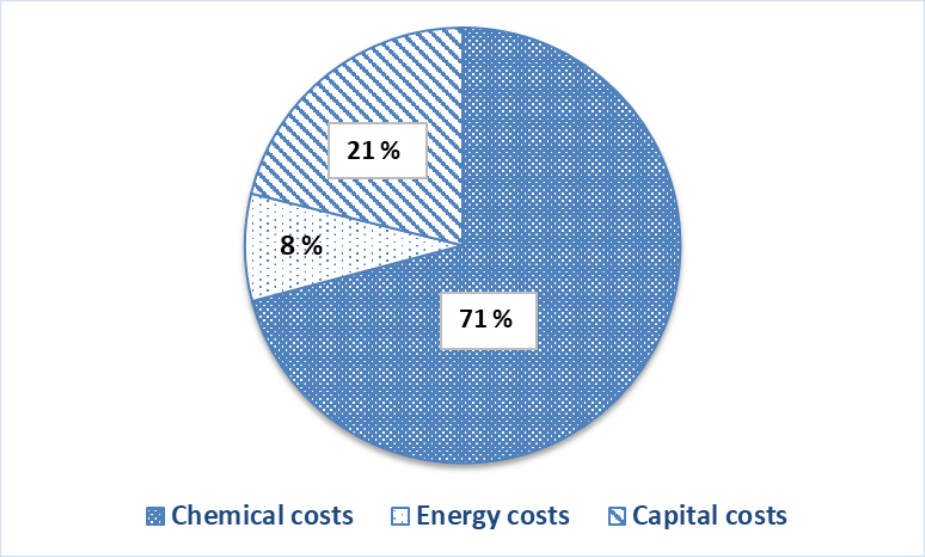


Figure 7-8: Overall cost distribution for phosphate adsorption on porous metal oxide

As can be seen from Figure 7-8, chemical costs, which includes the cost of the adsorbent, contributed to more than 70 % of the overall costs. A similar cost distribution was obtained for the hybrid ion exchange resins, although the percentage of chemical costs was slightly higher (Figure S7-13 in supporting information). Once the process is in operation, the process does not require much manual maintenance, except in the case of checking for the breakthrough (once the effluent P concentration exceeds the required level) and regenerating the adsorbent. Thus the labor costs for the process should ideally be minimal.

The other costs that are not considered in this calculation include the cost for waste generation. One time use biomass-based adsorbents can ideally be used directly as fertilizers provided they did not bind toxic materials like heavy metals and there is indeed a fertilizer value. For reusable adsorbents, although the excess chemicals in the regenerate stream are assumed to be completely reused, there could be an accumulation of other ions in this stream. In that case, occasionally a part of the regenerate stream would need to be bled. This stream might need to be neutralized and further treated before being discarded. Studies are needed on understanding the composition of the regenerate stream after multiple reuses.

7.5.3. Comparison with other technologies and defining the ideal conditions for adsorption

The ideal conditions for adsorption can be underlined by comparison with chemical precipitation. Chemical precipitation with iron salts is a commonly used technique to lower the phosphate concentrations in municipal wastewater (Sedlak 1991). Iron salts can be added near or slightly higher than stoichiometric Fe:P molar ratios to reduce phosphate concentrations to around 1 mg P/L. In practice, a Fe:P molar ratio between 1 to 2 is generally used in wastewater plants to achieve phosphate concentrations around 1 mg P/L (Paul et al. 2001). But reducing the phosphate concentrations below 1 mg P/L using chemical precipitation requires a significant increase in metal salt dosing due to the limitation by solubility product, which in turn leads to high sludge production, as well as due to the formation of metal hydroxides (Neethling 2013, Sedlak 1991). Figure 7-9 (a) shows the relation between required Fe:P molar ratio and the residual phosphate concentration based on data from a wastewater plant (Sedlak 1991). At residual phosphate concentration around 1 mg P/L, the ratio is near the stoichiometric region and the majority of the P removal is via precipitation. However, as the residual phosphate concentration decreases, the required ratio goes very high. In this zone, phosphate removal is mainly due to adsorption onto iron (hydr)oxide complexes (Sedlak 1991). To quantify the effects of this in terms of cost, Figure 7-9 (b) shows a comparison of P removal costs via reversible adsorption and chemical precipitation with iron at 3 different concentrations: 10 to 1 mg P/L, 1 to 0.1 mg P/L and 1 to 0.016 mg P/L. A lowest concentration of 0.016 mg P/L was chosen since this allows us to use the loading for porous iron oxides estimated at this concentration (Suresh Kumar et al. 2018). This does not include the capital costs, but the chemical costs for adsorption and the chemical as well as disposal costs due to sludge formation via chemical precipitation. For chemical precipitation with iron, a Fe:P molar ratio of 2, 20 and 100 are assumed for the concentration ranges of 10 to 1, 1 to 0.1 and 1 to 0.016 mg P/L (Table S7-10 in supporting information shows parameters used for the calculation). The chemical cost for chemical precipitation to bring phosphate concentration from 10 to 1 mg P/L was around $ 8/Kg P. This is in the same order of magnitude as estimated elsewhere (Paul et al. 2001). For adsorption, the chemical costs were calculated for porous metal oxide assuming that it is reused successfully for 30 cycles. Even if the equilibrium adsorption capacity for this adsorbent (FSP) at 1 mg P/L is considered as the practical loading value (Suresh Kumar et al. 2019), the cost to reduce phosphate concentrations from 10 to 1 mg P/L is around $ 35/Kg P. However, as the phosphate concentration goes lower, the costs for adsorption compete and eventually better those of precipitation (see Figure 7-9 (b)). This shows that adsorption is better suited for treating lower concentrations of phosphate.

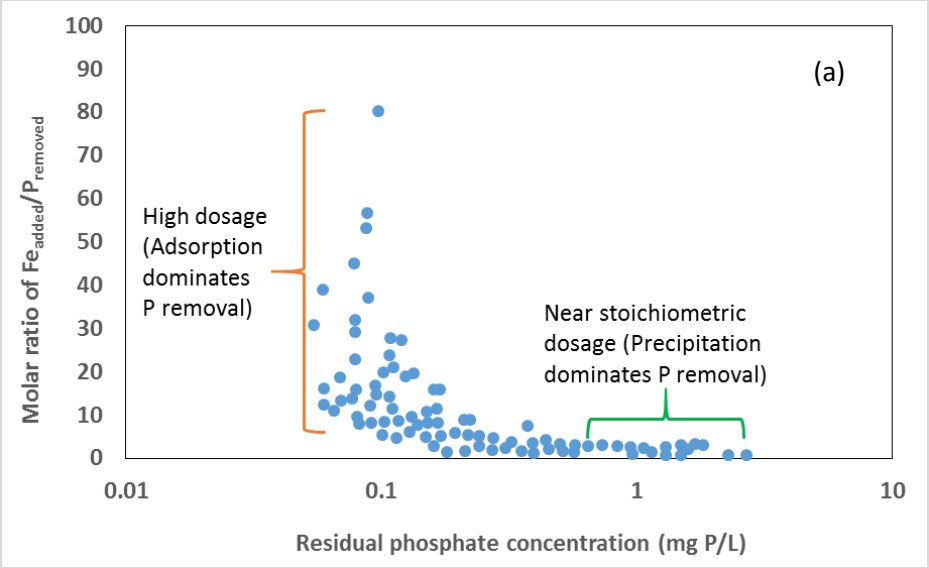


Figure 7-9: (a) Increment in Iron dosing as a function of residual phosphate concentration. The plot has been made using data extracted from (Sedlak 1991) using WebPlotDigitizer. (b) Comparison of chemical costs of reversible adsorption on porous metal oxides versus the cost related to chemical precipitation via iron dosing which includes the cost for chemical consumption and sludge disposal. Note that chemical precipitation is the term used to denote P removal by dosing iron salts, although the actual removal can happen via multiple mechanisms.

The overall cost for reversible adsorption estimated in this review was compared with the costs of other technologies that achieve ultra-low P concentrations (≤ 0.15 mg P/L). The technologies compared here are as follows:

i) Reversible adsorption (RAd) – This includes the estimates made in this review for overall costs to reduce phosphate from 1 to 0.1 mg P/L (denoted RAd-0.1) and from 1 to 0.016 mg P/L (denoted RAd-0.016) using porous metal oxide.

ii) Acti-Flo – In this approach, soluble phosphorus is first removed by dosing iron salts. The resulting flocs are weighed down with microsand in the presence of a polymer. After providing sufficient time in a mixing tank, the water is passed onto a clarifier which removes the microsand along with flocs (Bolton & Menk 2016). An effluent concentration of 0.17 mg P/L could be achieved using Acti-Flo process.

iii) Phoslock – Phoslock is a lanthanum modified bentonite that removes SRP by forming lanthanum phosphate precipitates. Cost estimation for Phoslock was based on the price of Phoslock (2750 €/ton) (Mackay et al. 2014) and on an average adsorption capacity of 9 mg P/g to reduce P concentrations to ≤ 0.05 mg P/L in surface water (Reitzel et al. 2013). This however does not include costs that might be incurred for dosing.

iv) Microalgae - Cost for P removal by microalgae was based on the P uptake by microalgae and the reported cost for microalgae production in Netherlands (Boelee 2013, de Vree 2016). The estimated cost is to reduce the P concentrations upto 0.15 mg P/L.

Figure 7-10 shows the cost comparison for P removal by these different methods. This includes the operational as well as capital costs wherever provided.

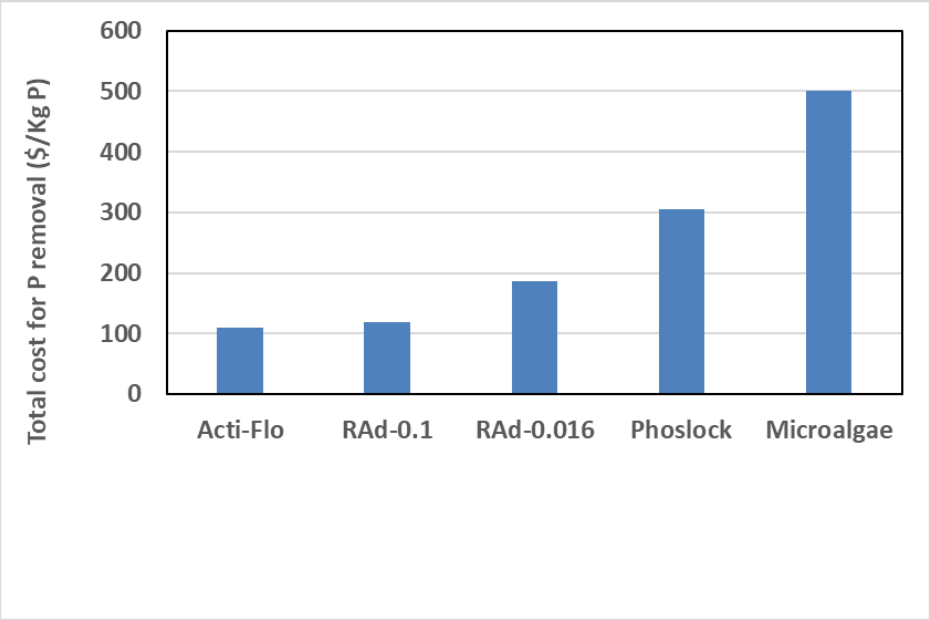


Figure 7-10: Total cost for P removal via different treatment methods that can reach ultra-low concentrations of P. Final effluent concentrations are: Acti-Flo = 0.17 mg P/L, Rad-0.1= 0.1 mg P/L, Rad-0.016 = 0.016 mg P/L, Phoslock = 0.05 mg P/L, Microalgae = 0.15 mg P/L.

As can be seen from Figure 7-10, RAd-0.1 along with Acti-Flo provide the least expensive options. There are other types of technologies like Acti-Flo, which include precipitation with metal salts aided by separation with sand (Newcombe et al. 2008, STOWA 2009). The metal salts dosed result in soluble phosphorus removal by precipitation as well as by forming metal (hydr)oxide complexes which adsorb the phosphorus (Newcombe et al. 2008). However, as discussed earlier in reference to Figure 7-9, P removal to concentrations lower than 0.1 mg P/L

would require a rather high dosing of these metal salts. Alternatively, the use of adsorption will be more suited for reducing phosphate to even lower concentrations. As can be seen from Figure 7-10, the cost of using reversible adsorption to reach a concentration of 0.1 mg P/L is about $ 120/Kg P. But a further reduction to a concentration 6 times lower, i.e. 0.016 mg P/L, increases the overall cost only by a factor 1.5, i.e. about $ 190/ Kg P. This is rather due to the high affinity of adsorbents which will imply a high adsorption capacity at lower P concentrations. Thus, reversible adsorption has the potential to give better economics compared to other methods when it is required to reduce the P concentrations further lower.

7.6. Conclusion

P removal to ultra-low concentrations is necessary to prevent eutrophication. Adsorption studies show a possibility to consistently reach such low concentrations of phosphate. However, despite an increasing interest in scientific literature, a wide spread implementation of phosphate adsorption on a commercial scale has not yet taken place. This may indicate that there are still important economic aspects that are not yet being addressed by the scientific community.

Therefore, this study performed an economic analysis of different types of adsorbents. A Monte Carlo simulation based scenario analysis showed that reusable adsorbents are more cost-effective than one time use low-cost adsorbents. Sensitivity analysis also showed that the most important parameters that govern chemical costs of adsorption are the adsorbent cost, practical loading, and the adsorbent reusability. An expensive adsorbent can still be part of a cost effective process provided it has a high lifetime. For e.g. the cost of adsorption by hybrid ion exchange resins is comparable with that of porous metal oxides even though the adsorbent cost was 3 to 5 times higher for the resins. This was possible due to the assumption that the hybrid ion exchange resins could be reused about 100 times compared to the 30 times by the porous metal oxides.

The literature review also showed the research gaps involved in determining the parameters that govern the economics. For instance, studies from the past 5 years show a big discrepancy between the adsorption capacity at 0.1 mg P/L ($q_{0.1}$) and the maximum adsorption capacity (q_{max}). Since adsorption is considered as a polishing step, it is necessary to have a high $q_{0.1}$. Practical loading is also governed by the adsorbent kinetics. Adsorption studies, in general, need to be done in realistic conditions since competing ions can either increase or decrease the adsorbent performance. Studies should focus on understanding the factors affecting adsorbent reusability so that a better estimation can be made regarding the adsorbent lifetime. Additionally, reusing the regenerate solution also needs more attention. Reusing the chemicals in the adsorption process is of economic and environmental significance.

7.7. Supporting information

7.7.1. Tables

*Table S7-4: Langmuir parameters for different adsorbents and their corresponding adsorption capacity at an equilibrium concentration of 0.1 mg P/L**

Adsorbent	**q_m (mg P/g)**	**K_L (L/mg P)**	**$q_{0.1}$ (mg P/g)**	**Reference**
CuFe2O4-2N-La	32.6	6.3	12.5	(Gu et al. 2018)
CuFe2O4-2N	9.9	0.14	0.14	(Gu et al. 2018)
CuFe2O4	8.3	0.9	0.69	(Gu et al. 2018)
ZnFe2O4	5.2	0.53	0.26	(Gu et al. 2018)
NiFe2O4	6.4	0.2	0.12	(Gu et al. 2018)
MgFe2O4	4.5	1.3	0.52	(Gu et al. 2018)
ACF-Zr-Fe	26.3	1.2	2.8	(Xiong et al. 2017)
NLZ	6.6	35.6	5.2	(He et al. 2016)
La-Z	14.8	0.38	0.54	(He et al. 2017)
MFB-MCs	128	0.05	0.59	(Jung et al. 2017)
NFS	0.39	1.5	0.05	(Wang et al. 2016)
RC-BOFS (0.8 – 2.3 mm)	2.8	0.16	0.04	(Park et al. 2017)
FMS-0.2 La	44.8	0.39	1.66	(Huang et al. 2015)
FMS-0.1 La	42.8	0.35	1.44	(Huang et al. 2015)

FMS-0.04 La	14.7	0.32	0.45	(Huang et al. 2015)
FMS-0.02 La	9.7	0.46	0.43	(Huang et al. 2015)
l-$Y(OH)_3$	75.9	1.9	12	(Kim et al. 2017)
Fe-CL	0.30	2.7	0.06	(Luo et al. 2017a)
Y-MnO_2	0.20	0.03	0.01	(Ge et al. 2016)
FMO-1	3.1	0.04	0.01	(Ge et al. 2016)
FMO-2	8.5	0.12	0.1	(Ge et al. 2016)
FMO-3	36.6	0.15	0.54	(Ge et al. 2016)
E33	8.4	2.5	1.7	(Lalley et al. 2015)
E33/AgI	6.7	1.1	0.67	(Lalley et al. 2015)
E33/AgII	9.1	2.1	1.6	(Lalley et al. 2015)
E33/Mn	6.1	0.73	0.42	(Lalley et al. 2015)
Pure-Zr-OH	38.8	0.06	0.24	(Luo et al. 2017b)
Dimethylamine Zr-OH	50.6	0.12	0.61	(Luo et al. 2017b)
N-Methylaniline Zr-OH	29.1	0.03	0.09	(Luo et al. 2017b)
N-Ethylmethylamine Zr-OH	28.7	0.03	0.09	(Luo et al. 2017b)
Diethylamine Zr-OH	21.8	0.06	0.13	(Luo et al. 2017b)

Hydrogel beads	19.7	0.07	0.14	(Wan et al. 2016)
NPS-HYCA	24.2	0.06	0.14	(Unuabonah et al. 2017)
iPS-HYCA	19.7	0.04	0.09	(Unuabonah et al. 2017)
NPP-HYCA	25.5	0.04	0.11	(Unuabonah et al. 2017)
iPP-HYCA	22.6	0.04	0.1	(Unuabonah et al. 2017)
$ZrO_2@Fe_3O_4$	16	46.2	13.1	(Fang et al. 2017)
$ZrO_2@SiO_2@Fe_3O_4$	6.3	45.1	5.2	(Fang et al. 2017)
Zr hydroxide	18.5	3.1	4.4	(Johir et al. 2016)
WDB	12	0.04	0.04	(Kizito et al. 2017)
CCB	10.4	0.03	0.03	(Kizito et al. 2017)
SDB	8.1	0.03	0.02	(Kizito et al. 2017)
RHB	10.1	0.03	0.03	(Kizito et al. 2017)
MG@La	72.7	0.52	3.6	(Rashidi Nodeh et al. 2017)
ZnFeZR-adsorbent	93.5	0.3	2.7	(Drenkova-Tuhtan et al. 2017)
$Fe_3O_4@ASC$	41.7	0.36	1.4	(Jiang et al. 2017)
NS	41.2	0.1	0.4	(Pan et al. 2014)

HMO@NS	28	0.83	2.1	(Pan et al. 2014)
MOD	47.4	0.65	2.9	(Xie et al. 2014)
Mg-Biochar	38	0.27	1	(Yao et al. 2013)
Phoslock	8.6	2.1	1.5	(Xu et al. 2017)
LAH-1/30	45.3	0.24	1	(Xu et al. 2017)
LAH-1/20	64.1	0.34	2.1	(Xu et al. 2017)
LAH-1/10	70.4	0.63	4.2	(Xu et al. 2017)
NT-25 La	4.6	0.31	0.13	(Kuroki et al. 2014)
am-ZrO_2	32.3	0.95	2.8	(Su et al. 2013)
GO-Zr	5.4	0.7	0.35	(Zong et al. 2013)
HA-MNP	9.4	0.09	0.08	(Rashid et al. 2017)
$La(OH)_3/Fe_3O_4$ (4:1)	83.5	1.7	12.4	(Wu et al. 2017)
20MMSB	121.2	0.02	0.23	(Li et al. 2016)
Fe-GAC-1	10.4	0.05	0.05	(Suresh Kumar et al. 2017)
Fe-GAC-2	10.8	0.13	0.14	(Suresh Kumar et al. 2017)
Fe-GAC-3	10.8	0.25	0.26	(Suresh Kumar et al. 2017)

*Certain studies expressed these values in terms of mg PO_4 instead of mg P. These were adjusted accordingly so that these terms are expressed in terms of mg P.

Table S7-5: Pseudo second order kinetic model constants for different adsorbents and the time taken to reach 90 % (t_{90}) of equilibrium adsorption capacity by these adsorbents

Adsorbent	**q_e (mg P/g)**	**K (g/(mg P min))**	**t_{90} (h)**	**Reference**
$CuFe_2O_4$-2N-La	29.8	4.1×10^{-3}	1.2	(Gu et al. 2018)
ACF-Zr-Fe	9.5	1.5×10^{-3}	10.3	(Xiong et al. 2017)
NLZ	2.5	2.2	0.03	(He et al. 2016)
La-Z	2.6	2.1	0.03	(He et al. 2017)
MFB-MCs	54	4.3×10^{-2}	0.06	(Jung et al. 2017)
NFS	0.16	1.5×10^{-1}	6	(Wang et al. 2016)
RC-BOFS (0.8-2.3 mm)	0.13	2.5	0.46	(Park et al. 2017)
FMS-0.1 La	2	9.7×10^{-2}	0.77	(Huang et al. 2015)
l-$Y(OH)_3$	79.6	2.7×10^{-4}	7.1	(Kim et al. 2017)
Pure-Zr-OH	25.8	3.1×10^{-3}	1.9	(Luo et al. 2017b)
Dimethylamine Zr-OH	36	1.2×10^{-2}	0.34	(Luo et al. 2017b)
N-Methylaniline Zr-OH	11.3	1.8×10^{-2}	0.72	(Luo et al. 2017b)

N-Ethylmethylamine Zr-OH	16.9	1.8×10^{-2}	0.48	(Luo et al. 2017b)
Diethylamine Zr-OH	12.4	1.2×10^{-2}	0.99	(Luo et al. 2017b)
Hydrogel beads	3.8	2.9×10^{-3}	13.8	(Wan et al. 2016)
$ZrO_2@Fe_3O_4$	4	1.7	0.02	(Fang et al. 2017)
$ZrO_2@SiO_2@Fe_3O_4$	3.9	2.4×10^{-1}	0.16	(Fang et al. 2017)
Zr hydroxide	15.3	1.7×10^{-1}	0.06	(Johir et al. 2016)
WDB	7.9	5.4×10^{-4}	35.3	(Kizito et al. 2017)
CCB	6.9	6×10^{-4}	36.3	(Kizito et al. 2017)
SDB	8.4	3.5×10^{-4}	51.5	(Kizito et al. 2017)
RHB	6.5	1×10^{-3}	22.5	(Kizito et al. 2017)
MG@La	5.4	1.1×10^{-2}	2.4	(Rashidi Nodeh et al. 2017)
ZnFeZR-adsorbent	10.5	5.9×10^{-1}	0.02	(Drenkova-Tuhtan et al. 2017)
$Fe_3O_4@ASC$	43.4	6.9×10^{-5}	49.7	(Jiang et al. 2017)
MOD	48.5	6.2×10^{-4}	5	(Xie et al. 2014)
Mg-Biochar	4.3	1.6×10^{-3}	21.2	(Yao et al. 2013)
am-ZrO_2	15.8	6.4×10^{-2}	0.15	(Su et al. 2013)
Go-Zr	4.3	2.2×10^{-2}	1.6	(Zong et al. 2013)

HA-MNP	0.97	2.2×10^{-1}	0.69	(Rashid et al. 2017)
Fe-GAC-1	4.6	4×10^{-4}	81.5	(Suresh Kumar et al. 2017)
Fe-GAC-2	6.5	2.8×10^{-4}	82.4	(Suresh Kumar et al. 2017)
Fe-GAC-3	7.1	8.8×10^{-4}	24	(Suresh Kumar et al. 2017)

Table S7-6: Variation in kinetic constants for different adsorbents as a function of temperature

Adsorbent	**Temperature (°C)**	**K (g/(mg P min))**	**Reference**
TDPA-KCl	20	1.66×10^{-2}	(Akar et al. 2010)
	30	1.91×10^{-2}	
	40	1.95×10^{-2}	
ACF-La	20	3.7×10^{-3}	(Liu et al. 2011)
	30	4×10^{-3}	
	40	5.6×10^{-3}	
	50	1×10^{-2}	
MFB-MCs	10	5.62×10^{-4}	(Jung et al. 2017)
	20	6.64×10^{-4}	
	30	8.18×10^{-4}	
Boehmite	20	6.97×10^{-3}	(Qian et al. 2017)
	30	3.83×10^{-3}	
	40	9.33×10^{-3}	
Fe-CL	25	2.76×10^{-2}	(Luo et al. 2017a)
	35	2.45×10^{-2}	
	45	2.76×10^{-2}	
Lanthanum modified bentonite	10	1.4×10^{-2}	(Haghseresht et al. 2009)
	23	2.8×10^{-2}	
	40	4.5×10^{-2}	

Fe(II)-treated biomass	10 20 30 40	1.59×10^{-2} 1.23×10^{-2} 9.51×10^{-3} 1.01×10^{-2}	(Aryal and Liakopoulou-Kyriakides 2011)
Iron hydroxide-eggshell waste	20 25 35 45	4.02×10^{-2} 6.81×10^{-2} 8.03×10^{-2} 1.31×10^{-1}	(Mezenner and Bensmaili 2009)
La(III)-loaded granular ceramic	20 40	1.97×10^{-3} 3.51×10^{-3}	(Chen et al. 2012)

*Table S7-7: Range of different parameters for estimating the chemical cost of adsorption**

(a) Waste biomass-based adsorbent (example used: rice husk) – No regeneration costs

Range of practical loading based on (Mor et al. 2016, Yadav et al. 2015)

Parameters	**Units**	**Minimum value**	**Maximum value**
Adsorbent cost (a1)	**$/Kg adsorbent**	0.1	0.2
Practical loading (a2)	**Moles P/Kg adsorbent**	0.01	0.02

(b) Porous metal oxide (example used: Ferrosorp)

Parameters	**Units**	**Minimum value**	**Maximum value**
Adsorbent cost (a1)	**$/Kg adsorbent**	3	6
Practical loading (a2)	**Moles P/Kg adsorbent**	0.05	0.1
OH to P ratio (c1)	**Moles OH/Mole P**	15	25
Adsorbent pore volume (c2)	**L/Kg adsorbent**	0.6	0.6
Concentration of NaOH (c3)	**Moles NaOH/L**	0.5	1

Cost of 100 % NaOH (c4)	**$/Mole NaOH**	0.03	0.03
H to Ca ratio (d1)	**Moles H/Mole Ca**	5	15
Ca practical loading (d2)	**Moles Ca/Kg adsorbent**	0	0.25
Cost of 100 % HCl (d3)	**$/Mole HCl**	0.003	0.003
Ca consumed for CaP formation (e1)	**Moles Ca/Mole P**	1.5	2.5
Cost of 100 % $CaCl_2$ (e2)	**$/Mole $CaCl_2$**	0.01	0.01
OH consumed for CaP formation (e3)	**Moles OH/Mole P**	0	0.5
Cost of 100 % CaP (e4)	**$/Mole CaP**	0.1	0.1
Number of regeneration cycles (n)		27	33

(c) Hybrid ion exchange resin (example used: BioPhree®)

Parameters	**Units**	**Minimum value**	**Maximum value**
Adsorbent cost (a1)	**$/Kg adsorbent**	15	20
Practical loading (a2)	**Moles P/Kg adsorbent**	0.04	0.08
OH to P ratio (c1)	**Moles OH/Mole P**	15	25
Adsorbent pore volume (c2)	**L/Kg adsorbent**	0.6	0.6
Concentration of NaOH (c3)	**Moles NaOH/L**	0.5	1
Cost of 100 % NaOH (c4)	**$/Mole NaOH**	0.03	0.03
H to Ca ratio (d1)	**Moles H/Mole Ca**	5	15

Ca practical loading (d2)	**Moles Ca/Kg adsorbent**	0	0.25
Cost of 100 % HCl (d3)	**$/Mole HCl**	0.003	0.003
Ca consumed for CaP formation (e1)	**Moles Ca/Mole P**	1.5	2.5
Cost of 100 % $CaCl_2$ (e2)	**$/Mole $CaCl_2$**	0.01	0.01
OH consumed for CaP formation (e3)	**Moles OH/Mole P**	0	0.5
Cost of 100 % CaP (e4)	**$/Mole CaP**	0.1	0.1
Number of regeneration cycles (n)		90	110

*Footnotes for Table S7-7

- The costs for all chemicals except the rice husk was provided by ICL fertilizers (Netherlands) as of May 2018. The cost for rice husk was based on the website information provided by the e-commerce company AliBaba (Last visited on May 2018).
- All parameter values except adsorbent cost (a1), number of regeneration cycles (n) and calcium consumption to form calcium phosphate (e1) were obtained based on the experiments from an earlier study (Suresh Kumar et al. 2018)
- Calcium consumption (e1) was based on values suggested by literature (Kuzawa et al. 2006, Song et al. 2002)
- Adsorbent cost (a1) was based on information provided by suppliers. For FSP, the higher end of this value was based on the fact that smaller adsorbent particles than the standard supply were used in the study (Suresh Kumar et al. 2018).

Table S7-8: Components used for calculating capital costs. The scenario considers two adsorbent columns running in series including regeneration with alkaline and acidic solutions for desorption and removal of surface precipitates, respectively, as depicted in figure S7-12. The text below the table further elaborates on the calculation of total equipment investment cost.

Parameters for capital costs	**Supplier/Origin**	**Volume per unit (L)**	**Cost per unit ($)**	**Number of units**	**Total cost ($)**
Adsorbent columns	Aquacom	300	800	2	1600
Regeneration tanks	Logisticon	1000	100	2	200
Pumps	Northern tool		300	4	1200
Crystallizer	Wetsus	300	1800	1	1800
Valves, piping and miscellaneous	Vaandjik, Bosta		1400		1400
					Overall cost = **6200**

Thus, the overall equipment cost for the pilot scale adsorption, which operates at flowrate of 1.5 m^3/h = $ 6200.

For a full-scale operation that operates at 500 m^3/h, these costs can be scaled up using the scale coefficient (Tribe and Alpine 1986). Using a scale coefficient of 0.6, results in equipment cost = $ 202,000.

Moreover, the total cost related to setting up the equipment, i.e. including the installation costs, can be calculated using the Lang factor (Wain 2014). Using the Lang factor for fluid processes, which is 4.8, the total equipment investment cost = $ 970,000.

Assuming an equipment lifetime of 10 years, an influent concentration = 1 mg P/L and the desired effluent concentration = 0.1 mg P/L, the capital cost in terms of P removed = $ 25/Kg P.

Table S7-9: Conditions used for calculating the energy costs

Parameters	**Units**	**Value**
Adsorbent bed volume	**m^3**	200
Adsorbent column height to diameter ratio		3
Volumetric flow rate	**m^3/h**	500
Superficial velocity	**m/s**	9×10^{-3}
Pump efficiency	**%**	90
Adsorbent particle size	**m**	2.5×10^{-4}
Bed void fraction		0.6
Density of liquid treated	**Kg/m^3**	1000
Electricity cost (as per United States)	**$/kWh**	0.12

*Table S7-10: Calculation of overall chemical and disposal cost for P removal via chemical precipitation**

Parameters	**Scenario - 1**	**Scenario - 2**	**Scenario - 3**
P_{in} (mg P/L)	10	1	1
P_{out} (mg P/L)	1	0.1	0.016
Fe to P molar ratio (β)	2	20	100
$FeCl_3$ consumed (Kg $FeCl_3$/Kg P)	10	105	524
Cost of 100 % $FeCl_3$ ($/Kg $FeCl_3$)	0.4	0.4	0.4
Cost due to FeCl3 consumption ($/Kg P)	4	42	210

Sludge produced (Kg dry matter/Kg P)	10	70	290
Cost for sludge treatment ($/dry matter)	0.4	0.4	0.4
Cost due to sludge generation ($/Kg P)	4	28	116
Overall chemical and disposal cost ($/Kg P)	8	70	326

*Cost of $FeCl_3$ was obtained from Brenntag (Netherlands),

Cost due to sludge production was based on the average costs for sewage sludge disposal in the Netherlands in 2015 (Waterschappen 2015),

The Fe to P molar ratio (β) for scenario-1 and scenario-2 was based on the average values from the data points in Figure 7-9 (a). For scenario-3 a value of 100 was chosen to be able to quantify the costs, but this number can actually be even higher, i.e. significant dosing of metal salts might be required such low phosphate concentrations (Esvelt et al. 2010).

Sludge produced was calculated using the model shown in equation S2.

7.7.2. Figures

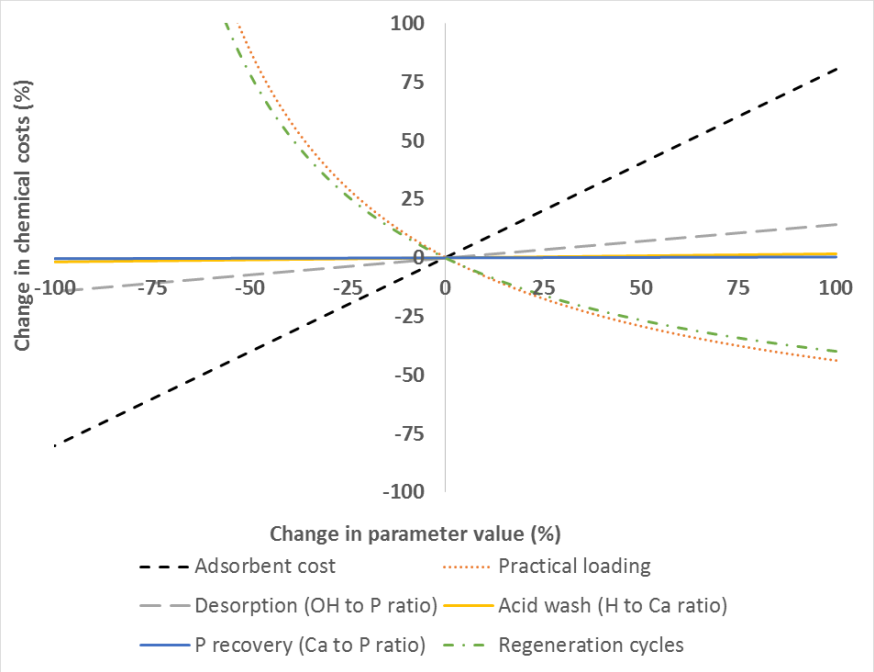


Figure S7-11: Sensitivity of different parameters to chemical costs of hybrid ion exchange resin

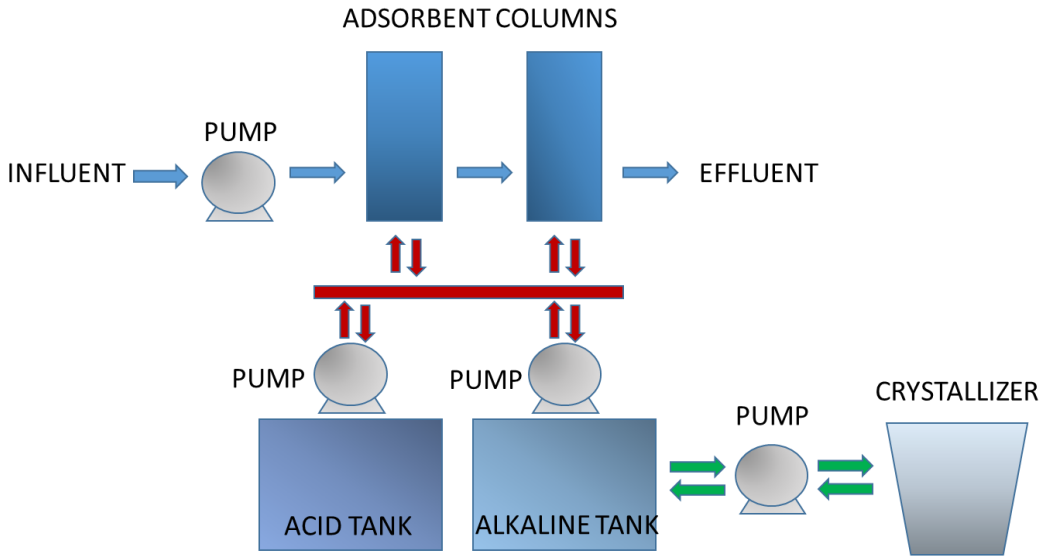


Figure S7-12: Schematic showing the main components used for pilot scale phosphate adsorption as listed in table S7-8. Blue arrows represent the flow for adsorption, red arrows for regeneration and green arrows for phosphate recovery via crystallization. Two adsorbent columns are present so that one column can keep adsorbing even while another is regenerated. The individual components in figure are not drawn to scale.

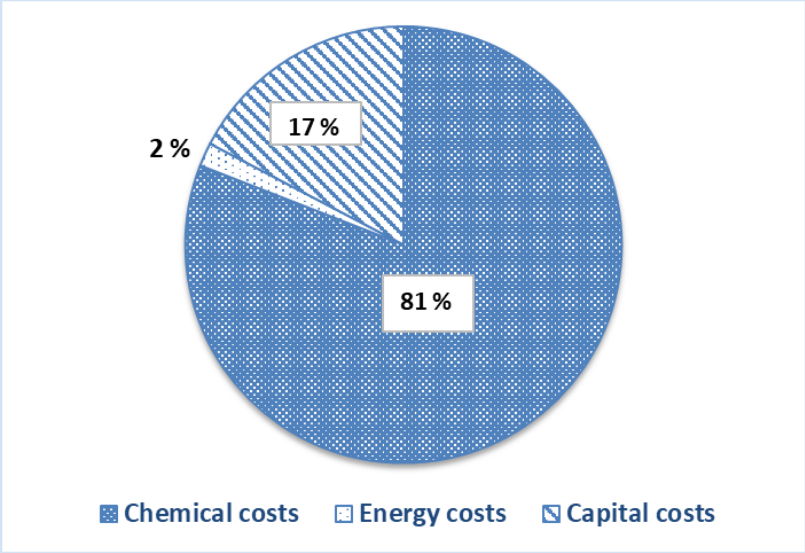


Figure S7-13: Overall cost distribution for phosphate adsorption on hybrid ion exchange resin

7.7.3. Equations

Equation S1: Ergun equation is given by:

$$\Delta P = \left[\frac{150 * \mu * L * (1-\varepsilon)^2 * v}{(D_p)^2 * (\varepsilon)^3}\right] + \left[\frac{1.75 * L * \rho * (1-\varepsilon) * (v)^2}{D_p * (\varepsilon)^3}\right]$$

Where,

μ = dynamic viscosity of the fluid (Kg/m*s),

L = Length of packed bed (m),

v = superficial velocity (m/s),

D_p = Particle diameter (m),

ε = Void fraction of bed,

ρ = Density of the fluid (Kg/m^3)

Equation S2: The sludge generated via chemical precipitation was calculated using the following equation (Veldkamp 1985):

$SFe = 3.50 + 3.37 * (Pin - Pout) + 2.79 * \beta * Pin$

Where,

S_{Fe} represents the sludge production due to iron dosing in mg dry solids/L,

P_{in}, P_{out} represent the influent and effluent phosphorus concentration,

β represents the molar ratio between the amount of metal salt added and total phosphorus concentration in the water.

Chapter - 8

Valorization of phosphate adsorption

"If you don't drive your business, you will be driven out of business."

- B.C. Forbes

8.1. Problem statement and the capability of adsorption

This thesis discusses adsorption as a technology for removing phosphate from dilute streams and reach very low phosphate concentrations. The need to reach low phosphate concentrations is primarily to combat eutrophication. Eutrophication has significant impacts on the ecosystem and the economy. The overall annual cost to prevent eutrophication in the US was estimated to be around $ 2.2 billion in 2009 (Dodds et al. 2009). The prevention of eutrophication paves way for a cleaner environment which provides a big benefit to sectors such as fishing, housing, recreation, and tourism.

Adsorption is a technology that can reduce phosphate down to concentrations lower than 10 µg P/L. It has the advantage of offering high throughputs, low footprint, minimal waste generation and contributing to a circular economy by recovering the phosphate and reusing the chemicals. Since the process is shown to be technically viable, the next question is how to create incentives for potential short and long-term actors that can help realize this at a commercial level.

8.2. Existing markets and potential customers

The chief market for phosphate adsorption is to prevent eutrophication. This is a theme for treating surface waters where phosphorus concentrations of less than 10 to 100 µg P/L are seen as a requirement. Adsorption can be used directly in surface water for controlling harmful algal bloom.

Municipal wastewater plants are point sources of phosphorus discharge and stringent limitations are already required in several municipalities in North America (USEPA 2007). Thus, sewage effluent polishing would be a potential application.

Phosphate removal to very low concentrations inhibits bacterial growth and hence adsorption has the potential to prevent biofilm formation (Sevcenco et al. 2015). This can be used to control biofouling in cooling towers or on membranes.

8.3. Cost analysis

For any technology to be applied it needs to have a market of customers, a process and driving forces for all actors. This includes an incentive for short-term as well as long-term actors. An economic analysis is a key requirement to assess the incentives.

Figure 8-1 (a) shows the chemical costs for phosphate adsorption for three types of adsorbents: a low-cost adsorbent which is only usable once, more expensive adsorbents based on porous metal oxides and hybrid ion exchange resins that can both be reused several times. It can be seen that the reusable adsorbents are cheaper than a single time use adsorbent.

Figure 8-1 (b) shows the respective cost distribution arising from chemical, energy and capital costs for the porous metal oxide adsorbent. It can be seen that chemical costs dominate the overall cost distribution. The hybrid ion exchange resin also showed a similar distribution, albeit with a higher fraction of the chemical costs, presumably due to the higher cost of the resins. The capital costs are based on scaling up the equipment used for a pilot study including costs considering their installation.

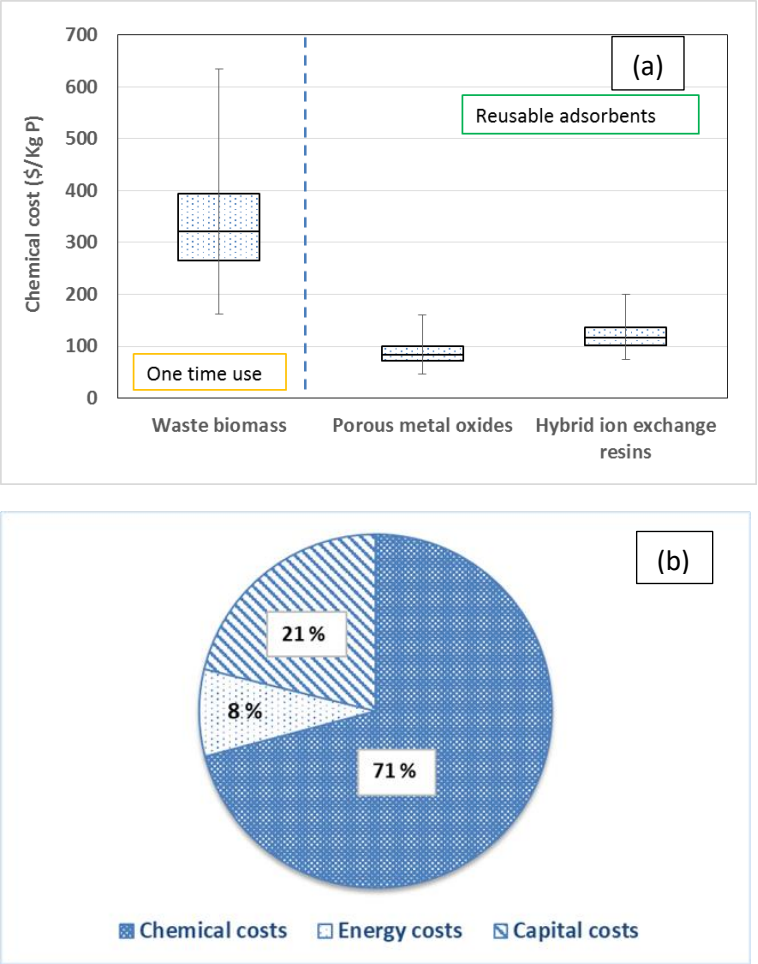


Figure 8-1: (a) Chemical costs for phosphate adsorption from 3 different types of adsorbents to reduce phosphate concentrations to 0.1 mg P/L (b) Cost distribution for porous metal oxides.

The cost for treatment is in the order of $ 100 to 200/ Kg P for the reusable adsorbents for reducing the phosphate concentration upto 0.016 mg P/L. It must be considered that this cost is for reaching effluent concentrations that are not usually reached by conventional techniques. Moreover, this cost does not include the potential economic and environmental benefits that come with preventing eutrophication.

8.4. Value to customers

The selling point of adsorption technology should be directed towards the environmental impact. Customers should be addressed about the possible benefits that will make the

investment worthy. Life cycle assessment will show the true benefits. The hiring of consultancies can help assess this value. For e.g. In UK, the annual price of waterside properties reduced by about $ 14 million due to eutrophication (Pretty et al. 2003). The corresponding damages due to reduced recreational values of water bodies and reduced revenues from the tourism industry were between $ 13 to 47 million, and $ 4 to 16 million, respectively. The price of residential properties, revenue due to recreational activities and tourism could increase by improving the quality of water near these places.

8.5. Example of application

The pollution of the Everglades (Florida) due to eutrophication has been seen as a very urgent issue and has led to the development of the George Barley Water Prize (GBWP). This is in the framework of a contest, offering a grand prize of 10 million USD to a team that can effectively reduce the total phosphorus concentrations to less than 10 µg P/L. The key factor here is to do this with a very small footprint and to have a cost that does not exceed 120 $/Kg P removed. This cost has been decided by consulting with various stakeholders including water treatment plants and waterboards.

Adsorption as a potential solution has already been demonstrated to successfully reduce phosphate at lab scales to less than 5 µg P/L and the research carried at Wetsus (European centre of excellence for sustainable water technology) has already been selected for testing a pilot scale operation treating real surface water.

Current requirements need to reduce total phosphorus (P) which includes soluble and particulate P. Since adsorption only targets the soluble P, depending on the extent of particulate P, there might be a need to combine adsorption with other techniques like flocculation or filtration. However, as suggested by various studies, a better criteria in the future would be to focus on bioavailable P instead of total P (Gerdes and Kunst 1998). This has been shown to be predominantly soluble reactive P/phosphate. Hence adsorption would again be at the forefront to remove the bioavailable P.

The pilot scale study of the GBWP has been conducted in Canada where the temperatures are lower than in Florida. This would show that the technology is applicable across various conditions. The pilot study by Wetsus combines adsorption with flocculation to remove the particulate P. The adsorbent is reusable by regeneration and the phosphate can be recovered from the regenerate stream by the formation of calcium phosphate crystals. These can be used as raw materials for fertilizers. A biodegradable flocculant like chitosan is used to remove the particulate P and this can be used as direct fertilizer for agriculture.

Although some technologies like combination of precipitation with membrane filtration, wetlands can reduce P to levels less than 10 µg P/L, they need excess addition of metal salts leading to more sludge formation, or need very high land area. Adsorption technology used for the GBWP has an estimated area that is 100 times smaller than a wetland and the reuse of the

chemicals lead to minimal waste generation. This is seen by the fact that many of the competitors in the pilot test of the GBWP use technology based on adsorption.

8.6. Potential business model

There are different types of business models that are possible with this technology. This can be a product model where the whole setup is sold to customers (like water boards), or service model where customers are charged per unit volume of water treated or per mass of P removed. A manufacturer model would mean selling only adsorbents or equipment to a retailer, whereas franchise model would involve selling products developed by certain brand and paying a royalty.

Since the upfront investment is high for adsorption, a service model can be envisioned to begin with. Adsorption technology has a small footprint, allowing it to be built as a modular unit. The initial cost of the set up will be taken by the service provider and the customers will be charged per unit volume of water treated or per mass of phosphate removed. The adsorbent regeneration can also be done in a centralized way so that the customers do not need to have to use harsh chemicals on their site. A business model canvas can be used to visualize the different steps involved (Osterwalder and Pigneur 2010). The business model canvas in Figure 8-2 shows the scenario for a service model for adsorption.

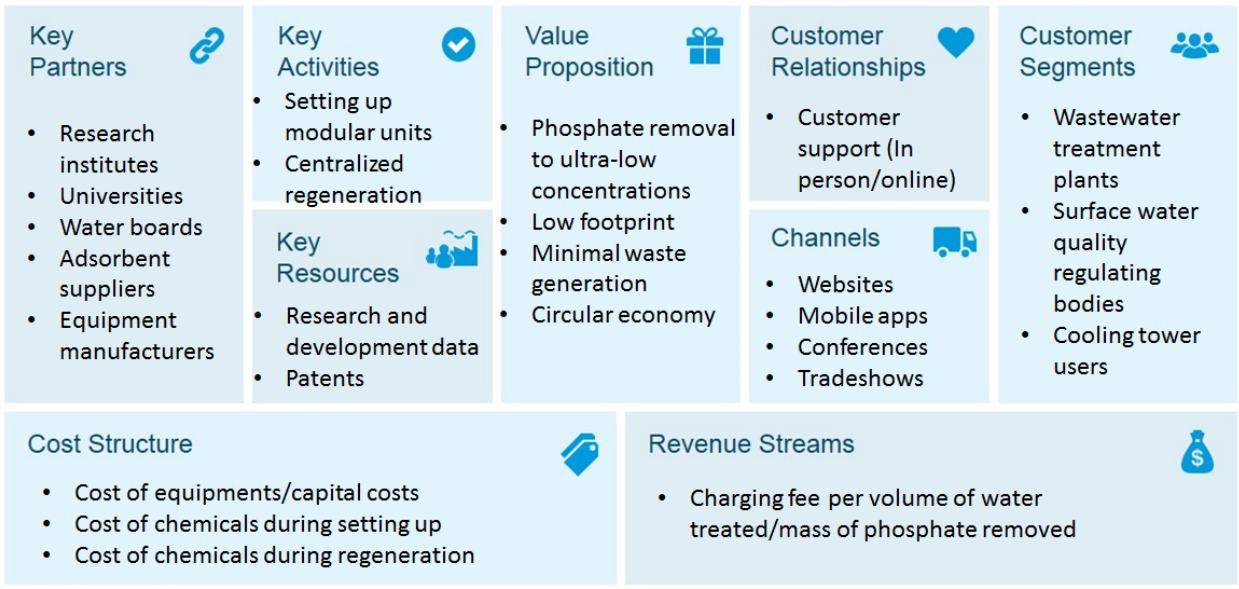


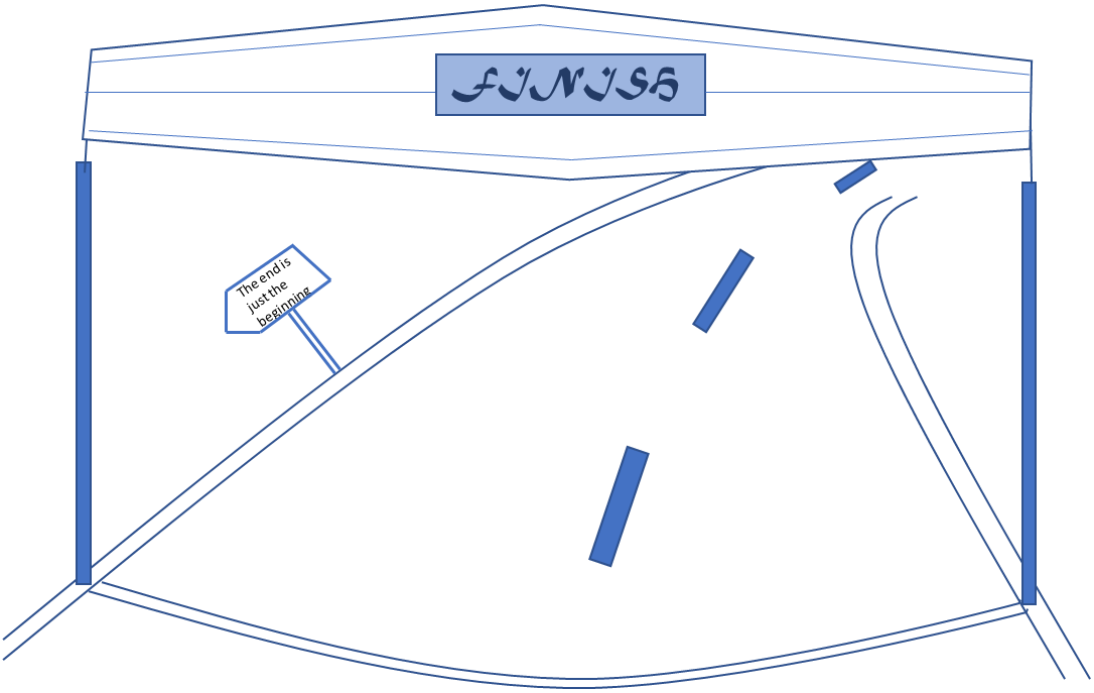
Figure 8-2: Business model canvas for a service model of phosphate adsorption

Figure 8-2 shows the different components involved in realizing the service model for phosphate adsorption. The value proposition will be based on the environmental needs to achieve very low P concentration. The customers will typically include anyone needing such low P concentrations, like surface water authorities, wastewater treatment plants, tourist and recreational industries, and users requiring biofouling control, for instance in cooling towers.

The generation of revenue will come from the cost charged for treating water, whereas research and development will be key for continuous improvement. As the market grows, the service model can be turned into a product model where the adsorbent along with the setup can be sold as a product. In an effort to combat eutrophication, future legislation regarding permissible phosphorus discharge levels from different sources will likely get stringent. Thus, phosphate adsorption can currently be seen as an emerging market with a high potential for expansion in the future.

Chapter - 9

Conclusion and outlook



Adsorption as a technology can remove phosphate effectively to concentrations lower than 10 µg P/L. Even before the commencement of this research, phosphate adsorption from aqueous solutions had been extensively studied and suggested as a potential polishing step for wastewater effluent. However, the problem with phosphate adsorption studies were the huge variations in adsorbents and the conditions in which they were tested in. This made it difficult to gather information on the essential phosphate adsorbent characteristics for application in effluent polishing. Moreover, despite the huge number of phosphate adsorption studies, there was insufficient information on the factors needed to successfully implement this as an economically viable technology.

The goal of this thesis was thus based on two important questions:

I) What are the parameters that can be optimized for making adsorption an economically viable technology?
II) How can these essential parameters be optimized using scientific research?

From this work, it follows that the main parameters were the adsorbent cost, the practical adsorption capacity, and the reusability of the adsorbent and the regeneration chemicals. High surface area adsorbents investigated to improve the phosphate adsorption at lower phosphate concentrations (adsorbent affinity) showed that just considering the surface area is not enough. Iron oxide coated onto granular activated carbon (Fe-GACs) showed that phosphate adsorption affinity could be attributed to the area coming from pores larger than 3 nm. GACs had 90% or more of their surface area coming from micropores (pore size < 2 nm). The micropores in the GAC could not be coated with iron oxide thereby leaving most of the surface area unusable for phosphate adsorption. Granular porous metal oxides exhibited phosphate adsorption in such micropores but the presence of pores larger than 10 nm favoured the phosphate adsorption kinetics by allowing faster diffusion.

Biogenic iron oxides studied because of their reportedly high phosphate adsorption affinity were found to remove soluble phosphate via multiple mechanisms. This involved adsorption on the solid phase as well as removal via precipitation and/or adsorption onto suspended complexes released from the biogenic iron oxides. The phosphate removed via such mechanisms are not recoverable by regeneration of the adsorbent. Moreover, the phosphate removal capacity of biogenic iron oxides purely from an adsorption perspective was lower than that of chemical iron oxides (more than 3 times lower than granular ferric hydroxide (GEH)). Thus chemical iron oxides are more suited for phosphate adsorption. However, biogenic iron oxides could play an important role in phosphorus mobilization in the environment, or in the removal of contaminants like arsenic, where the recovery is not a big focus.

A suitable reusable adsorbent should have good stability and be easily regenerable. Using Mössbauer spectroscopy, it was found that adsorbents used in municipal wastewater effluent changed their iron oxide composition to a small extent (from 0 to 10 %) within 3 reuse cycles. Amongst all other ions present in the wastewater, the most significant effect on adsorbent reusability came from the effect of calcium. Calcium ions present in the wastewater played a dual role. On one hand, it enhances the phosphate adsorption by making the adsorbent surface

more electropositive. On the other hand, it forms surface precipitates. An acidic treatment step was required in the regeneration step to release the surface precipitates and make the adsorbent reusable. A proper understanding of the mechanism of surface precipitation can help optimize the phosphate adsorption as well as adsorbent reusability. For instance, the adsorption of calcium could be controlled by fine-tuning the adsorbent surface charge.

Economic analysis showed that reusing high-cost adsorbents is cheaper than using a low cost one-time use adsorbent provided the adsorbent lifetime is sufficiently high. The chemical cost for adsorption was around $ 100/Kg P for porous metal oxides as well hybrid ion exchange adsorbents, provided they had a lifetime around 30 and 100 cycles, respectively. Sensitivity analysis showed that adsorbent cost, practical adsorption capacity and adsorbent lifetime significantly impacted the chemical costs. Adsorption is most favourable for reducing phosphate concentrations to less than 0.1 mg P/L. Other techniques such as precipitation are economically more favourable for treating water with higher concentrations of phosphate.

The studies in this thesis have revealed ways to improve the phosphate adsorption kinetics and adsorbent reusability. The economic evaluation has pointed out the essential parameters pertaining to costs and highlighted the research gaps. A pilot installation (in the context of the George Barley Water Prize) for phosphate adsorption from surface water has been realized during this timeframe, showcasing the feasibility of this technology. The next step would be to apply phosphate adsorption on a full scale. Further research on phosphate adsorption can still contribute to improving the adsorbent performance and lowering the costs further.

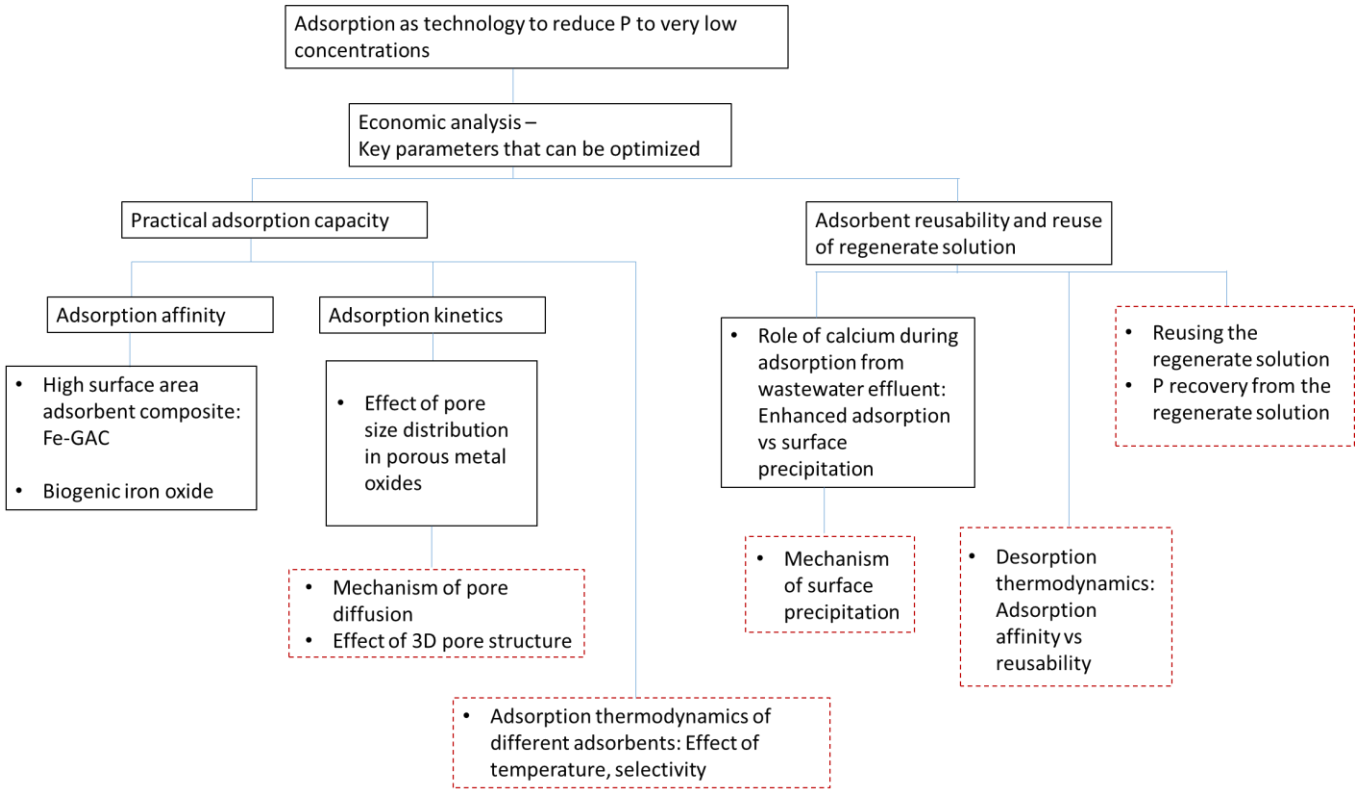


Figure 9-1: Research framework for phosphate adsorption showing the studies undertaken in this thesis along with future directions (dashed boxes)

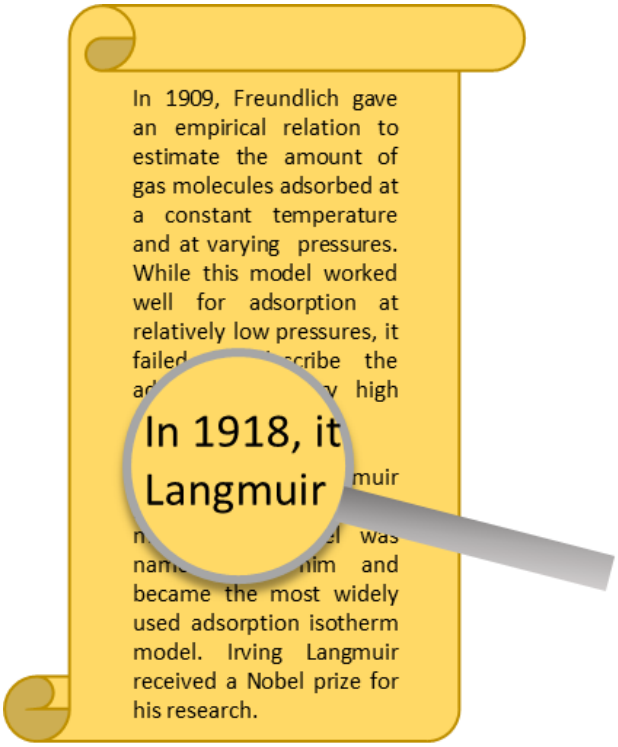
Figure 9-1 shows the studies undertaken in this thesis and the rationale behind them, also highlighting (in dashed boxes) studies to be undertaken in the future.

Studies aimed toward fundamental understanding of phosphate interaction on the adsorbents can improve the adsorption capacity at low phosphate concentrations (adsorption affinity). Calorimetry measurements can be used to determine the thermodynamic constants which will help understand the adsorption affinity. Use of X-Ray absorption spectroscopy and Mössbauer spectroscopy can help determine the type of interaction and binding energy of phosphate towards adsorbents like iron oxides. Studies investigating the three-dimensional structure of porous adsorbents will help improve the adsorption kinetics. From a reusability point of view, future studies need to determine the best practices for recovering the desorbed phosphate and reusing the regenerate solution. This will be essential to minimize the waste generation as well having lower chemical costs.

For water boards as well as stakeholders that plan to take phosphate adsorption to a commercial level, the work in this thesis shows that adsorption has the potential to be used for sewage effluent polishing. The pilot study in the framework of the George Barley Water Prize also used adsorption to remove phosphate from surface water. Economic analysis shows that reversible adsorption is the way to go, as the overall chemical costs can be lowered if the chemicals are reused. This thesis also gives information to existing adsorbent producers, specifically to producers of porous metal oxides, as to what adsorbent characteristics can be optimized to improve phosphate adsorption. For researchers, the information present as well as missing in this thesis will hopefully give leads as what can be done further in the field of phosphate adsorption as a polishing step.

Current legislations do not always require to reach very low phosphate concentrations (< 0.1 mg P/L). However, as more stringent regulations on nutrient discharge are applied, the market for phosphate adsorption will increase. While the goal to reduce phosphate discharge will be based on the need for combating eutrophication, it is worthwhile to pause and visualize what could become the ultimate goal of municipal as well as industrial wastewater treatment plants. On one hand, human society in general will move further towards resource recovery from all sorts of wastewater. While this is currently being done to a large extent in municipal wastewater plants, the loop is not 100 % complete. A 100 % resource recovery implies that even trace amounts of materials need to be prevented from escaping in the wastewater effluent. This will need a combination two things: i) development of analytical techniques that detect extremely low concentrations ii) technologies that can remove resources at such dilute streams. Such an approach will turn the idea of waste generation into rerouting of resources. The usage of the term waste disposal might actually cease and would be replaced by a term like resource rerouting. While when exactly this would happen will be a speculation, it will need technologies that can facilitate selective removal at trace concentrations and complete reusability of the chemicals involved. Adsorption will have a very big potential in such a future.

References


In 1909, Freundlich gave an empirical relation to estimate the amount of gas molecules adsorbed at a constant temperature and at varying pressures. While this model worked well for adsorption at relatively low pressures, it
high
In 1918, it
Langmuir
and became the most widely used adsorption isotherm model. Irving Langmuir received a Nobel prize for his research.

Abbas, M.N. (2015) Phosphorus removal from wastewater using rice husk and subsequent utilization of the waste residue. Desalination and Water Treatment 55(4), 970-977.

Abdala, D.B., Northrup, P.A., Arai, Y. and Sparks, D.L. (2015) Surface loading effects on orthophosphate surface complexation at the goethite/water interface as examined by extended X-ray Absorption Fine Structure (EXAFS) spectroscopy. Journal of Colloid and Interface Science 437, 297-303.

Abma, W.R., Schultz, C.E., Mulder, J.W., van der Star, W.R.L., Strous, M., Tokutomi, T., van Loosdrecht, M.C.M., 2007. Full-scale granular sludge Anammox process. Water Science & Technology 55 (8-9), 27.

ACHS, 2009. Review of the Feasibility of Recycling Phosphates at Sewage Treatment Plants in The UK - Executive Summary. Department for Environment, Food and Rural Affairs, 32 pp.

Adam, C., Peplinski, B., Michaelis, M., Kley, G., Simon, F.G., 2009. Thermochemical treatment of sewage sludge ashes for phosphorus recovery. Waste Management 29 (3), 1122–1128.

Ahoranta, S.H., Kokko, M.E., Papirio, S., Özkaya, B. and Puhakka, J.A. (2016) Arsenic removal from acidic solutions with biogenic ferric precipitates. Journal of hazardous materials 306, 124-132.

Akar, S.T., Tosun, I., Ozcan, A. and Gedikbey, T. (2010) Phosphate removal potential of the adsorbent material prepared from thermal decomposition of alunite ore–KCl mixture in environmental cleanup. Desalination 260(1), 107-113.

Al Mahrouqi, D., Vinogradov, J. and Jackson, M.D. (2017) Zeta potential of artificial and natural calcite in aqueous solution. Advances in Colloid and Interface Science 240, 60-76.

Altomare, C., Norvell, W.A., Bjorkman, T., Harman, G.E., 1999. Solubilization of phosphates and micronutrients by the plant-growth-promoting and biocontrol fungus Trichoderma harzianum Rifai 1295-22. Applied and Environmental Microbiology 65 (7), 2926–2933.

Anderson, D.M., Glibert, P.M. and Burkholder, J.M. (2002) Harmful algal blooms and eutrophication: Nutrient sources, composition, and consequences. Estuaries 25(4), 704-726.

Antelo, J., Arce, F. and Fiol, S. (2015) Arsenate and phosphate adsorption on ferrihydrite nanoparticles. Synergetic interaction with calcium ions. Chemical Geology 410, 53-62.

Antelo, J., Arce, F., Avena, M., Fiol, S., López, R. and Macías, F. (2007) Adsorption of a soil humic acid at the surface of goethite and its competitive interaction with phosphate. Geoderma 138(1), 12-19.

Antelo, J., Avena, M., Fiol, S., López, R. and Arce, F. (2005) Effects of pH and ionic strength on the adsorption of phosphate and arsenate at the goethite–water interface. Journal of Colloid and Interface Science 285(2), 476-486.

Arai, Y., Sparks, D.L., 2001. ATR-FTIR Spectroscopic Investigation on Phosphate Adsorption Mechanisms at the Ferrihydrite-Water Interface. Journal of Colloid and Interface Science 241 (2), 317–326.

Aryal, M. and Liakopoulou-Kyriakides, M. (2011) Equilibrium, kinetics and thermodynamic studies on phosphate biosorption from aqueous solutions by Fe(III)-treated Staphylococus xylosus biomass: Common ion effect. Colloids and Surfaces A: Physicochemical and Engineering Aspects 387(1), 43-49.

Ashekuzzaman, S.M. and Jiang, J.-Q. (2017) Improving the Removal of Phosphate in Secondary Effluent of Domestic Wastewater Treatment Plant.

Ashley, K., Cordell, D. and Mavinic, D. (2011) A brief history of phosphorus: from the philosopher's stone to nutrient recovery and reuse. Chemosphere 84(6), 737-746.

Atienza–Martínez, M., Gea, G., Arauzo, J., Kersten, S.R.A., Kootstra, A.M.J., 2014. Phosphorus recovery from sewage sludge char ash. Biomass and Bioenergy 65, 42–50.

Atkinson, K. (1989) An Introduction to Numerical Analysis, Wiley.

Aubain, P., Gazzo, A., Le Mous, J., Mugnier, E., Brunet, H., Landrea, B., 2002. Disposal and Recycling Routes for Sewage Sludge February. European Commission, 1-25.

Awual, M.R., Jyo, A., Ihara, T., Seko, N., Tamada, M. and Lim, K.T. (2011) Enhanced trace phosphate removal from water by zirconium(IV) loaded fibrous adsorbent. Water Research 45(15), 4592-4600.

Awual, M.R., Shenashen, M.A., Jyo, A., Shiwaku, H. and Yaita, T. (2014) Preparing of novel fibrous ligand exchange adsorbent for rapid column-mode trace phosphate removal from water. Journal of Industrial and Engineering Chemistry 20(5), 2840-2847.

B., P.A., S., H.T., R., R.B. and M., R.B. (2008) Structure and dynamics of phosphate ion in aqueous solution: An ab initio QMCF MD study. Journal of Computational Chemistry 29(14), 2330-2334.

Bache, B.W., 1964. Aluminum And Iron Phosphate Studies Relating To Soils. Journal of Soil Science 15 (1), 110–116.

Bai, Y., Yang, T., Liang, J. and Qu, J. (2016) The role of biogenic Fe-Mn oxides formed in situ for arsenic oxidation and adsorption in aquatic ecosystems. Water Research 98, 119-127.

Barrett, E.P., Joyner, L.G. and Halenda, P.P. (1951) The Determination of Pore Volume and Area Distributions in Porous Substances. I. Computations from Nitrogen Isotherms. Journal of the American Chemical Society 73(1), 373-380.

Barrón, V. and Torrent, J. (1996) Surface Hydroxyl Configuration of Various Crystal Faces of Hematite and Goethite. Journal of Colloid and Interface Science 177(2), 407-410.

Barron, V., Herruzo, M., Torrent, J., 1988. Phosphate Adsorption by Aluminous Hematites of Different Shapes. Soil Science Society of America Journal 52 (3), 647.

Beck, R.E. and Schultz, J.S. (1972) Hindrance of solute diffusion within membranes as measured with microporous membranes of known pore geometry. Biochimica et Biophysica Acta (BBA)-Biomembranes 255(1), 273-303.

Beecher, N., Harrison, E., 2005. Risk perception, risk communication, and stakeholder involvement for biosolids management and research. Journal of łdots, 122–128.

Benjamin, M.M. (2010) Water Chemistry, Waveland Press, Incorporated.

Biber, M.V., dos Santos, A.M., Stumm, W., 1994. The coordination chemistry of weathering: IV. Inhibition of the dissolution of oxide minerals. Geochimica et Cosmochimica Acta 58 (9), 1999–2010.

Biswas, B.K., Inoue, K., Harada, H., Ohto, K., Kawakita, H., 2009. Leaching of phosphorus from incinerated sewage sludge ash by means of acid extraction followed by adsorption on orange waste gel. Journal of Environmental Sciences 21 (12), 1753–1760.

Blackall, L.L., Crocetti, G.R., Saunders, A.M. and Bond, P.L. (2002) A review and update of the microbiology of enhanced biological phosphorus removal in wastewater treatment plants. Antonie van Leeuwenhoek 81(1), 681-691.

Blaney, L.M., Cinar, S., SenGupta, A.K., 2007. Hybrid anion exchanger for trace phosphate removal from water and wastewater. Water research 41 (7), 1603–1613.

Boelee, N.C. (2013) Microalgal biofilms for wastewater treatment.

Boelee, N.C., Temmink, H., Janssen, M., Buisman, C.J.N. and Wijffels, R.H. (2011) Nitrogen and phosphorus removal from municipal wastewater effluent using microalgal biofilms. Water Research 45(18), 5925-5933.

Boels, L., Keesman, K.J. and Witkamp, G.J. (2012) Adsorption of phosphonate antiscalant from reverse osmosis membrane concentrate onto granular ferric hydroxide. Environ Sci Technol 46(17), 9638-9645.

Böhnke, B., Diering, B., Zuckut, S.W., 1997. Cost-effective wastewater treatment process for removal of organics and nutrients. Water Eng. Manag. 144 (7), 18–21.

Bolan, N.S., Robson, A.D., Barrow, N.J., 1987. Effects of vesicular-arbuscular mycorrhiza on the availability of iron phosphates to plants. Plant Soil 99 (2-3), 401–410.

Bolton & Menk, I. (2016) Ultra-Low Phosphorus Removal Pilot Study: City of Mankato, Minnesota.

Bonneville, S., Behrends, T., van Cappellen, P., 2009. Solubility and dissimilatory reduction kinetics of iron(III) oxyhydroxides: A linear free energy relationship. Geochimica et Cosmochimica Acta 73 (18), 5273–5282.

Borch, T., Fendorf, S., 2007. Phosphate Interactions with Iron (Hydr)oxides: Mineralization Pathways and Phosphorus Retention upon Bioreduction, in: , Adsorption of Metals by Geomedia II: Variables, Mechanisms, and Model Applications, vol. 7. Developments in Earth and Environmental Sciences. Elsevier, pp. 321–348.

Borggaard, O. (2006) Influence of iron oxides on the surface area of soil.

Borggaard, O.K., 1983. Effect of Surface Area and Mineralogy of Iron Oxides on Their Surface Charge and Anion-Adsorption Properties. Clays and Clay Minerals 31 (3), 230–232.

Borggaard, O.K., Jorgensen, S.S., Moberg, J.P., Rabenlange, B., 1990. Influence of Organic Matter on Phosphate Adsorption by Aluminum and Iron Oxides in Sandy Soils. Journal of Soil Science 41 (3), 443–449.

Borggaard, O.K., Raben-Lange, B., Gimsing, A.L. and Strobel, B.W. (2005) Influence of humic substances on phosphate adsorption by aluminium and iron oxides. Geoderma 127(3), 270-279.

Boström, B., Andersen, J.M., Fleischer, S. and Jansson, M. (1988) Exchange of phosphorus across the sediment-water interface. Hydrobiologia 170(1), 229-244.

Brandt, R.C., Elliott, H.A., O'Connor, G.A., 2004. Water-Extractable Phosphorus in Biosolids: Implications for Land-Based Recycling. Water Environ Res 76 (2), 121–129.

Buhmann, A. and Papenbrock, J. (2013) Biofiltering of aquaculture effluents by halophytic plants: Basic principles, current uses and future perspectives. Environmental and Experimental Botany 92, 122-133.

Cabrera, F., Arambarri, P.d., Madrid, L., Toga, C.G., 1981. Desorption of phosphate from iron oxides in relation to equilibrium pH and porosity. Geoderma 26 (3), 203–216.

CanadianWaterNetwork (2018) Canada's Challenges and Opportunities to Address Contaminants in Wastewater; Supporting Document 2: Wastewater Treatment Practice and Regulations in Canada and Other Jurisdictions.

Canfield, D.E., 1989. Reactive iron in marine sediments. Geochimica et Cosmochimica Acta 53 (3), 619–632.

Caraco, N.F., Cole, J.J., Likens, G.E., 1989. Evidence for sulphate-controlled phosphate release from sediments of aquatic systems. Nature (341), 316–318.

Cardoso, I., Kuyper, T., 2006. Mycorrhizas and tropical soil fertility. Agriculture, Ecosystems & Environment 116 (1-2), 72–84.

Carliell-Marquet, C., 2014. Sustainable Phosphorus Summit.

Carliell-Marquet, C., Cooper, J., 2014. Towards closed-loop phosphorus management for the UK Water Industry, in: Sustainable Phosphorus Summit.

Carliell-Marquet, C., Oikonomidis, I., Wheatley, A., Smith, J., 2009. Inorganic profiles of chemical phosphorus removal sludge. Proceedings of the ICE - Water Management 163 (2), 65–77.

Carpenter, S.R., Caraco, N.F., Correll, D.L., Howarth, R.W., Sharpley, A.N. and Smith, V.H. (1998) Nonpoint pollution of surface waters with phosphorus and nitrogen. Ecological Applications 8(3), 559-568.

Carvalho, L., McDonald, C., Hoyos, C., Mischke, U., Phillips, G., Borics, G., Poikane, S., Skjelbred, B., Solheim Anne, L., Wichelen, J. and Cardoso Ana, C. (2013) Sustaining recreational quality of European lakes: minimizing the health risks from algal blooms through phosphorus control. Journal of Applied Ecology 50(2), 315-323.

Catrouillet, C., Davranche, M., Dia, A., Bouhnik-Le Coz, M., Marsac, R., Pourret, O., Gruau, G., 2014. Geochemical modeling of Fe(II) binding to humic and fulvic acids. Chemical Geology 372, 109–118.

Çeçen, F. and Aktaş, Ö. (2011) Activated Carbon for Water and Wastewater Treatment, pp. 265-318, Wiley-VCH Verlag GmbH & Co. KGaA.

Chacon, N., Silver, W.L., Dubinsky, E.A., Cusack, D.F., 2006. Iron Reduction and Soil Phosphorus Solubilization in Humid Tropical Forests Soils: The Roles of Labile Carbon Pools and an Electron Shuttle Compound. Biogeochemistry 78 (1), 67–84.

Charles, W., Cord-Ruwisch, R., Ho, G., Costa, M., Spencer, P., 2006. Solutions to a combined problem of excessive hydrogen sulfide in biogas and struvite scaling. Water Science & Technology 53 (6), 203.

Chen, N., Feng, C., Zhang, Z., Liu, R., Gao, Y., Li, M. and Sugiura, N. (2012) Preparation and characterization of lanthanum(III) loaded granular ceramic for phosphorus adsorption from aqueous solution. Journal of the Taiwan Institute of Chemical Engineers 43(5), 783-789.

Chen, Y., Cheng, J.J., Creamer, K.S., 2008. Inhibition of anaerobic digestion process: A review. Bioresour. Technol. 99 (10), 4044–4064.

Cheng, X., Chen, B., Cui, Y., Sun, D., Wang, X., 2015. Iron(III) reduction-induced phosphate precipitation during anaerobic digestion of waste activated sludge. Separation and Purification Technology 143, 6–11.

Chitrakar, R., Tezuka, S., Sonoda, A., Sakane, K., Ooi, K. and Hirotsu, T. (2006) Phosphate adsorption on synthetic goethite and akaganeite. Journal of Colloid and Interface Science 298(2), 602-608.

Chubar, N.I., Kanibolotskyy, V.A., Strelko, V.V., Gallios, G.G., Samanidou, V.F., Shaposhnikova, T.O., Milgrandt, V.G. and Zhuravlev, I.Z. (2005) Adsorption of phosphate ions on novel inorganic ion exchangers. Colloids and Surfaces A: Physicochemical and Engineering Aspects 255(1), 55-63.

Chunming Su and Suarez, D.L. (1997) In situ infrared speciation of adsorbed carbonate on aluminum and iron oxides. Clays and Clay Minerals 45(6), 814-825.

Clark, T., Stephenson, T. and Pearce, P.A. (1997) Phosphorus removal by chemical precipitation in a biological aerated filter. Water Research 31(10), 2557-2563.

Clarke, B.O., Smith, S.R., 2011. Review of 'emerging' organic contaminants in biosolids and assessment of international research priorities for the agricultural use of biosolids. Environment International 37 (1), 226–247.

Clesceri, L.S., Greenberg, A. E., & Eaton, A. D. (1998) Standard Methods for the Examination of Water and Wastewater. 20th edn. , Amer Public Health Assn.

Colombo, C., Barron, V., Torrent, J., 1994. Phosphate adsorption and desorption in relation to morphology and crystal properties of synthetic hematites. Geochimica et Cosmochimica Acta 58 (4), 1261–1269.

Conley, D.J., Paerl, H.W., Howarth, R.W., Boesch, D.F., Seitzinger, S.P., Havens, K.E., Lancelot, C., Likens, G.E., 2009. Ecology. Controlling eutrophication: nitrogen and phosphorus. Science 323 (5917), 1014–1015.

Connor, P.A. and McQuillan, A.J. (1999) Phosphate Adsorption onto TiO2 from Aqueous Solutions: An in Situ Internal Reflection Infrared Spectroscopic Study. Langmuir 15(8), 2916-2921.

Cooper, J., Lombardi, R., Boardman, D., Carliell-Marquet, C., 2011. The future distribution and production of global phosphate rock reserves. Resources, Conservation and Recycling 57 (January), 78–86.

Cordell, D., Drangert, J.-O. and White, S. (2009) The story of phosphorus: Global food security and food for thought. Global Environmental Change 19(2), 292-305.

Corma, A., Fornés, V., Martín-Aranda, R.M., García, H. and Primo, J. (1990) Zeolites as base catalysts: Condensation of aldehydes with derivatives of malonic esters. Applied Catalysis 59(1), 237-248.

Cornel, P., Jardin, N., Schaum, C., 2004. Möglichkeiten einer Rückgewinnung von Phosphor aus Klärschlammasche: Teil 1: Ergebnisse von Laborversuchen zur Extraktion von Phosphor. GWF Wasser 145 (9), 627–632.

Cornel, P., Schaum, C., 2009. Phosphorus recovery from wastewater: needs, technologies and costs. Water Science & Technology 59 (6), 1069–1076.

Cornell, R.M. and Schwertmann, U. (2004) The Iron Oxides, Wiley-VCH Verlag GmbH & Co. KGaA.

Cornell, R.M. and Schwertmann, U. (2006) The Iron Oxides: Structure, Properties, Reactions, Occurrences and Uses, Wiley.

Cornell, R.M., Schwertmann, U., 2003. The iron oxides: Structure, properties, reactions, occurrences, and uses, 2nd ed. Wiley-VCH, Weinheim.

Correll, D.L. (1999) Phosphorus: a rate limiting nutrient in surface waters. Poult Sci 78(5), 674-682.

Cracknell, R.F., Gubbins, K.E., Maddox, M. and Nicholson, D. (1995) Modeling Fluid Behavior in Well-Characterized Porous Materials. Accounts of Chemical Research 28(7), 281-288.

Cullen, N., Baur, R., Schauer, P., 2013. Three years of operation of North America's first nutrient recovery facility. Water Science & Technology 68 (4), 763–768.

Cumbal, L. and SenGupta, A.K. (2005) Arsenic Removal Using Polymer-Supported Hydrated Iron(III) Oxide Nanoparticles: Role of Donnan Membrane Effect. Environmental Science & Technology 39(17), 6508-6515.

Dakora, F.D., Phillips, D.A., 2002. Root exudates as mediators of mineral acquisition in low-nutrient environments. Plant Soil 245 (1), 35–47.

Daou, T.J., Begin-Colin, S., Grenèche, J.M., Thomas, F., Derory, A., Bernhardt, P., Legaré, P. and Pourroy, G. (2007) Phosphate Adsorption Properties of Magnetite-Based Nanoparticles. Chemistry of Materials 19(18), 4494-4505.

Davis, J.A., Hayes, K.F. (Eds.), 1987. Geochemical Processes at Mineral Surfaces. ACS symposium series. American Chemical Society, Washington D.C.

De Ridder, M., De Jong, S., Polchar, J., Lingemann, S., 2012. Risks and opportunities in the global phosphate rock market: Robust strategies in times of uncertainty. Rapport / Centre for Strategic Studies no. 17 | 12 | 12. The Hague Centre for Strategic Studies, Den Haag.

de Vet, W.W.J.M., Dinkla, I.J.T., Rietveld, L.C. and van Loosdrecht, M.C.M. (2011) Biological iron oxidation by Gallionella spp. in drinking water production under fully aerated conditions. Water Research 45(17), 5389-5398.

de Vet, W.W.J.M., van Loosdrecht, M.C.M. and Rietveld, L.C. (2012) Phosphorus limitation in nitrifying groundwater filters. Water Research 46(4), 1061-1069.

de Vree, J.H. (2016) Outdoor production of microalgae, Wageningen University.

De-Bashan, L.E., Bashan, Y., 2004. Recent advances in removing phosphorus from wastewater and its future use as fertilizer (1997-2003). Water research 38 (19), 4222–4246.

Deliyanni, E.A., Peleka, E.N. and Lazaridis, N.K. (2007) Comparative study of phosphates removal from aqueous solutions by nanocrystalline akaganéite and hybrid surfactant-akaganéite. Separation and Purification Technology 52(3), 478-486.

Deng, D., Kim, B.-S., Gopiraman, M. and Kim, I.S. (2015) Needle-like MnO2/activated carbon nanocomposites derived from human hair as versatile electrode materials for supercapacitors. RSC Advances 5(99), 81492-81498.

Desmidt, E., Ghyselbrecht, K., Zhang, Y., Pinoy, L., Van der Bruggen, B., Verstraete, W., Rabaey, K., Meesschaert, B., 2015. Global Phosphorus Scarcity and Full-Scale P-Recovery Techniques: A Review. Critical Reviews in Environmental Science and Technology 45 (4), 336–384.

Diaz, I., Barron, V., Del Campillo, M. C., Torrent, J., 2009. Vivianite (ferrous phosphate) alleviates iron chlorosis in grapevine. VITIS 48 (3), 107–113.

Dierberg, F.E., DeBusk, T.A., Jackson, S.D., Chimney, M.J. and Pietro, K. (2002) Submerged aquatic vegetation-based treatment wetlands for removing phosphorus from agricultural runoff: response to hydraulic and nutrient loading. Water Research 36(6), 1409-1422.

Dodds, W.K. and Whiles, M.R. (2010) Freshwater Ecology (Second Edition), pp. 469-507, Academic Press, London.

Dodds, W.K., Bouska, W.W., Eitzmann, J.L., Pilger, T.J., Pitts, K.L., Riley, A.J., Schloesser, J.T. and Thornbrugh, D.J. (2009) Eutrophication of U.S. Freshwaters: Analysis of Potential Economic Damages. Environmental Science & Technology 43(1), 12-19.

Donatello, S., Cheeseman, C.R., 2013. Recycling and recovery routes for incinerated sewage sludge ash (ISSA): a review. Waste Management 33 (11), 2328–2340.

Dong, S., Wang, Y., Zhao, Y., Zhou, X. and Zheng, H. (2017) La3+/La(OH)3 loaded magnetic cationic hydrogel composites for phosphate removal: Effect of lanthanum species and mechanistic study. Water Research 126, 433-441.

Drenkova-Tuhtan, A., Schneider, M., Franzreb, M., Meyer, C., Gellermann, C., Sextl, G., Mandel, K. and Steinmetz, H. (2017) Pilot-scale removal and recovery of dissolved phosphate from secondary wastewater effluents with reusable ZnFeZr adsorbent @ Fe3O4/SiO2 particles with magnetic harvesting. Water Research 109, 77-87.

DWA, 2005. Stand der Klarschlammbehandlung und Entsorgung in Deutschland, 66 pp.

Egle, L., Rechberger, H., Zessner, M., 2014. Endbericht Phosphorrückgewinnung aus dem Abwasser, Wien, 323 pp.

Elliott, H.A., O'Connor, G.A., 2007. Phosphorus management for sustainable biosolids recycling in the United States. Soil Biology and Biochemistry 39 (6), 1318–1327.

Elzinga, E.J., Sparks, D.L., 2007. Phosphate adsorption onto hematite: an in situ ATR-FTIR investigation of the effects of pH and loading level on the mode of phosphate surface complexation. Journal of Colloid and Interface Science 308 (1), 53–70.

Emerson D, V.W.d. (2015) The Role of FeOB in Engineered Water Ecosystems: A Review. Journal - American Water Works Association.

Erickson, A., Gulliver, J. and T. Weiss, P. (2007) Enhanced Sand Filtration for Storm Water Phosphorus Removal.

Eriksson, J., 2001. Concentrations of 61 trace elements in sewage sludge, farmyard manure, mineral fertiliser, precipitation and in oil and crops. Swedish Environmental Protection Agency Stockholm, Sweden.

Esvelt, L., Esvelt, M., Walker, B. and Hendron, L. (2010) Pilot Studies for Reducing RPWRF Effluent TP for Discharge to the Spokane River. Proceedings of the Water Environment Federation 2010(16), 937-947.

EuropeanCommission (2017) 9th Technical assessment on UWWTD implementation.

Eynard, A., Campillo, M.C., Barron, V., Torrent, J., 1992. Use of vivianite (Fe3(PO4)2.8H2O) to prevent iron chlorosis in calcareous soils. Fertilizer Research 31 (1), 61–67.

Fang, L., Huang, L., Holm, P.E., Yang, X., Hansen, H.C.B. and Wang, D. (2015) Facile upscaled synthesis of layered iron oxide nanosheets and their application in phosphate removal. Journal of Materials Chemistry A 3(14), 7505-7512.

Fang, L., Shi, Q., Nguyen, J., Wu, B., Wang, Z. and Lo, I.M.C. (2017a) Removal Mechanisms of Phosphate by Lanthanum Hydroxide Nanorods: Investigations using EXAFS, ATR-FTIR, DFT, and Surface Complexation Modeling Approaches. Environmental Science & Technology 51(21), 12377-12384.

Fang, L., Wu, B. and Lo, I.M.C. (2017b) Fabrication of silica-free superparamagnetic ZrO2@Fe3O4 with enhanced phosphate recovery from sewage: Performance and adsorption mechanism. Chemical Engineering Journal 319, 258-267.

Fischer, F., Bastian, C., Happe, M., Mabillard, E., Schmidt, N., 2011. Microbial fuel cell enables phosphate recovery from digested sewage sludge as struvite. Bioresour. Technol. 102 (10), 5824–5830.

Fischer, F., Zufferey, G., Sugnaux, M., Happe, M., 2015. Microbial electrolysis cell accelerates phosphate remobilisation from iron phosphate contained in sewage sludge. Environmental science: Processes & impacts 17 (1), 90–97.

Foo, K.Y. and Hameed, B.H. (2010) Insights into the modeling of adsorption isotherm systems. Chemical Engineering Journal 156(1), 2-10.

Fortin, D. and Langley, S. (2005) Formation and occurrence of biogenic iron-rich minerals. Earth-Science Reviews 72(1), 1-19.

Freundlich, H. (1907) Über die adsorption in lösungen. Zeitschrift für physikalische Chemie 57(1), 385-470.

Frimmel, F., 1999. Basic characterization of reference NOM from Central Europe - Similarities and differences. Environment International 25 (2-3), 191–207.

Froelich Philip, N. (1988) Kinetic control of dissolved phosphate in natural rivers and estuaries: A primer on the phosphate buffer mechanism1. Limnology and Oceanography 33(4part2), 649-668.

Frossard, E., Bauer, J.P., Lothe, F., 1997. Evidence of vivianite in FeSO4-flocculated sludges. Water research 31 (10), 2449–2454.

Fu, Z., Wu, F., Song, K., Lin, Y., Bai, Y., Zhu, Y., Giesy, J.P., 2013. Competitive interaction between soil-derived humic acid and phosphate on goethite. Applied Geochemistry 36, 125–131.

Gahoonia, T.S., Claassen, N., Jungk, A., 1992. Mobilization of phosphate in different soils by ryegrass supplied with ammonium or nitrate. Plant Soil 140 (2), 241–248.

Gálvez, N., 1999. Effect of Phosphate on the Crystallization of Hematite, Goethite, and Lepidocrocite from Ferrihydrite. Clays and Clay Minerals 47 (3), 304–311.

García-Mateos, F.J., Ruiz-Rosas, R., Marqués, M.D., Cotoruelo, L.M., Rodríguez-Mirasol, J. and Cordero, T. (2015) Removal of paracetamol on biomass-derived activated carbon: Modeling the fixed bed breakthrough curves using batch adsorption experiments. Chemical Engineering Journal 279, 18-30.

Gardner, W.K., Barber, D.A., Parbery, D.G., 1983. The acquisition of phosphorus by Lupinus albus L. Plant Soil 70 (1), 107–124.

Ge, H., Zhang, L., Batstone, D.J., Keller, J., Yuan, Z., 2013. Impact of Iron Salt Dosage to Sewers on Downstream Anaerobic Sludge Digesters: Sulfide Control and Methane Production. J. Environ. Eng. 139 (4), 594–601.

Ge, X., Song, X., Ma, Y., Zhou, H., Wang, G., Zhang, H., Zhang, Y., Zhao, H. and Wong, P.K. (2016) Fabrication of hierarchical iron-containing MnO2 hollow microspheres assembled by thickness-tunable nanosheets for efficient phosphate removal. Journal of Materials Chemistry A 4(38), 14814-14826.

Geelhoed, J.S., van Riemsdijk, W., Findenegg, G.R., 1999. Simulation of the effect of citrate exudation from roots on the plant availability of phosphate adsorbed on goethite. Eur J Soil Science 50 (3), 379–390.

Genz, A., Kornmüller, A. and Jekel, M. (2004) Advanced phosphorus removal from membrane filtrates by adsorption on activated aluminium oxide and granulated ferric hydroxide. Water Research 38(16), 3523-3530.

Geraarts, B., Koetse, E., Loeffen, P., Reitsma, B., Gaillard, A., 2007. Fosfaatterugwinning uit ijzerarm slib van rioolwaterzuiveringsinrichtingen. STOWA, 83 pp. http://www.stowa.nl/Upload/publicaties2/mID_4924_cID_3914_74684671_STOWA 2007 31.pdf.

Gerdes, P. and Kunst, S. (1998) Bioavailability of phosphorus as a tool for efficient P reduction schemes. Water Science and Technology 37(3), 241-247.

Gerke, J. (2010) Humic (Organic Matter)-Al(Fe)-Phosphate Complexes: An Underestimated Phosphate Form in Soils and Source of Plant-Available Phosphate. 175(9), 417-425.

Gerke, J., 1993. Phosphate adsorption by humic/Fe-oxide mixtures aged at pH 4 and 7 and by poorly ordered Fe-oxide. Geoderma 59 (1-4), 279–288.

Gerke, J., Hermann, R., 1992. Adsorption of Orthophosphate to Humic-Fe-Complexes and to Amorphous Fe-Oxide. Zeitschrift für Pflanzenernährung und Bodenkunde 155 (3), 233–236.

Gerke, J., Römer, W., Beissner, L., 2000. The quantitative effect of chemical phosphate mobilization by carboxylate anions on P uptake by a single root. II. The importance of soil and plant parameters for uptake of mobilized P. J. Plant Nutr. Soil Sci. 163 (2), 213–219.

Ghassemi, M., Recht, H.L., 1971. Phosphate Precipitation with Ferrous Iron. Water Pollution Control Research Series, 64 pp.

Gil, R.R., Ruiz, B., Lozano, M.S., Martín, M.J. and Fuente, E. (2014) VOCs removal by adsorption onto activated carbons from biocollagenic wastes of vegetable tanning. Chemical Engineering Journal 245, 80-88.

Goldberg, S., Sposito, G., 1985. On the mechanism of specific phosphate adsorption by hydroxylated mineral surfaces: A review. Communications in Soil Science and Plant Analysis 16 (8), 801–821.

Greenberg, S.A., Chang, T.N. and Anderson, E. (1960) INVESTIGATION OF COLLOIDAL HYDRATED CALCIUM SILICATES. I. SOLUBILITY PRODUCTS. The Journal of Physical Chemistry 64(9), 1151-1157.

Gu, A.Z., Saunders, A., Neethling, J.B., Stensel, H.D. and Blackall, L.L. (2008) Functionally relevant microorganisms to enhanced biological phosphorus removal performance at full-scale wastewater treatment plants in the United States. Water Environ Res 80(8), 688-698.

Gu, W., Li, X., Xing, M., Fang, W. and Wu, D. (2018) Removal of phosphate from water by amine-functionalized copper ferrite chelated with La(III). Science of The Total Environment 619-620, 42-48.

Gutierrez, O., Park, D., Sharma, K.R., Yuan, Z., 2010. Iron salts dosage for sulfide control in sewers induces chemical phosphorus removal during wastewater treatment. Water research 44 (11), 3467–3475.

Guzmán, G., Alcantara, E., Barrón, V. and Torrent, J. (1994) Phytoavailability of phosphate adsorbed on ferrihydrite, hematite, and goethite. Plant and soil 159, 219-225.

Haghseresht, F., Wang, S. and Do, D.D. (2009) A novel lanthanum-modified bentonite, Phoslock, for phosphate removal from wastewaters. Applied Clay Science 46(4), 369-375.

Han, C., Lalley, J., Iyanna, N. and Nadagouda, M.N. (2017) Removal of phosphate using calcium and magnesium-modified iron-based adsorbents. Materials Chemistry and Physics 198, 115-124.

Harder, E.C. (1919) Iron-depositing Bacteria and Their Geologic Relations, U.S. Government Printing Office.

Hashimoto, H., Yokoyama, S., Asaoka, H., Kusano, Y., Ikeda, Y., Seno, M., Takada, J., Fujii, T., Nakanishi, M. and Murakami, R. (2007) Characteristics of hollow microtubes consisting of amorphous iron oxide nanoparticles produced by iron oxidizing bacteria, Leptothrix ochracea. Journal of Magnetism and Magnetic Materials 310(2, Part 3), 2405-2407.

He, Y., Lin, H., Dong, Y. and Wang, L. (2017) Preferable adsorption of phosphate using lanthanum-incorporated porous zeolite: Characteristics and mechanism. Applied Surface Science 426, 995-1004.

He, Y., Lin, H., Dong, Y., Liu, Q. and Wang, L. (2016) Simultaneous removal of ammonium and phosphate by alkaline-activated and lanthanum-impregnated zeolite. Chemosphere 164, 387-395.

Heiberg, L., Koch, C.B.K.C., J. Henning S., Hansen, H. B. C., 2012. Vivianite precipitation and phosphate sorption following iron reduction in anoxic soils. J. Environ. Qual. 41 (3), 938–949.

Heim, C., Simon, K., Ionescu, D., Reimer, A., De Beer, D., Quéric, N.-V., Reitner, J. and Thiel, V. (2015) Assessing the utility of trace and rare earth elements as biosignatures in microbial iron oxyhydroxides. 3(6).

Hermann, L., 2009. Rückgewinnung von Phosphor aus der Abwasserreinigung. Eine Bestandsaufnahme. Umwelt Wissen 0929, 196 pp.

Hermann, L., 2014. A review of innovations in mineral fertilizer production, in: 16th World Fertilizer Congress of CIEC, pp. 105–108.

Herrmann, H., Nolde, J., Berger, S. and Heise, S. (2016) Aquatic ecotoxicity of lanthanum – A review and an attempt to derive water and sediment quality criteria. Ecotoxicol Environ Saf 124, 213-238.

Hey, M.J., Hilton, A.M. and Bee, R.D. (1994) The formation and growth of carbon dioxide gas bubbles from supersaturated aqueous solutions. Food Chemistry 51(4), 349-357.

Higgins, M.J., Murthy, S., 2006. Understanding factors affecting polymer demand for thickening and dewatering. Water Environment Research Foundation; IWA Publishing, Alexandria, Va, London.

Hinsinger, P., 2001. Bioavailability of soil inorganic P in the rhizosphere as affected by root-induced chemical changes: a review. Plant Soil 237 (2), 173–195.

Ho, Y.S. and McKay, G. (1999) Pseudo-second order model for sorption processes. Process Biochemistry 34(5), 451-465.

Hoagland, P., Anderson, D.M., Kaoru, Y. and White, A.W. (2002) The economic effects of harmful algal blooms in the United States: Estimates, assessment issues, and information needs. Estuaries 25(4), 819-837.

Hongshao, Z. and Stanforth, R. (2001) Competitive Adsorption of Phosphate and Arsenate on Goethite. Environmental Science & Technology 35(24), 4753-4757.

Huang, W., Yu, X., Tang, J., Zhu, Y., Zhang, Y. and Li, D. (2015) Enhanced adsorption of phosphate by flower-like mesoporous silica spheres loaded with lanthanum. Microporous and Mesoporous Materials 217, 225-232.

Huang, W., Zhu, Y., Tang, J., Yu, X., Wang, X., Li, D. and Zhang, Y. (2014) Lanthanum-doped ordered mesoporous hollow silica spheres as novel adsorbents for efficient phosphate removal. Journal of Materials Chemistry A 2(23), 8839-8848.

Huang, W.-Y., Li, D., Liu, Z.-Q., Tao, Q., Zhu, Y., Yang, J. and Zhang, Y.-M. (2014) Kinetics, isotherm, thermodynamic, and adsorption mechanism studies of La(OH)3-modified exfoliated vermiculites as highly efficient phosphate adsorbents. Chemical Engineering Journal 236, 191-201.

Huang, X.L., Shenker, M., 2004. Water-Soluble and Solid-State Speciation of Phosphorus in Stabilized Sewage Sludge. Journal of Environment Quality 33 (5), 1895.

Huang, Y., Yang, J.-K. and Keller, A.A. (2014) Removal of Arsenic and Phosphate from Aqueous Solution by Metal (Hydr-)oxide Coated Sand. ACS Sustainable Chemistry & Engineering 2(5), 1128-1138.

Hupfer, M. and Lewandowski, J. (2008) Oxygen Controls the Phosphorus Release from Lake Sediments – a Long-Lasting Paradigm in Limnology. International Review of Hydrobiology 93(4-5), 415-432.

Hvitved-Jacobsen, T., Vollertsen, J., Nielsen, A.H., 2013. Sewer processes: Microbial and chemical process engineering of sewer networks, 2nd ed. ed. CRC Press, Boca Raton.

Ingrid Chorus, I.R.F.H.J.S.J.B. (2000) HEALTH RISKS CAUSED BY FRESHWATER CYANOBACTERIA IN RECREATIONAL WATERS. Journal of Toxicology and Environmental Health, Part B 3(4), 323-347.

Ismail, Z.Z. (2012) Kinetic study for phosphate removal from water by recycled date-palm wastes as agricultural by-products. International Journal of Environmental Studies 69(1), 135-149.

Ito, A., Umita, T., Aizawa, J., Takachi, T., Morinaga, K., 2000. Removal of heavy metals from anaerobically digested sewage sludge by a new chemical method using ferric sulfate. Water research 34 (3), 751–758.

J. Torrent, U.S., V. Barron (1992) Fast and slow phosphate sorption by goethite-rich natural materials. Clays and Clay Minerals 40(1), 14-21.

Jan Oleszkiewicz, D.K., Tanner Devlin, Monireh Laksharizadeh, Qiuyan Yuan (2015) Options for Improved Nutrient Removal and Recovery from Municipal Wastewater in the Canadian Context

Jarvie, H.P., Neal, C. and Withers, P.J.A. (2006) Sewage-effluent phosphorus: A greater risk to river eutrophication than agricultural phosphorus? Science of The Total Environment 360(1), 246-253.

Jetten, M., Horn, S., van Loosdrecht, M.C.M., 1997. Towards a more sustainable municipal wastewater treatment system. Water Science & Technology 35 (9), 171–180.

Jiang, D., Amano, Y. and Machida, M. (2017) Removal and recovery of phosphate from water by a magnetic Fe3O4@ASC adsorbent. Journal of Environmental Chemical Engineering 5(5), 4229-4238.

Jiang, J.-Q. and Graham, N.J. (1998) Pre-polymerised inorganic coagulants and phosphorus removal by coagulation- a review. Water Sa 24(3), 237-244.

Johir, M.A.H., Pradhan, M., Loganathan, P., Kandasamy, J. and Vigneswaran, S. (2016) Phosphate adsorption from wastewater using zirconium (IV) hydroxide: Kinetics, thermodynamics and membrane filtration adsorption hybrid system studies. Journal of Environmental Management 167, 167-174.

Jonasson, R.G., Ronald, M.R., Giuliacci, M.E., Tazaki, K., 1988. Surface reactions of goethite with phosphate. Journal of the Chemical Society, Faraday Transactions 1: Physical Chemistry in Condensed Phases 84 (7), 2311.

Ju, X., Hou, J., Tang, Y., Sun, Y., Zheng, S. and Xu, Z. (2016) ZrO2 nanoparticles confined in CMK-3 as highly effective sorbent for phosphate adsorption. Microporous and Mesoporous Materials 230, 188-195.

Jung, K.-W., Lee, S. and Lee, Y.J. (2017) Synthesis of novel magnesium ferrite (MgFe2O4)/biochar magnetic composites and its adsorption behavior for phosphate in aqueous solutions. Bioresource Technology 245, 751-759.

Kahiluoto, H., Kuisma, M., Ketoja, E., Salo, T., Heikkinen, J., 2015. Phosphorus in manure and sewage sludge more recyclable than in soluble inorganic fertiliser. in revision 49 (4), 2115–2122.

Kalaitzidou, K., Mitrakas, M., Raptopoulou, C., Tolkou, A., Palasantza, P.-A. and Zouboulis, A. (2016a) Pilot-Scale Phosphate Recovery from Secondary Wastewater Effluents. Environmental Processes 3(1), 5-22.

Kappler, A., Benz, M., Schink, B., Brune, A., 2004. Electron shuttling via humic acids in microbial iron(III) reduction in a freshwater sediment. FEMS Microbiology Ecology 47 (1), 85–92.

Karau, A., Benken, C., Thommes, J. and Kula, M.R. (1997) The influence of particle size distribution and operating conditions on the adsorption performance in fluidized beds. Biotechnol Bioeng 55(1), 54-64.

Karlsson, T., Persson, P., 2010. Coordination chemistry and hydrolysis of Fe(III) in a peat humic acid studied by X-ray absorption spectroscopy. Geochimica et Cosmochimica Acta 74 (1), 30–40.

Karlsson, T., Persson, P., 2012. Complexes with aquatic organic matter suppress hydrolysis and precipitation of Fe(III). Chemical Geology 322-323, 19–27.

Kartal, B., Kuenen, J.G., van Loosdrecht, M.C.M., 2010. Sewage Treatment with Anammox. Science 328 (5979), 702–703.

Karthikeyan, K.G., Tshabalala, M.A., Wang, D. and Kalbasi, M. (2004) Solution Chemistry Effects on Orthophosphate Adsorption by Cationized Solid Wood Residues. Environmental Science & Technology 38(3), 904-911.

Kato, F., Kitakoji, H., Oshita, K., Takaoka, M., Takeda, N., Matsumoto, T., 2006. Extraction efficiency of phosphate from pre-coagulated sludge with NaHS. Water Science & Technology 54 (5), 119.

Katsoyiannis, I.K., I.A. & Zouboulis, Anastasios & Ζουμπούλης, A.I. (2016) Use of Iron- and Manganese-Oxidizing Bacteria for the Combined Removal of Iron, Manganese and Arsenic from Contaminated Groundwater. Water Quality Research Journal of Canada. 41.

Keesman, K.J. (2011) System identification: an introduction, Springer Science & Business Media.

Kelessidis, A., Stasinakis, A.S., 2012. Comparative study of the methods used for treatment and final disposal of sewage sludge in European countries. Waste Management 32 (6), 1186–1195.

Khare, N., Martin, J.D., Hesterberg, D.L., 2007. Phosphate bonding configuration on ferrihydrite based on molecular orbital calculations and XANES fingerprinting. Geochimica et Cosmochimica Acta 71 (18), 4405–4415.

Kidd, P.S., Dominguez-Rodriguez, M.J., Diaz, J., Monterroso, C., 2007. Bioavailability and plant accumulation of heavy metals and phosphorus in agricultural soils amended by long-term application of sewage sludge. Chemosphere 66 (8), 1458–1467.

Kim, J., Deng, Q. and Benjamin, M.M. (2008) Simultaneous removal of phosphorus and foulants in a hybrid coagulation/membrane filtration system. Water Research 42(8), 2017-2024.

Kim, J., Li, W., Philips, B.L. and Grey, C.P. (2011) Phosphate adsorption on the iron oxyhydroxides goethite ([small alpha]-FeOOH), akaganeite ([small beta]-FeOOH), and lepidocrocite ([gamma]-FeOOH): a 31P NMR Study. Energy & Environmental Science 4(10), 4298-4305.

Kim, M., Kim, H. and Byeon, S.H. (2017) Layered Yttrium Hydroxide l-Y(OH)3 Luminescent Adsorbent for Detection and Recovery of Phosphate from Water over a Wide pH Range. ACS Appl Mater Interfaces 9(46), 40461-40470.

Kizito, S., Luo, H., Wu, S., Ajmal, Z., Lv, T. and Dong, R. (2017) Phosphate recovery from liquid fraction of anaerobic digestate using four slow pyrolyzed biochars: Dynamics of adsorption, desorption and regeneration. Journal of Environmental Management 201, 260-267.

Klencsár, Z. (1997) Mössbauer spectrum analysis by Evolution Algorithm. Nuclear Instruments and Methods in Physics Research Section B: Beam Interactions with Materials and Atoms 129(4), 527-533.

Klüpfel, L., Piepenbrock, A., Kappler, A., Sander, M., 2014. Humic substances as fully regenerable electron acceptors in recurrently anoxic environments. Nature Geosci 7 (3), 195–200.

Knowlton, K.F., Radcliffe, J.S., Novak, C.L. and Emmerson, D.A. (2004) Animal management to reduce phosphorus losses to the environment. J Anim Sci 82 E-Suppl, E173-195.

Ko, I., Kim, J.-Y. and Kim, K.-W. (2005) Adsorption properties of soil humic and fulvic acids by hematite. Chemical Speciation & Bioavailability 17(2), 41-48.

Kolbe, F., Weiss, H., Morgenstern, P., Wennrich, R., Lorenz, W., Schurk, K., Stanjek, H. and Daus, B. (2011) Sorption of aqueous antimony and arsenic species onto akaganeite. Journal of Colloid and Interface Science 357(2), 460-465.

Korving, L., 2012. Trends in slibontwatering. STOWA, 108 pp.

Krogstad, T., Sogn, T., Asdal, A.A., Smund, A., 2005. Influence of chemically and biologically stabilized sewage sludge on plant-available phosphorus in soil. Ecological Engineering 25 (1), 51–60.

Kumar, R.A., Velayudhan, K.T., Ramachandran, V., Bhai, R.S., Unnikrishnan, G. and Vasu, K. (2010) Adsorption and removal kinetics of phosphonate from water using natural adsorbents. Water Environ Res 82(1), 62-68.

Kunaschk, M., Schmalz, V., Dietrich, N., Dittmar, T. and Worch, E. (2015) Novel regeneration method for phosphate loaded granular ferric (hydr)oxide – A contribution to phosphorus recycling. Water Research 71, 219-226.

Kuroki, V., Bosco, G.E., Fadini, P.S., Mozeto, A.A., Cestari, A.R. and Carvalho, W.A. (2014) Use of a La(III)-modified bentonite for effective phosphate removal from aqueous media. Journal of Hazardous Materials 274, 124-131.

Kuzawa, K., Jung, Y.-J., Kiso, Y., Yamada, T., Nagai, M. and Lee, T.-G. (2006) Phosphate removal and recovery with a synthetic hydrotalcite as an adsorbent. Chemosphere 62(1), 45-52.

L. Correll, D. (1998) The Role of Phosphorus in the Eutrophication of Receiving Waters: A Review.

Lackner, S., Gilbert, E.M., Vlaeminck, S.E., Joss, A., Horn, H., van Loosdrecht, M.C.M., 2014. Full-scale partial nitritation/anammox experiences-an application survey. Water research 55, 292–303.

Lalley, J., Han, C., Li, X., Dionysiou, D.D. and Nadagouda, M.N. (2016) Phosphate adsorption using modified iron oxide-based sorbents in lake water: Kinetics, equilibrium, and column tests. Chemical Engineering Journal 284, 1386-1396.

Lalley, J., Han, C., Mohan, G.R., Dionysiou, D.D., Speth, T.F., Garland, J. and Nadagouda, M.N. (2015) Phosphate removal using modified Bayoxide[registered sign] E33 adsorption media. Environmental Science: Water Research & Technology 1(1), 96-107.

Landers, J., Gor, G.Y. and Neimark, A.V. (2013) Density functional theory methods for characterization of porous materials. Colloids and Surfaces A: Physicochemical and Engineering Aspects 437, 3-32.

Langenkamp, H., Part, P., Erhardt, W., Prüess, A., 2001. Organic contaminants in sewage sludge for agricultural use October 2001. European Commission, Joint Research Centre, Institute for Environment and Sustainability. http://www.eu.nl/environment/waste/sludge/presentations/11_pruess.pdf.

Langer, M., Vaananen, J., Boulestreau, M., Miehe, U., Bourdon, C. and Lesjean, B. (2017) Advanced phosphorus removal via coagulation, flocculation and microsieve filtration in tertiary treatment. Water Sci Technol 75(12), 2875-2882.

Langeveld, C.P., Wolde, K.W., 2013. Phosphate recycling in mineral fertiliser production, in: Proceedings International Fertiliser Society 717. International Fertiliser Society, UK, p. 24.

Langmuir, I. (1918) THE ADSORPTION OF GASES ON PLANE SURFACES OF GLASS, MICA AND PLATINUM. Journal of the American Chemical Society 40(9), 1361-1403.

Laridi, R., Auclair, J.C. and Benmoussa, H. (2005) Laboratory and Pilot-scale Phosphate and Ammonium Removal by Controlled Struvite Precipitation Following Coagulation and Flocculation of Swine Wastewater. Environ Technol 26(5), 525-536.

Larsen, O., Postma, D., 2001. Kinetics of reductive bulk dissolution of lepidocrocite, ferrihydrite, and goethite. Geochimica et Cosmochimica Acta 65 (9), 1367–1379.

Leckie, J., Stumm, W., 1970. Phosphate precipitation, in: Gloyna, E.F., Eckenfelder, W.W. (Eds.), Water Quality Improvement By Physical and Chemical Processes. University of Texas Press, Austin, pp. 237–249.

Lente, G., Magalhães, M. E. A., Fábián, I., 2000. Kinetics and Mechanism of Complex Formation Reactions in the Iron(III)−Phosphate Ion System at Large Iron(III) Excess. Formation of a Tetranuclear Complex. Inorganic Chemistry 39 (9), 1950–1954.

Leo, C.P., Chai, W.K., Mohammad, A.W., Qi, Y., Hoedley, A.F. and Chai, S.P. (2011) Phosphorus removal using nanofiltration membranes. Water Sci Technol 64(1), 199-205.

Levlin, E., Lowen, M., Stark, K., Hultman, B., 2002. Effects of phosphorus recovery requirements on Swedish sludge management. Water Science & Technology 46 (4-5), 435–440.

Li, J., 2005. Effects of Fe(III) on floc characteristics of activated sludge. J. Chem. Technol. Biotechnol. 80 (3), 313–319.

Li, L. and Stanforth, R. (2000) Distinguishing Adsorption and Surface Precipitation of Phosphate on Goethite (α-FeOOH). Journal of Colloid and Interface Science 230(1), 12-21.

Li, M., Liu, J., Xu, Y. and Qian, G. (2016) Phosphate adsorption on metal oxides and metal hydroxides: A comparative review. Environmental Reviews 24(3), 319-332.

Li, R., Wang, J.J., Zhou, B., Awasthi, M.K., Ali, A., Zhang, Z., Lahori, A.H. and Mahar, A. (2016) Recovery of phosphate from aqueous solution by magnesium oxide decorated magnetic biochar and its potential as phosphate-based fertilizer substitute. Bioresource Technology 215, 209-214.

Li, W.-W., Sheng, G.-P., Zeng, R., Liu, X.-W. and Yu, H.-Q. (2012) China's wastewater discharge standards in urbanization: Evolution, challenges and implications: Evolution, challenges and implications.

Liese, A. and Hilterhaus, L. (2013) Evaluation of immobilized enzymes for industrial applications. Chem Soc Rev 42(15), 6236-6249.

Likosova, E.M., Keller, J., Rozendal, R.A., Poussade, Y., Freguia, S., 2013. Understanding colloidal FeSx formation from iron phosphate precipitation sludge for optimal phosphorus recovery. Journal of Colloid and Interface Science 403, 16–21.

Lin, J., Zhan, Y., Wang, H., Chu, M., Wang, C., He, Y. and Wang, X. (2017) Effect of calcium ion on phosphate adsorption onto hydrous zirconium oxide. Chemical Engineering Journal 309, 118-129.

Liu, B., Li, A.M., Xia, M.F. and Zhu, Z.L. (2012) Preparation of manganese oxide supported on activated carbon and its application in catalytic ozonation of 4-chlorophenol, pp. 2285-2288, Trans Tech Publ.

Liu, J., Wan, L., Zhang, L. and Zhou, Q. (2011) Effect of pH, ionic strength, and temperature on the phosphate adsorption onto lanthanum-doped activated carbon fiber. Journal of Colloid and Interface Science 364(2), 490-496.

Liu, J., Zhou, Q., Chen, J., Zhang, L. and Chang, N. (2013) Phosphate adsorption on hydroxyl–iron–lanthanum doped activated carbon fiber. Chemical Engineering Journal 215–216, 859-867.

Liu, Y. (2005) Phosphorus flows in China - Physical profiles and environmental regulations; ISBN 90-8504-196-1

Liu, Y.-T. and Hesterberg, D. (2011) Phosphate Bonding on Noncrystalline Al/Fe-Hydroxide Coprecipitates. Environmental Science & Technology 45(15), 6283-6289.

Lobartini, J.C., Tan, K.H. and Pape, C. (1998) Dissolution of aluminum and iron phosphate by humic acids. Communications in Soil Science and Plant Analysis 29(5-6), 535-544.

Lodder, R., Meulenkamp, R., Notenboom, G., 2011. Fosfaatterugwinning in communale afvalwaterzuiveringsinstallaties. STOWA, 111 pp.

Loganathan, P., Vigneswaran, S., Kandasamy, J. and Bolan, N.S. (2014) Removal and Recovery of Phosphate From Water Using Sorption. Critical Reviews in Environmental Science and Technology 44(8), 847-907.

Lothenbach, B. and Nonat, A. (2015) Calcium silicate hydrates: Solid and liquid phase composition. Cement and Concrete Research 78, 57-70.

Lotti, T., Kleerebezem, R., Kip, C., Hendrickx, T. L. G., Kruit, J., Hoekstra, M., van Loosdrecht, M.C.M., 2014. Anammox growth on pretreated municipal wastewater. Environ. Sci. Technol. 48 (14), 7874–7880.

Lovley, D.R., 1997. Microbial Fe(III) reduction in subsurface environments. FEMS Microbiology Reviews 20 (3-4), 305–313.

Lovley, D.R., Coates, J.D., Blunt-Harris, E.L., Phillips, E.J.P., Woodward, J.C., 1996. Humic substances as electron acceptors for microbial respiration. Nature 382 (6590), 445–448.

Lovley, D.R., Fraga, J.L., Blunt-Harris, E.L., La Hayes, Phillips, E.J.P., Coates, J.D., 1998. Humic substances as a mediator for microbially catalyzed metal reduction. Acta Hydrochemica et Hydrobiologica 26 (3), 152–157.

Lovley, D.R., Holmes, D.E., Nevin, K.P., 1991. Dissimilatory Fe(III) and Mn(IV) Reduction. Microbiol Reviews 49, 219–286.

Lǔ, J., Liu, H., Liu, R., Zhao, X., Sun, L. and Qu, J. (2013) Adsorptive removal of phosphate by a nanostructured Fe–Al–Mn trimetal oxide adsorbent. Powder Technology 233, 146-154.

Lu, Q., He, Z.L., Stoffella, P.J., 2012. Land Application of Biosolids in the USA: A Review. Applied and Environmental Soil Science 2012, 1–11.

Lüderitz, V. and Gerlach, F. (2002) Phosphorus Removal in Different Constructed Wetlands. Acta Biotechnologica 22(1-2), 91-99.

Luedecke, C., Hermanowicz, S.W., Jenkins, D., 1989. Precipitation of ferric phosphate in activated-sludge - A chemical model and its verification. Water Science & Technology 21 (4-5), 325–337.

Luo, X., Liu, C., Yuan, J., Zhu, X. and Liu, S. (2017) Interfacial Solid-Phase Chemical Modification with Mannich Reaction and Fe(III) Chelation for Designing Lignin-Based Spherical Nanoparticle Adsorbents for Highly Efficient Removal of Low Concentration Phosphate from Water. ACS Sustainable Chemistry & Engineering 5(8), 6539-6547.

Luo, X., Wang, X., Bao, S., Liu, X., Zhang, W. and Fang, T. (2016) Adsorption of phosphate in water using one-step synthesized zirconium-loaded reduced graphene oxide. Scientific Reports 6, 39108.

Luo, X., Wu, X., Reng, Z., Min, X., Xiao, X. and Luo, J. (2017b) Enhancement of Phosphate Adsorption on Zirconium Hydroxide by Ammonium Modification. Industrial & Engineering Chemistry Research 56(34), 9419-9428.

Lürling, M., Waajen, G. and van Oosterhout, F. (2014) Humic substances interfere with phosphate removal by lanthanum modified clay in controlling eutrophication. Water Research 54, 78-88.

M, B.L., TM, A.L. and Cees, O. (2016) - Growth Rate and Morphology of a Single Calcium Carbonate Crystal on Polysulfone Film Measured with Time Lapse Raman Micro Spectroscopy. Journal of Analytical & Bioanalytical Techniques 7(4), 321.

Maccoux, M.J., Dove, A., Backus, S.M. and Dolan, D.M. (2016) Total and soluble reactive phosphorus loadings to Lake Erie: A detailed accounting by year, basin, country, and tributary. Journal of Great Lakes Research 42(6), 1151-1165.

Maccoux, M.J., Dove, A., Backus, S.M. and Dolan, D.M. (2016) Total and soluble reactive phosphorus loadings to Lake Erie: A detailed accounting by year, basin, country, and tributary. Journal of Great Lakes Research 42(6), 1151-1165.

Macdonald, G.K., Bennett, E.M., Potter, P.A., Ramankutty, N., 2011. Agronomic phosphorus imbalances across the world's croplands 108 (7), 3086–3091.

Mackay, E.B., Maberly, S.C., Pan, G., Reitzel, K., Bruere, A., Corker, N., Douglas, G., Egemose, S., Hamilton, D., Hatton-Ellis, T., Huser, B., Li, W., Meis, S., Moss, B., Lürling, M., Phillips, G., Yasseri, S. and Spears, B.M. (2014) Geoengineering in lakes: welcome attraction or fatal distraction? Inland Waters 4(4), 349-356.

Mahmood, T., Saddique, M.T., Naeem, A., Westerhoff, P., Mustafa, S. and Alum, A. (2011) Comparison of Different Methods for the Point of Zero Charge Determination of NiO. Industrial & Engineering Chemistry Research 50(17), 10017-10023.

Maier, W., Weidelener, A., Krampe, J., Rott, I., 2005. Entwicklung eines Verfahrens zur Phosphat-Rückgewinnung aus ausgefaultem Nassschlam oder entwässertem Faulschlamm als gut pflanzenverfügbares Magnesium-Ammonium-Phosphat (MAP): Schlussbericht: Teil 1: Zusammenfassung und Wertung der Ergebnisse, 160 pp.

Mao, Y., Ninh Pham, A., Xin, Y. and David Waite, T. (2012) Effects of pH, floc age and organic compounds on the removal of phosphate by pre-polymerized hydrous ferric oxides. Separation and Purification Technology 91, 38-45.

Martin, B.D., Parsons, S.A., Jefferson, B., 2009. Removal and recovery of phosphate from municipal wastewaters using a polymeric anion exchanger bound with hydrated ferric oxide nanoparticles. Water Science & Technology 60 (10), 2637–2645.

Martin, R.R., Tazaki, K., St. Smart, R.C., 1988. Direct Observation of Phosphate Precipitation in the Goethite/Phosphate System. Soil Science Society of America Journal 52 (5), 1492.

Matthias, T. (2004) Nanoporous Materials: Science and Engineering, pp. 317-364, PUBLISHED BY IMPERIAL COLLEGE PRESS AND DISTRIBUTED BY WORLD SCIENTIFIC PUBLISHING CO.

Mc, L.J.R., Ryden J, C. and Syers J, K. (1981) SORPTION OF INORGANIC PHOSPHATE BY IRON- AND ALUMINIUM- CONTAINING COMPONENTS. Journal of Soil Science 32(3), 365-378.

McLaughlin, J.R., Ryden, J.C., Syers, J.K., 1981. Sorption of inorganic-phosphate by iron containing and aluminum containing components. Journal of Soil Science 32 (3), 365–377.

Mekonnen Mesfin, M. and Hoekstra Arjen, Y. (2017) Global Anthropogenic Phosphorus Loads to Freshwater and Associated Grey Water Footprints and Water Pollution Levels: A High-Resolution Global Study. Water Resources Research 54(1), 345-358.

Mezenner, N.Y. and Bensmaili, A. (2009) Kinetics and thermodynamic study of phosphate adsorption on iron hydroxide-eggshell waste. Chemical Engineering Journal 147(2), 87-96.

Mia, S., Dijkstra, F.A. and Singh, B. (2017) Aging Induced Changes in Biochar's Functionality and Adsorption Behavior for Phosphate and Ammonium. Environ Sci Technol 51(15), 8359-8367.

Midorikawa, I., Aoki, H., Omori, A., Shimizu, T., Kawaguchi, Y., Kassai, K. and Murakami, T. (2008) Recovery of high purity phosphorus from municipal wastewater secondary effluent by a high-speed adsorbent. Water Science and Technology 58(8), 1601.

Mikutta, C., Kretzschmar, R., 2011. Spectroscopic Evidence for Ternary Complex Formation between Arsenate and Ferric Iron Complexes of Humic Substances. Environ. Sci. Technol. 45 (22), 9550–9557.

Miller, M., O'Connor, G.A., 2009. The Longer-Term Phytoavailability of Biosolids-Phosphorus. Agronomy Journal 101 (4), 889.

Ming, H., Yu, H., Wei, H., Liu, Y., Li, H., He, X., Huang, H., Kang, Z., 2011. Composition and morphology control of Fex(PO4)y(OH)z·nH2O microcrystals. Crystal Research and Technology 46 (7), 711–717.

Miot, J., Benzerara, K., Morin, G., Bernard, S., Beyssac, O., Larquet, E., Kappler, A., Guyot, F., 2009. Transformation of vivianite by anaerobic nitrate-reducing iron-oxidizing bacteria. Geobiology 7 (3), 373–384.

Mitchell, S. and Ullman, J. (2016) Removal of Phosphorus, BOD, and Pharmaceuticals by Rapid Rate Sand Filtration and Ultrafiltration Systems. Journal of Environmental Engineering 142, 06016006.

Moore, P.B., 1969. Basic ferric phosphates: a crystallochemical principle. Science 164 (3883), 1063–1064.

Moore, P.B., 1970. Crystal chemistry of the basic iron phosphates. The American Mineralogist 55.

Mor, S., Chhoden, K. and Ravindra, K. (2016) Application of agro-waste rice husk ash for the removal of phosphate from the wastewater. Journal of Cleaner Production 129, 673-680.

Moreira, R.F.P.M., Vandresen, S., Luiz, D.B., José, H.J. and Puma, G.L. (2017) Adsorption of arsenate, phosphate and humic acids onto acicular goethite nanoparticles recovered from acid mine drainage. Journal of Environmental Chemical Engineering 5(1), 652-659.

Morris, A.J., Hesterberg, D.L., 2012. Iron(III) Coordination and Phosphate Sorption in Peat Reacted with Ferric or Ferrous Iron. Soil Science Society of America Journal 76 (1), 101.

Morse, G., Brett, S., Guy, J., Lester, J., 1998. Review: Phosphorus removal and recovery technologies. Science of The Total Environment 212 (1), 69–81.

Morse, J., Millero, F.J., Cornwell, J., Rickard, D., 1987. The chemistry of the hydrogen sulfide and iron sulfide systems in natural waters. Earth-Science Reviews 24 (1), 1–42.

Moss, L., Donovan, J.F., Carr, S., Stone, L., Polo, C., Khunjar, W., Latimer, R., Jeyanayagam, S., Beecher, N., McFadden, L., 2013. Enabling the future-Advancing Resource Recovery from Biosolids.

Munch, J.C., Ottow, J. C. G., 1983. Reductive transformation mechanism of ferric oxides in hydromorphic soils. Ecological Bulletins, 383–394.

Murad, E. (1988a) The Mössbauer spectrum of "well"-crystallized ferrihydrite. Journal of Magnetism and Magnetic Materials 74(2), 153-157.

Murad, E. (1988b) Iron in Soils and Clay Minerals. Stucki, J.W., Goodman, B.A. and Schwertmann, U. (eds), pp. 309-350, Springer Netherlands, Dordrecht.

Murad, E. and Cashion, J. (2004) Mössbauer Spectroscopy of Environmental Materials and Their Industrial Utilization, pp. 159-188, Springer US, Boston, MA.

Murad;, E. and Schwertmann, U. (1980) The Moessbauer spectrum of ferrihydrite and its relations to those of other iron oxides. American Mineralogist 65(9-10), 1044-1049.

Namasivayam, C. and Sangeetha, D. (2004) Equilibrium and kinetic studies of adsorption of phosphate onto ZnCl2 activated coir pith carbon. Journal of Colloid and Interface Science 280(2), 359-365.

Nanzer, S., Oberson, A., Berger, L., Berset, E., Hermann, L., Frossard, E., 2014. The plant availability of phosphorus from thermo-chemically treated sewage sludge ashes as studied by 33P labeling techniques. Plant Soil 377 (1-2), 439–456.

Neethling, J. (2013) Optimizing chemical phosphorus removal. Technical Conference and Exposition Ohio Water Environment Association (OWEA).

Nelson, P. and Oades, J.M. (1998) Organic matter, sodicity and soil structure.

Newcombe, R.L., Rule, R.A., Hart, B.K. and Möller, G. (2008) Phosphorus Removal from Municipal Wastewater by Hydrous Ferric Oxide Reactive Filtration and Coupled Chemically Enhanced Secondary Treatment: Part I—Performance. Water Environment Research 80(3), 238-247.

Ngo, H.-H. and Guo, W. (2009) Membrane fouling control and enhanced phosphorus removal in an aerated submerged membrane bioreactor using modified green bioflocculant. Bioresource Technology 100(18), 4289-4291.

Nguyen, T.A.H., Ngo, H.H., Guo, W.S., Zhang, J., Liang, S., Lee, D.J., Nguyen, P.D. and Bui, X.T. (2014) Modification of agricultural waste/by-products for enhanced phosphate removal and recovery: Potential and obstacles. Bioresource Technology 169, 750-762.

Nielsen, A.H., Lens, P., Vollertsen, J., Hvitved-Jacobsen, T., 2005. Sulfide–iron interactions in domestic wastewater from a gravity sewer. Water research 39 (12), 2747–2755.

Nielsen, P.H., 1996. The significance of microbial Fe(III) reduction in the activated sludge process. Water Science & Technology 34 (5-6), 129–136.

Nixon, S.W. (1995) Coastal marine eutrophication: A definition, social causes, and future concerns. Ophelia 41(1), 199-219.

Nowak, O., Enderle, P., Varbanov, P., 2015. Ways to optimize the energy balance of municipal wastewater systems: lessons learned from Austrian applications. Journal of Cleaner Production 88, 125–131.

Nowak, O., Keil, S., Fimml, C., 2011. Examples of energy self-sufficient municipal nutrient removal plants. Water Science & Technology 64 (1), 1.

Nriagu, J.O., 1972. Stability of vivianite and ion-pair formation in the system Fe3(PO4)2-H3PO4H3PO4-H2O. Geochimica et Cosmochimica Acta 36 (4), 459–470.

Nriagu, J.O., Dell, C.I., 1974. Diagenetic formation of iron phosphates in recent lake sediments. American Mineralogist 59, 934–946.

O'Connor, G.A., Sarkar, D., Brinton, S.R., Elliott, H.A., Martin, F.G., 2004. Phytoavailability of Biosolids Phosphorus. Journal of Environment Quality 33 (2), 703.

Oehmen, A., Lemos, P.C., Carvalho, G., Yuan, Z., Keller, J., Blackall, L.L. and Reis, M.A.M. (2007) Advances in enhanced biological phosphorus removal: From micro to macro scale. Water Research 41(11), 2271-2300.

Oleszkiewicz, J., James L. B., 2006. Nutrient removal technology in North America and the European Union: A review. Water Qual.Res.J. Canada 41 (4), 449–462.

Oliver, I.W., McLaughlin, M.J., Merrington, G., 2005. Temporal trends of total and potentially available element concentrations in sewage biosolids: a comparison of biosolid surveys conducted 18 years apart. Science of The Total Environment 337 (1-3), 139–145.

Olofsson, U., Bignert, A., Haglund, P., 2012. Time-trends of metals and organic contaminants in sewage sludge. Water research 46 (15), 4841–4851.

Osmari, T.A., Gallon, R., Schwaab, M., Barbosa-Coutinho, E., Severo, J.B. and Pinto, J.C. (2013) Statistical Analysis of Linear and Non-Linear Regression for the Estimation of Adsorption Isotherm Parameters. Adsorption Science & Technology 31(5), 433-458.

Osterwalder, A. and Pigneur, Y. (2010) Business model generation: a handbook for visionaries, game changers, and challengers, John Wiley & Sons.

P.M.J. Janssen, A.F.v.N., P. van der Pijl , P.J. Roeleveld, A. Visser, N. Wortel (2006) STOWA-Filtratie-Technikien RWZI's; ISBN 90.5773.341.2.

Pan, B., Han, F., Nie, G., Wu, B., He, K. and Lu, L. (2014) New Strategy To Enhance Phosphate Removal from Water by Hydrous Manganese Oxide. Environmental Science & Technology 48(9), 5101-5107.

Parfitt, R.L. (1979) Advances in Agronomy. Brady, N.C. (ed), pp. 1-50, Academic Press.

Parfitt, R.L., Atkinson, R.J. and Smart, R.S.C. (1975) The Mechanism of Phosphate Fixation by Iron Oxides 1. Soil Science Society of America Journal 39(5), 837-841.

Parfitt, R.L., Atkinson, R.J., 1976. Phosphate adsorption on goethite (α-FeOOOH). Nature 264 (5588), 740–742.

Parfitt, R.L., Atkinson, R.J., Smart, R.S.C., 1975. The Mechanism of Phosphate Fixation by Iron Oxides1. Soil Science Society of America Journal 39 (5), 837.

Park, J.-H., Wang, J.J., Kim, S.-H., Cho, J.-S., Kang, S.-W., Delaune, R.D. and Seo, D.-C. (2017) Phosphate removal in constructed wetland with rapid cooled basic oxygen furnace slag. Chemical Engineering Journal 327, 713-724.

Patrick, W.H., Gotoh, S., Williams, B.G., 1973. Strengite dissolution in flooded soils and sediments. Science 179 (4073), 564–565.

Paul, E., Laval, M.L. and Sperandio, M. (2001) Excess sludge production and costs due to phosphorus removal. Environ Technol 22(11), 1363-1371.

Peak, F., Sparks, 1999. An in Situ ATR-FTIR Investigation of Sulfate Bonding Mechanisms on Goethite. Journal of Colloid and Interface Science 218 (1), 289–299.

Pédrot, M., Le Boudec, A., Davranche, M., Dia, A., Henin, O., 2011. How does organic matter constrain the nature, size and availability of Fe nanoparticles for biological reduction? Journal of Colloid and Interface Science 359 (1), 75–85.

Peretyazhko, T., Sposito, G., 2005. Iron(III) reduction and phosphorus solubilization in humid tropical forest soils. Geochimica et Cosmochimica Acta 69 (14), 3643–3652.

Persson, P., Nilsson, N., Sjöberg, S., 1996. Structure and Bonding of Orthophosphate Ions at the Iron Oxide-Aqueous Interface. Journal of Colloid and Interface Science 177 (1), 263–275.

Petzet, S., Cornel, P., 2011. Towards a complete recycling of phosphorus in wastewater treatment – options in Germany. Water Science & Technology 64 (1), 29.

Petzet, S., Peplinski, B., Cornel, P., 2012. On wet chemical phosphorus recovery from sewage sludge ash by acidic or alkaline leaching and an optimized combination of both. Water research 46 (12), 3769–3780.

Pham, A.N., Rose, A.L., Feltz, A.J., Waite, T.D., 2004. The effect of dissolved natural organic matter on the rate of removal of ferrous iron in fresh waters, in: Natural Organic Material Research: Innovations and Applications for Drinking Water. IWA Publishing, pp. 213–219.

Piepenbrock, A., Behrens, S., Kappler, A., 2014a. Comparison of Humic Substance- and Fe(III)-Reducing Microbial Communities in Anoxic Aquifers. Geomicrobiology Journal 31 (10), 917–928.

Piepenbrock, A., Schröder, C., Kappler, A., 2014b. Electron transfer from humic substances to biogenic and abiogenic Fe(III) oxyhydroxide minerals. Environ. Sci. Technol. 48 (3), 1656–1664.

Pinnekamp, J., Everding, W., Gethke, K., Montag, D., Weinfurtner, K., Sartorius, C., Horn, J. von, Tettenborn, F., Gäth, S., Waida, C., Fehrenbach, H., Reinhardt, J.L., 2011. Phosphorrecycling – Ökologische und wirtschaftliche Bewertung verschiedener Verfahren und Entwicklung eines strategischen Verwertungskonzepts für Deutschland, 463 pp.

Pokhrel, D. and Viraraghavan, T. (2009) Biological filtration for removal of arsenic from drinking water. Journal of Environmental Management 90(5), 1956-1961.

Posth, N.R., Canfield, D.E., Kappler, A., 2014. Biogenic Fe(III) minerals: From formation to diagenesis and preservation in the rock record. Earth-Science Reviews 135, 103–121.

Poulton, S.W., Krom, M.D., Raiswell, R., 2004. A revised scheme for the reactivity of iron (oxyhydr)oxide minerals towards dissolved sulfide. Geochimica et Cosmochimica Acta 68 (18), 3703–3715.

Pratt, C., Parsons, S.A., Soares, A., Martin, B.D., 2012. Biologically and chemically mediated adsorption and precipitation of phosphorus from wastewater. Current opinion in biotechnology 23 (6), 890–896.

Pretty, J.N., Mason, C.F., Nedwell, D.B., Hine, R.E., Leaf, S. and Dils, R. (2003) Environmental Costs of Freshwater Eutrophication in England and Wales. Environmental Science & Technology 37(2), 201-208.

Prill, T. and Schladitz, K. (2013) Simulation of FIB-SEM images for analysis of porous microstructures. Scanning 35(3), 189-195.

Prochnow, L.I., Chien, S.H., Carmona, G., Dillard, E.F., Henao, J., Austin, E.R., 2008. Plant Availability of Phosphorus in Four Superphosphate Fertilizers Varying in Water-Insoluble Phosphate Compounds. Soil Science Society of America Journal 72 (2), 462.

Puccia, V., Luengo, C., Avena, M., 2009. Phosphate desorption kinetics from goethite as induced by arsenate. Colloids and Surfaces A: Physicochemical and Engineering Aspects 348 (1-3), 221–227.

Qian, J., Shen, M., Wang, P., Wang, C., Hu, J., Hou, J., Ao, Y., Zheng, H., Li, K. and Liu, J. (2017) Co-adsorption of perfluorooctane sulfonate and phosphate on boehmite: Influence of temperature, phosphate initial concentration and pH. Ecotoxicol Environ Saf 137, 71-77.

R. Kadlec, R.K. (1996) Treatment wetlands. Lewis Publishers, Boca Raton, FL.

Ragsdale, D., 2007. Advanced Wastewater Advanced Wastewater Treatment to Achieve Low Concentration of Phosphorus, 73 pp.

Rashid, M., Price, N.T., Gracia Pinilla, M.Á. and O'Shea, K.E. (2017) Effective removal of phosphate from aqueous solution using humic acid coated magnetite nanoparticles. Water Research 123, 353-360.

Rashidi Nodeh, H., Sereshti, H., Zamiri Afsharian, E. and Nouri, N. (2017) Enhanced removal of phosphate and nitrate ions from aqueous media using nanosized lanthanum hydrous doped on magnetic graphene nanocomposite. J Environ Manage 197, 265-274.

Rasmussen, H., Bruus, J.H., Keiding, K., Nielsen, P.H., 1994. Observations on dewaterability and physical, chemical and microbiological changes in anaerobically stored activated sludge from a nutrient removal plant. Water research 28 (2), 417–425.

Rasmussen, H., Nielsen, P.H., 1996. Iron reduction in activated sludge measured with different extraction techniques. Water research 30 (3), 551–558.

Recht, H.L., Ghassemi, M., 1970. Kinetics and mechanism of precipitation and nature of the precipitate obtained in phosphate removal from wastewater using aluminum (III) and iron (III) salts. Water Pollution Control Research Series. University of Michigan, 77 pp.

Recillas, S., Garcia, A., Gonzalez, E., Casals, E., Puntes, V., Sanchez, A. and Font, X. (2012) Preliminary study of phosphate adsorption onto cerium oxide nanoparticles for use in water purification; nanoparticles synthesis and characterization. Water Sci Technol 66(3), 503-509.

Reid, R.K., Reid, C. P. P., Szaniszlo, P.J., 1985. Effects of synthetic and microbially produced chelates on the diffusion of iron and phosphorus to a simulated root in soil. Biol Fert Soils 1 (1), 45–52.

Reijnders, L. (2014) Phosphorus resources, their depletion and conservation, a review. Resources, Conservation and Recycling 93, 32-49.

Reitzel, K., Andersen, F.Ø., Egemose, S. and Jensen, H.S. (2013) Phosphate adsorption by lanthanum modified bentonite clay in fresh and brackish water. Water Research 47(8), 2787-2796.

Rentz, J. A.; Turner, I. P.; Ullman, J. L. Removal of phosphorus from solution using biogenic iron oxides. Water Research 2009, 43, 2029–2035, DOI 10.1016/j.watres.2009.02.021.

Rentz, J.A., Turner, I.P. and Ullman, J.L. (2009) Removal of phosphorus from solution using biogenic iron oxides. Water Research 43(7), 2029-2035.

Richardson, C.J., King, R.S., Qian, S.S., Vaithiyanathan, P., Qualls, R.G. and Stow, C.A. (2007) Estimating Ecological Thresholds for Phosphorus in the Everglades. Environmental Science & Technology 41(23), 8084-8091.

Ridgway, H.F., Means, E.G. and Olson, B.H. (1981) Iron bacteria in drinking-water distribution systems: elemental analysis of gallionella stalks, using x-ray energy-dispersive microanalysis. Applied and environmental microbiology 41(1), 288-297.

Rietra, R.P.J.J., Hiemstra, T. and van Riemsdijk, W.H. (2001) Interaction between Calcium and Phosphate Adsorption on Goethite. Environmental Science & Technology 35(16), 3369-3374.

Riffaldi, R., Sartori, F., Levi-Minzi, R., 1982. Humic substances in sewage sludges. Environmental Pollution 3 (2), 139–146.

Rivera-Utrilla, J., Sánchez-Polo, M., Gómez-Serrano, V., Álvarez, P.M., Alvim-Ferraz, M.C.M. and Dias, J.M. (2011) Activated carbon modifications to enhance its water treatment applications. An overview. Journal of Hazardous Materials 187(1–3), 1-23.

Robinson, K.G., Robinson, C.H., Raup, L.A., Markum, T.R., 2012. Public attitudes and risk perception toward land application of biosolids within the south-eastern United States. Journal of Environmental Management 98, 29–36.

Roden, E.E., Edmonds, J.W., 1997. Phosphate mobilization in iron-rich anaerobic sediments: Microbial Fe(III) oxide reduction versus iron-sulfide formation. Archiv für Hydrobiologie 139 (3), 347–378.

Roldan, R., Barron, V., Torrent, J., 2002. Experimental alteration of vivianite to lepidocrocite in a calcareous medium. clay miner 37 (4), 709–718.

Römer, W., 2006. Vergleichende Untersuchungen zur Pflanzenverfügbarkeit von Phosphat aus verschiedenen P-Recycling-Produkten im Keimpflanzenversuch. J. Plant Nutr. Soil Sci. 169 (6), 826–832.

Rouquerol, J., Avnir, D., Fairbridge, C., Everett, D., Haynes, J., Pernicone, N., Ramsay, J., Sing, K. and Unger, K. (1994) Recommendations for the characterization of porous solids (Technical Report). Pure and applied chemistry 66(8), 1739-1758.

Russel, J.D., Parfitt, R.L., Frasser, A.R., Farmer, V.C., 1974. Surface structures of gibbsite goethite and phosphated goethite. Nature 248 (5445), 220–221.

Russo, V., Tesser, R., Trifuoggi, M., Giugni, M. and Di Serio, M. (2015) A dynamic intraparticle model for fluid–solid adsorption kinetics. Computers & Chemical Engineering 74, 66-74.

Russo, V., Trifuoggi, M., Di Serio, M. and Tesser, R. (2017) Fluid-Solid Adsorption in Batch and Continuous Processing: A Review and Insights into Modeling. Chemical Engineering & Technology 40(5), 799-820.

Samie, I.F., Römer, W., 2001. Phosphorus availability to maize plants from sewage sludge treated with Fe compounds, in: Horst, W.J., Schenk, M.K., Bürkert, A., Claassen, N., Flessa, H., Frommer, W.B., Goldbach, H., Olfs, H.W., Römheld, V., Sattelmacher, B., Schmidhalter, U., Schubert, S., Wirén, N., Wittenmayer, L. (Eds.), Plant Nutrition. Springer Netherlands, Dordrecht, pp. 846–847.

Sang Won, L., Kim, S.J., In-Bo, S., Seongtae, B. and Chul Sung, K. (2005) Mössbauer studies of nano-size controlled iron oxide for biomedical applications. IEEE Transactions on Magnetics 41(10), 4114-4116.

Sano, A., Kanomata, M., Inoue, H., Sugiura, N., Xu, K.-Q., Inamori, Y., 2012. Extraction of raw sewage sludge containing iron phosphate for phosphorus recovery. Chemosphere 89 (10), 1243–1247.

Schindler, D.W., Carpenter, S.R., Chapra, S.C., Hecky, R.E. and Orihel, D.M. (2016) Reducing Phosphorus to Curb Lake Eutrophication is a Success. Environmental Science & Technology 50(17), 8923-8929.

Schipper, W.J., Klapwijk, A., Potjer, B., Rulkens, W.H., Temmink, B.G., Kiestra, F.D., Lijmbach, A.C., 2001. Phosphate recycling in the phosphorus industry. Environmental technology 22 (11), 1337–1345.

Schipper, W.J., Korving, L. (Eds.), 2009. Full-scale plant test using sewage sludge ash as raw material for phosphorus production.

Schröder, J.J., Cordell, D., Smit, A.L., Rosemarin, A., 2010. Sustainable use of phosphorus. Wageningen University and Research Centre, 140 pp.

Schröder, J.J., Smit, A.L., Cordell, D., Rosemarin, A., 2011. Improved phosphorus use efficiency in agriculture: a key requirement for its sustainable use. Chemosphere 84 (6), 822–831.

Schulz, H.D., Zabel, M., 2006. Marine geochemistry, 2nd rev., updated and extended ed. ed. Springer, Berlin, New York.

Schwertmann, U. and Cornell, R.M. (2000) Iron Oxides in the Laboratory: Preparation and Characterization, Wiley.

Schwertmann, U., 1966. Inhibitory Effect of Soil Organic Matter on the Crystallization of Amorphous Ferric Hydroxide. Nature 212 (5062), 645–646.

Schwertmann, U., 1970. Influence of various simple organic anions on formation of goethite and hematite from amorphous ferric hydroxide. Geoderma 3 (3), 207–214.

Schwertmann, U., Carlson, L. and Fechter, H. (1984) Iron oxide formation in artificial ground waters. Schweizerische Zeitschrift für Hydrologie 46(2), 185-191.

Schwertmann, U., Wagner, F., Knicker, H., 2005. Ferrihydrite–Humic Associations: Magnetic Hyperfine Interactions. Soil Science Society of America Journal 69 (4), 1009.

Sedlak, R.I. (1991) Phosphorus and nitrogen removal from municipal wastewater: principles and practice, CRC press.

Sellner, B.M., Hua, G., Ahiablame, L.M., Trooien, T.P., Hay, C.H. and Kjaersgaard, J. (2017) Evaluation of industrial by-products and natural minerals for phosphate adsorption from subsurface drainage. Environ Technol, 1-12.

Senesi, N., Sposito, G., Holtzclaw, K.M., Bradford, G.R., 1989. Chemical Properties of Metal-Humic Acid Fractions of a Sewage Sludge-Amended Aridisol. Journal of Environment Quality 18 (2), 186.

Sengupta, S. and Pandit, A. (2011) Selective removal of phosphorus from wastewater combined with its recovery as a solid-phase fertilizer. Water Research 45(11), 3318-3330.

Sevcenco, A.-M., Paravidino, M., Vrouwenvelder, J.S., Wolterbeek, H.T., van Loosdrecht, M.C.M. and Hagen, W.R. (2015) Phosphate and arsenate removal efficiency by thermostable ferritin enzyme from Pyrococcus furiosus using radioisotopes. Water Research 76, 181-186.

Sharpley, A. (2016) Managing agricultural phosphorus to minimize water quality impacts. Scientia Agricola 73, 1-8.

Shin, E.W., Han, J.S., Jang, M., Min, S.-H., Park, J.K. and Rowell, R.M. (2004) Phosphate Adsorption on Aluminum-Impregnated Mesoporous Silicates: Surface Structure and Behavior of Adsorbents. Environmental Science & Technology 38(3), 912-917.

Shuang, C., Wang, M., Zhou, Q., Zhou, W. and Li, A. (2013) Enhanced adsorption and antifouling performance of anion-exchange resin by the effect of incorporated Fe3O4 for removing humic acid. Water Research 47(16), 6406-6414.

Sibanda H, M. and Young S, D. (1986) Competitive adsorption of humus acids and phosphate on goethite, gibbsite and two tropical soils. Journal of Soil Science 37(2), 197-204.

Sigg, L. and Stumm, W. (1981) The interaction of anions and weak acids with the hydrous goethite (α-FeOOH) surface. Colloids and Surfaces 2(2), 101-117.

Sing, K. (2001) The use of nitrogen adsorption for the characterisation of porous materials. Colloids and Surfaces A: Physicochemical and Engineering Aspects 187-188, 3-9.

Sing, K.S. (1985) Reporting physisorption data for gas/solid systems with special reference to the determination of surface area and porosity (Recommendations 1984). Pure and applied chemistry 57(4), 603-619.

Sing, K.S.W., Everett, D.H., Haul, R.A.W., Moscou, L., Pierotti, R.A., Rouquerol, J. and Siemieniewska, T. (2008) Handbook of Heterogeneous Catalysis, Wiley-VCH Verlag GmbH & Co. KGaA.

Singer, P.C., 1972. Anaerobic control of phosphate by ferrous iron: Anaerobic control of phosphate by ferrous iron. Journal Water Pollution Control Federation 44 (4), 663.

Singer, P.C., Stumm, W., 1969. Oxygenation of ferrous iron: The rate determining step in the formation of acidic mine drainage. Water Pollution Control Research Series, 150 pp.

Sjöstedt, C., Persson, I., Hesterberg, D., Kleja, D.B., Borg, H., Gustafsson, J.P., 2013. Iron speciation in soft-water lakes and soils as determined by EXAFS spectroscopy and geochemical modelling. Geochimica et Cosmochimica Acta 105, 172–186.

Smith, S., Kim, G., Doan, L. and Roh, H. (2014) Improving biological phosphorus removal in membrane bioreactors - A pilot study.

Smith, S., Takacs, I., Murthy, S., Daigger, G.T., Szabo, A., 2008. Phosphate complexation model and its implications for chemical phosphorus removal. Water Environ Res 80 (5), 428–438.

Smith, S.R., 2009. Organic contaminants in sewage sludge (biosolids) and their significance for agricultural recycling. Philosophical transactions. Series A, Mathematical, physical, and engineering sciences 367 (1904), 4005–4041.

Smith, V.H., Tilman, G.D. and Nekola, J.C. (1999) Eutrophication: impacts of excess nutrient inputs on freshwater, marine, and terrestrial ecosystems. Environmental Pollution 100(1), 179-196.

Smolders, A.J.P., Lamers, L. P. M., Lucassen, E. C. H. E. T., Van Der Velde, G., Roelofs, J. G. M., 2006. Internal eutrophication: How it works and what to do about it—a review. Chemistry and Ecology 22 (2), 93–111.

Song, H., Li, X., Zhang, Y., Wang, H., Li, H. and Huang, J. (2014) A nanocomposite of needle-like MnO2 nanowires arrays sandwiched between graphene nanosheets for supercapacitors. Ceramics International 40(1, Part A), 1251-1255.

Song, Y., Hahn, H.H. and Hoffmann, E. (2002a) The Effect of Carbonate on the Precipitation of Calcium Phosphate. Environ Technol 23(2), 207-215.

Song, Y., Hahn, H.H. and Hoffmann, E. (2002b) Effects of solution conditions on the precipitation of phosphate for recovery: A thermodynamic evaluation. Chemosphere 48(10), 1029-1034.

Sorkina, T.A., Polyakov, A.Y., Kulikova, N.A., Goldt, A.E., Philippova, O.I., Aseeva, A.A., Veligzhanin, A.A., Zubavichus, Y.V., Pankratov, D.A., Goodilin, E.A., Perminova, I.V., 2014.

Nature-inspired soluble iron-rich humic compounds: new look at the structure and properties. J Soils Sediments 14 (2), 261–268.

Sparks, D.L., 2003. Sorption Phenomena on Soils, in: Environmental Soil Chemistry. Elsevier, pp. 133–186.

Sperling, M.v. (2016) Urban wastewater treatment in Brazil. Department of Sanitary and Environmental Engineering, Federal University of Minas Gerais, Brazil.

Spiess, A.-N. and Neumeyer, N. (2010) An evaluation of R(2)as an inadequate measure for nonlinear models in pharmacological and biochemical research: a Monte Carlo approach. BMC Pharmacology 10, 6-6.

Sposito, G. (1987) Geochemical Processes at Mineral Surfaces, pp. 217-228, American Chemical Society.

Stevenson, F.J., 1994. Humus chemistry: Genesis, composition, reactions, 2nd ed ed. Wiley, New York.

Stoch, P., Szczerba, W., Bodnar, W., Ciecinska, M., Stoch, A., Burkel, E., 2014. Structural properties of iron-phosphate glasses: spectroscopic studies and ab initio simulations. Physical chemistry chemical physics: PCCP 16 (37), 19917–19927.

STOWA (2009) 1-Step filter als effluentpolishings-techniek. ISBN 978.90.5773.456.4.

Stumm, W., 1997. Reactivity at the mineral-water interface: dissolution and inhibition. Colloids and Surfaces A: Physicochemical and Engineering Aspects 120 (1-3), 143–166.

Stumm, W., Morgan, J.J., 1996. Aquatic chemistry: Chemical equilibria and rates in natural waters, 3rd ed. ed. Environmental science and technology. Wiley, New York.

Stumm, W., Sigg, L., Sulzberger, B., 1992. Chemistry of the solid-water interface: processes at the mineral-water and particle-water in natural systems. A Wiley-Intersciece publication. Wiley, New York.

Su, C. and Puls, R.W. (2001) Arsenate and Arsenite Removal by Zerovalent Iron: Effects of Phosphate, Silicate, Carbonate, Borate, Sulfate, Chromate, Molybdate, and Nitrate, Relative to Chloride. Environmental Science & Technology 35(22), 4562-4568.

Su, Y., Cui, H., Li, Q., Gao, S. and Shang, J.K. (2013) Strong adsorption of phosphate by amorphous zirconium oxide nanoparticles. Water Research 47(14), 5018-5026.

Subramanyam, B. and Das, A. (2009) Linearized and non-linearized isotherm models comparative study on adsorption of aqueous phenol solution in soil. International Journal of Environmental Science & Technology 6(4), 633-640.

Sukačová, K., Trtílek, M. and Rataj, T. (2015) Phosphorus removal using a microalgal biofilm in a new biofilm photobioreactor for tertiary wastewater treatment. Water Research 71, 55-63.

Sun, X., Imai, T., Sekine, M., Higuchi, T., Yamamoto, K., Kanno, A. and Nakazono, S. (2014) Adsorption of phosphate using calcined Mg3–Fe layered double hydroxides in a fixed-bed column study. Journal of Industrial and Engineering Chemistry 20(5), 3623-3630.

Sundareshwar, P.V., Morris, J.T., 1999. Phosphorus sorption characteristics of intertidal marsh sediments along an estuarine salinity gradient. Limnol. Oceangr. 44 (7), 1693–1701.

Suresh Kumar, P., Ejerssa, W.W., Wegener, C.C., Korving, L., Dugulan, A.I., Temmink, H., van Loosdrecht, M.C.M. and Witkamp, G.-J. (2018) Understanding and improving the reusability of phosphate adsorbents for wastewater effluent polishing. Water Research 145, 365-374.

Suresh Kumar, P., Korving, L., Keesman, K.J., van Loosdrecht, M.C.M. and Witkamp, G.-J. (2019) Effect of pore size distribution and particle size of porous metal oxides on phosphate adsorption capacity and kinetics. Chemical Engineering Journal 358, 160-169.

Suresh Kumar, P., Prot, T., Korving, L., Keesman, K.J., Dugulan, I., van Loosdrecht, M.C.M. and Witkamp, G.-J. (2017) Effect of pore size distribution on iron oxide coated granular activated carbons for phosphate adsorption – Importance of mesopores. Chemical Engineering Journal 326, 231-239.

Suschka, J., Machnicka, A., Poplawski, S., 2001. Phosphate recovery from iron phosphate sludge. Environmental technology 22, 1295–1301.

Suzuki, T., Hashimoto, H., Itadani, A., Matsumoto, N., Kunoh, H. and Takada, J. (2012) Silicon and phosphorus linkage with iron via oxygen in the amorphous matrix of Gallionella ferruginea stalks. Applied and environmental microbiology 78(1), 236-241.

Svanks, K., 1971. Precipitation of Phosphates from Water with Ferrous Salts. United States. Office of Water Resources Research; Ohio State University. Water Resources Center. http://hdl.handle.net/1811/36304.

Szabo, A., Takacs, I., Murthy, S., Daigger, G.T., Licskó, I., Smith, S., 2008. Significance of Design and Operational Variables in Chemical Phosphorus Removal. Water Environ Res 80 (5), 407–416.

Talebi Atouei, M., Rahnemaie, R., Goli Kalanpa, E. and Davoodi, M.H. (2016) Competitive adsorption of magnesium and calcium with phosphate at the goethite water interface: Kinetics, equilibrium and CD-MUSIC modeling. Chemical Geology 437, 19-29.

Tawfik, D.S. and Viola, R.E. (2011) Arsenate replacing phosphate - alternative life chemistries and ion promiscuity. Biochemistry 50(7), 1128-1134.

Tchobanoglous, G., Burton, F.L., Stensel, H.D., 2013. Wastewater engineering: Treatment and reuse, 5th ed. ed. McGraw-Hill Higher Education; McGraw-Hill [distributor], New York, London.

Theis, T.L., Singer, P.C., 1974. Complexation of iron(II) by organic matter and its effect on iron(II) oxygenation. Environ. Sci. Technol. 8 (6), 569–573.

Thistleton, J., Clark, T., Pearce, P., Parsons, S.A., 2001. Mechanisms of Chemical Phosphorus Removal. Process Safety and Environmental Protection 79 (6), 339–344.

Thomas, A.E., 1965. Phosphat-Elimination in der Belebtschlammanlage von Männedorf und Phosphat-Fixation in See- und Klärschlamm. Vierteljahrschr. Naturforsch. Ges. Zürich 110, 419–434.

Thommes, M. (2004) Nanoporous Materials: Science and Engineering, pp. 317-364, PUBLISHED BY IMPERIAL COLLEGE PRESS AND DISTRIBUTED BY WORLD SCIENTIFIC PUBLISHING CO.

Tilley, 2005. Supplementary Material to Part 3: Reactions and Transformations, in: , Understanding Solids. John Wiley & Sons, Ltd, pp. 531–542.

Torrent, J., Barrón, V., Schwertmann, U., 1990. Phosphate Adsorption and Desorption by Goethites Differing in Crystal Morphology. Soil Science Society of America Journal 54 (4), 1007.

Tran, H.N., You, S.-J., Hosseini-Bandegharaei, A. and Chao, H.-P. (2017) Mistakes and inconsistencies regarding adsorption of contaminants from aqueous solutions: A critical review. Water Research 120, 88-116.

Tribe, M.A. and Alpine, R.L.W. (1986) Scale economies and the "0.6 rule". Engineering Costs and Production Economics 10(4), 271-278.

Tuutijärvi, T., Repo, E., Vahala, R., Sillanpää, M. and Chen, G. (2012) Effect of Competing Anions on Arsenate Adsorption onto Maghemite Nanoparticles. Chinese Journal of Chemical Engineering 20(3), 505-514.

UK technical advisory group, 2008. UK environmental standards and conditions (Phase 1): Water Framework Directive.

Unuabonah, E.I., Agunbiade, F.O., Alfred, M.O., Adewumi, T.A., Okoli, C.P., Omorogie, M.O., Akanbi, M.O., Ofomaja, A.E. and Taubert, A. (2017) Facile synthesis of new amino-functionalized agrogenic hybrid composite clay adsorbents for phosphate capture and recovery from water. Journal of Cleaner Production 164, 652-663.

Urano, K. and Tachikawa, H. (1991) Process development for removal and recovery of phosphorus from wastewater by a new adsorbent. II. Adsorption rates and breakthrough curves. Industrial & Engineering Chemistry Research 30(8), 1897-1899.

USEPA, 2009. Targeted National Sewage Sludge Survey Sampling and Analysis Technical Report (January).

USEPA, U.S.E.P.A. (2000) Nutrient Criteria Technical Guidance Manual - Lakes and Reservoirs.

USEPA, U.S.E.P.A. (2007) Advanced Wastewater Treatment to Achieve Low Concentration of Phosphorus.

USEPA, U.S.E.P.A. (2015) A compilation of cost data associated with the impacts and control of nutrient pollution.

van den Brand, T.P.H., Roest, K., Brdjanovic, D., Chen, G.H., van Loosdrecht, M.C.M., 2014. Influence of acetate and propionate on sulphate-reducing bacteria activity. Journal of applied microbiology 117 (6), 1839–1847.

van der Grift, B., Behrends, T., Osté, L.A., Schot, P.P., Wassen, M.J. and Griffioen, J. (2016) Fe hydroxyphosphate precipitation and Fe(II) oxidation kinetics upon aeration of Fe(II) and

phosphate-containing synthetic and natural solutions. Geochimica et Cosmochimica Acta 186, 71-90.

van Vuuren, D.P., Bouwman, A., Beusen, A., 2010. Phosphorus demand for the 1970–2100 period: A scenario analysis of resource depletion. Global Environmental Change 20 (3), 428–439.

Végh, K.R., Füleky, G.Y. and Varró, T. (1990) Plant Nutrition — Physiology and Applications: Proceedings of the Eleventh International Plant Nutrition Colloquium, 30 July–4 August 1989, Wageningen, The Netherlands. van Beusichem, M.L. (ed), pp. 147-151, Springer Netherlands, Dordrecht.

Veldkamp, R.G. (1985) Modeling Phosphate Sludge Production. Water Science and Technology 17(2-3), 107-119.

Violante, A. and Pigna, M. (2002) Competitive Sorption of Arsenate and Phosphate on Different Clay Minerals and Soils. 66(6), 1788-1796.

Vohla, C., Kõiv, M., Bavor, H.J., Chazarenc, F. and Mander, Ü. (2011) Filter materials for phosphorus removal from wastewater in treatment wetlands—A review. Ecological Engineering 37(1), 70-89.

Volesky, B. (2007) Biosorption and me. Water Research 41(18), 4017-4029.

Vrouwenvelder, J.S., Beyer, F., Dahmani, K., Hasan, N., Galjaard, G., Kruithof, J.C. and Van Loosdrecht, M.C.M. (2010) Phosphate limitation to control biofouling. Water Research 44(11), 3454-3466.

Wain, Y.A. (2014) Updating the Lang Factor and Testing its Accuracy, Reliability and Precision as a Stochastic Cost Estimating Method. PM World Journal 3(10).

Walker J., R., R., Halliday, D. (2014) Haliday and Resnick Fundamental of Physics.

Wan, J., Tao, T., Zhang, Y., Liang, X., Zhou, A. and Zhu, C. (2016) Phosphate adsorption on novel hydrogel beads with interpenetrating network (IPN) structure in aqueous solutions: kinetics, isotherms and regeneration. RSC Advances 6(28), 23233-23241.

Wang, W., Ma, C., Zhang, Y., Yang, S., Shao, Y. and Wang, X. (2016) Phosphate adsorption performance of a novel filter substrate made from drinking water treatment residuals. Journal of Environmental Sciences 45, 191-199.

Wang, X., Liu, F., Tan, W., Li, W., Feng, X. and Sparks, D. (2013) Characteristics of Phosphate Adsorption-Desorption Onto Ferrihydrite: Comparison With Well-Crystalline Fe (Hydr)Oxides. Soil Science 178, 1-11.

Wang, Z., Nie, E., Li, J., Yang, M., Zhao, Y., Luo, X. and Zheng, Z. (2012) Equilibrium and kinetics of adsorption of phosphate onto iron-doped activated carbon. Environmental Science and Pollution Research 19(7), 2908-2917.

Wang, Z., Shen, D., Shen, F. and Li, T. (2016) Phosphate adsorption on lanthanum loaded biochar. Chemosphere 150, 1-7.

Waterschappen, U.v. (2015) Bedrijfsvergelijking Zuiveringsbeheer 2015 (BVZ 2015).

Wathugala, A.G., Suzuki, T. and Kurihara, Y. (1987) Removal of nitrogen, phosphorus and COD from waste water using sand filtration system with Phragmites Australis. Water Research 21(10), 1217-1224.

Weber, K.A., Achenbach, L.A., Coates, J.D., 2006. Microorganisms pumping iron: anaerobic microbial iron oxidation and reduction. Nature reviews. Microbiology 4 (10), 752–764.

WEF, 2011. Nutrient removal. WEF manual of practice no. 34. McGraw-Hill; WEF Press, New York, Alexandria, Va.

Weir, C.C. and Soper, R.J. (1963) INTERACTION OF PHOSPHATES WITH FERRIC ORGANIC COMPLEXES. Canadian Journal of Soil Science 43(2), 393-399.

Wen, Z., Zhang, Y. and Dai, C. (2014) Removal of phosphate from aqueous solution using nanoscale zerovalent iron (nZVI). Colloids and Surfaces A: Physicochemical and Engineering Aspects 457, 433-440.

Wendt von, H., 1973. Die Kinetik typischer Hydrolysereaktionen von mehrwertigen Kationen. Chimia (27), 575–588.

Weng, L., Van Riemsdijk, W.H. and Hiemstra, T. (2012) Factors controlling phosphate interaction with iron oxides. J Environ Qual 41(3), 628-635.

Whalley, M., Laidlaw, S., Steel, P., and Shiskowski, D. (2013) Meeting ultra-low effluent phosphorus in small, cold-climate WWTFs. Proc. Water Environ. Fed.

Wijnja, H. and Schulthess, C.P. (2000) Vibrational Spectroscopy Study of Selenate and Sulfate Adsorption Mechanisms on Fe and Al (Hydr)oxide Surfaces. Journal of Colloid and Interface Science 229(1), 286-297.

Wilfert, P., Kumar, P.S., Korving, L., Witkamp, G.-J. and van Loosdrecht, M.C.M. (2015) The Relevance of Phosphorus and Iron Chemistry to the Recovery of Phosphorus from Wastewater: A Review. Environmental Science & Technology 49(16), 9400-9414.

Wu, B., Fang, L., Fortner, J.D., Guan, X. and Lo, I.M.C. (2017) Highly efficient and selective phosphate removal from wastewater by magnetically recoverable La(OH)3/Fe3O4 nanocomposites. Water Research 126, 179-188.

Wu, R.S.S. (1999) Eutrophication, Water Borne Pathogens and Xenobiotic Compounds: Environmental Risks and Challenges. Marine Pollution Bulletin 39(1), 11-22.

Wu, R.S.S., Lam, K.H., Lee, J.M.N. and Lau, T.C. (2007) Removal of phosphate from water by a highly selective La(III)-chelex resin. Chemosphere 69(2), 289-294.

Xie, F., Wu, F., Liu, G., Mu, Y., Feng, C., Wang, H. and Giesy, J.P. (2014a) Removal of Phosphate from Eutrophic Lakes through Adsorption by in Situ Formation of Magnesium Hydroxide from Diatomite. Environmental Science & Technology 48(1), 582-590.

Xie, J., Wang, Z., Fang, D., Li, C. and Wu, D. (2014b) Green synthesis of a novel hybrid sorbent of zeolite/lanthanum hydroxide and its application in the removal and recovery of phosphate from water. Journal of Colloid and Interface Science 423, 13-19.

Xie, J., Wang, Z., Lu, S., Wu, D., Zhang, Z. and Kong, H. (2014c) Removal and recovery of phosphate from water by lanthanum hydroxide materials. Chemical Engineering Journal 254, 163-170.

Xie, Q., Li, Y., Lv, Z., Zhou, H., Yang, X., Chen, J. and Guo, H. (2017) Effective Adsorption and Removal of Phosphate from Aqueous Solutions and Eutrophic Water by Fe-based MOFs of MIL-101. Scientific Reports 7(1), 3316.

Xiong, W., Tong, J., Yang, Z., Zeng, G., Zhou, Y., Wang, D., Song, P., Xu, R., Zhang, C. and Cheng, M. (2017) Adsorption of phosphate from aqueous solution using iron-zirconium modified activated carbon nanofiber: Performance and mechanism. Journal of Colloid and Interface Science 493, 17-23.

Xu, R., Zhang, M., Mortimer, R.J. and Pan, G. (2017) Enhanced Phosphorus Locking by Novel Lanthanum/Aluminum-Hydroxide Composite: Implications for Eutrophication Control. 51(6), 3418-3425.

Xue, Y., Hou, H. and Zhu, S. (2009) Characteristics and mechanisms of phosphate adsorption onto basic oxygen furnace slag. Journal of Hazardous Materials 162(2), 973-980.

Yadav, D., Kapur, M., Kumar, P. and Mondal, M.K. (2015) Adsorptive removal of phosphate from aqueous solution using rice husk and fruit juice residue. Process Safety and Environmental Protection 94, 402-409.

Yamashita, K., Miyake, T., Fukuoka, H., Midorikawa, I., Shimizu, T. and Hashimoto, T. (2013) High Efficiency Adsorbent System for Phosphorus Removal and Recovery from Filtrated Water of Anaerobic Digestion Sludge. Proceedings of the Water Environment Federation 2013(19), 133-142.

Yang, J., Yuan, P., Chen, H.-Y., Zou, J., Yuan, Z. and Yu, C. (2012) Rationally designed functional macroporous materials as new adsorbents for efficient phosphorus removal. Journal of Materials Chemistry 22(19), 9983-9990.

Yao, W., Millero, F.J., 1996. Oxidation of hydrogen sulfide by hydrous Fe(III) oxides in seawater. Marine Chemistry 52 (1), 1–16.

Yao, Y., Gao, B., Chen, J. and Yang, L. (2013) Engineered Biochar Reclaiming Phosphate from Aqueous Solutions: Mechanisms and Potential Application as a Slow-Release Fertilizer. Environmental Science & Technology 47(15), 8700-8708.

Ye, Y., Ngo, H.H., Guo, W., Liu, Y., Li, J., Liu, Y., Zhang, X. and Jia, H. (2017) Insight into chemical phosphate recovery from municipal wastewater. Sci Total Environ 576, 159-171.

Ye, Z., Shen, Y., Ye, X., Zhang, Z., Chen, S. and Shi, J. (2014) Phosphorus recovery from wastewater by struvite crystallization: Property of aggregates. Journal of Environmental Sciences 26(5), 991-1000.

Yildiz, E. (2004) Phosphate removal from water by fly ash using crossflow microfiltration. Separation and Purification Technology 35(3), 241-252.

Yoon, S.-Y., Lee, C.-G., Park, J.-A., Kim, J.-H., Kim, S.-B., Lee, S.-H. and Choi, J.-W. (2014) Kinetic, equilibrium and thermodynamic studies for phosphate adsorption to magnetic iron oxide nanoparticles. Chemical Engineering Journal 236, 341-347.

Yuan, X., Bai, C., Xia, W., Xie, B. and An, J. (2015) Phosphate adsorption characteristics of wasted low-grade iron ore with phosphorus used as natural adsorbent for aqueous solution. Desalination and Water Treatment 54(11), 3020-3030.

Zach-Maor, A., Semiat, R. and Shemer, H. (2011a) Adsorption–desorption mechanism of phosphate by immobilized nano-sized magnetite layer: Interface and bulk interactions. Journal of Colloid and Interface Science 363(2), 608-614.

Zach-Maor, A., Semiat, R. and Shemer, H. (2011b) Synthesis, performance, and modeling of immobilized nano-sized magnetite layer for phosphate removal. Journal of Colloid and Interface Science 357(2), 440-446.

Zelmanov, G. and Semiat, R. (2011) Phosphate removal from water and recovery using iron (Fe +3)oxide/hydroxide nanoparticles-based agglomerates suspension (AggFe) as adsorbent. Environmental Engineering and Management Journal 10, 1923-1933.

Zeng, L., Li, X. and Liu, J. (2004) Adsorptive removal of phosphate from aqueous solutions using iron oxide tailings. Water Research 38(5), 1318-1326.

Zhang, G., Liu, H., Liu, R. and Qu, J. (2009) Removal of phosphate from water by a Fe–Mn binary oxide adsorbent. Journal of Colloid and Interface Science 335(2), 168-174.

Zhang, L., Wan, L., Chang, N., Liu, J., Duan, C., Zhou, Q., Li, X. and Wang, X. (2011) Removal of phosphate from water by activated carbon fiber loaded with lanthanum oxide. Journal of Hazardous Materials 190(1–3), 848-855.

Zhang, L., Zhou, Q., Liu, J., Chang, N., Wan, L. and Chen, J. (2012) Phosphate adsorption on lanthanum hydroxide-doped activated carbon fiber. Chemical Engineering Journal 185-186, 160-167.

Zhang, Y., Pan, B., Shan, C. and Gao, X. (2016) Enhanced Phosphate Removal by Nanosized Hydrated La(III) Oxide Confined in Cross-linked Polystyrene Networks. Environmental Science & Technology 50(3), 1447-1454.

Zheng, X., Sun, P., Han, J., Song, Y., Hu, Z., Fan, H. and Lv, S. (2014) Inhibitory factors affecting the process of enhanced biological phosphorus removal (EBPR) – A mini-review. Process Biochemistry 49(12), 2207-2213.

Zhou, J., Yang, S., Yu, J. and Shu, Z. (2011) Novel hollow microspheres of hierarchical zinc–aluminum layered double hydroxides and their enhanced adsorption capacity for phosphate in water. Journal of Hazardous Materials 192(3), 1114-1121.

Zhou, Q., Wang, X., Liu, J. and Zhang, L. (2012) Phosphorus removal from wastewater using nano-particulates of hydrated ferric oxide doped activated carbon fiber prepared by Sol–Gel method. Chemical Engineering Journal 200–202, 619-626.

Zhu, Z., Zeng, H., Zhu, Y., Yang, F., Zhu, H., Qin, H. and Wei, W. (2013) Kinetics and thermodynamic study of phosphate adsorption on the porous biomorph-genetic composite of

α-Fe2O3/Fe3O4/C with eucalyptus wood microstructure. Separation and Purification Technology 117, 124-130.

Zong, E., Wei, D., Wan, H., Zheng, S., Xu, Z. and Zhu, D. (2013) Adsorptive removal of phosphate ions from aqueous solution using zirconia-functionalized graphite oxide. Chemical Engineering Journal 221, 193-203.

Zong, E., Wei, D., Wan, H., Zheng, S., Xu, Z. and Zhu, D. (2013) Adsorptive removal of phosphate ions from aqueous solution using zirconia-functionalized graphite oxide. Chemical Engineering Journal 221, 193-203.

Acknowledgments



I see several similarities between my first marathon and my PhD. And I mean it in an exciting way. Sure, there is the challenge aspect, but there is also so much more, its packed with events. One meets with so many people, some in short phases, some for a longer time. Some at the beginning, some at the end, and perhaps some for the entire duration. Some whose names will stay with me for a long time, and some whose names I never got to ask. And yet, each and every single person I met contributed to my experience and played a role in helping me complete my marathon. And in the process, I also learnt so much more about myself. I will not be able to acknowledge them all in entirety within a few pages, but this section will at least serve to remind me that there is so much more to it.

Wetsus has been at the heart of my PhD experience. Several of my academic, as well as extracurricular activities, have revolved around Wetsus. Chess was one of my favorites. Jan (de Groot), I am glad that you reciprocated that day near Albert Heijn. That led to a lasting friendship amidst great battles on the chessboard. Ilse and Chris, I have enjoyed several games with you both. Pau, you almost shocked me with your version 2 during the Wetsus chess tournament. That was one of the most breathtaking games I played in Wetsus. Jan-Willem, you got me interested in playing fast chess. Jorrit, that was one truly magical game we played.

I picked up my running skills during my PhD. Fei, you were the first to get me interested in outdoor running in Leeuwarden. Jouke, you showed me that it is possible to have interesting discussions during long runs. I also remember how good the juice tasted after returning home from the long runs. Jai, I learned many technical things during my runs with you. Roel and Philipp Kuntke, being part of your triathlon team was a lot of fun. And to think that at one point we were contemplating four events in a row. Anthony, Bianca, and Hester, listening to your stories and experiences were encouraging. Henk, I never got to run with you, but seeing and waving to you during my runs in Leeuwarden always gave me a boost.

Trienke and Jannie, you have been my ice cream buddies. Those moments were great. Taking a short break towards La Venezia or Puur or Min12 (preferably in that order) helped me to get through busy days.

Not many people were a fan of the horror genre, but I still managed to get an enthusiastic group of friends to be part of horror movie nights. Sofia, Hector, Yang, Yin, Marianne (Heegstra), you guys were awesome to have along for gripping movies. I remember some movies scared me so much that I had trouble getting sleep during those nights.

Although I didn't pick up my Dutch language skills, the Dutch lessons constituted to interesting sessions nevertheless. Gerbrich, I tied to practice the Dutch G every time I pronounced your name. I think I have never met an alphabet quite like the Dutch G. Henriette, you were so supportive and motivating towards all of us in your classes. You inspired me further to appreciate teaching.

Wetsus also resulted in broadening my musical taste. Being part of the Wetsus band was one of the most rewarding experiences for me. Sofia, Brahzil, Ricardo, Jorrit, Fabian, Victor, Stan, Pau, Louis, Gonzalo, it was incredible playing along with you all. Ricardo, you were symbolic of the guitar guys, always overpowering the sounds from the piano. And yet Blackbird was one of my most unique experiences. Fabian, you were very kind to me. You would easily give up your explosive drumming style to accompany me with my minimalistic tunes. Stan, just one session of jamming with you and I played chords that I never knew existed. Louis, I absolutely

loved your different style of piano playing. Sofia, you lent your voice for some of the songs that I enjoyed playing the most on piano. Brazhil, you created an atmosphere that everyone enjoyed being part of. Victor, your cello playing was a beautiful complement to the piano. And yet we only heard ourselves when the guitarists mellowed down. Gonzalo, I loved your enthusiasm in trying out different styles. Jorrit, we couldn't have asked for a better leader for our band. I will miss playing with you all.

Working with school students from the Wetsus Honours programs was also an activity I enjoyed a lot. Marco, Jan Jurjen, your enthusiasm with this program is feverish. Jorn, Marte, Silke, Tim, Roald, Sanne, Lyssia, I wanted to let you know that you all are amazing. You guys do stuff that I never thought about during my school days. Lisette, Koon and Jos, it's also nice that you guys are actively bringing and engaging young minds in Wetsus.

I also got to teach courses in Van Hall Larenstein during my PhD years. Paula, and Leo, it was fun to do the courses thrice in a row. Every occasion brought new questions from students and opportunities to improve. Nelleke and Petra, you guys also facilitated presentations with college students. I always enjoyed those interactions.

During the course of my PhD, I had several officemates. Natasha, Nirajan, Enver, Fei, and Maria, I shared an office space with you guys in the old Wetsus building. Natasha, I still remember your explanation on using the calendar in the webmail. It proved quite handy for me ever since. Enver and Fei, we had a legendary barbecue at the very beginning of my PhD. Maria, you were someone whose very presence can uplift the surroundings. You often invited yourself to my house, and that helped me open up a bit. Jouke, Sam, Mariana Rodriguez, Pau, Rebeca, Gosha, Hector, Lina, Emanuel, Diego, Kaustub, you guys make our office space the way it is. I have shared memorable incidents with you all in that space. Our office dinners were also something that I looked forward to.

An exciting part of being at Wetsus was also the chance to experience weddings from different cultures. Gosha and Pawel, your wedding gave me an opportunity to visit your wonderful country. I enjoyed the ceremony and I understood the meaning of a true wedding feast that night. Sam and Sanne, witnessing yours at the community farm, was quite an experience. I met with some very interesting people during the wedding. Of course, the trip at the Leeuwarden beach was also reminiscent. Ricardo and Lina, to have an ocean as the backdrop was a setting from a movie for me. What can I say, I am just guessing who is on the list next?

The Wetsus canteen is one the usual places to catch up with colleagues. That brings me to Gerben, and Riet, who were integral in maintaining it. Riet, you were always warm and friendly which made me walk by the canteen even if it was just to say a hi.

The 2nd floor of Wetsus feels relatively calmer than the 1st, but it does host important people. Cees, I enjoyed the guided walk by the Rijs forest. Johannes, you made me feel at home in Hemelum, a place many of my Dutch colleagues did not know about. Bert, I must admit that I had a dream when I was asked to write a review paper at the end of my 1st year. And guess who I was talking to in the dream. But talking with you in person was quite the contrary, it gave me confidence that it's doable. Nynke, Anke, Helena, Linda, Geke, Jeanette, Roely, you all made sure that administrative things went as smooth as possible. Jeanette, it was nice once in a while to discuss music with you. Esther, Tineke, and Jannie, saying hi to you all was often my first experience when I entered Wetsus. The finance team of Albert, Lucy, Jan, and Klaudia also

made it easy for me in terms of expense claims. Rienk, the martial arts/computer guy, was always eager to troubleshoot IT related challenges. Gerrit, your discussions while making orders from Canada were helpful and vital during the pilot study. Elmar, you often came up with fascinating stories and questions. I am still awaiting an answer.

Maarten (Biesheuvel), I liked your feedbacks after my presentations. I would like to call them constructive. Martijn (Wagterveld), you were often a quick source for relevant numbers. Martijn (Bijmans), you knew a thing or two (or maybe three) about taste, and it was fun to hop along with your choices. Heleen, along with Ingrid, you were responsible for organizing courses that I found helpful. Karel and Hardy (I was about to type Laurel and Hardy), it was nice to collaborate with you both during my research. Both were fruitful, and more importantly, I learned more about the topics.

The support provided by the lab/analytical team made it really easy for me to focus just on the experiments. Janneke, Mieke, Marianne, Lisette, Ton and Jelmer, you guys are a big advantage for Wetsus PhDs. Mieko, you were always willing to answer queries and I found it very comfortable to ask you for suggestions. You were also of great help when I had my first student. Janneke, you organized SEM classes which were very useful. Marianne, your style of music brought a smile in the lab. Ton, your discussions during Raman analysis kept me awake in the dark room. Lisette, it was cool to discuss about birds and drawings with you. Jelmer, you are the movie star who helped me so often with my microscope samples.

Building setups for experiments were easier due to the technical team including Wim, Jan (Tuinstra), Harm, Ernst, Jan Jurjen, John and Harrie. You guys were not helpful just with PhD related work, but also helped us with the George Barley Prize related experimental setup. Ernst, it was nice to hear you play the piano sometimes too. Wiebe, apart from biking the Elf Steden, you helped maintain the humidity in the piano at Wetsus. That was an important help for me.

Adam, Olivier, and Mikele, making the movie for the Geroge Barley prize was also one of my funniest experiences during my PhD. All those fiddling around with the camera, holding the mike at awkward angles, doing breathing exercises, holding out the dialogues in our hands, using a dubbed over voice; after that shoot, I decided acting was not my cup of tea. But jokes apart, you guys made a great movie.

Where would have I been without my former students and friends? Thomas, it already feels like you have been there throughout my PhD. I had a terrific time working with you. Remember that day when we were trying to solve something regarding the porosity and we sat pretty much for an hour or more just discussing the possible scenarios. And the trip in Ameland also sticks in the mind. Kevin, your iron man presentation comes to mind when I think of you. You managed so well when I was initially not around and almost carried your work singlehandedly. Raimonda, I will remember how you and Philipp made fun of my drawing, but that only brings a smile to my face. Having you around for the biogenic study as well for the George Barley Prize lab stage was an asset. Not to forget that you create a nice working space around others. Wondesen, I somehow felt you deserved more than what you got. You did really well with the reusability study, but for me, it was our discussions outside Wetsus that were more fun. Whether it be in the wastewater plant or at the Wok place. Carita, you solved the final piece in my PhD research and did it impressively. It is fair to say that my PhD would not have been the same without you all.

I was also lucky that we had theme members who were actively engaged in the discussions during the theme meetings. Outi, Wout, Kees, Mathias, you all made the discussions meaningful and enjoyable. There were also very good questions asked during the presentations with the STOWA committee.

I also had collaborators from outside Wetsus who helped me with my research. Iulian Dugulan and Kees Goubitz's collaboration was very important for the research. Dap Hartmann gave useful insights into the valorization of the thesis. Miranda Verhulst from TUD was very helpful with organizing important meetings and handling administrative stuff regarding the PhD. Koos, Frank, Miriam, and Ad gave valuable support during the pilot study in Canada.

Doing an MBA along with the PhD sounded challenging, but it was comforting to have some colleagues from Wetsus who also signed up for it. Terica and Natashca, I am sure we have been in group events that had a more exciting atmosphere than the MBA meetups. But nevertheless, it stands outs as a different experience. Without having any colleagues, it could have felt more challenging.

Going to music festivals, concerts and parties also made for very interesting experiences. Patrick, Marriane, Jan, Roel, Sebastian, Adam, Sam, Prithvi you all have been part of my experiences. Patrick, I have had some of my most funny and best experiences with you. You are a great dancer although you probably did not expect the dance with Jan. Roel, you made a great host for Halloween.

Celebrating Indian festivals and getting together for traditional cooking became more frequent during the final years of my PhD. This was in no small amount due to my desi friends Jai, Nimmy, Suyash, Swaroopa, Haniel, Indresh, Kaustub, Advait, Aniket, Prithvi, Nandini, Namratha, Varun. It felt nice to be with you all for traditional get-togethers. Nimmy, I think the midnight wakeup and the milk potato experience will be hard to forget, but it was fun (at least for some). Jai, your commitment to your actions was inspiring. Namratha, your voice sounded even more impressive to me during the playback. I enjoyed our music sessions. Elango, we spanned a range of interesting and thoughtful conversations during our meetups in Delft.

There are so many more events with people from Wetsus. Rik, I remember watching the movie in the cinema and getting surprised when for you the scene was obvious. Of course that makes sense. Jaap, talking with you has gotten me to know more about massages. Victor Ajao, it was awesome to be part of the team along with you. And your dubbed voice was such a highlight in the video. Lucia, I will remember your reaction when I first showed you my picture with the mustache. And that you were quite vocal in supporting veggie food at the events. Klaudia, for someone who finds chess so boring, you still managed to bring in nice discussions when Jan used to go for a break. And of course you were the one who introduced me to twin peaks. Victor Torres, I had no idea about the caravan, but otherwise, I thought we had a lot of fun during our times at Delft. Mariane Rodrigues, it was nice to be able to enjoy spicy food with you. Aga and Slawek the genius, you shared interesting but sometimes also mystical stories. Janneke, the Mo gymnastics was a great idea. Jordi, Joao, Pedro, Pom, Dries, Vytautas, Zlatica, Joeri, Anna, Jan Willem, Tania, Caspar, Gerwin, Karine, Paulina, Rachel, Andrew, Sandra, Steffen, Hakan, Gijs, Maarten, Enas, Hanieh, Anthonie, Ehmad, I had interesting discussions with each and every one of you. It ranged from topics on trying sweet potato fries to time traveling. Carlo, it was nice to discuss music and education with you. Good luck with your ongoing marathon.

Now it's time for me to get to the core team of my research. Geert-Jan, I remember the day when we walked by the Oldehove during our theme's inaugural dinner. There popped the question on whether the Oldehove was really tilted or if it was my imagination. I found out the next day. Apart from having discussions on my project, I enjoyed our discussions regarding music and different civilizations. I admire the fact that you are not only helpful but that you like helping as many people as possible. Your excitement towards results also makes it a lot of fun to do research with you. Mark, you were very accessible by emails and I found that very helpful for making decisions in different situations. You gave useful suggestions, relevant contacts and often encouraged me to think about future options.

Leon, the professional, or that is at least how we saw you at the beginning. It did take me some time to get aligned with your style of working, but you made a big impact on how my PhD shaped. I have learned a lot from you, and also due to your constant pushing to go one step further. I think that has equipped me with some handy attributes. You also provided me with plenty of opportunities, including the George Barley Water Prize and I am quite happy that I could be a part of your team.

Philipp(ino), you accompanied me for a majority of my marathon. There were countless things we did together (remember that expression), but I particularly liked the open discussions we had while we were in Delft. And of course, all the fun we had while collaborating and working with students.

I did have my share of experiences outside Wetsus as well. Janneke, I enjoyed learning the violin from you. I personally did find it a more challenging instrument to learn than the piano, but it still has me in awe whenever I hear its sound. Joh, I often refer to you as my youngest friend. You show me that age is just a number. Going out with you and hearing your stories often provided me with a new perspective. I also need to mention Herre for that great trip he took us on, which covered the 12th city of Friesland. And Janneke's driving felt like straight from a James Bond movie.

Charu and Indranil, you guys were like a family away from home. Apart from your unconditional support, Indranil's ability to improvise while I was playing music kept me hooked. And not to forget the little one. Running around together with Harihar was amongst the activities I enjoyed the most during my thesis writing.

There were also people whose name I never asked but still contributed to my experience. The lady with the dog who greeted me whenever I used to go on a run, the lady outside the shop who would always return a smile. And there were people whose name I know, but I never met them again., Piet, that one night at Groningen was unlike any other.

I also went travelling with my friends studying abroad who organized exotic trips around Europe. Anbu, Dinesh, Jothi, Sakthi, Prakash, Ram, Vignesh, our trips were a good mix of fun and adventure. Mariane, Olof, Maxim, I also had interesting trips with you guys, ranging from traveling around in the Netherlands to climbing on the Alps. Linda and Harald, you guys played a definitive role in getting me interested in the field of research. Harald, the explanation you gave me on gas molecules is still one of my favorite scientific ones.

Finally, but most importantly I would like to thank my parents, my brother and all my family members for their support. Mom and dad, without you I would not have been able to start this marathon in the first place. Your support throughout my education meant a lot to me.

I have run a few marathons so far and I must admit that for all its similarities, the PhD marathon is still unlike any other. I am very grateful to each and every one who has been a part of this.

Curriculum vitae



Prashanth Suresh Kumar was born on September 10th, 1988 in Jamshedpur, India. He completed his B.Tech in Biotechnology in 2010 under Anna University. During his Bachelor's thesis, he worked on phenol biodegradation in an inverse fluidized biofilm reactor. He pursued his M.Sc in Applied Biotechnology in Uppsala University, Sweden. His master's thesis was on arsenic adsorption using cryogels in Lund University. He completed his M.Sc in 2012 and continued research in the field of his master's thesis at Lund University. During this time, he worked on producing and characterizing cryogels incorporated with metal hydroxides.

In late 2013 Prashanth started his PhD work on reversible adsorption of phosphate from wastewater. This project was started in the Netherlands in collaboration with Delft University of Technology and Wetsus, European centre of excellence for sustainable water technology. During his PhD, he was involved in working with students from the WaterCampus Honours program. Being involved with his team of school students who won the WaterCampus science fair award twice in a row ranks amongst his happiest achievements. Prashanth was also part of the Wetsus team that participated in the George Barley Water Prize, a contest aimed to solve the phosphorus pollution in the Everglades, Florida. In early 2018, Prashanth followed up his doctoral research with a pilot study in Canada in the context of the George Barley Water Prize. The results of his PhD work are presented in this thesis.

List of publications

Suresh Kumar, P., Korving, L., Keesman, K.J., van Loosdrecht, M.C.M. and Witkamp, G.-J. (2019) Effect of pore size distribution and particle size of porous metal oxides on phosphate adsorption capacity and kinetics. Chemical Engineering Journal 358, 160-169.

Suresh Kumar, P., Ejerssa, W.W., Wegener, C.C., Korving, L., Dugulan, A.I., Temmink, H., van Loosdrecht, M.C.M. and Witkamp, G.-J. (2018) Understanding and improving the reusability of phosphate adsorbents for wastewater effluent polishing. Water Research 145, 365-374.

Suresh Kumar, P., Prot, T., Korving, L., Keesman, K.J., Dugulan, I., van Loosdrecht, M.C.M. and Witkamp, G.-J. (2017) Effect of pore size distribution on iron oxide coated granular activated carbons for phosphate adsorption – Importance of mesopores. Chemical Engineering Journal 326, 231-239.

Buliauskaitė, R., Wilfert, P., Suresh Kumar, P., de Vet, W.W.J.M., Witkamp, G.-J., Korving, L. and van Loosdrecht, M.C.M. (2018) Biogenic iron oxides for phosphate removal. Environmental Technology, 1-7.

Wilfert, P., Kumar, P.S., Korving, L., Witkamp, G.-J. and van Loosdrecht, M.C.M. (2015) The Relevance of Phosphorus and Iron Chemistry to the Recovery of Phosphorus from Wastewater: A Review. Environmental Science & Technology 49(16), 9400-9414.

In submission: Adsorption as technology for achieving ultra-low concentrations of phosphate: Research gaps and economic analysis, Suresh Kumar, P., Korving, L., van Loosdrecht, M.C.M. and Witkamp, G.-J.